

**The E.S.R. Spectra of Some
Aromatic Radical Ions**

A Thesis submitted for the degree
of Doctor of Philosophy in the
Faculty of Science of the
University of London

By
Kai-Mo Ng

The Christopher Ingold Laboratories
University College London
20 Gordon Street
London WC1H 0AJ

October 1993

ProQuest Number: 10017389

All rights reserved

INFORMATION TO ALL USERS

The quality of this reproduction is dependent upon the quality of the copy submitted.

In the unlikely event that the author did not send a complete manuscript and there are missing pages, these will be noted. Also, if material had to be removed, a note will indicate the deletion.



ProQuest 10017389

Published by ProQuest LLC(2016). Copyright of the Dissertation is held by the Author.

All rights reserved.

This work is protected against unauthorized copying under Title 17, United States Code.
Microform Edition © ProQuest LLC.

ProQuest LLC
789 East Eisenhower Parkway
P.O. Box 1346
Ann Arbor, MI 48106-1346

Acknowledgements

I would like to express my sincere thanks to my supervisor Professor A.G. Davies for his invaluable guidance, understanding and encouragement throughout the course of this work. I therefore wish to take this opportunity to convey my thanks to him not only his help with my PhD but also support whenever I needed it.

I would like to take this opportunity to thank Dr. B.P. Roberts for his help and advice.

I also wish to thank Dr. D.V. Avila for helping me when I first started this work, and Drs. H.S. Dang and J. Cai for looking after me throughout my PhD years.

Special thanks to my parent and Ms. Y.L. Lee for their patience and encouragement during my period of study.

Finally, I would like to thank the Overseas Research Student committee for the award an O.R.S. Research Scholarship (1990-93) and a Departmental Studentship from University College London.

Abstract

This thesis reports the results of investigations concerning the generation of radical cations, and the nuclear and electronic structures of some aromatic radical ions.

The radical ions were generated in fluid solution, and then identified and characterised by electron spin resonance (e.s.r.) spectroscopy. The interpretation was confirmed by computer simulation.

The generation of radical cations by electron-transfer from an electron-rich arene to an electron-acceptor, 2,3-dichloro-5,6-dicyano-1,4-quinone (DDQ) in trifluoroacetic acid (TFAH) in the presence of stronger acids (eg. MeSO_3H , $\text{CF}_3\text{SO}_3\text{H}$) was examined. This technique can generate the radical cations which we had failed to make previously such as the benzo[1,2:4,5]dicyclobutene radical cation. The most important result with this method is the observation of the e.s.r. spectra of a number of benzo-crown ethers (eg. benzo-18-crown-6, benzo-15-crown-5) and their complexes.

The e.s.r. spectra of a series of strained benzocyclobutene and benzocyclopentene radical cations were observed. The McConnell-type Q-values have been derived. The S.O.M.O. of these strained radical cations is the Ψ_A M.O., and it is suggested that the ordering of the energy levels (Ψ_A above Ψ_S) in these ring-strained compounds is a manifestation of the Mills-Nixon effect, and results from rehybridisation of the strained molecular frame work.

The e.s.r. spectra of 1,3-benzodioxole radical cations have been observed and characterised. The coupling constants of the aliphatic protons ($-\text{OCH}_3$ or $-\text{OCH}_2\text{O}-$) can be explained in terms of the molecular orbital theory of hyperconjugation, and the Whiffen effect.

The e.s.r. spectra of the radical cations of benzo-[1,2-b:4,5-b']-bis-1,4-dioxane, 1,3-dioxolo[4,5-g]benzo-1,4-dioxane, 6,7-dimethyl-1,4-benzodioxane, 6,7-dimethoxy-1,4-benzodioxane and 5,8-di-*tert*-butyl-1,4-benzodioxane have been observed and analysed. In all five radical cations, the *pseudo*-axial and *pseudo*-equatorial protons of the methylene groups in the half-chair dioxene rings are distinguished by different hyperfine coupling constants, and simulation of the spectra over a range of temperatures has given the Arrhenius plots for the ring inversions.

When certain substituted benzo-1,4-dioxanes and benzo-1,3-dioxoles are treated with mercury(II) trifluoroacetate in TFAH, the e.s.r. spectra of the mercurated arene radical cations were observed. The aromatic protons with a small hyperfine coupling constant are replaced by mercury and satellites due to ^{199}Hg hyperfine coupling can be observed. Mercuration also increases the g-value of the radical cations, and the ratio $\underline{a}(^{199}\text{Hg})/\underline{a}(^1\text{H}) = 13-14$ is obtained. Replacement of trifluoroacetate anion by the fluorosulphonate anion, gave an increase of $\underline{a}(^{199}\text{Hg})$ of about 14% as the electronegativity of the anion increased.

The radical anions and cations of benzo[b]biphenylene, binaphthylene and tribenzo[12]annulene were examined. In the case of benzo[b]biphenylene and binaphthylene. The hyperfine coupling constants of the radical cations are *less* than those of the radical anions, and the pairing principle of alternant hydrocarbons appears to break down.

Abbreviations

DDQ	2,3-Dichloro-5,6-dicyano-1,4-quinone
DME	1,2-Dimethoxyethane
DMF	<i>N,N</i> -Dimethylformamide
DMSO	Dimethyl sulphoxide
eV	Electron volt
ENDOR	Electron nuclear double resonance
E.s.r.	Electron spin resonance
H.O.M.O.	Highest occupied molecular orbital
L.U.M.O.	Lowest unoccupied molecular orbital
M.O.	Molecular orbital
N.m.r.	Nuclear magnetic resonance
S.O.M.O.	Singly occupied molecular orbital
THF	Tetrahydrofuran
TFA	Trifluoroacetate
TFAH	Trifluoroacetic acid

Contents

	Page
Acknowledgements	2
Abstract	3
Abbreviations	5
1. Introduction	
1.1. Background	10
1.2. Generation of Radical Ions	11
1.2.1. Radical Anions	12
1.2.2. Radical Cations	13
1.3. Counterion Coupling	17
1.4. Interactions and Reactions	18
1.5. Electron Spin Resonance Spectroscopy	
1.5.1. Theory	19
1.5.2. Hyperfine Coupling Constants	20
1.5.3. Molecular Orbital Calculations	25
References	27
2. DDQ Method for Generating Some Unusual Radical Cations	
2.1. Background	30
2.2. Results	32
2.2.1. Benzo[1,2:4,5]dicyclobutene	32
2.2.2. 1,3,5-Tri- <i>tert</i> -butylbenzene	32
2.2.3. 1,4-Di- <i>tert</i> -butylbenzene	33
2.2.4. Mesitylene	33
2.2.5. Benzo-18-crown-6	36
2.2.6. Benzo-15-crown-5	37
2.2.7. Dibenzo-18-crown-6	38
2.2.8. 4,5-Dimethoxybenzo-15-crown-5	38
2.3. Discussion	44
2.3.1. Benzo-crown Ethers	44

2.3.2. Advantages and Disadvantages of the DDQ Method	45
References	47
3. Radical Cations of Some Benzocyclobutenes and Benzocyclopentenes	
3.1. Background	48
3.2. Results	52
3.2.1. Benzocyclobutenes	52
3.2.1a. 3,6-Dimethylbenzo[1,2:4,5]dicyclobutene	53
3.2.1b. 3,4,5,6-Tetramethylbenzocyclobutene	53
3.2.1c. Benzo[1,2:4,5]dicyclobutene	54
3.2.2. Benzocyclopentenes	54
3.2.2a. 3,6-Dimethylbenzo[1,2:4,5]dicyclopentene	58
3.2.2b. 3,4,5,6-Tetramethylbenzocyclopentene	58
3.2.2c. 3,6-Dimethylbenzocyclopentene	59
3.3. Discussion	65
3.3.1. Benzocyclobutenes	65
3.3.2. Benzocyclopentenes	70
3.3.3. Benzocyclohexenes	71
References	74
4. Conformational Inversion of Derivatives of Benzo-1,4-dioxane Radical Cations	
4.1. Background	76
4.2. Results	78
4.2.1. Benzo[1,2-d:4,5-d']bis-1,4-dioxane	79
4.2.2. 1,3-Dioxolo[4,5-g]benzo-1,4-dioxane	79
4.2.3. 6,7-Dimethylbenzo-1,4-dioxane	83
4.2.4. 6,7-Dimethoxybenzo-1,4-dioxane	84
4.2.5. 5,8-Di- <i>tert</i> -butylbenzo-1,4-dioxane	84
4.3. Discussion	93
References	96

5. Radical Cations of Alkoxybenzenes	
5.1. Background	97
5.2. Results	99
5.2.1. Benzo[1,2-d:4,5-d']bis-1,3-dioxole	99
5.2.2. 5,6-Dimethoxybenzo-1,3-dioxole	99
5.2.3. 3,6-Di- <i>tert</i> -butyl-1,2-dimethoxybenzene	100
5.2.4. 5,6-Dimethylbenzo-1,3-dioxole	100
5.2.5. 1,2-Dimethoxy-4,5-dimethylbenzene	105
5.2.6. 1,2,4,5-Tetramethoxybenzene	105
5.2.7. Benzo[1,2-d:3,4-d']bis-1,3-dioxole	106
5.3. Discussion	112
5.3.1. Hyperfine Coupling to the Protons in OCH ₃ and OCH ₂ O Groups	112
References	115
6. Mercuration of Aromatic Radical Cations	
6.1. Background	116
6.2. Results	121
6.2.1. Biphenylene	121
6.2.2. 1,4,5,8-Tetramethylbiphenylene	122
6.2.3. Dibenzodioxin	123
6.2.4. 2,5-Diphenylpyrrole	127
6.2.5. 2-Methylbiphenylene	128
6.2.6. Benzo[1,2-d:4,5-d']bis-1,4-dioxane	131
6.2.7. 1,3-Dioxolo[4,5-g]benzo-1,4-dioxane	132
6.2.8. 5,6-Dimethylbenzo-1,3-dioxole	133
6.2.9. 4,7-Di- <i>tert</i> -butylbenzo-1,3-dioxole	134
6.2.10. 6,7-Dimethylbenzo-1,4-dioxane and benzo[1,2-d:3,4- d']bis-1,3-dioxole	135
6.3. Discussion	144
6.3.1. ¹⁹⁹ Hg Satellites	144
6.3.2. Site of Mercuration	145

6.3.3. Mercuration of Benzo[1,2-d:4,5-d']bis-1,4-dioxane, 1,3-Dioxolo[4,5-g]benzo-1,4-dioxane and 5,6-Dimethylbenzo-1,3-dioxole	145
6.3.4. The Ratio $\underline{a}(^{199}\text{Hg})/\underline{a}(^1\text{H})$	146
6.3.5. Mechanism of Mercuration	150
6.3.6. Trifluoroacetylation	151
References	152
7. Radical Ions of Benzenoid Systems	
7.1. Background	154
7.2. Results	156
7.2.1. Benzo[b]biphenylene	156
7.2.2. Binaphthylene	159
7.2.3. Tribenzo[12]annulene	160
7.3. Discussion	165
7.3.1. Benzo[b]biphenylene and Binaphthylene	165
7.3.2. Tribenzo[12]annulene	166
References	167
8. Experimental	
8.1. Synthesis	168
8.2. E.s.r. Spectroscopy	184
8.3. Preparation of Samples for e.s.r. Spectroscopy	184
8.3.1. Oxidants	184
8.3.2. Reductants	186
8.4. N.m.r. Spectroscopy	187
References	188

Chapter 1. Introduction

1.1. Background.

Organic radical ions have played an important part in e.s.r. spectroscopy. Neutral radicals in fluid solution usually self-react at a diffusion-control rate and have a very short life-time, usually less than a second. If the e.s.r. spectra of these neutral radicals are to be recorded, they therefore have to be generated continuously within the e.s.r. spectrometer cavity by special techniques such as flow-mixing of the reagents as they enter the cavity or *in situ* irradiation with electrons, or with u.v. light.

The techniques for generating radical ions are quite different. Radical anions and radical cations are often longer lived, sometime indefinitely so, probably due partly to their Coulombic repulsion. With this slower decay rate, it is relatively easy to obtain strong and well resolved e.s.r. spectra of the radical ions.

Radical ions decay not only by self-reaction, but by other routes such as loss of a proton from a radical cation.

Much of the early work on the e.s.r. spectra of organic radicals involved radical ions. In 1953 Weissman¹ published the first set of papers on organic radicals, and these included the anthracene, naphthalene, and mono-, di-, and tri-nitrobenzene radical anions and the radical cation of *N,N,N',N'*-tetramethyl-p-phenylene diamine, known as Wurster's blue, and then in 1955 Fraenkel² reported the spectra of semiquinone and semidione radical anions.

Most of the principles governing hyperfine coupling in the neutral radicals and radical ions which are still used today were developed from studies on radical anions in the 1950's and 1960's and are discussed in Gerson's *High Resolution E.S.R. Spectroscopy* (1970)³ and in *Radical Ions* (1968) edited by Kaiser and Kevan.⁴

However the experimental techniques have improved greatly, particularly for generating radical cations and the studies have been extended to many more structural types. An extensive listing of the e.s.r. data on organic radical ions, with references, is given in three editions of Landolt-Börnstein⁵.

Radical cations are often derived from highly alkylated conjugated π -systems. This polyalkylation provides (a) steric protection against decay, and (b) reduction of the ionisation energies. In this case, the unpaired electron is delocalised over all the π -centres resulting in hyperfine coupling by many alkyl groups. This can give rise to a very complicated e.s.r. spectrum which cannot be analysed, and electron nuclear double resonance (ENDOR) spectroscopy⁶ may then be employed to identify the hyperfine coupling constants, but the technique of ENDOR spectroscopy will not be discussed in this thesis.

The new techniques for the generation of radical ions include γ -irradiation of solutions of substrates in solid matrices such as frozen Freons for radical cations⁷, or ethers for radical anions. This technique is best for smaller molecules, and unstable radical ions, and can be used for generating radical cations from molecules with high ionisation energies (*ca.* 11eV), such as alkanes. It is less useful for handling the radical cations from larger π -conjugated systems, which involves the resolution of complex spectra containing a large number of closely spaced lines. The e.s.r. spectra recorded by this technique are anisotropic because of the restricted molecular tumbling motion; but this anisotropy provides a great deal of information about the electron configuration of the molecule.

A second technique which is being increasingly used is the generation of radical cations in activated zeolites.⁸ The organic molecule must be small enough to be adsorbed in the activated zeolites. It can be used to generate radical cations from substrates with ionisation energies up to about 11eV. Again, the e.s.r. spectra are to some degree anisotropic, due to the orientation-dependent spin coupling of the radicals inside the channels.

This thesis will concentrate on the e.s.r. spectra of radical ions in fluid solution, for which the spectra are isotropic.

1.2. Generation of Radical Anions and Radical Cations.

In principle, a radical anion of a π -conjugated system can be prepared by addition of an electron into the Lowest Unoccupied Molecular Orbital (L.U.M.O.), and the Singly Occupied Molecular Orbital (S.O.M.O.) of the radical anion corresponds with the L.U.M.O. of the parent (ArH). On the other hand a radical cation is formed by removal

of an π -electron from the Highest Occupied Molecular Orbital (H.O.M.O.), and now the S.O.M.O. of the radical cation corresponds with the H.O.M.O. of the parent ArH. The electron occupancy of a neutral π -conjugated molecule⁸ and its corresponding radical anion and cation are illustrated in (Figure 1.0).

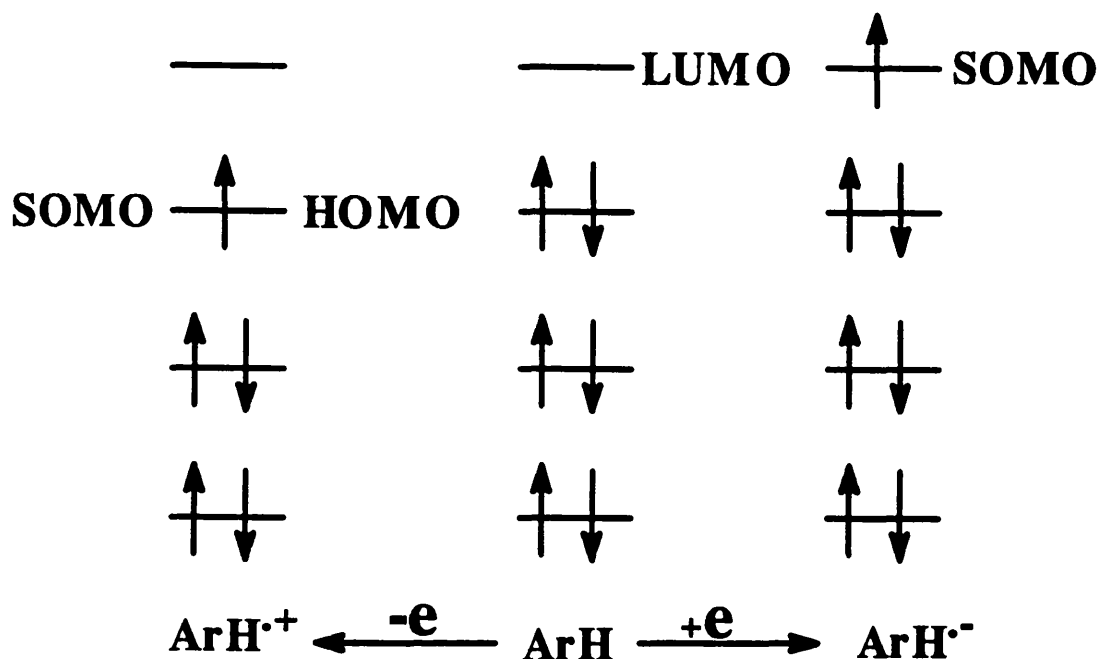
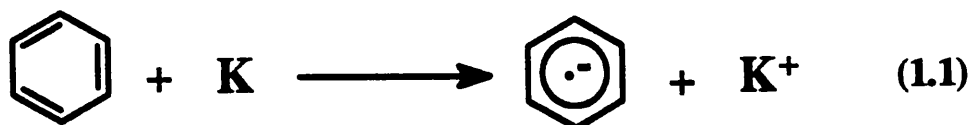


Figure 1.0 Orbital occupancy in ArH, ArH^{•-} and ArH^{•+}.

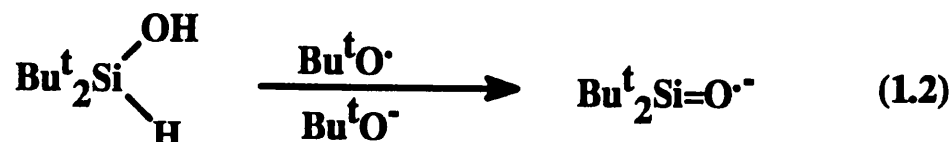
1.2.1. Radical Anions.

The most convenient techniques for generating radical anions in fluid solution are as follows:

(a). A radical anion can be prepared by treating a substrate with an alkali metal (such as potassium or sodium), or its alloy (eg. sodium/potassium) in a polar solvent (such as 1,2-dimethoxyethane or tetrahydrofuran rather than a non-polar hydrocarbon) which helps to solvate the metal cations (equation (1.1)), which are formed. If necessary, a good ligand for the metal cations may be used, particularly a crown ether that will further stabilise the metal cation to avoid complication due to counter ion coupling, and the electron transfer can be assisted by sonication.



(b) A radical anion can be regarded as the conjugate base of a protic neutral radical and the application of this principle can be illustrated by the formation of the di-*tert*-butyl-silanone radical anion by the abstraction of a hydrogen atom and hydride anion from the corresponding silanol by a *tert*-butoxyl radical (from the photolysis of di-*tert*-butyl peroxide) and a *tert*-butoxide anion respectively (equation (1.2)).



(c) Radical anions can also be prepared by cathodic reduction, and Ohya Nishiguchi¹⁰ has described a convenient cell for *in situ* electrolysis. This technique deserves more attention as it is applicable under neutral conditions over a wide range of temperature.

1.2.2. Radical Cations.

No single method is available for the generation of radical cations equivalent to the alkali metal route to radical anions. A variety of methods is available as shown in Table 1.0, and the choice of the technique to be used is still largely empirical. The methods [(a)-(f)] may be used in conjunction with photolysis.

Table 1.0.

No.	Conditions
(a)	With protic acids (eg. H_2SO_4 , $\text{CF}_3\text{SO}_3\text{H}$ and $\text{FSO}_3\text{H}/\text{SO}_2$)
(b)	With Lewis acids (eg. AlCl_3 , BF_3 , SbCl_3 and SbCl_5)
(c)	With oxidising metal ions (eg. Co^{3+} , Ce^{4+} , Hg^{2+} and Tl^{3+})
(d)	With π -conjugated electron-acceptors (eg. DDQ)
(e)	With aminium radical cations (eg. $(4\text{-BrC}_6\text{H}_4)_3\text{N}^+\text{SbCl}_6^-$)
(f)	Protonation of a neutral radical
(g)	Electrolysis

Sometimes dissolution of a substrate in a protic acid (eg. $\text{CF}_3\text{CO}_2\text{H}$), will be sufficient to generate the radical cation; a stronger acid (eg. $\text{FSO}_3\text{H}/\text{SO}_2$) may be used for substrates with higher ionisation energies. For example, a solution of anthracene (An) in $\text{FSO}_3\text{H}/\text{SO}_2$ ¹¹ showed the ^1H n.m.r. spectrum of the anthracenium carbon cations $(\text{An.H})^+$ resulting from protonation at the 9-position, and the same solution showed the e.s.r. spectrum of the anthracene radical cation $(\text{An})^{\cdot+}$ resulting from removal of an electron (Figure 1.1).

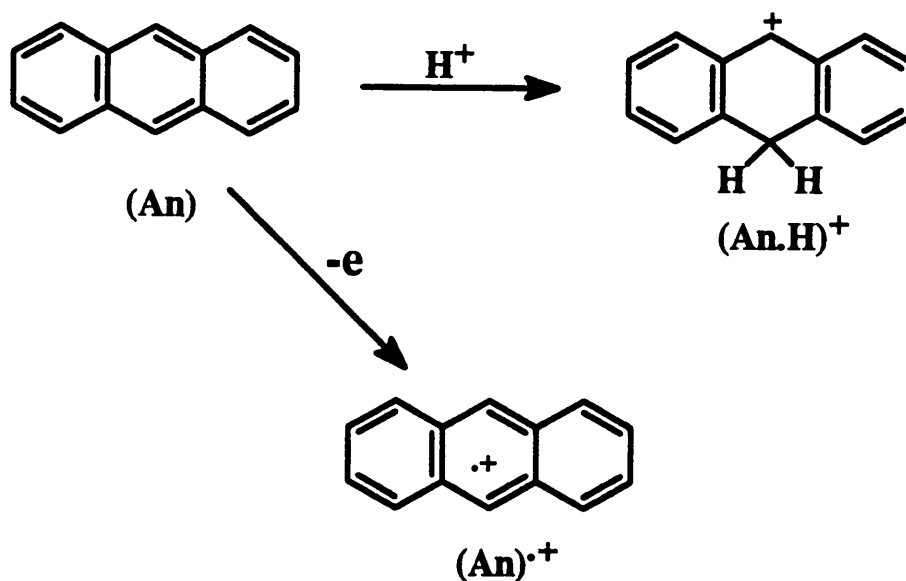


Figure 1.1 Formation of $(\text{An.H})^+$ and $(\text{An})^{\cdot+}$.



The mechanism by which protic acids bring about the formation of arene radical cations are not certain (and the possible effect of laboratory light has often been ignored). The most reasonable mechanisms would appear to be the electron-transfer from an arene (ArH) to the ground state (or photoexcited) protonated arene¹² (equation 1.3) or from the photoexcited arene to the dimer of trifluoroacetic acid, where back electron-transfer is avoided by rapid dissociation of the counterion $(\text{CF}_3\text{CO}_2\text{H})_2^-$ into trifluoroacetate anion and dihydroxy trifluoroethyl radical (equation 1.4).

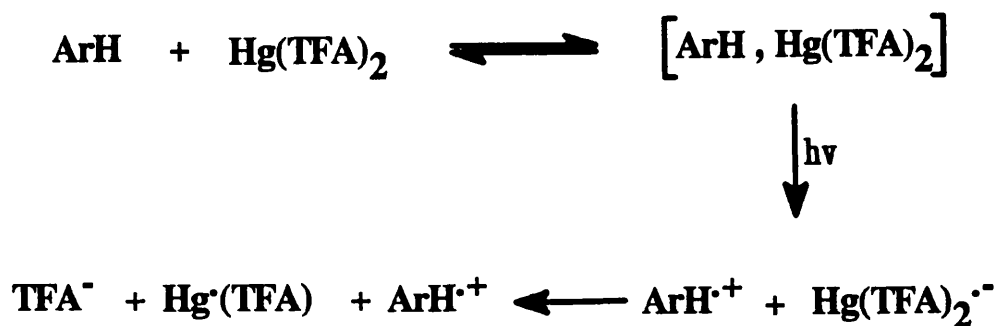


A variety of Lewis acids have been used for the generation of radical cations. Aluminium trichloride has been most commonly used, especially in dichloromethane, and can be used for substrates with ionisation energies less than ca. 8eV. Other reagents such as AsCl_3 , BF_3 , SbCl_3 and SbCl_5 ¹⁴ have also been used. The main advantage of this technique is that it can be used at low temperatures, and variable temperature studies can be carried out.

Metal ion oxidations have been carried out with cobalt(III),¹⁵ cerium(IV),¹⁶ mercury(II),¹⁷ thallium(III)¹⁸ and lead(IV),¹⁹ usually in TFAH.

Both cobalt(III) and cerium(IV) have been used only in a flow system, which is costly in reagent, solvent and substrate. Recently, a modification of this method has been suggested^{ed} for cerium(IV), using other acid media (such as acetic acid²⁰) under static conditions.

Mercury(II) trifluoroacetate or thallium(III) trifluoroacetate are usually used in photolytic, static systems, and the mechanism for $\text{Hg}(\text{TFA})_2/\text{TFAH}$ is shown in equation (1.5). The arene and $\text{Hg}(\text{TFA})_2$ form a charge-transfer complex that undergoes photoinduced electron-transfer and back electron-transfer is minimized by dissociation of the radical anion $\text{Hg}(\text{TFA})_2^-$.



Equation (1.5)

Under these conditions, a number of substrates undergo mercuration in the aromatic ring;²¹ the detail of the mercuration will be discussed in Chapter 6.

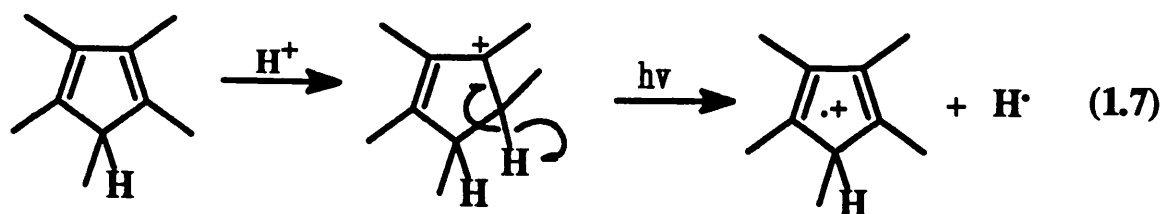
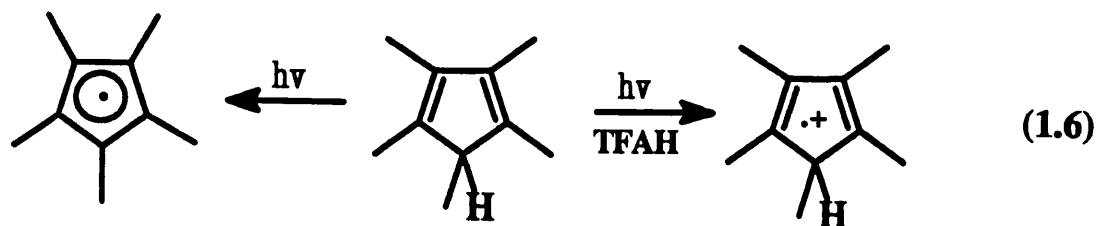
In an alternative procedure, which probably follows a similar mechanism, the arene is treated with $\text{Tl}(\text{TFA})_3/\text{TFAH}$; the charge transfer complex now involves the ion $\text{Tl}(\text{TFA})_2^+$.

A radical cation can be generated by electron-transfer from an electron rich donor (e.g. an arene) to a π -conjugated electron-acceptor (e.g. 2,3-dichloro-5,6-dicyanobenzoquinone (DDQ)), [see Chapter 2 for details].

Triarylamminium radical cation salts may be used as one-electron oxidants which remove an electron from a substrate. Tris(4-bromophenyl)aminium hexachloroantimonate, $(4\text{-BrC}_6\text{H}_4)_3\text{N}^+\text{SbCl}_6^-$, which is commercially available and the tris(2,4-dibromophenyl)aminium hexachloroantimonate²² is readily accessible.

An alternative potential route to radical cations is the protonation of a neutral radical. This technique has been already demonstrated in this research group. For example, photolysis of pentamethylcyclopentadiene ($\text{Me}_5\text{C}_5\text{H}$) under neutral conditions shows the e.s.r. spectrum of the pentamethylcyclopentadienyl radical, and it was predicted that the same procedure in TFAH should show the spectrum of the pentamethylcyclopentadiene radical cation²³ (equation 1.6).

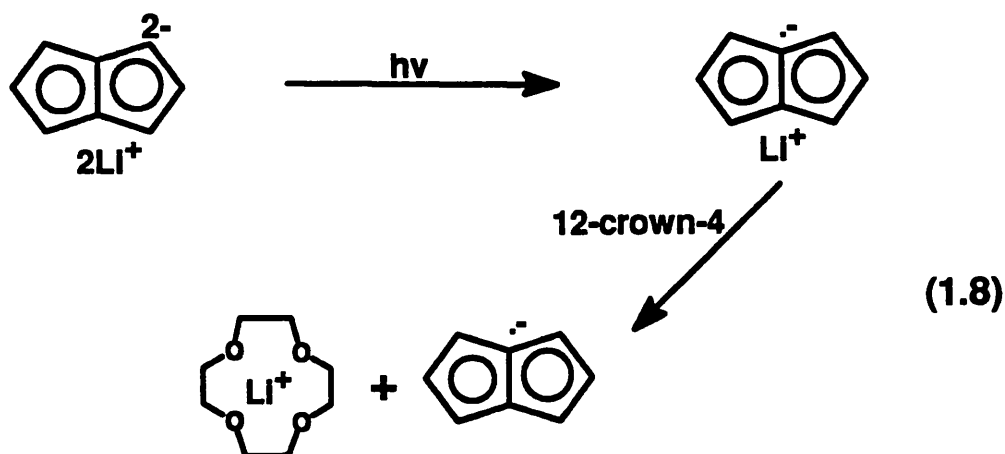
Indeed it does, but the mechanism seems to be oxidation of the substrate $\text{Me}_5\text{C}_5\text{H}$ by the photoexcited cation $\text{Me}_5\text{C}_5\text{H}_2^+$ (equation 1.7).



1.3. Counterion Coupling

The alkali metals all have nuclear spin, and frequently, radical anions show hyperfine coupling to an alkali metal counterion [^7Li (92.6%), ^{23}Na (100%), ^{39}K (93.1%), all with $I = 3/2$; ^{85}Rb (72.8%), $I = 5/2$; ^{87}Rb (27.2%), $I = 3/2$; ^{133}Cs (100%), $I = 7/2$.].

For example, irradiation of the dianion of dihydropentalene with u.v. light induces electron-transfer to the lithium cation, and the e.s.r. spectrum of the pentalene radical anion can be recorded. The spectrum consists of a quintet of triplets and each line is further split into a 1:1:1:1 quartet due to coupling with the lithium counter-ion;²⁴ if 12-crown-4 is added, this complexes the lithium cation and the coupling to the lithium counter-ion is broken (equation 1.8).



1.4. Interactions and Reactions

E.s.r. spectroscopy is a very sensitive technique in that the spectra can be recorded from solutions ca. $10^{-6}M$ in radicals. The spectrum of the radical anion or cation which is observed will be that of the compound in solution with the highest electron affinity and or lowest ionisation energy respectively. If impurities have a lower ionisation energy than the principal substrate, this can cause misleading results when radical cations are generated. For example, tetraphenylene prepared from the thermolysis of biphenylene continues to show the e.s.r. spectrum of the biphenylene radical cation until it is purified by chromatography.

Another phenomenon we must beware of is the interactions and reactions which the radical ions may undergo in solution. These are rare with radical anions, but common with radical cations.

The most common example is the charge-transfer interaction between a radical cation ($ArH^{\cdot+}$) and its precursor (ArH), which is illustrated in equation (1.9).

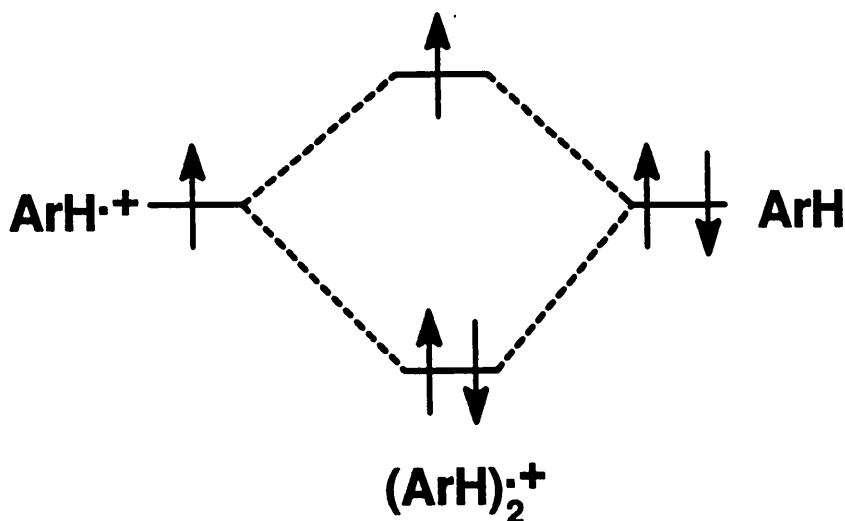
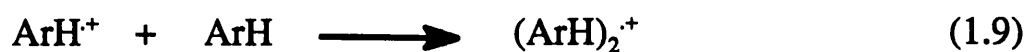
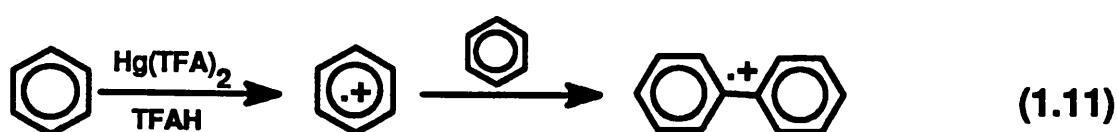
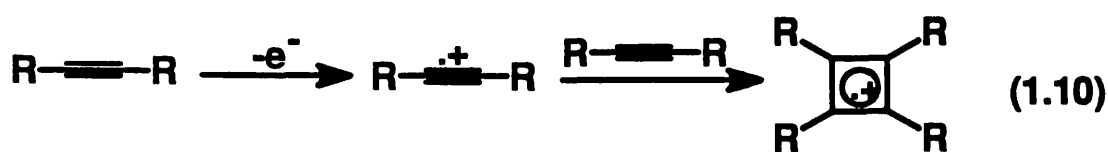


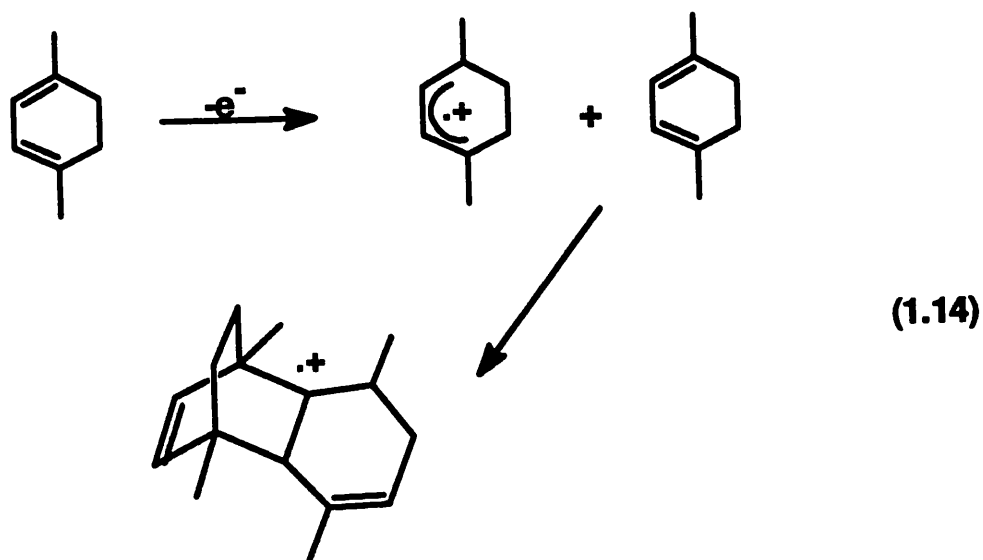
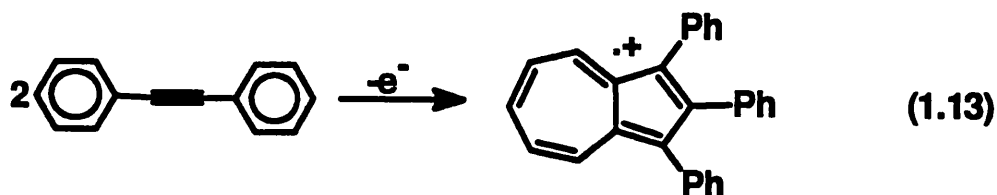
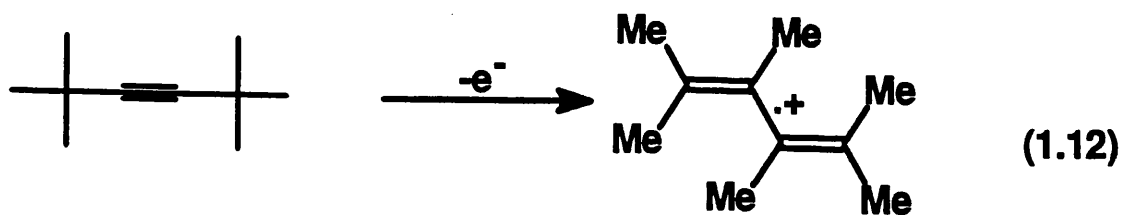
Figure 1.2. Frontier orbital interaction of $ArH^{\cdot+}$ and ArH .

For example, the structure of the anthracene dimer radical cation showed two anthracene molecules which are apparently held in eclipsing positions.²⁵ This phenomenon can be understood in terms of the interaction between the S.O.M.O. of the radical cation and the H.O.M.O. of the precursor. The electron is equally shared between the two molecules as illustrated in Figure 1.2, and the spectrum shows hyperfine coupling to twice the number of protons of each type, at approximately half the coupling constant show by ArH^+ . For example, the benzene radical cation with $\underline{a}(6\text{H})$ 4.44 G forms $(\text{C}_6\text{H}_6)_2^+$ with $\underline{a}(12\text{H})$ 2.16 G, and the anthracene radical cation with $\underline{a}(2\text{H})$ 6.47 G, $\underline{a}(4\text{H})$ 3.08 G, $\underline{a}(4\text{H})$ 1.38 G forms $(\text{C}_{10}\text{H}_{10})_2^+$ with $\underline{a}(4\text{H})$ 3.25 G, $\underline{a}(8\text{H})$ 1.42 G, $\underline{a}(8\text{H})$ 0.71 G.

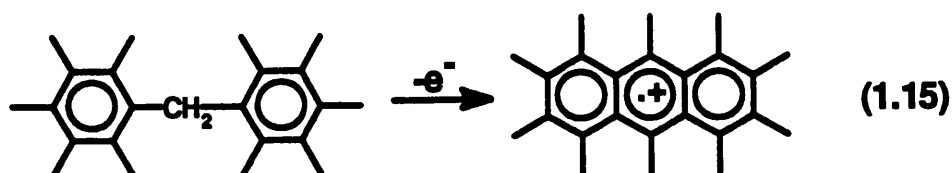
The dimers $(\text{ArH})_2^+$ may interact further by covalent bonding and leading to the formation of a secondary radical cations. For example, dialkylacetylene radical cations react with their parent molecules to give tetraalkylcyclobutene radical cations²⁶ (equation 1.10), and treatment of benzene with $\text{Hg}(\text{TFA})_2/\text{TFAH}$ leads to the radical cation of biphenyl²⁷(equation 1.11).



Radical cations may also be formed with intramolecular rearrangement. The detailed mechanism of the rearrangement involved is often not clear as to whether this occurs through a cation or radical cation. Thus di-*tert*-butyl acetylene with aluminium trichloride in CH_2Cl_2 shows the e.s.r. spectrum of the hexamethylbutadiene radical cation²⁸ (equation 1.12), diphenyl acetylene shows the spectrum of the triphenylazulene radical cation²⁹ (equation 1.13), and 1,4-dimethylcyclohexene shows the spectrum of the radical cation of the tricyclic Diels-Alder adduct between the precursor and the 1,4-dimethylcyclohexene radical cation³⁰ (equation 1.14).



Sometimes, this kind of the rearrangement can mislead the interpretation, for example, Kochi³¹ reported the e.s.r. spectrum of bis(pentamethylphenyl)methane radical cation derived from oxidation of the parent molecule, but actually, the spectrum is due to the octmethylanthracene radical cation^{32,33} formed from a complex rearrangement (equation 1.15).



1.5. Electron Spin Resonance Spectroscopy

1.5.1. Theory

Electron spin resonance (e.s.r.) spectroscopy is a powerful tool for probing the properties of a singly occupied molecular orbital (S.O.M.O.). E.s.r. is particularly important because of its high specificity for detecting, identifying and monitoring reactive paramagnetic intermediates in chemical reactions.

An electron has an intrinsic angular momentum called spin, just like a proton. The electron has two energy states ($M_s = +\frac{1}{2}$ and $M_s = -\frac{1}{2}$). In the absence of an external magnetic field, these two energy states are degenerate. Upon application of an external magnetic field, these energy states are no longer degenerate and establish a separation between the two energy states (ΔE), which is proportional to the strength of the applied external magnetic field (Figure 1.3).

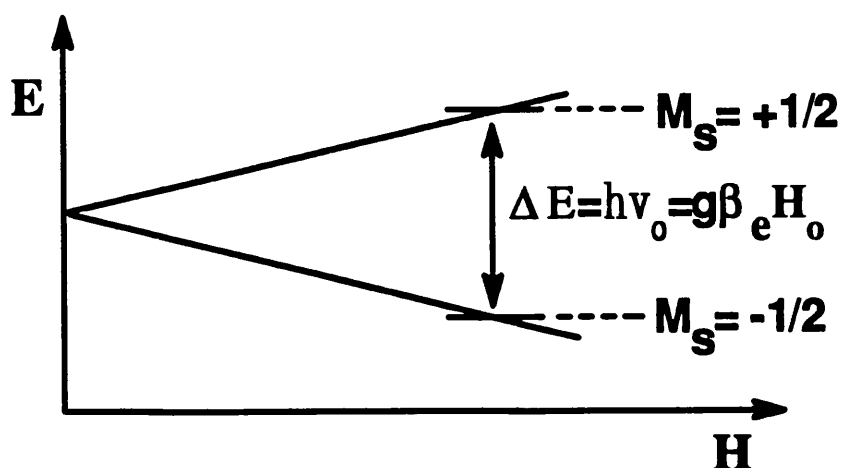


Figure 1.3. Energy states of an electron in an applied external magnetic field.

Transitions from one energy level to the other, in which the electron changes its spin state, occur when the system is exposed to electromagnetic radiation with a resonance frequency ν_0 . This frequency ν_0 is determined by the resonance condition and is described by equation 1.16:

$$\Delta E = h\nu_0 = g\beta_e H_0 \quad (1.16)$$

where h is Planck's constant, β_e is a constant called the Bohr magneton, H_0 is the strength of the applied magnetic field, and g is a constant called the g -factor ($g = 2.0023$ for a free electron).

1.5.2. Hyperfine coupling constants

The coupling constant to the α -hydrogen of a neutral radical (or radical ion), $\underline{a}(H_\alpha)$, is directly proportional to the spin density, $\rho_{C\alpha}$, on the α -carbon atom, C_α , adjacent to the α -hydrogen and is described by the McConnell³⁴ equation (equation 1.17).

$$\underline{a}(H_\alpha) = \rho_{C\alpha} Q \quad (1.17)$$

Q is the proportionality constant known as the McConnell constant.

The spin density ρ_i is the difference between two electron densities $\rho_i(\alpha)$ and $\rho_i(\beta)$ relating to electrons differing in their spin quantum number M_s (equation 1.18).

$$\rho_i = \rho_i(\alpha) - \rho_i(\beta) \quad (1.18)$$


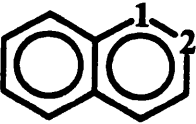
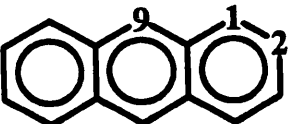
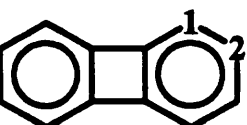
ρ_i is the spin density in the region i of the molecule and $\rho_i(\alpha)$ is the density of electrons with $M_s = +\frac{1}{2}(\alpha)$ and $\rho_i(\beta)$ is the density of electron with $M_s = -\frac{1}{2}(\beta)$.

Considering the methyl radical, the hyperfine coupling of the α -hydrogen arises by the *spin polarisation* mechanism with $\underline{a}(H_\alpha) = -23.04$ G. As shown in Figure 1.4, the unpaired electron in the $2p_z$ orbital interacts with the two bonding electrons in the (C-H) σ -bond. According to Hund's rule of maximum multiplicity, the electron near the carbon

nucleus has the same spin as that of the unpaired electron and the electron close to the hydrogen nucleus has opposite spin, thus there is a negative spin density on the α -hydrogen [$\rho_{C\alpha}(\beta) > \rho_{C\alpha}(\alpha)$] and the coupling is negative.

The literature shows that there is a variation in the constant Q between corresponding radical anions and cations. The pairing theorem³⁵⁻³⁷ states that, in a given alternant hydrocarbon, the spin densities for the corresponding positions in the radical anion and cation should be identical. The hyperfine coupling constants for the radical cation are usually larger than those of the corresponding radical anion which implies the constant Q depends on the charge concentration in the singly occupied p-orbital at the carbon atom.^{38,39} Table 1.2 illustrates a comparison of radical ion hyperfine coupling constants of some alternant hydrocarbons.

Table 1.2: Proton coupling constants in some alternant hydrocarbon radical ions.

Radical ions of	P	$\underline{a}(\text{H}_p)/G$ for ArH^+	$\underline{a}(\text{H}_p)/G$ for ArH^-
	1	4.43	3.75
	1	5.54	4.95
	2	2.06	1.87
	1	3.06	2.74
	2	1.38	1.51
	9	6.53	5.34
	1	0.21	0.21
	2	3.69	2.86

Hyperfine coupling to β -hydrogens is usually larger than to the α -hydrogens, for example in the ethyl radical, CH_3CH_2 ; $\underline{a}(2\text{H}_\alpha) = 22.2$ G and $\underline{a}(3\text{H}_\beta) = 26.9$ G. The β -

hydrogen coupling constant is due partly to the spin polarisation mechanism (Figure 1.5a), but mainly to *hyperconjugation* (Figure 1.5b).

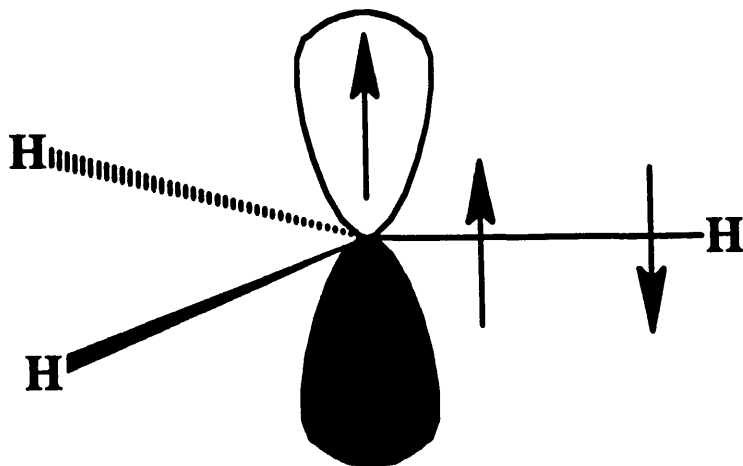


Figure 1.4.: The spin polarisation of a methyl radical.

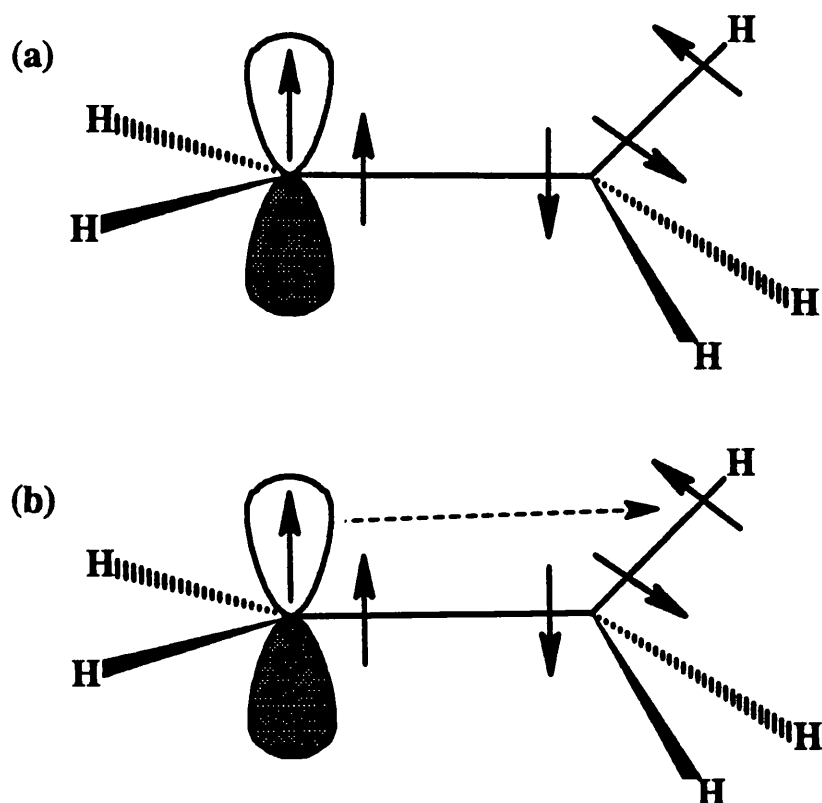


Figure 1.5. A qualitative representation of (a) spin polarisation and (b) hyperconjugation involving spin transfer from the singly occupied 2p-orbital to the C_{β} - H_{β} bond in the ethyl radical.

The β -hydrogen coupling constant, $\underline{a}(\text{H}_\beta)$, can be described by the Heller-McConnell⁴⁰ equation (equation 1.19).

$$\underline{a}(\text{H}_\beta) = \rho_{\text{C}\alpha}(\text{A} + \text{B}\cos^2\theta) \quad (1.19)$$

θ is the dihedral angle between the singly occupied p-orbital and the β -CH bond as shown in Figure 1.6, and A (*ca.* 1 G) and B (*ca.* 54 G) are constants relating to the spin polarisation and hyperconjugation respectively.

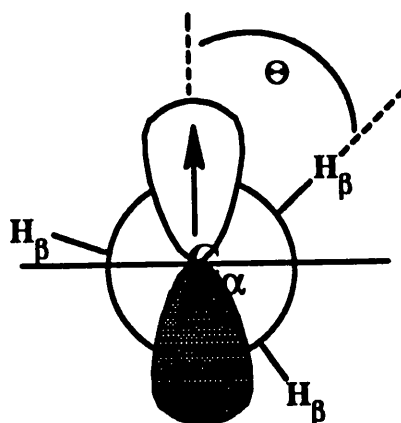


Figure 1.6. Orientation of the methyl group in an ethyl radical.

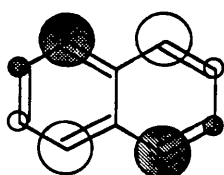
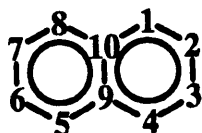
1.5.3. Molecular orbital calculations

Hückel molecular orbital (H.M.O.) theory⁴¹ provides the simplest method for calculating the π -electron density at the carbon atoms in the π -system which sometimes can facilitate the interpretation of the e.s.r. spectra of the radicals.

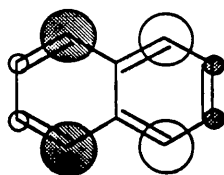
Alternant π -systems have a particular advantage, because the H.M.O. spin densities c^2 (c = Hückel coefficient) at the carbon atoms will then be the same in the radical anion and cation. Since the coupling constants of radical anions are smaller than those of the corresponding radical cations, the constant Q for radical anions is smaller than that for radical cations.

This principle can be illustrated by applying H.M.O. theory to the naphthalene radical anion and cation (Figure 1.7 and Table 1.3). This prediction can be improved by a more advanced McLachlan⁴² treatment.

Consider the orbitals of the naphthalene radical cation (Ψ_5) and anion (Ψ_6).



$$\Psi_5 = 0.425\phi_1 + 0.263\phi_2 - 0.263\phi_3 - 0.425\phi_4 + 0.425\phi_5 + 0.263\phi_6 - 0.263\phi_7 - 0.425\phi_8 + 0.0\phi_9 + 0.0\phi_{10}$$



$$\Psi_6 = 0.425\phi_1 - 0.263\phi_2 - 0.263\phi_3 + 0.425\phi_4 - 0.425\phi_5 + 0.263\phi_6 + 0.263\phi_7 - 0.425\phi_8 + 0.0\phi_9 + 0.0\phi_{10}$$

Figure 1.7. Molecular orbitals of naphthalene radical ions.

Positions	c^2	$\underline{a}(\text{H})/\text{G}$ for ArH^-		$\underline{a}(\text{H})/\text{G}$ for ArH^+	
		(Exp.)	(Cal.)	(Exp.)	(Cal.)
1,4,5,8	0.181	4.95	4.07	5.54	4.82
2,3,6,7	0.069	1.87	1.55	2.06	1.84

Table 1.3: Comparison of calculated and experimental values of the hyperfine coupling constant for the naphthalene radical anion and cation.

References

1. D. Lipkin, D.E. Paul, J. Yournsend and S.T. Weissman, *Science*, 1953, **117**, 534.
2. B. Venkatarman and G.K. Fraenkel, *J. Am. Chem. Soc.*, 1955, **77**, 2707; *J. Chem. Phys.*, 1955, **23**, 588.
3. F. Gerson, *High Resolution E.S.R. Spectroscopy*, Wiley-Verlag Chemie, Weinheim, 1970.
4. E.T. Kaiser and L. Kevan, *Radical ions*, Interscience, New York, 1968.
5. Landolt-Börnstein, Numerical Data and Functional Relationships in Science and Technology, 1965, Vol. II/1; 1980, Vol. II/9d1; 1980, Vol. II/9d2; 1988, Vol. II/17f; 1990, Vol. II/17h.
6. L. Kevan and L.D. Kispert, *Electron Spin Double Resonance Spectroscopy*, Wiley, New York, 1976.
7. M.C.R. Symons, *Chem. Soc. Rev.*, 1984, **13**, 393.
8. E. Roduner, L-M. Wu, R. Crockett and C.J. Rhodes, *Catal. Lett.*, 1992, 373.
9. A.G. Davies and J.L. Courtneidge, *Acc. Chem. Res.*, 1987, **20**, 90.
10. A.G. Davies and A.G. Neville, *J. Organomet. Chem.*, 1992, **436**, 255.
11. A.G. Davies and C.J. Shields, *J. Chem. Soc. Perkin Trans. 2*, 1989, 1001.
12. J.L. Courtneidge, A.G. Davies, C.J. Shields and S.N. Yazdi, *J. Chem. Soc., Perkin Trans. 2*, 1988, 799.
13. L. Ebersson and F. Radner, *Act. Chem. Scand.*, 1992, **46**, 630.
14. I.C. Lewis and L.S. Singer, *J. Chem. Phys.*, 1965, **43**, 2712.
15. R.M. Dessau, S. Shih and E.I. Heiba, *J. Am. Chem. Soc.*, 1970, **92**, 412.
16. W.T. Dixon and D. Murphy, *J. Chem. Soc., Perkin Trans. 2*, 1976, 1823.
17. W. Lau, J.C. Huffman and J.K. Kochi, *J. Am. Chem. Soc.*, 1982, **104**, 5515.
18. I.H. Elson and J.K. Kochi, *J. Am. Chem. Soc.*, 1984, **106**, 7100.
19. F.A. Neugebauer, S. Bamberger and W.R. Groh, *Chem. Ber.*, 1975, **108**, 2406.

20. X-K. Jiang, C-X. Zhao and Y-F. Gong, *J. Phys. Org. Chem.*, 1991, 4, 1.
21. A.G. Davies and D.C. McGuchan, *Organometallics*, 1991, 10, 329.
22. W. Schmidt and E. Stechan, *Chem. Ber.*, 1980, 113, 577.
23. J.L. Courtneidge, A.G. Davies, C.J. Shieids and S.N. Yazdi, *J. Chem. Soc., Perkin Trans. 2*, 1988, 799.
24. D. Wilhelm, J.L. Courtneidge, T. Clark and A.G. Davies, *J. Chem. Soc., Chem. Commun.*, 1984, 810.
25. F. Gerson, *Topics in Current Chem.*, 1983, 115, 57.
26. J.L. Courtneidge, A.G. Davies, E. Lusztzk and J. Lusztzyk, *J. Chem. Soc., Perkin Trans. 2*, 1984, 155.
27. T. Clark, J.L. Courtneidge, A.G. Davies, and D. Wilhelm, *J. Chem. Soc., Perkin Trans. 2*, 1984, 1197.
28. J.L. Courtneidge and A.G. Davies, *J. Chem. Soc., Chem. Commun.*, 1984, 136.
29. C.J. Cooksey, J.L. Courtneidge, A.G. Davies, P.S. Gregory, J.C. Evans and C.C. Rowlands, *J. Chem. Soc., Perkin Trans. 2*, 1988, 807.
30. A.G. Davies and R. Hay-Motherwell, *J. Chem. Soc., Perkin Trans. 2*, 1988, 2099.
31. S. Sankararaman, W. Lau and J.K. Kochi, *J. Chem. Soc., Chem. Commun.*, 1991, 396.
32. L. Ebersson and F. Radner, *J. Chem. Soc., Chem. Commun.*, 1991, 1233.
33. R. Sebastiano, J.D. Korp and J.K. Kochi, *J. Chem. Soc., Chem. Commun.*, 1991, 1481.
34. H.M. McConnell and D.B. Chestnut, *J. Chem. Phys.*, 1958, 28, 107.
35. C.A. McDowell and J.R. Rowlands, *Canad. J. Chem.*, 1960, 38, 503.
36. A. Carrington and J. dos Santos-Viega, *Mol. Phys.*, 1962, 5, 288.
37. J.R. Bolton, P.R. Hindle and J. dos Santos-Viega, *J. Chem. Phys.*, 1968, 48, 4703.
38. J.R. Bolton, *J. Chem. Phys.*, 1965, 43, 309.

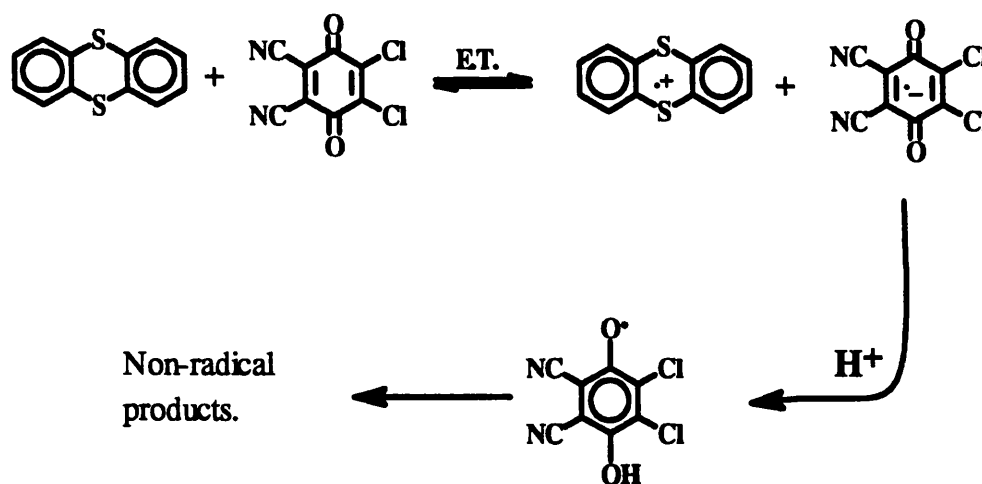
39. J.P. Colpa and J.R. Bolton, *Mol. Phys.*, 1963, **6**, 273.
40. C. Heller and H.M. McConnell, *J. Chem. Phys.*, 1960, **32**, 1535.
41. A. Streitwieser Jnr., *Molecular Orbital Theory for Chemists*, J. Wiley and Sons, Inc., New York, 1961.
42. A.D. McLachlan, *Mol. Phys.*, 1960, **3**, 233.

Chapter 2. DDQ Method for Generating Some Unusual Radical Cations.

2.1. Background.

There is much current interest in experimental and theoretical aspects of radical cation chemistry¹ as has been described in Chapter 1. A number of techniques are available for observing the e.s.r. spectra of radical cations in fluid solution. Nevertheless, we still have amassed a number of compounds for which all of these methods has failed, including treatment with H_2SO_4 , $\text{CF}_3\text{CO}_2\text{H}$, $\text{FSO}_3\text{H}/\text{SO}_2$, $\text{Hg}(\text{TFA})_2$, and $\text{Tl}(\text{TFA})_3$, and triarylamminium radical cations. In most cases, the electron transfer may be assisted by photolysis, and there is still a constant search for better procedures for generating radical cations.

We have been interested in observing the e.s.r. spectra of the benzo-crown ethers for a long time, because this should provide a way of studying conformational change in the crown ether rings and the interaction with metal ions.



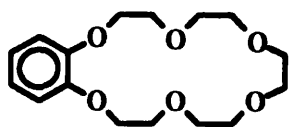
Scheme 2.0. Formation of thianthrene radical cation.

At the suggestion of Professor Lennart Eberson (Lund), we have followed up some work of Handoo and Gadru² who showed that a mixture of thianthrene (2.0) and 2,3-

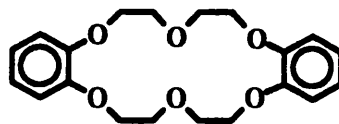
dichloro-5,6-dicyano-1,4-benzoquinone (DDQ) in dichloromethane with a few drops of trifluoroacetic acid gave the e.s.r. spectrum of the thianthrene radical cation (2.0)⁺. It appears that electron transfer gives the thianthrene radical cation and DDQ radical anion, and back electron transfer is prevented by the rapid protonation of the DDQ radical anion (Scheme 2.0).

Thianthrene is very readily oxidised, and this technique does not work for our problem compounds.

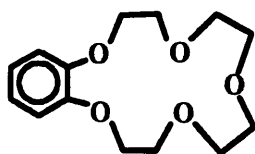
We report here an e.s.r. study of the formation of radical cations by an extension of this technique, using trifluoroacetic acid containing DDQ with photolysis, and if necessary, a stronger acid (such as CF₃SO₃H or MeSO₃H).



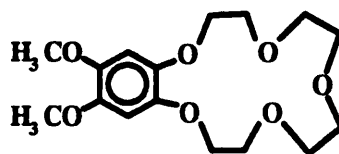
(2.4)



(2.6)



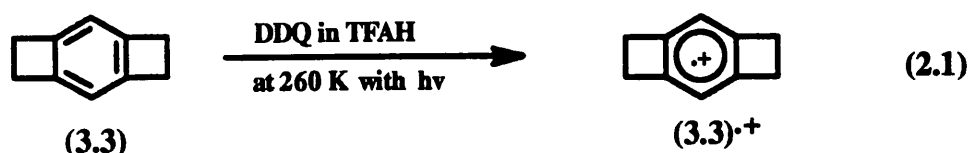
(2.5)



(2.5)

2.2. Results.

2.2.1. Benzo[1,2:4,5]dicyclobutene (3.3)

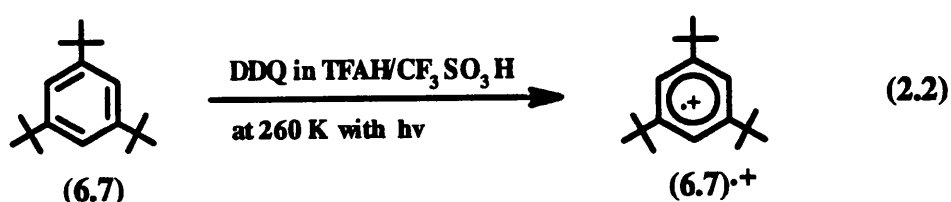


A number of different methods have been tried to generate the (3.3) radical cation, but all failed; these included the systems $\text{Ti}(\text{TFA})_3/\text{TFAH}$, $\text{Hg}(\text{TFA})_2/\text{TFAH}$ and $\text{FSO}_3\text{H}/\text{SO}_2$.

When compound (3.3) was dissolved in trifluoroacetic acid containing DDQ at 260 K it gave deep blue-purple solution. No e.s.r. spectrum was observed without photolysis. If this sample was irradiated with strong unfiltered U.V. light, an e.s.r. spectrum of the benzo[1,2:4,5]dicyclobutene radical cation (3.3)^{•+} was recorded, with $a(8\text{H})$ 14.25 G, $a(2\text{H})$ 0.93 G, g 2.0026.

The e.s.r. spectrum disappeared when the U.V. light was cut off, but the same spectrum reappeared when the photolysis was resumed.

2.2.2. 1,3,5-Tri-*tert*-butylbenzene (6.7)



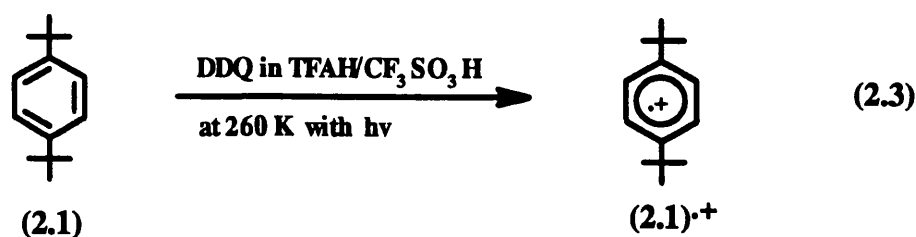
The e.s.r. spectrum of the 1,3,5-tri-*tert*-butylbenzene radical cation (6.7)^{•+} [$a(3\text{H})$ 5.17 G and $a(27\text{H})$ 0.65 G] has been observed previously by Dessau and Shih³, and by Davies and McGuchan⁴, who oxidised (6.7) with cobaltic trifluoroacetate in trifluoroacetic acid in a rapid mixing flow system at room temperature, and by photolysis of the solution in trifluoroacetic acid containing mercury(II) trifluoroacetate at 260 K, respectively.

The compound (6.7) failed to show the spectrum of the radical cation by treatment

with other oxidants (e.g. $\text{AlCl}_3/\text{CH}_2\text{Cl}_2$, $\text{Ti}(\text{TFA})_3/\text{TFAH}$, $\text{FSO}_3\text{H}/\text{SO}_2$).

When compound (6.7) was dissolved in trifluoroacetic acid containing DDQ at 260 K it gave a yellowish solution. We could not observe any e.s.r. spectrum of $(6.7)^+$, with or without photolysis. If a few drops of trifluoromethane sulphonic acid were added to the sample containing (6.7) and DDQ in TFAH at 260 K it gave a yellowish solution. A strong e.s.r. spectrum of $(6.7)^+$ was observed when this sample was irradiated with 30% U.V. light. Again, the formation of the radical cation was dependent on photolysis.

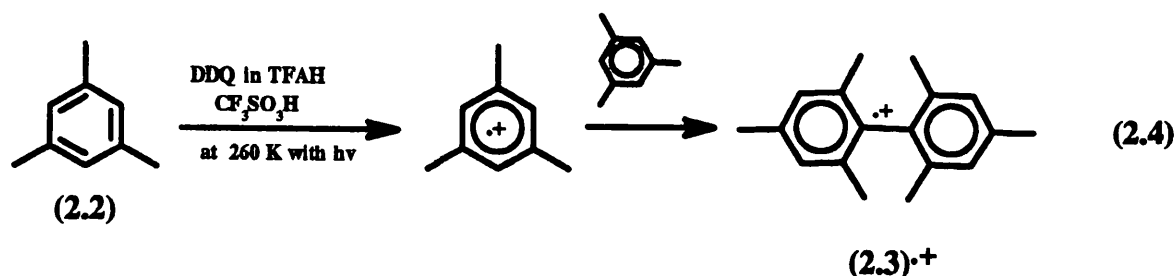
2.2.3. 1,4-Di-*tert*-butylbenzene (2.1)



The 1,4-di-*tert*-butylbenzene radical cation $(2.1)^{\bullet+}$ spectrum has been observed previously only in trifluoroacetic acid containing cobaltic ion in a flow system.³

If a few drops of $\text{CF}_3\text{SO}_3\text{H}$ was added to a solution of compound (2.1) in trifluoroacetic acid containing DDQ at 260 K it gave yellowish solution that showed the e.s.r. spectrum of the radical cation $(2.1)^{\bullet+}$ with $\underline{a}(4\text{H})$ 0.94 G and $\underline{a}(18\text{H})$ 1.89 G, and g 2.0024, without photolysis. The best spectrum of $(2.1)^{\bullet+}$ was recorded when the sample was photolysed with 10% U.V. light (Figure 2.1).

2.2.4. Mesitylene (2.2)



A deep blue-purple solution was formed, when mesitylene (2.2) was added to a solution of trifluoroacetic acid containing DDQ, together with a few drops of $\text{CF}_3\text{SO}_3\text{H}$ at 260 K. In the dark, this solution gave no e.s.r. spectrum. If this solution was irradiated

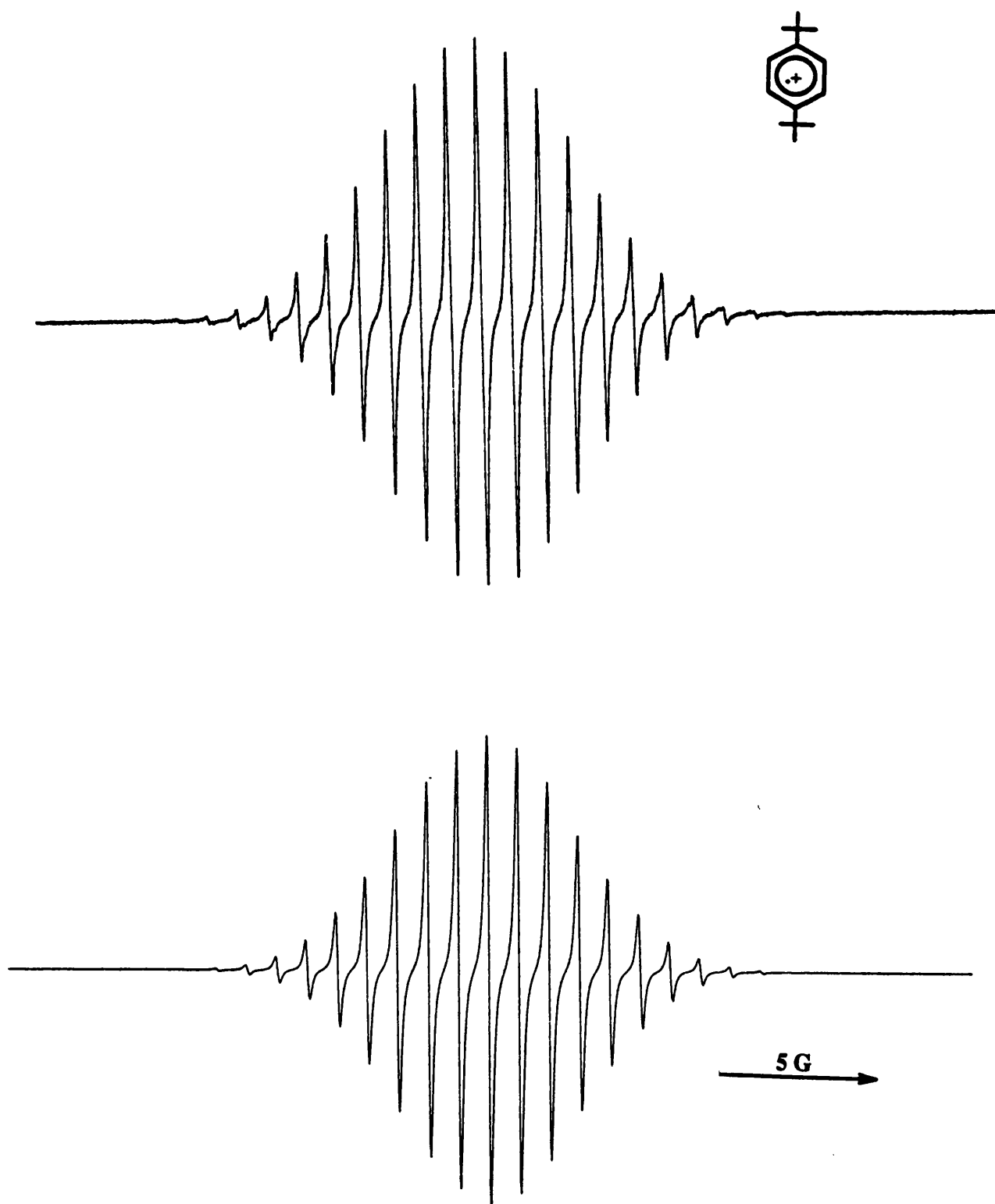


Figure 2.1. E.s.r. spectrum (top) and simulation (bottom) of the 1,4-di-*tert*-butylbenzene radical cation (2.1)⁺ in DDQ-TFAH-CF₃SO₃H at 260 K.

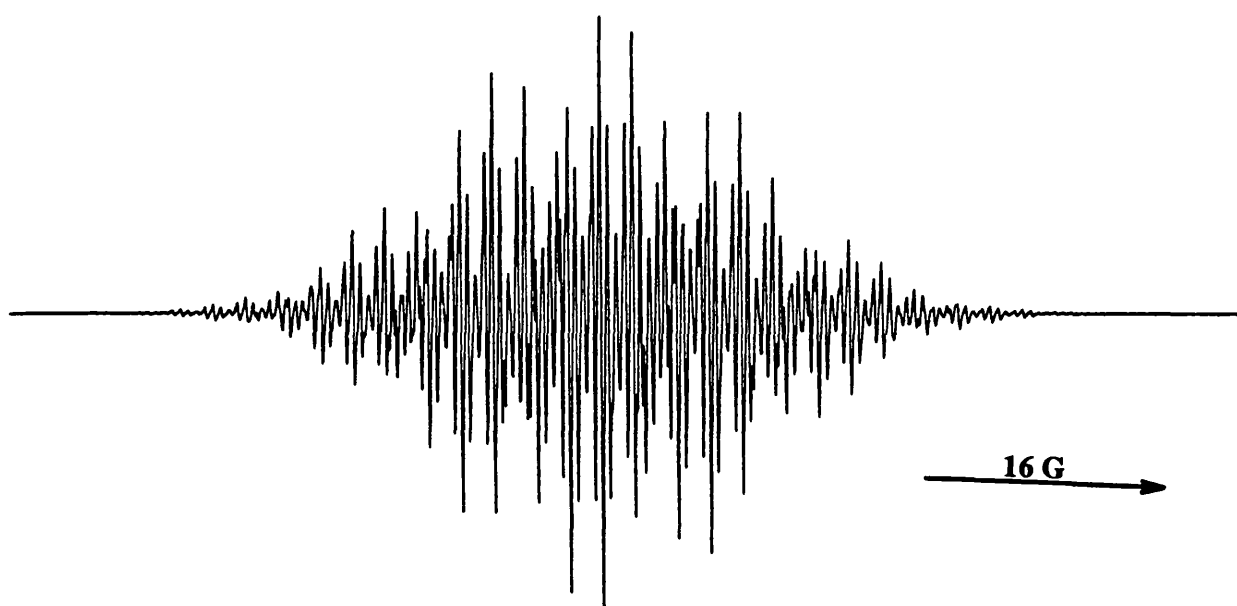
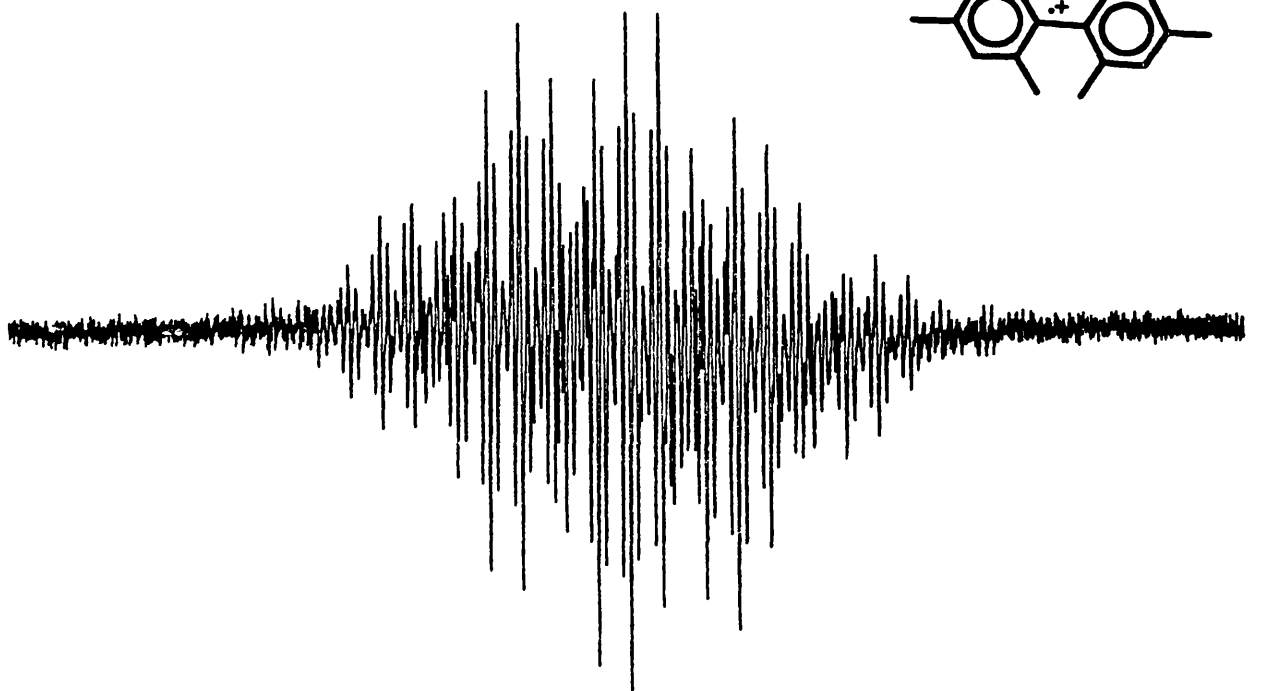
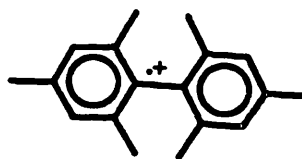


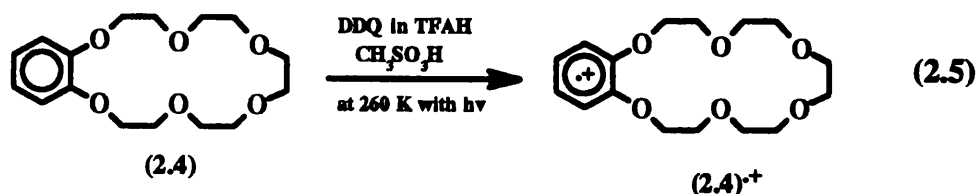
Figure 2.2. E.s.r. spectrum obtained from mesitylene (2.2) in DDQ-TFAH-CF₃SO₃H at 260 K showing (2.3)⁺ (top) and simulation (bottom).

with 10% U.V. light filtered through Pyrex it showed the spectrum which is illustrated in Figure 2.2, with $\underline{a}(6\text{H})$ 6.99 G, $\underline{a}(12\text{H})$ 2.10 G and $\underline{a}(4\text{H})$ 0.503 G, and g 2.0026.

We assign the spectrum in Figure 2.2 to the 2,4,6,2',4',6'-hexamethylbiphenyl radical cation (2.3)⁺. The same spectrum had been reported by Ishizu and his co-workers when compound (2.3) was treated with $\text{SbCl}_5/\text{CH}_2\text{Cl}_2$.⁵

The compound (2.3)⁺ is probably formed in the same way as biphenyl radical cation is formed from benzene, as described in Chapter 1. Presumably, with mesitylene (2.3), the mesitylene radical cation is first formed, which then reacts rapidly with a further mesitylene. Compound (2.3) has been reported to be formed from the parent mesitylene in trifluoroacetic acid containing cobaltic ion.⁶

2.2.5. Benzo-18-crown-6 (2.4)



This is the first time that the e.s.r. spectrum of a benzo-crown ether radical cation has been observed.

When benzo-18-crown-6 (2.4) was dissolved in a solution of trifluoroacetic acid containing DDQ and a few drops of methanesulphonic acid at 260 K, it gave a yellowish solution. If this solution was irradiated with 30% U.V. light at 307 K it showed the spectrum in Figure 2.3b, with $\underline{a}(2\text{H})$ 4.95 G and $\underline{a}(4\text{H})$ 3.97 G and any coupling to the 2 protons at the *para*-aromatic position was lost in the linewidth [ΔH_{pp} 0.66 G]; g 2.0036. The spectrum 2.3b can be simulated reasonably well in terms of the above hyperfine coupling constants (Figure 2.3c). The unpaired electron is localised mainly in the Ψ_A molecular orbital of the benzene ring and is showing large interaction with the aromatic protons at the 4- and 5- positions and the methylene protons close to the aromatic ring. These values are similar to those of the 1,2-dimethoxybenzene radical cation (5.10)⁺, which shows $\underline{a}(6\text{H})$ 3.33 G, $\underline{a}(2\text{H})$ 0.16 G and $\underline{a}(2\text{H})$ 4.89 G, and g 2.0037.

At lower temperature the spectrum shows a strong alternating linewidth effect

associated with the development of conformational non-equivalence of these methylene protons on the e.s.r. time scale (Figure 2.3a).

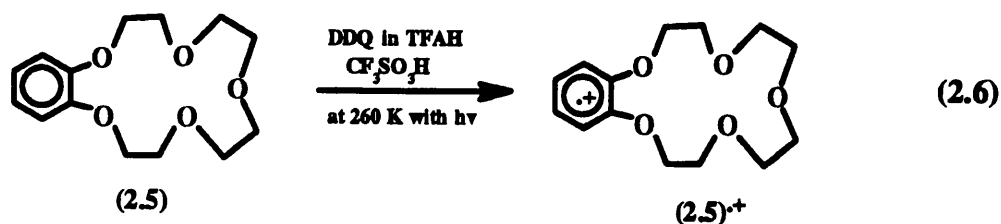
The problem with this technique is the solvent: trifluoroacetic acid freezes at 258 K, and it is not suitable for low temperature studies.

A number of alternative solvents were tested, such as dichloromethane, 1,3-dichloropropane and propanoic acid which might allow studies at lower temperature. Unfortunately, all these attempts gave rise to complicated e.s.r. spectra which could not be analysed. The cause of this complication is probably the formation of ring opened species.

If sodium acetate is added to the solution, there is little change of the spectrum above room temperature, but the upper limit of the conformational changes occur at about 10°C higher than before. This implies that the inclusion of the sodium cation in the crown ether ring renders the ring more rigid. These effects are parallel to those which can be observed by N.M.R. spectroscopy.⁷

We have found the metal ions (Na^+ , K^+) also stabilise the crown ether radical cation. Above about 323 K, the $(2.4)^+$ spectrum changes irreversibly to a more complicated spectrum which we have not yet been able to interpret in detail, but we believe to be associated with loss of proton and/or ring opening. However, if metal ions are present these changes do not occur until significantly higher temperatures ($\approx 10\text{-}15^\circ\text{C}$).

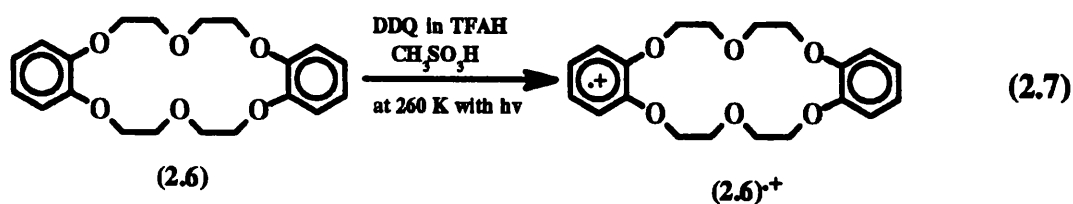
2.2.6. Benzo-15-crown-5 (2.5)



The e.s.r. spectra of the radical cation of benzo-15-crown-5 $(2.5)^+$ can be observed by irradiating a solution of compound (2.5) in trifluoroacetic acid containing DDQ. At 317 K this solution gives the spectrum which is illustrated in Figure 2.4b with $\underline{a}(4\text{H})$ 4.15 G, $\underline{a}(2\text{H})$ 4.97 G and ΔH_{pp} 0.48 G, and g 2.0035, which implies that the S.O.M.O. of the benzo-15-crown-5 radical cation $(2.5)^+$ has the Ψ_A configuration.

At 260 K, the spectrum of (2.5)⁺ shows a similar alternating linewidth effect which is illustrated in the spectrum 2.4a. Again, the solvent (TFAH) did not allow low temperature studies. Again, both Na⁺ and K⁺ ions stabilised the radical cation.

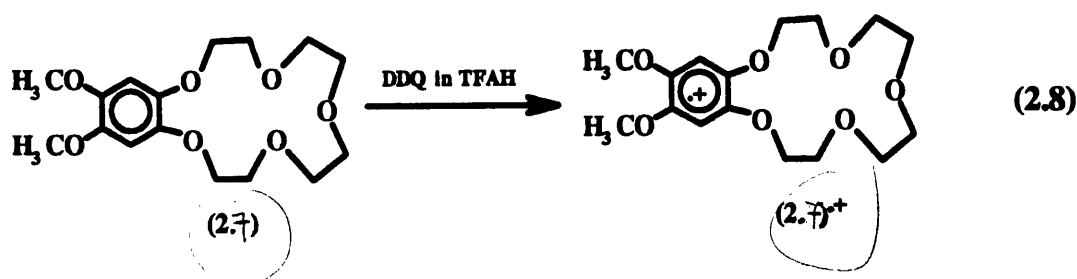
2.2.7. Dibenzo-18-crown-6 (2.6)



The best e.s.r. spectrum of the dibenzo-18-crown-6 radical cation (2.6)⁺ was obtained when a solution containing compound (2.6), DDQ, and MeSO₃H in TFAH was irradiated with 100% Pyrex-filtered U.V. light at 260 K. The spectrum which is illustrated in Figure 2.5 shows the familiar spectrum of the *o*-benzo-crown ether moiety and shows that the unpaired electron is localised mainly on one benzene ring with the Ψ_A configuration. If the temperature of the sample was raised above about 273 K, the spectrum changed irreversibly.

If sodium acetate or potassium acetate was added to the solution, the radical cation (2.6)⁺ was stable up to about 288 K.

2.2.8. 4,5-Dimethoxybenzo-15-crown-5 (2.7)



In the dark, 4,5-dimethoxybenzo-15-crown-5 (2.7) in trifluoroacetic acid containing DDQ gave rise to a strong e.s.r. spectrum of (2.7)⁺. The spectrum at 319 K, is shown in the Figure 2.6c, with $\underline{a}(4H)$ 2.74 G, $\underline{a}(6H)$ 2.24 G, $\underline{a}(2H)$ 0.92 G and $\underline{a}(4H)$ 0.08 G.

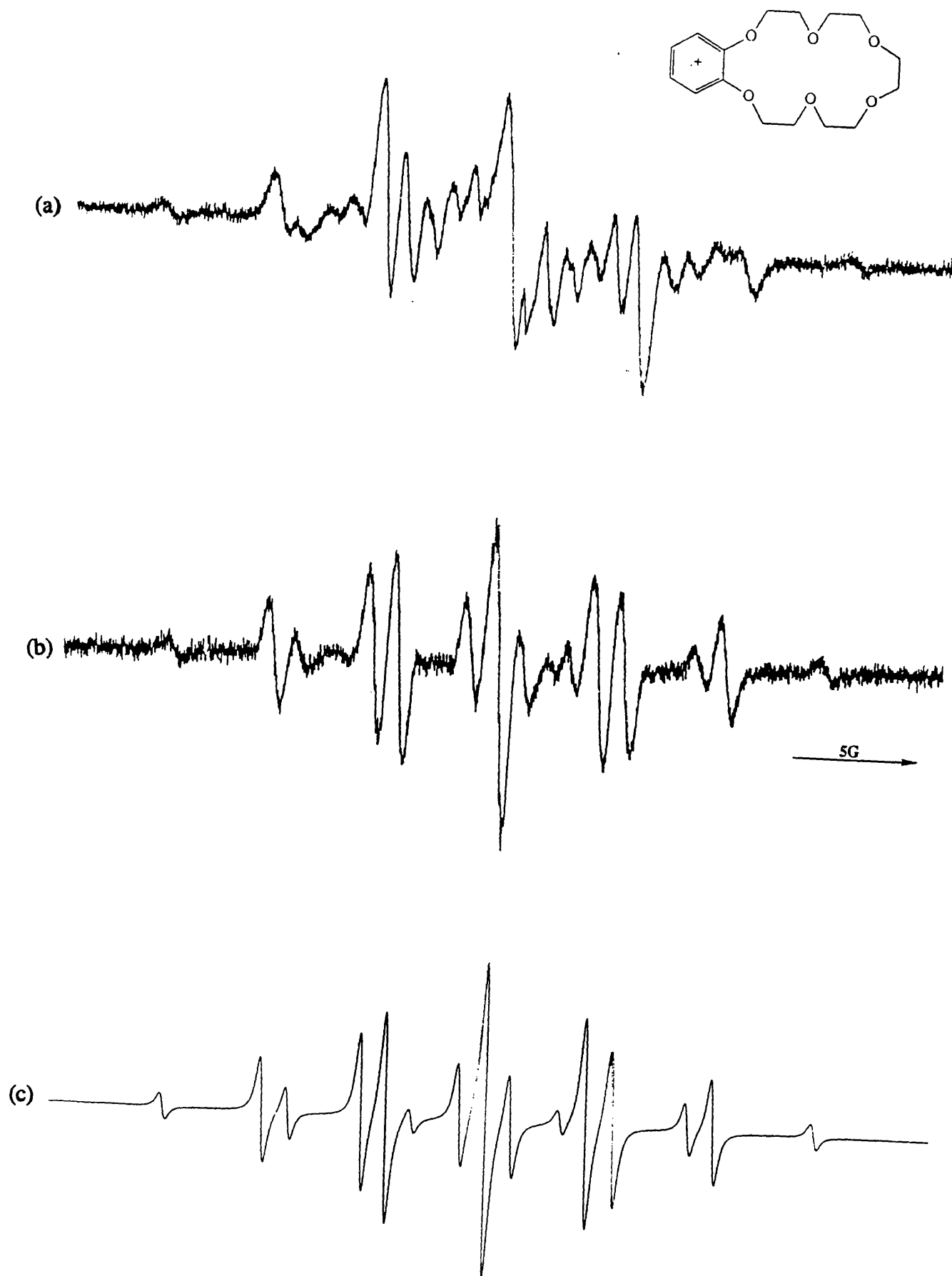


Figure 2.3. E.s.r. spectra of the benzo-18-crown-6 radical cation (2.4)⁺ in DDQ-TFAH-MeSO₃H at (a) 260 K, (b) 307 K and (c) simulation of spectrum 2.3b.

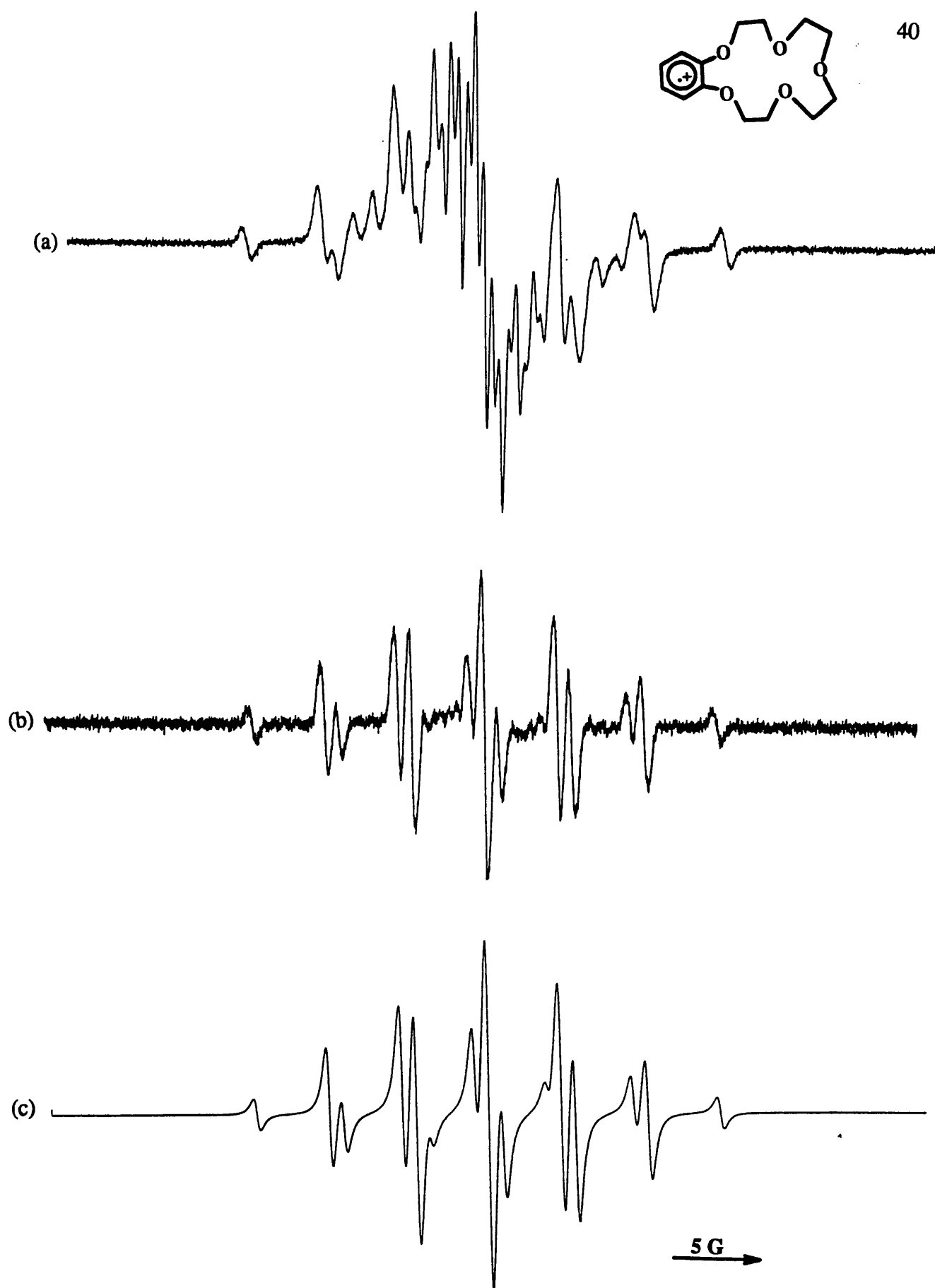


Figure 2.4. E.s.r. spectra of the benzo-15-crown-5 radical cation (2.5)⁺ in DDQ/TFAH at (a) 260 K, (b) 313 K and (c) simulation of spectrum 2.4b.

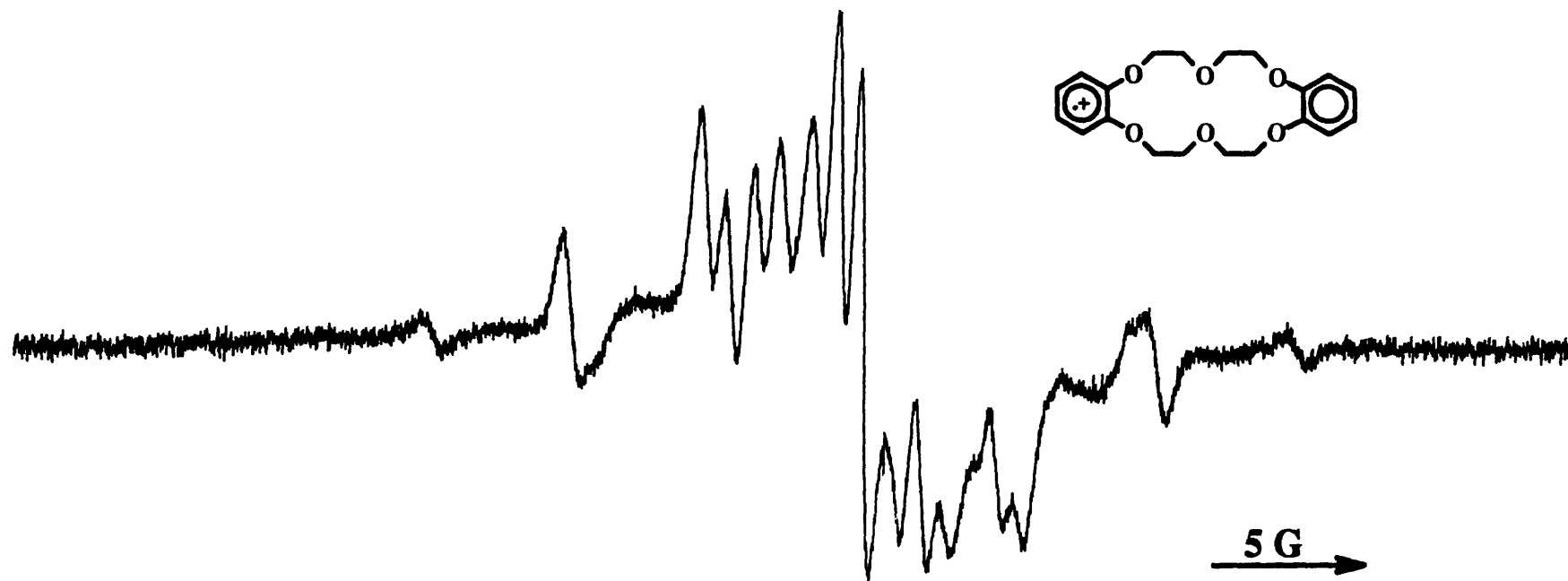


Figure 2.5. E.s.r. spectrum of the dibenzo-18-crown-6 radical cation (2.6)⁺ in DDQ-TFAH-MeSO₃H at 260 K.

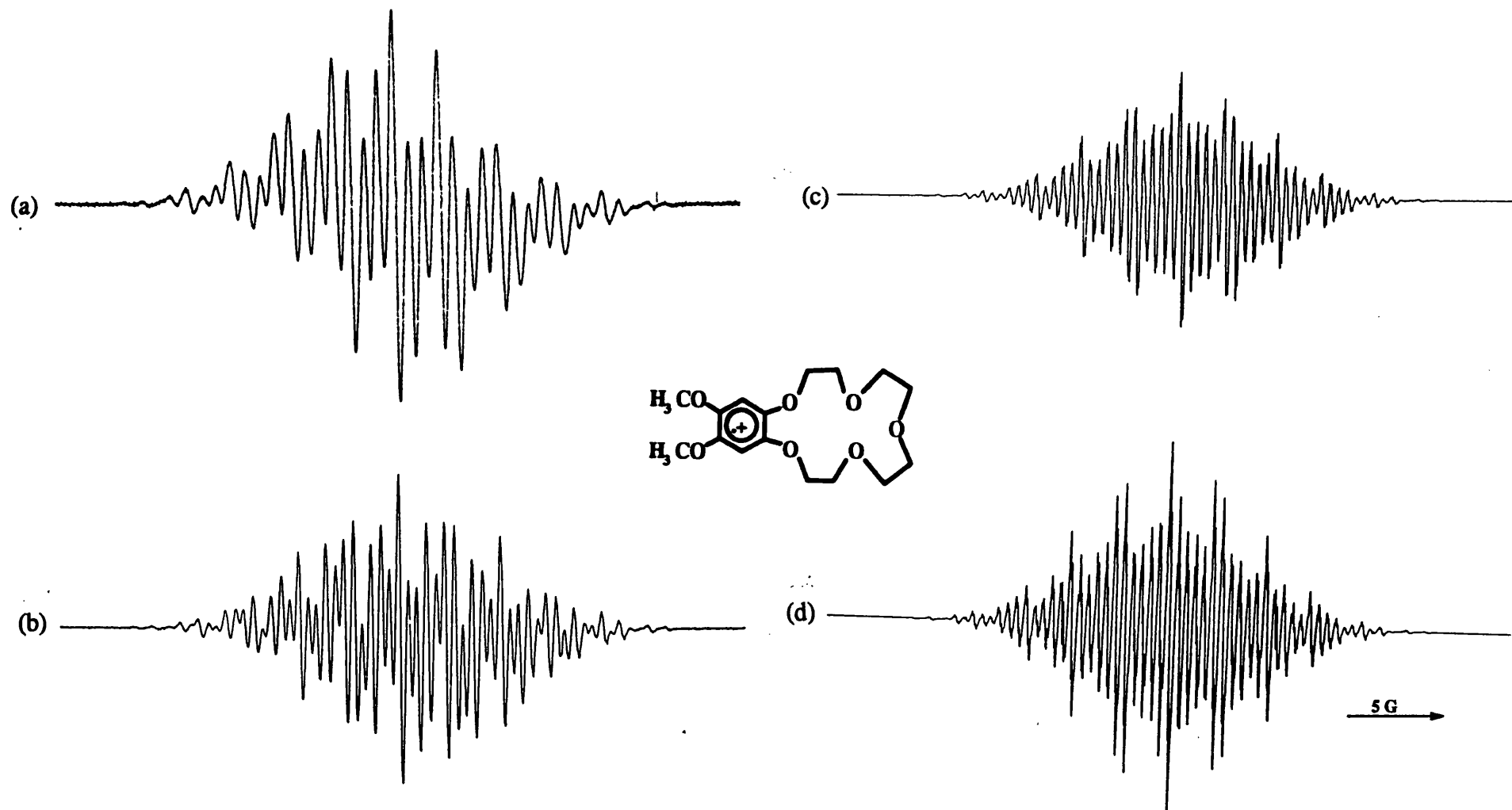


Figure 2.6. E.s.r. spectra of the 4,5-dimethoxybenzo-15-crown-5 radical cation (2.5)⁺ in DDQ-ClCH₂CH₂CH₂Cl-TFAH at (a) 213 K (b) 260 K, (c) 319 K and (d) simulation of spectrum 2.6c.

If $(2.7)^+$ was prepared in dichloromethane containing DDQ and a few drops of trifluoroacetic acid, the spectra over the temperature range 203-319 K could be recorded. At about 213 K, the spectrum seemed to have reached the lower limit of the conformational changes and remained unchanged at lower temperature. We were unable to obtain a convincing simulation of the spectrum 2.6a. The cause of this complication is not fully understood (see discussion). It is impossible to obtain the energy barrier of the ring inversion without knowing the correct values of the hyperfine coupling constants of $(2.7)^+$ at the lower limit.

The e.s.r. spectrum suggest that the radical cation $(2.7)^+$ has the unpaired electron principally in the Ψ_A molecular orbital. These hyperfine coupling constants are comparable with those of the 1,2,4,5-tetramethoxybenzene radical cation $(5.7)^+$: $a(12H)$ 2.20 G and $a(2H)$ 0.86 G, and g 2.0040.

2.3. Discussion

2.3.1. Benzo-crown ethers

We are not aware of any reports of the e.s.r. spectra of benzo-crown ether radical cations, though there is related work in the literature on radical anions derived from tetracyano-benzo-crown ethers,⁸ quinone-based crown ethers,^{9,10} and of non-aromatic crown ether "solvating" the electrons derived from alkali metals.¹¹

2.3.1a. Unusual conformational changes.

In the present studies, the conformational changes of the radical cation (2.7)⁺ spectra at the lowest temperature seem to be very complex. The cause of this complication is not known, but we note that this benzo-crown ether radical cation contains a large flexible macrocyclic ring, and which could undergo a number of conformational changes. Also we have not yet reached a temperature low enough to freeze out conformational change on the e.s.r. time scale.

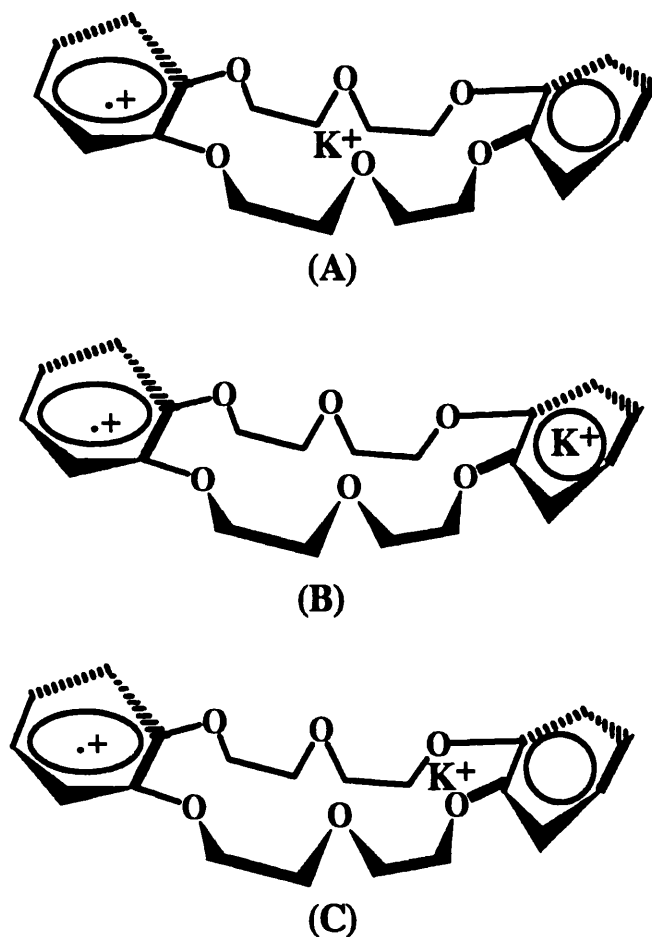
2.3.1b. Structural details

The structure of dibenzo-18-crown-6 radical cation and of its potassium complex [(2.6)⁺/K⁺] are particularly interesting, with respect to the distance between the aromatic rings and the location of the metal cation. Our experiments provide no information on this aspect.

Crystallographic studies by Bright and Truter¹² for the parent dibenzo-18-crown-6, and its Na⁺ and Rb⁺ complexes, provide a basis for understanding the conformational properties of (2.6)⁺/K⁺. They claimed that the conformation of the macrocycle is very similar for metal-free and for complexed crowns. The angle between the planes containing the aromatic rings varies, but all the C-O bonds of the 1,2-dioxyethane bridge were found to adopt a *gauche*-conformation.

Coordination of alkali metal cations could involve either or both of the two distinct electron-rich sites on the radical cation [(B) or (C) in Scheme 2.1]. On the basis of the e.s.r. spectra results, metal cation complex crowns shows no redistribution of the spin

densities of the aromatic ring which might suggest that the metal cation is some distance away from the radical cation π -centre due to Columbic repulsion.



Scheme 2.1. Various alternative structures for $(2.6)^{+\cdot}/K^+$.

2.3.2. Advantages and Disadvantages of the DDQ Method

With this modified DDQ method, we are able to observe the e.s.r. spectra of some new and interesting radical cations (e.g. benzo-crown ethers), which have been inaccessible previously.

There are some advantages and disadvantages with this DDQ technique at the present stage of its development.

Advantage:

- (a) The radical cations are generated in a static system, which consumes less reagent, solvent and substrate than the flow method.
- (b) The cost of the 2,3-dichloro-5,6-dicyano-1,4-benzoquinone (DDQ) is much less than that of thallium(III) trifluoroacetate or mercury(II) trifluoroacetate.
- (c) For substrates with higher ionisation energies, photolysis is essential for generation of the radical cations, making it possible to control the formation of the radical cation. In the past, we have often neglected the effect of laboratory light, which may have been crucial in some of our experiments.

Disadvantage:

- (a) At the present investigation, this technique is not generally suitable for low temperature studies.

References

1. J.C. Courtneidge and A.G. Davies, *Acc. Chem. Res.*, 1987, **20**, 97.
2. K.L. Handoo and K. Gadru, *Current Science*, 1986, **55**, 920.
3. R.M. Dessan, S. Shih and E.I. Heiba, *J. Am. Chem. Soc.*, 1970, **92**, 412.
4. A.G. Davies and D.C. McGuchan, *Organometallics*, 1991, **10**, 329.
5. K. Ishizu, M. Ohuchi and M. Suga, *Bull. Chem. Soc. Japan*, 1973, **46**, 2932.
6. L.L. Miller, G.D. Nordblom and E.A. Mayeda, *J. Org. Chem.*, 1972, **37**, 916.
7. M. Payne and M.R. Truter, *Unpublished Work*.
8. S. Mazur, V.M. Dixit and F. Gerson, *J. Am. Chem. Soc.*, 1980, **102**, 5343.
9. R.E. Wolf and S.R. Cooper, *J. Am. Chem. Soc.*, 1984, **106**, 4646.
10. M. Delgado, R.E. Wolf, J.R. Hartman, G. McCafferty, R. Yagbasan, S.C. Rawle, D.J. Watkin and S.R. Cooper, *J. Am. Chem. Soc.*, 1992, **114**, 8983.
11. D.M. Holten, A.S. Ellaboudry, R.N. Edmonds and P.P. Edwards, *Proc. Roy. Soc.*, 1988, **A415**, 121.
12. D. Bright and M.R. Truter, *J. Chem. Soc. B*, 1970, 1544.

Chapter 3. Radical Cations of Some Benzocyclobutenes and Benzocyclopentenenes

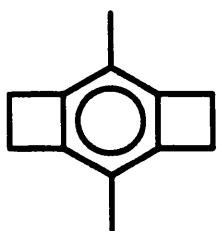
3.1. Background

As described in Chapter 1, the rules governing the interpretation of the e.s.r. hyperfine coupling to hydrogen in the α - or β -position of many π -conjugated organic radical anions and cations are well established.¹ In recent years however, we have found a number of compounds which appear not to obey these simple rules. These compounds which show anomalous results appear to have the common factor of substantial steric strain resulting from angle strain induced by small rings (benzocyclobutenes and benzocyclopentenenes).

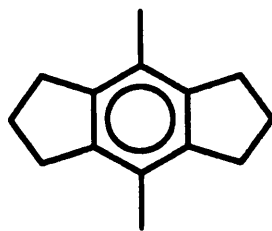
The aim of the project is to synthesise a series of compounds with structures which might be expected to be subject to angle strain. The radical cations could then be generated in solution and the e.s.r. spectra analysed and compared with the prediction of the simple McConnell and Heller-McConnell models in order to identify any effect resulting from the angle strained.

As yet the principal relevant compounds which have been described on a variety of benzocyclobutenes and benzocyclopentenenes. For synthesising the benzocyclobutenes, the technique of flash vacuum pyrolysis has been developed.

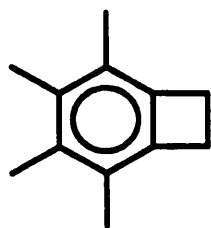
This chapter discusses the e.s.r. spectra which we have observed in fluid solution of the radical cations of the following molecules:



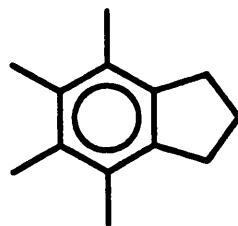
(3.1)



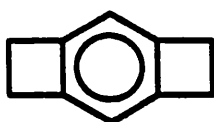
(3.4)



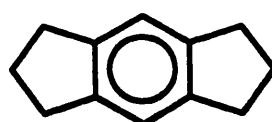
(3.2)



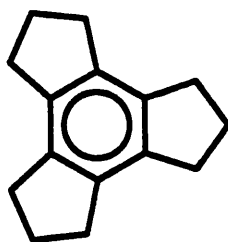
(3.5)



(3.3)



(3.6)



(3.7)

Hyperfine coupling to α -hydrogen results from *spin polarisation*, and is directly proportional to the unpaired electron density ($\rho_{C\alpha}$) at the α -carbon atom (C_α) as described by the McConnell equation [eqn. (3.1)].

$$\underline{a}(H_\alpha) = \rho_{C\alpha} Q_\alpha \quad (3.1)$$

Hyperfine coupling to β -hydrogen is described in the Heller-McConnell equation [eqn. (3.2)]. It is similarly proportional to the unpaired electron density ($\rho_{C\alpha}$) at the α -carbon atom (C_α), but involves both a *spin polarisation* term (A) and a second term ($B\cos^2\theta$) which is due to *hyperconjugation*.

$$\underline{a}(H_\beta) = \rho_{C\alpha}(A + B\cos^2\theta) \quad (3.2)$$

For a given alkyl group in which the angle θ can be taken to be constant, this equation can be reduced to the form of equation 3.3.

$$\underline{a}(H_\beta) = \rho_{C\alpha} Q_\beta \quad (3.3)$$

The unpaired electron density term $\rho_{C\alpha}$ in alkyl-benzenes will vary from 1/6, as it is in benzene or hexamethylbenzene, if the pattern of alkyl substitution breaks the degeneracy of the Ψ_S and Ψ_A orbitals of the benzene ring. For example Figure 3.1 shows how the methyl groups in durene, by inductive and hyperconjugative electron release, destabilise the Ψ_A orbital which has a high coefficient ($\sqrt{1/4}$) at the points of attachment, above that of the Ψ_S orbital in which the relevant coefficients are only $\sqrt{1/12}$. The unpaired electron is thus located in the Ψ_A orbital, and shows a hyperfine coupling pattern reflecting the electron distribution in this orbital, namely $\underline{a}(4CH_3)$ 10.70 G and $\underline{a}(2H)$ 0.80 G;² and the ionisation energy as shown by photoelectron spectroscopy (P.E.S.) is reduced from 9.24 eV as it is in benzene to 8.07 eV.³

An improved (McLachlan) treatment replaces the unpaired electron densities in equations (3.1) and (3.2) by the spin densities.⁴

We have been interested in the potential effect of steric strain upon this simple model, and the correlation between the information on electron distribution provided by e.s.r spectroscopy on one hand, and photoelectron spectroscopy on the other.

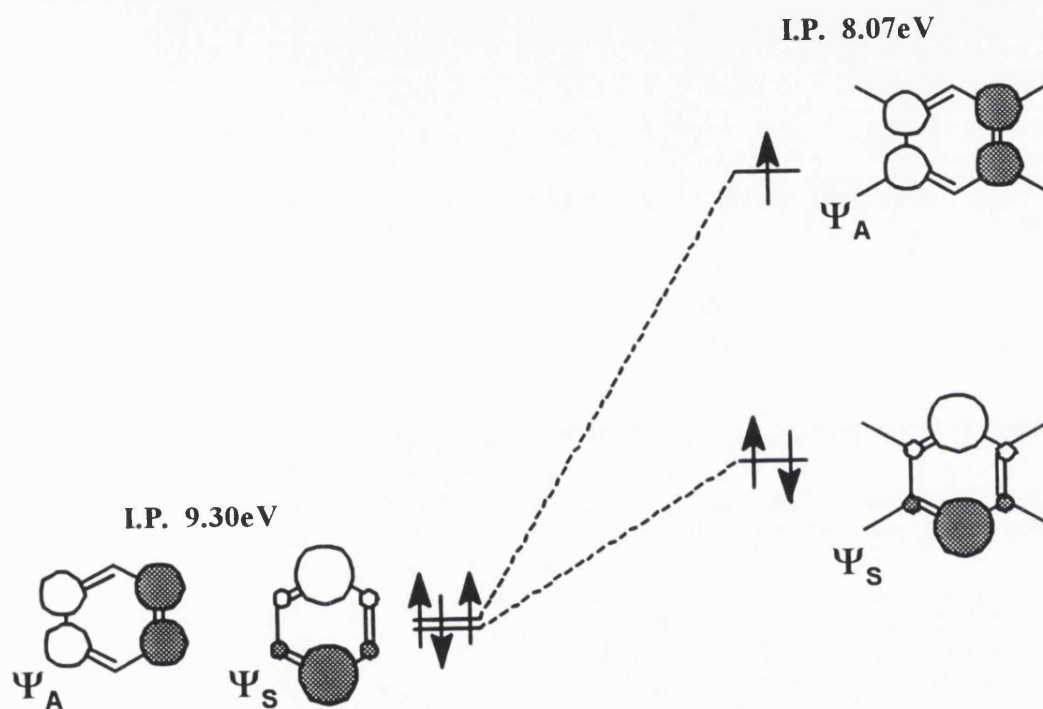
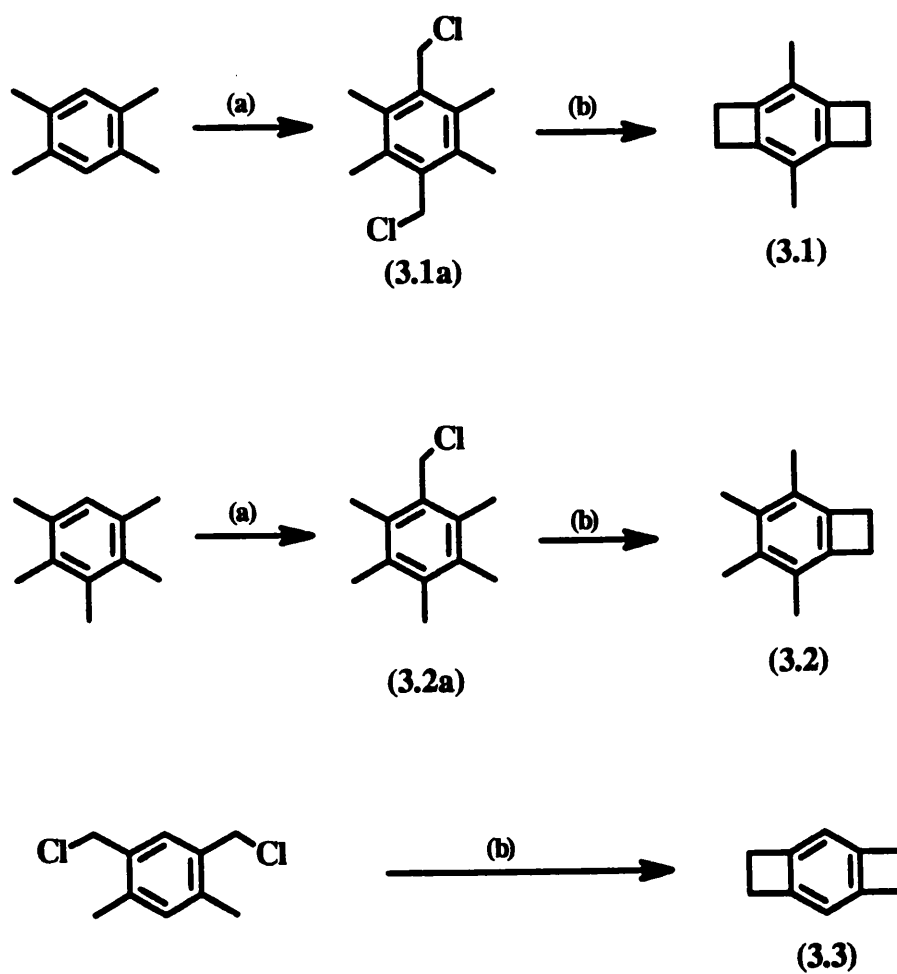


Figure 3.1

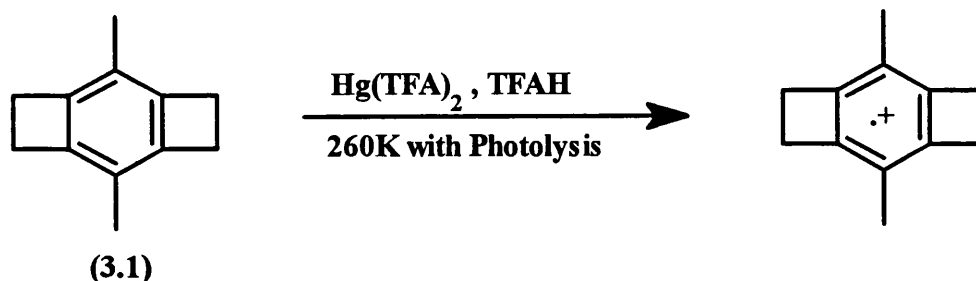
3.2. Results

3.2.1. Benzocyclobutenes.- The benzocyclobutenes (3.1, 3.2 and 3.3) were prepared by flash vacuum pyrolysis of *ortho*-methyl(chloromethyl)arenes (see Scheme 3.1).



Scheme 3.1. Conditions: (a) CH_2O and conc. HCl ; (b) $700\text{ }^\circ\text{C}$ at 0.05 mmHg .

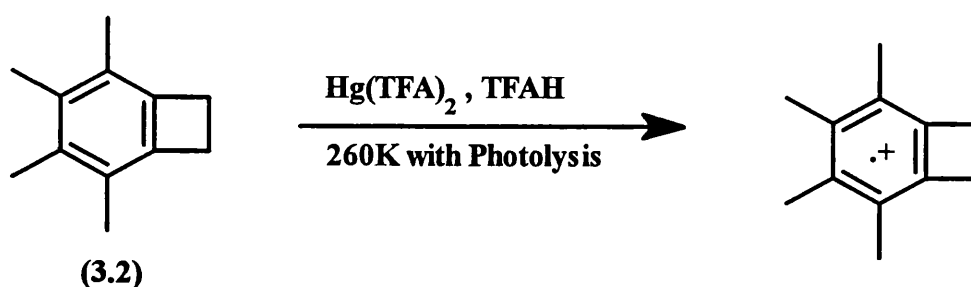
3.2.1a. 3,6-Dimethylbenzo[1,2:4,5]dicyclobutene radical cation (3.1)



When compound (3.1) was added to a solution of trifluoroacetic acid (TFAH) containing mercury(II) trifluoroacetate at -13°C it gave a yellowish solution. This solution showed no e.s.r. spectrum without photolysis, but a strong and persistent spectrum of the 3,6-dimethylbenzo[1,2:4,5]dicyclobutene radical cation (3.1)⁺ was observed when this sample was irradiated with U.V. light which was attenuated to 30% of its intensity by a neutral filter, and passed through Pyrex glass.

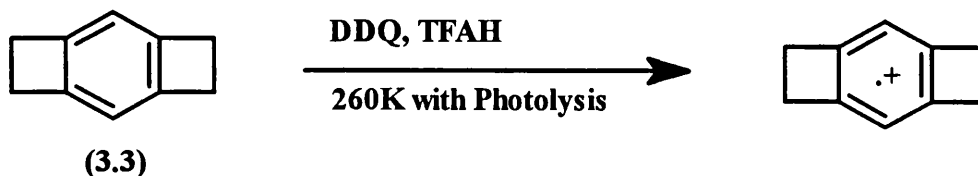
The e.s.r. spectrum of (3.1)⁺ is shown in Figure 3.2, and this spectrum has been analysed and confirmed by computer simulation: $\underline{a}(8\text{H}, 4\text{CH}_2)$ 13.84 G, $\underline{a}(6\text{H}, 2\text{Me})$ 0.68 G and g 2.0025.

3.2.1b. 3,4,5,6-Tetramethylbenzocyclobutene radical cation (3.2)



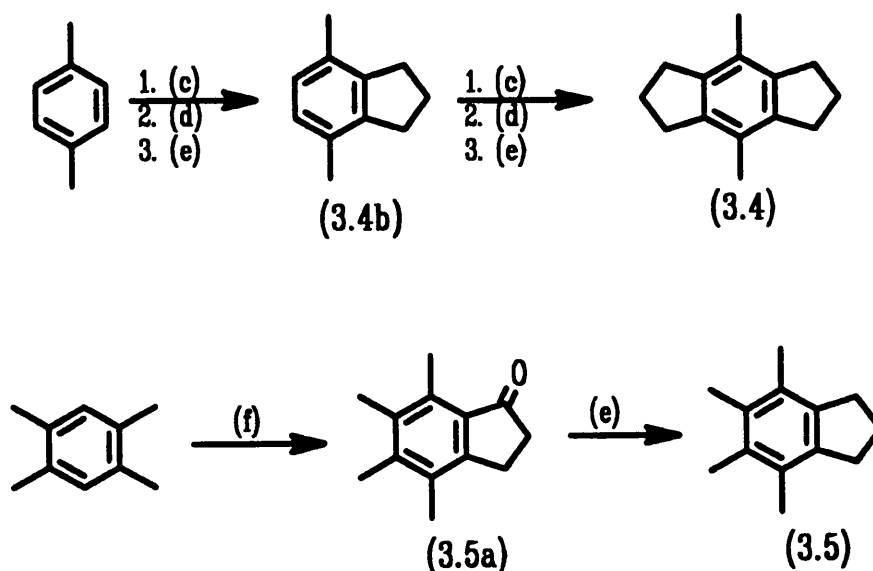
A yellowish solution was obtained, when compound (3.2) was added to TFAH containing mercury(II) trifluoroacetate at -13°C . The spectrum of the radical cation spectrum of (3.2)⁺ was observed on photolysis of this solution with filtered U.V. light, and this can be simulated using the following hyperfine coupling constants: $\underline{a}(4\text{H}, 2\text{CH}_2)$ 11.87 G, $\underline{a}(6\text{H}, 2\text{Me})$ 10.72 G and $\underline{a}(6\text{H}, 2\text{Me})$ 0.24 G, and g 2.0025 (see Figure 3.3).

3.2.1c. Benzo[1,2:4,5]dicyclobutene radical cation (3.3)

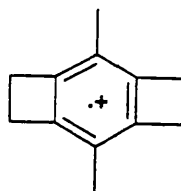


A solution of the compound (3.3) and 2,3-dichloro-5,6-dicyanoquinone (DDQ) was dissolved in TFAH at -13°C . A deep blue-purple solution was formed. This solution give no e.s.r. spectrum without photolysis. When this solution was irradiated with unfiltered U.V. light, an e.s.r. spectrum was observed which we assign to the (3.3)⁺ radical cation with the following hyperfine coupling constants $a(8\text{H}, 4\text{CH}_2)$ 14.25 G and $a(2\text{H}, \text{ArH})$ 0.93 G, and g 2.0026 (see Figure 3.4).

3.2.2. Benzocyclopentenes.- The benzocyclopentenes (3.4, 3.5 and 3.6) were prepared by Friedel Crafts annelation with β -chloropropionyl chloride, then Clemmensen reduction (see Scheme 3.2), and the benzotricyclopentene (3.7) was prepared by trimerisation of cyclopentanone.



Scheme 3.2. Conditions: (c) $\text{ClCH}_2\text{CH}_2\text{COCl}/\text{AlCl}_3$; (d) conc. H_2SO_4 ; (e) $\text{Zn}(\text{Hg})/\text{conc. HCl}$ and (f) $\text{ClCH}_2\text{CH}_2\text{CO}_2\text{Et}/\text{AlCl}_3$.



55

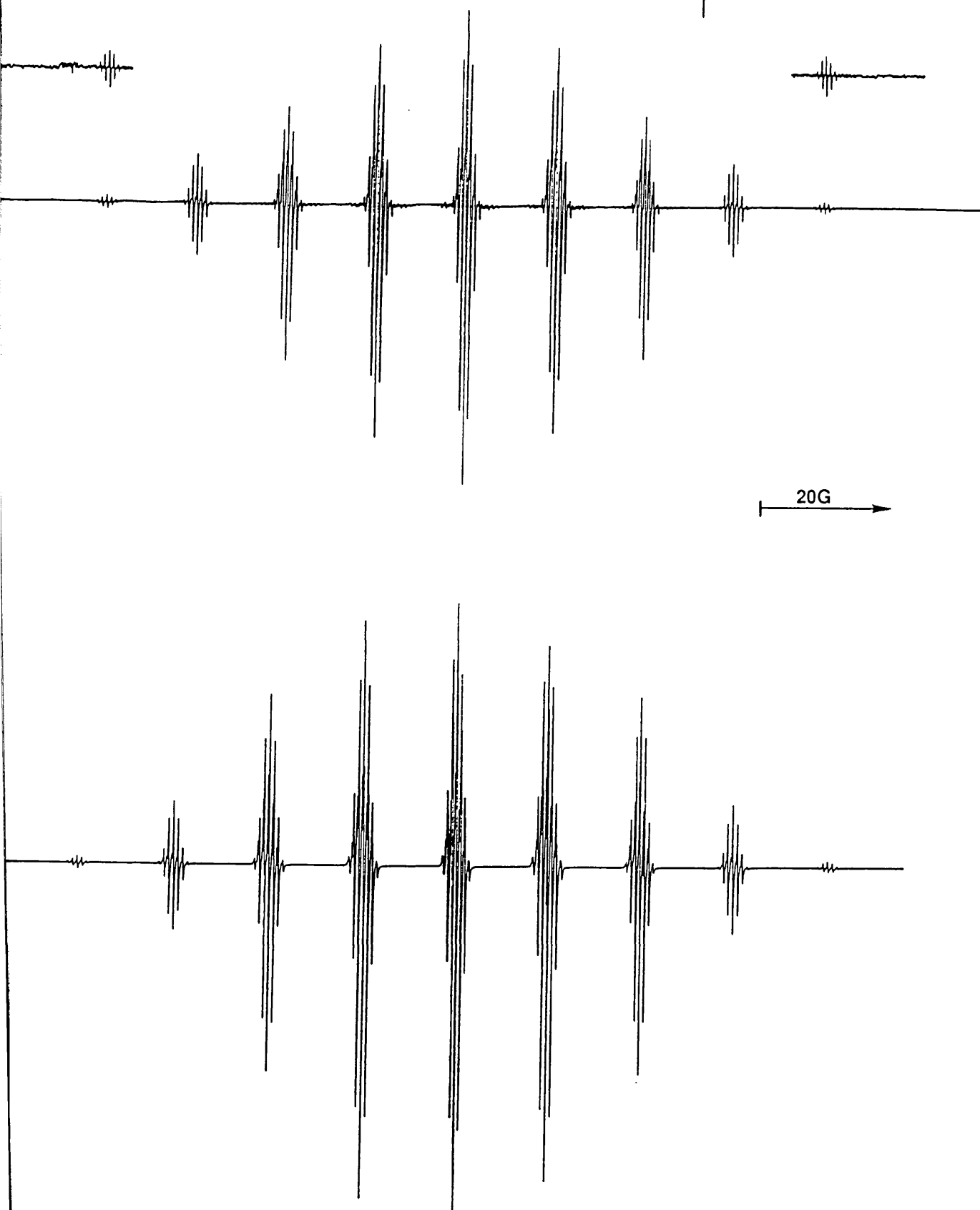


Figure 3.2. E.s.r. spectrum (top) and simulation (bottom) of the 3,6-dimethylbenzo[1,2:4,5]dicyclobutene radical cation (3.1)⁺ in TFAH/Hg(TFA)₂ at 260 K.

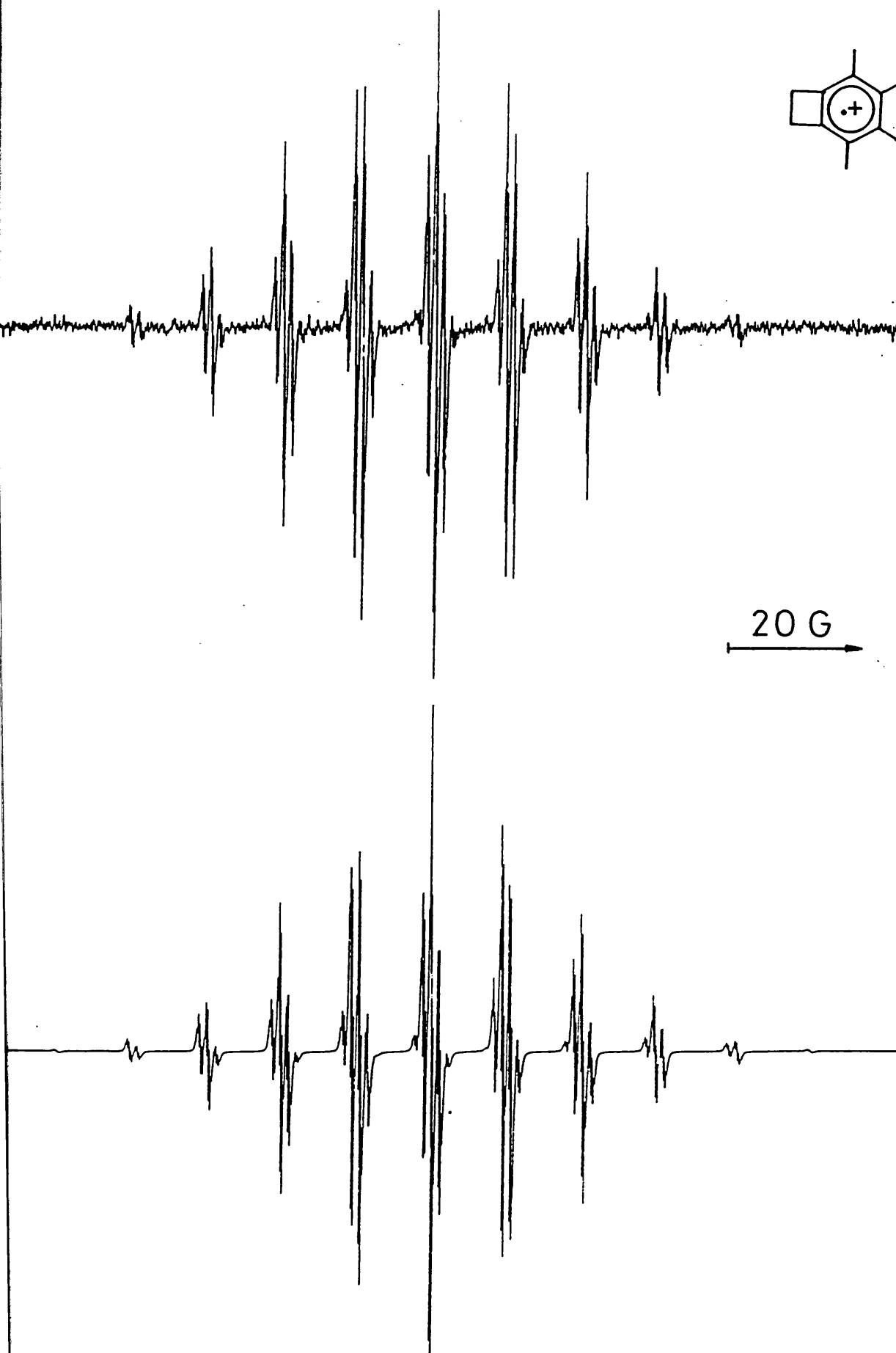


Figure 3.3. E.s.r. spectrum (top) and simulation (bottom) of the 3,4,5,6-tetramethylbenzocyclobutene radical cation (3.2)⁺ in TFAH/Hg(TFA)₂ at 260 K.

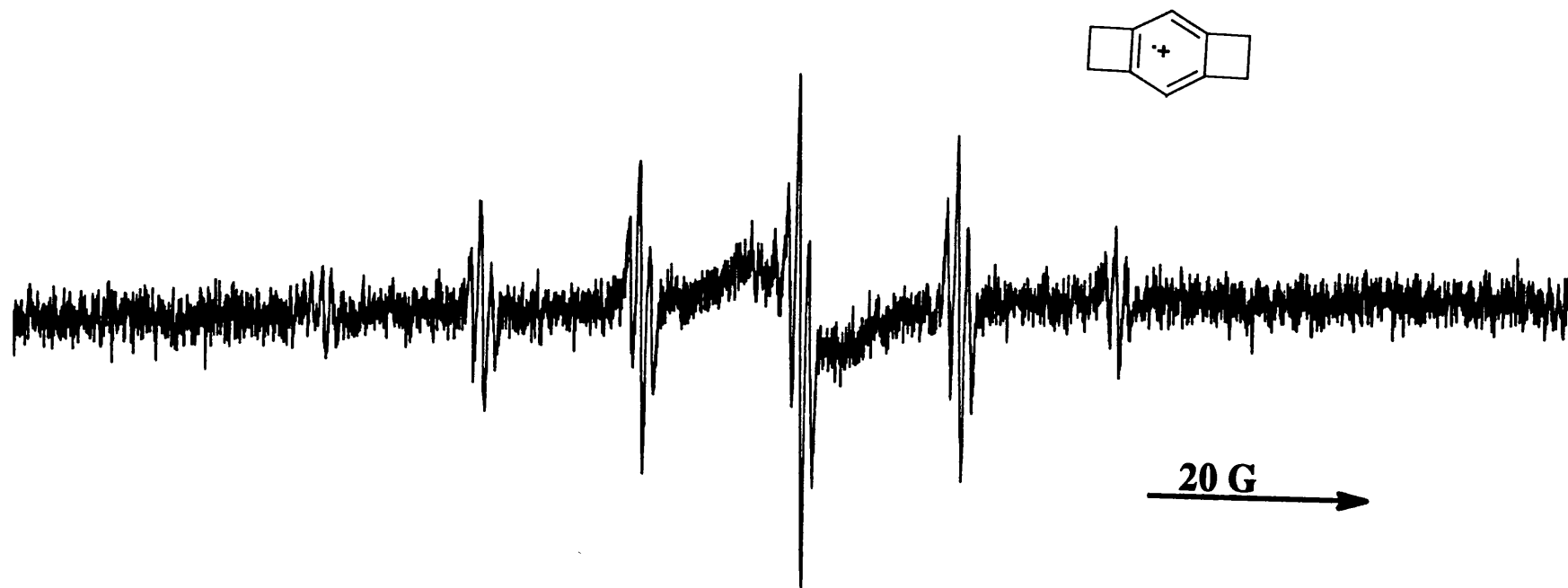
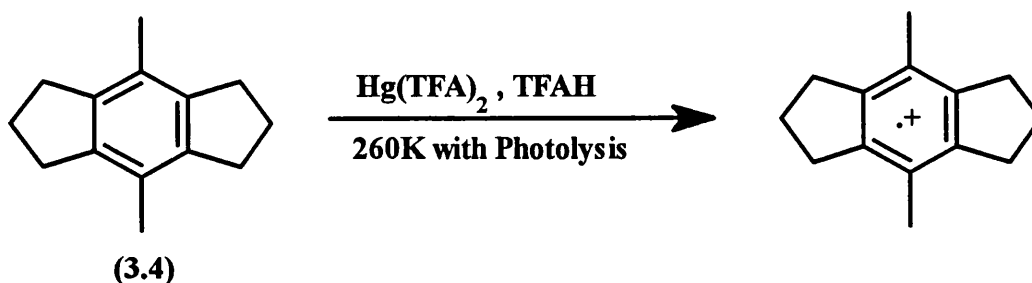


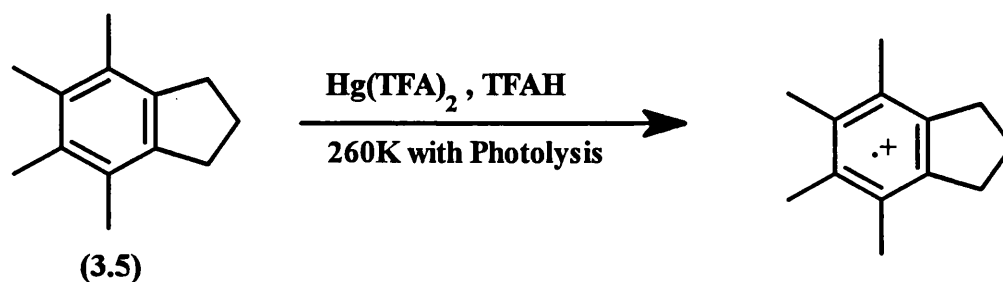
Figure 3.4. E.s.r. spectrum of the benzo[1,2:4,5]dicyclobutene radical cation (3.3)⁺ in TFAH/Hg(TFA)₂ at 260 K.

3.2.2a. 3,6-Dimethylbenzo[1,2:4,5]dicyclopentene radical cation (3.4)

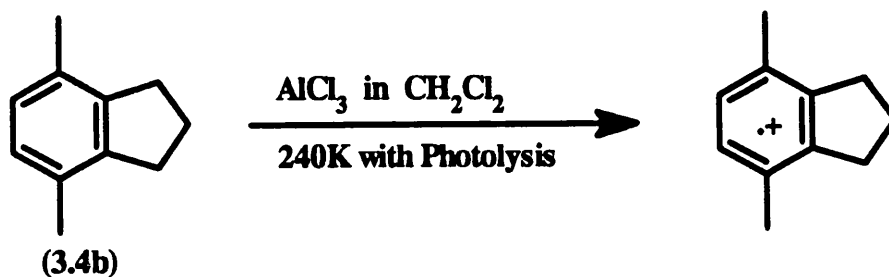


When compound (3.4) was added to a solution of TFAH containing thallium(III) trifluoroacetate at $-13\text{ }^{\circ}\text{C}$ it gave a yellowish solution. Without photolysis, this solution gave a strong and persistent e.s.r. spectrum of the 3,6-dimethylbenzo[1,2:4,5]-dicyclopentene radical cation (3.4)⁺, which is shown in Figure 3.5, with the hyperfine coupling constants: $\underline{a}(8\text{H}, 4\text{CH}_2)$ 18.37 G, $\underline{a}(6\text{H}, 2\text{Me})$ 0.64 G and $\underline{a}(4\text{H}, 2\text{CH}_2)$ 0.64 G, and g 2.0027.

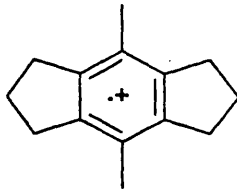
3.2.2b. 3,4,5,6-Tetramethylbenzocyclopentene radical cation (3.5)



Compound (3.5) was added to a solution of TFAH containing mercury(II) trifluoroacetate at $-13\text{ }^{\circ}\text{C}$ to give a pale yellowish solution. A strong and persistent e.s.r. spectrum of 3,4,5,6-tetramethylbenzocyclopentene radical cation (3.5)⁺ was obtained, when this solution was irradiated with 30% U.V. light. It showed $\underline{a}(4\text{H}, 2\text{CH}_2)$ 18.09 G, $\underline{a}(2\text{H}, \text{CH}_2)$ 0.68 G, $\underline{a}(6\text{H}, 2\text{Me})$ 8.86 G and $\underline{a}(6\text{H}, 2\text{Me})$ 0.68 G, and g 2.00247 (Figure 3.6).

3.2.2c. 3,6-Dimethylbenzocyclopentene radical cation (3.4b)

When a sample of (3.4b) was dissolved in a mixture of anhydrous AlCl_3 and CH_2Cl_2 at $-13\text{ }^\circ\text{C}$ and irradiated with full U.V. light, a strong and complicated e.s.r. spectrum was observed which has a large quintet due to coupling to the 4 equivalent β -methylene protons in the cyclopentene ring $\underline{a}(4\text{H}, 2\text{CH}_2)$ 13.3 G (Figure 3.7).



60

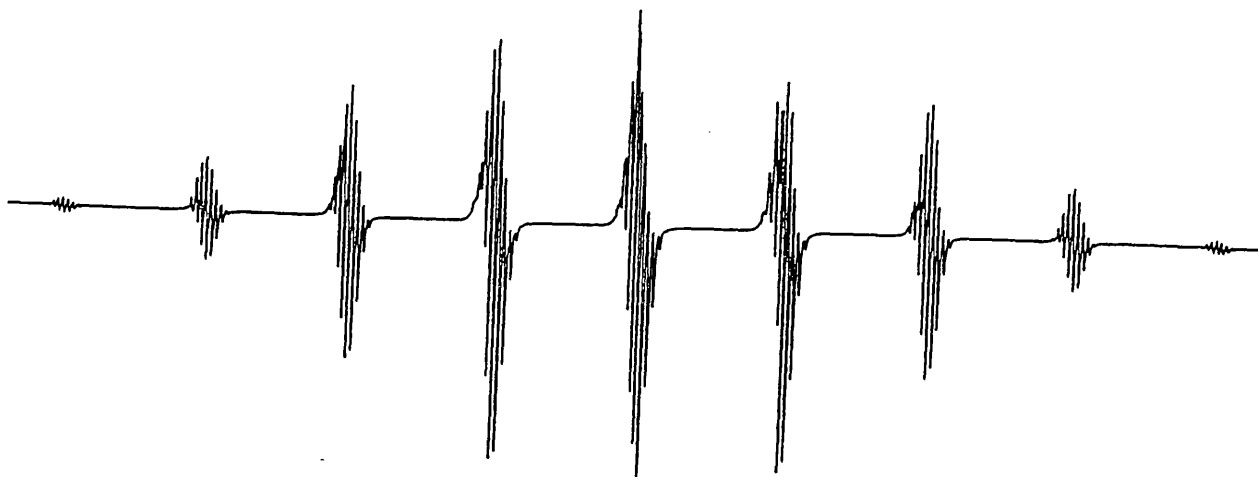
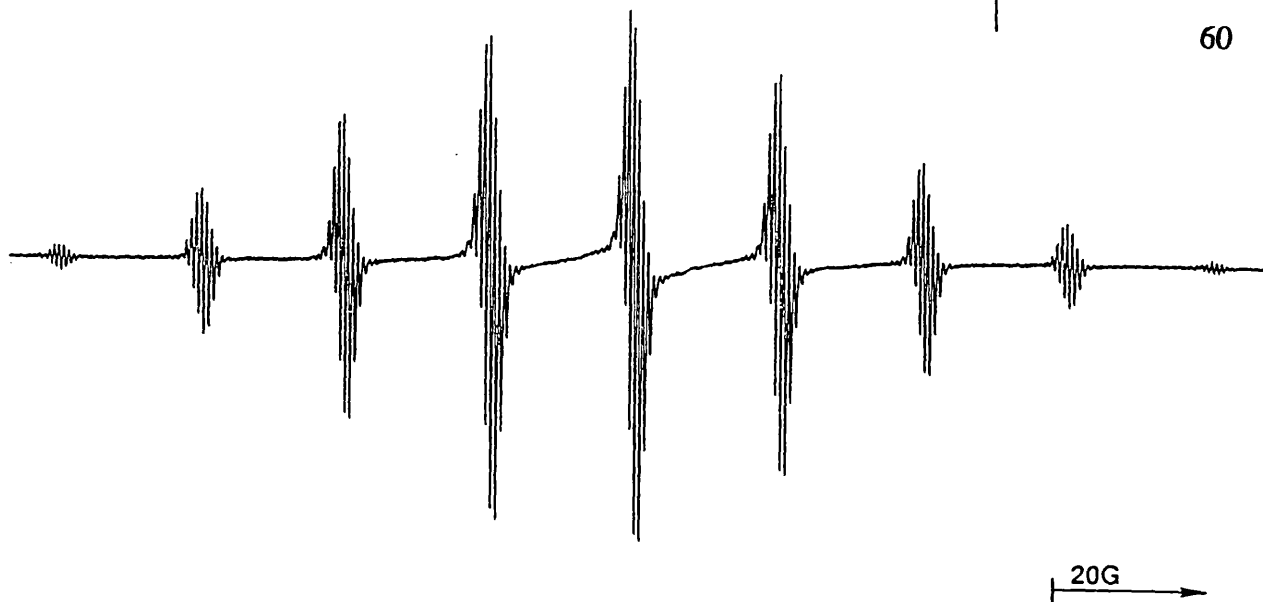


Figure 3.5. E.s.r. spectrum (top) and simulation (bottom) of the 3,6-dimethylbenzo[1,2:4,5]dicyclopentene radical cation (3.4)⁺ in TFAH/Tl(TFA)₃ at 260 K.

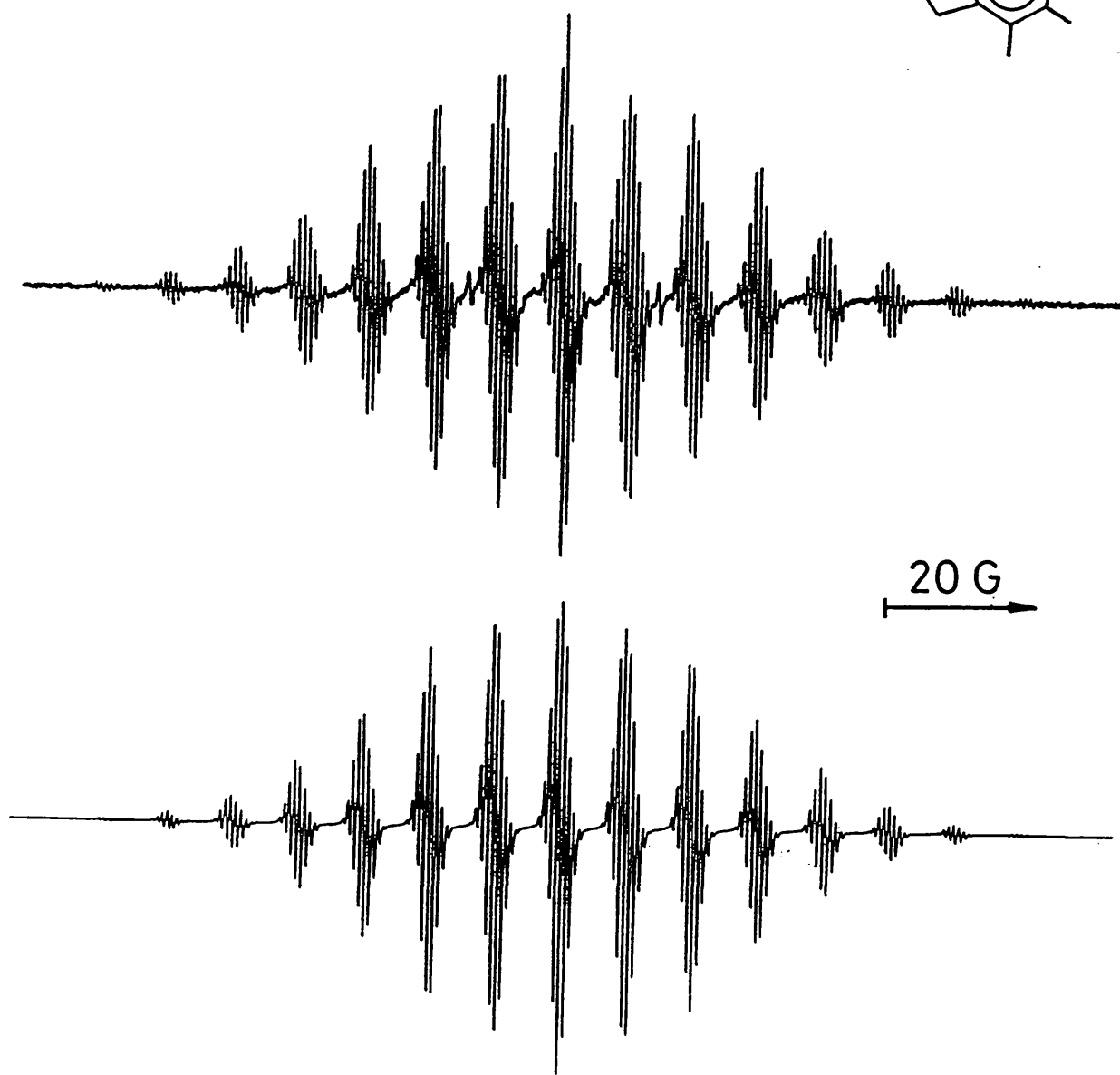
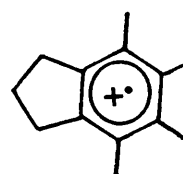


Figure 3.6. E.s.r. spectrum (top) and simulation (bottom) of the 3,4,5,6-tetramethylbenzocyclopentene radical cation (3.5)⁺ in TFAH/Hg(TFA)₂ at 260 K.

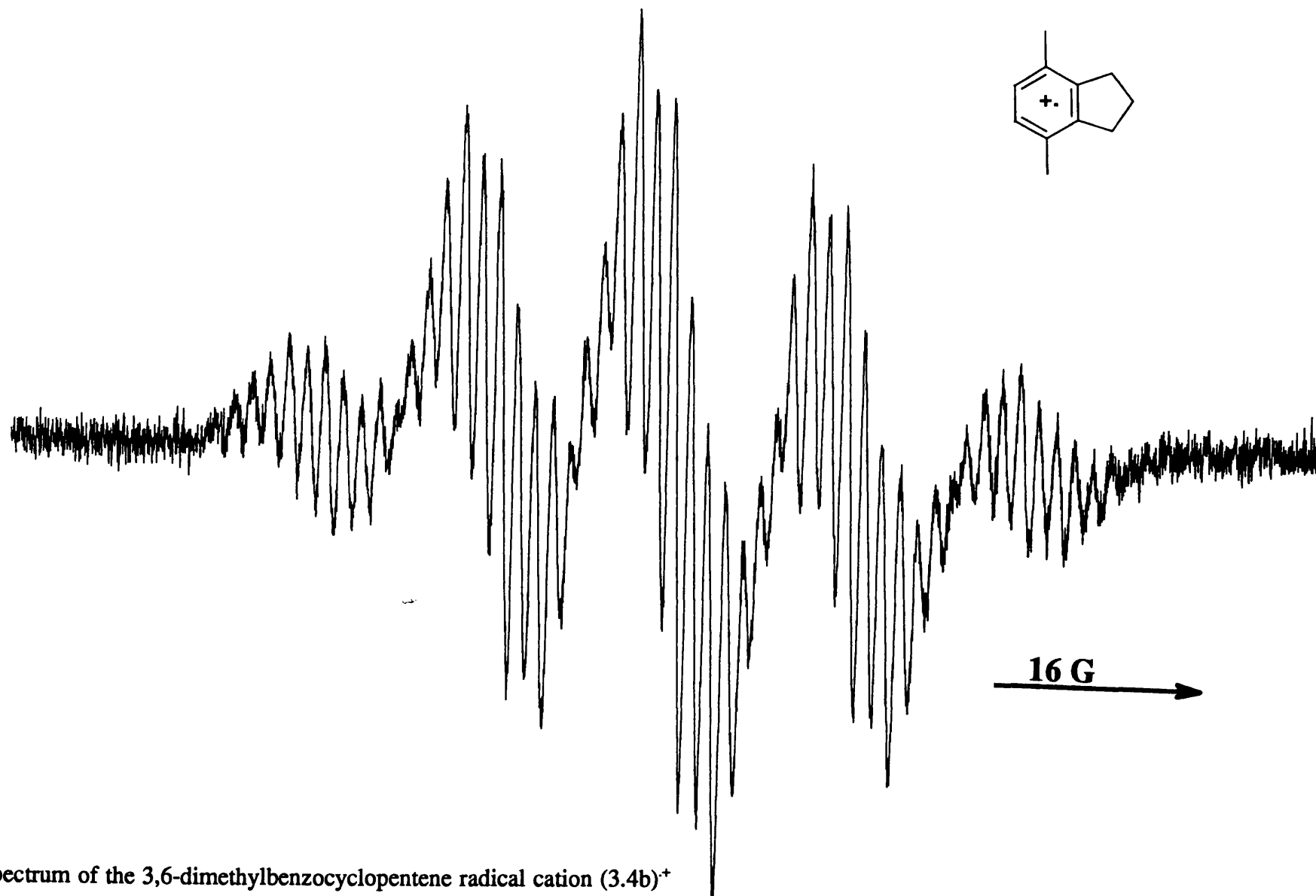


Figure 3.7. E.s.r. spectrum of the 3,6-dimethylbenzocyclopentene radical cation (3.4b)⁺ in CH₂Cl₂/AlCl₃ at 260 K.

Table 3.1 E.S.R. Spectra of radical cations


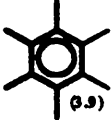
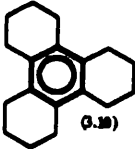
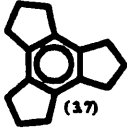
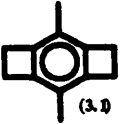
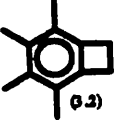

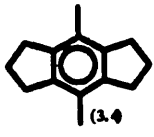
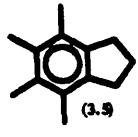
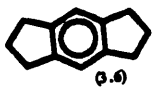
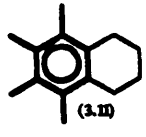
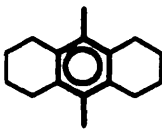
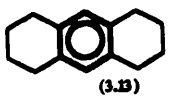
Compound	Condns. ^a	$\underline{a}(nH)/G$	$\rho_{C\alpha}$	$\Sigma\rho_{C\alpha}$	S.O.M.O.	Ref.
 (3.8)	A	6 H 4.43	0.17	(1)	A + S	<i>b</i>
 (3.9)	B	6 Me 6.5	0.17	(1)	A + S	<i>f</i>
 (3.10)	D	6 CH ₂ 10.24	0.17	(1)	A + S	<i>d</i>
 (3.7)	C	6 CH ₂ 11.49 3 CH ₂ 0.34	0.17	(1)	A + S	<i>c</i>
 (3.1)	B	2 Me 0.68 4 CH ₂ 13.84	—	(1)	A	<i>f</i>
 (3.2)	B	2 Me 0.24 2 Me 10.72 2 CH ₂ 11.87	0.06 0.275 0.207	1.01	A	<i>f</i>
 (3.3)	E	2 H 0.93 4 CH ₂ 14.25	0.035 0.249	1.07	A	<i>f</i>

Table 3.1 (continued) Compound	Condns.	$\underline{a}(nH)/G$	$\rho_{C\alpha}$	$\Sigma\rho_{C\alpha}$	S.O.M.O.	Ref.
 (3.4)	C	2 Me 0.64 4 CH ₂ 18.37 2 CH ₂ 0.64	0.019 0.266	1.10	A	<i>f</i>
 (3.5)	B	2 Me 0.68 2 Me 8.86 2 CH ₂ 18.09 2 CH ₂ 0.68	0.018 0.223 0.262	1.01	A	<i>f</i>
 (3.6)	F	2 H 0 4 CH ₂ 19.2	0 0.279	1.11	A	<i>c</i>
 (3.11)	C	2 Me 9.34 2 Me 2.39 2 CH ₂ 3.7 2 CH ₂ 1.38	0.240 0.061	0.65	S	<i>c</i>
 (3.12)	C	2 Me 9.27 4 CH ₂ 3.65	0.238 0.059	0.71	S	<i>c</i>
 (3.13)	D	2 H 0 4 CH ₂ 15.5	0 0.252	1.01	A	<i>c</i>

^aConditions: A, H₂SO₄ at 163 K; B, TFAH/Hg(TFA)₂ at 260 K; C, TFAH/Tl(TFA)₃ at 260 K; D, CH₂Cl₂/AlCl₃ at RT; E, TFAH/DDQ at 260 K; F, TFAH/Co(OAc)₂ at RM. ^bM.K.Carter and G.Vincow, *J. Am. Chem. Soc.*, 1970, 92, 292. ^cD.V.Avila, *Ph.D. Thesis*, 1990. ^dD.V.Avila, A.G.Davies and M.L.Girbal, *Tetrahedron*, 1990, 46, 1999. ^eR.M. Dessau and S.Shih, *J. Chem. Phys.*, 1970, 53, 3169. ^fPresent work.

3.3. Discussion

In order to use equations (3.1) and (3.3) for determining local unpaired electron densities in these substituted benzene radical cations, we have to derive first the Q values by equations (3.1) and (3.3) from the symmetrical hexasubstituted benzenes (3.7 - 3.10) for H (26.6 G), and CH₃ (39.0 G), and for the α-CH₂ groups in fused cyclopentene (68.9 G), and cyclohexene (61.4 G) rings, assuming that in each radical cation, the local unpaired electron density ρ_{Cα} is 1/6. As benzotricyclobutene (8.14) was not available, we derived the Q value indirectly for the CH₂ group in the cyclobutene ring from compound (3.1) as described below.

From these Q values we can then reverse the argument and convert observed hyperfine coupling constants in other radical cations into local unpaired electron densities ρ_{Cα}. These values of ρ_{Cα} and those of Σρ_{Cα} are given in Table 3.1.

Then, we use this principle to derive from compound (3.1) the Q_b value for the CH₂CH₂ group of a cyclobutene ring. The observed value of $\underline{a}(6\text{H}, 2\text{CH}_3)$ 0.68 G, corresponds to ρ 0.0174, by equation (3.3). If the total unpaired electron density is taken to be unity, the unpaired electron density at each of the points of fusion of the cyclobutene rings must be 0.241, and use of the observed value of $\underline{a}(8\text{H}, 4\text{CH}_2)$ 13.84 G, then gives to Q_b 57.3 G, for the CH₂CH₂ group in the cyclobutene ring.

If we use this Q value to calculate the total unpaired electron density in compound (3.2) and compound (3.3), we obtained values 1.006 and 1.07 respectively, close to unity. This gives us confidence that, if it is applied with caution, this way of analysing the data can be useful.

3.3.1. Benzocyclobutenes:-

In the benzocyclobutenes, the electronic configuration (S.O.M.O.) of the radical cation which is indicated by the E.S.R. spectra is the result of the breaking of the degeneracy of the Ψ_A and Ψ_S benzene orbitals by the alkyl substituents.

Comparison the results of the vertical ionisation energies^{3,6,7} for the related methylated benzenes and cyclobutene-annelated benzenes (Figure 3.8) (3.9) and (3.14), (3.15) and (3.3), and (3.16) and (3.17), suggests that a pair of *ortho*-methyl groups repels electrons *more* strongly than does a cyclobutene (cyclo-(CH₂)₂) group. But the e.s.r.

spectra show clearly that the radical cations (3.1)⁺ and (3.2)⁺ have the unpaired electron situated principally in the Ψ_A M.O.: the unpaired electron density at the 3,6-positions carrying methyl groups in (3.1)⁺ is 0.01 and (3.2)⁺ is 0.006, and at the other four (or 1,2,4,5-) positions it is correspondingly high.

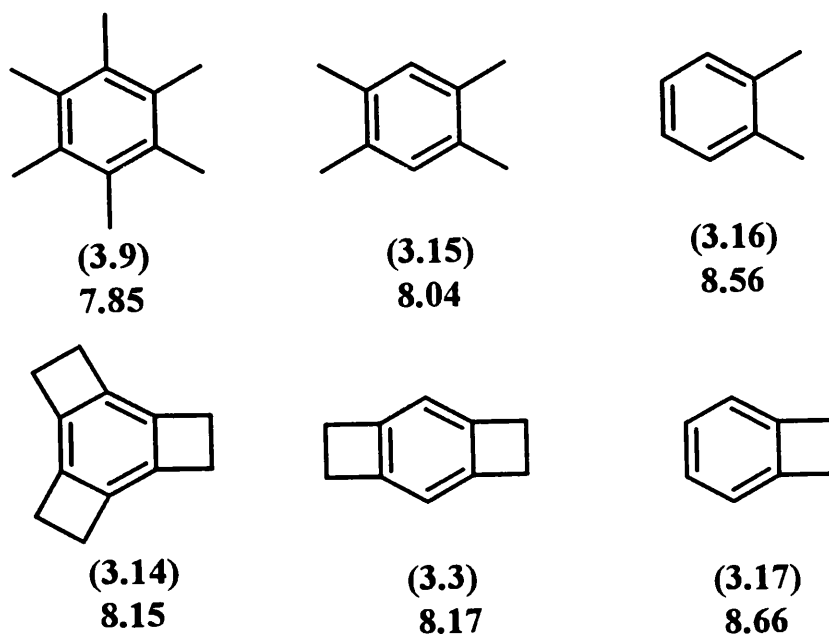


Figure 3.8. Vertical ionisation energies (eV).

These benzocyclobutenes [(3.1) and (3.2)] can be regarded as derivatives of the orbitally degenerate hexamethylbenzene (3.9) in which *ortho* pairs of methyl groups have been replaced by a cyclo-(CH₂)₂ groups. The S.O.M.O. is Ψ_A in which the cyclo-(CH₂)₂ groups are concentrated at the centre of high (1/4) unpaired electron density, and the methyl groups lie in the nodal plane. Usually, these would be taken to imply that the cyclo-(CH₂)₂ groups repel electrons *more* strongly than do an *ortho* pair of methyl groups.

However, this is contrary to the results of photoelectron spectroscopy (Figure 3.8) which imply that a cyclo-(CH₂)₂ group repels electrons *less* strongly than do an *ortho* pair of methyl groups, so that the S.O.M.O. in (3.1)⁺ and (3.2)⁺ should be the Ψ_S M.O..

These photoelectron spectra, however, relate to molecules in the gas phase, whereas our e.s.r. spectra relate to radical cations in solution where they will be heavily solvated. In order to check that the same sequence holds for the ionisation energies in solution, we have therefore oxidised a mixture of hexamethylbenzene (3.9) and 3,6-dimethylbenzo[1,2:4,5]dicyclobutene (3.1), and of (3.9) and 3,4,5,6-tetramethylbenzocyclobutene (3.2) under conditions where each compound separately gives a strong e.s.r. spectrum of the long-lived corresponding radical cation. In these experiments, the radical cation which is observed should be derived from the arene with the lower ionisation energy, and indeed with both mixtures showed a strong e.s.r. spectrum of the hexamethylbenzene (3.9)⁺ radical cation (see Figure 3.9). From a similar experiment, a mixture of 3,6-dimethylbenzo[1,2:4,5]dicyclobutene (3.1) and 3,4,5,6-tetramethylbenzocyclobutene (3.2) showed a spectrum which was less well defined, but related principally to (3.2)⁺. These results thus imply that an *ortho* pair of methyl groups repel electrons *more* strongly than does a cyclo-CH₂CH₂ group, and support the results obtained from the P.E.S. gas phase studies.

We suggest that this apparent contradiction between the results of the e.s.r. spectra and the ionisation energies may be another example of the Mills and Nixon effect,⁸ in which the chemical and physical properties of an aromatic nucleus are perturbed when it is fused to a small ring. Recent studies involving, in particular, N.M.R. spectroscopy,^{9,22} X-ray diffraction,^{10,11} and *ab initio* M.O. calculations^{7,12,13} suggest that the rehybridisation occurs to the (*ipso*) carbon atom at the ring junction, as first suggest by Finnegan¹⁴ and by Streitwieser.¹⁵ To relieve the angle strain in the small ring, the aromatic (*ipso*) carbon atoms undergo rehybridisation from sp² to place more p-character in the bonds subtending the strained angle, and hence more s-character in the bond to the *ortho* position. This *ipso-ortho* bond will therefore be polarised with a partial negative (δ^-) charge on the *ipso* carbon atom and a partial positive (δ^+) on the *ortho* carbon atom as shown in Figure 3.10. This polar structure will stabilise the Ψ_s M.O. which has a high coefficient ($\sqrt{1/3}$) on each *ortho* carbon, and destabilise Ψ_A which has a high coefficient ($\sqrt{1/4}$) on each *ipso* carbon. This interplay of the electronic (inductive and hyperconjugative) and stereoelectronic (Mills-Nixon) effect is illustrated in Figure 3.11.

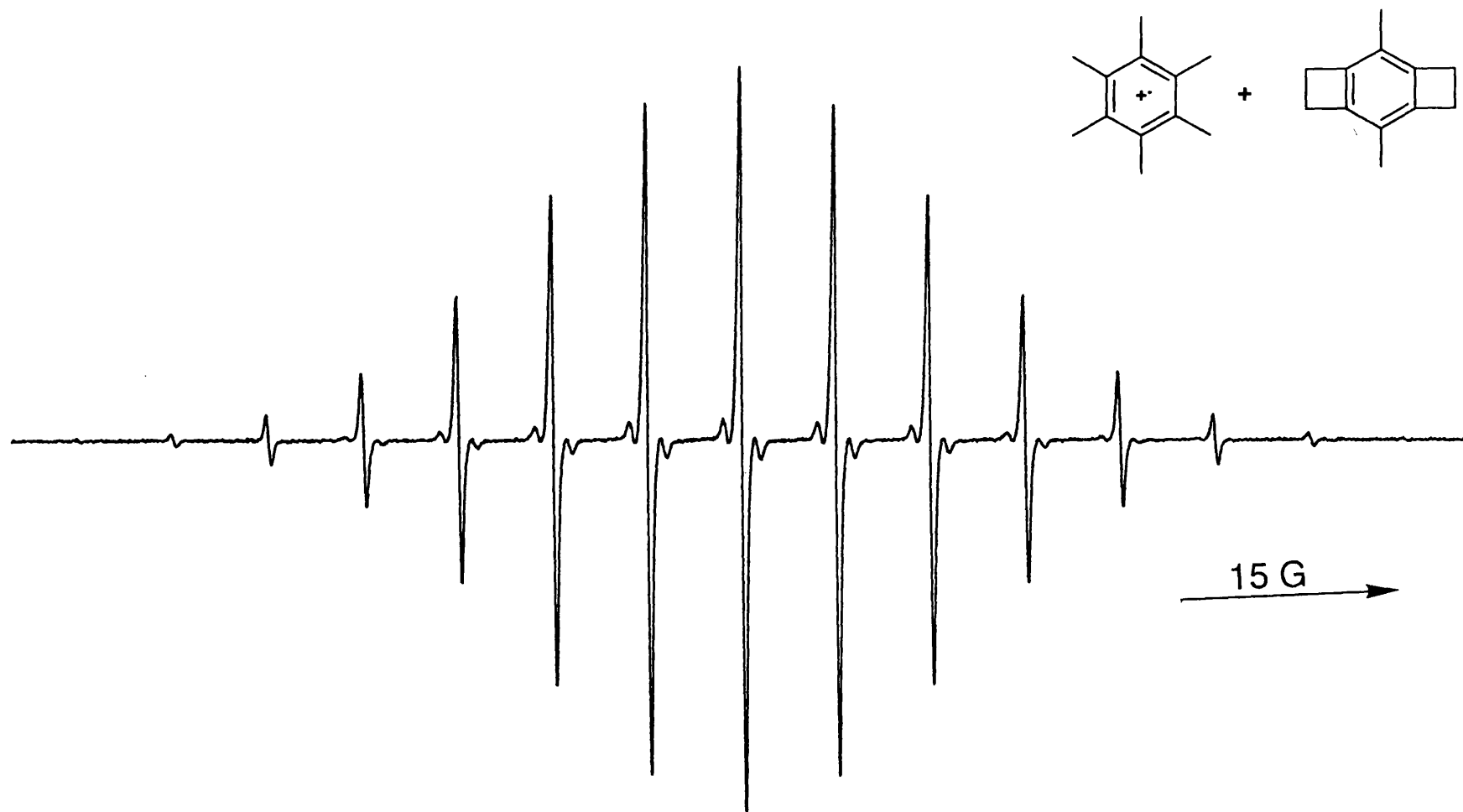


Figure 3.9. E.s.r. spectrum obtained from a mixture of 3,6-dimethylbenzo[1,2:4,5]dicyclobutene (3.1) and hexamethylbenzene (3.9) in TFAH/Hg(TFA)₂ at 260 K showing hexamethylbenzene radical cation (3.9)⁺.

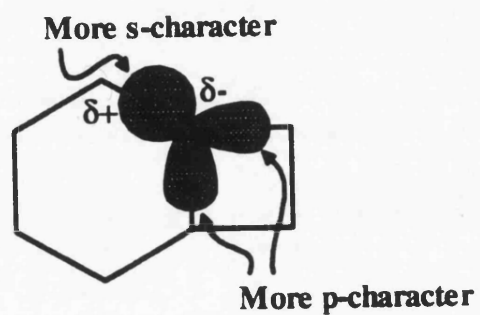


Figure 3.10. Finnegan-Streitwieser model of rehybridisation.

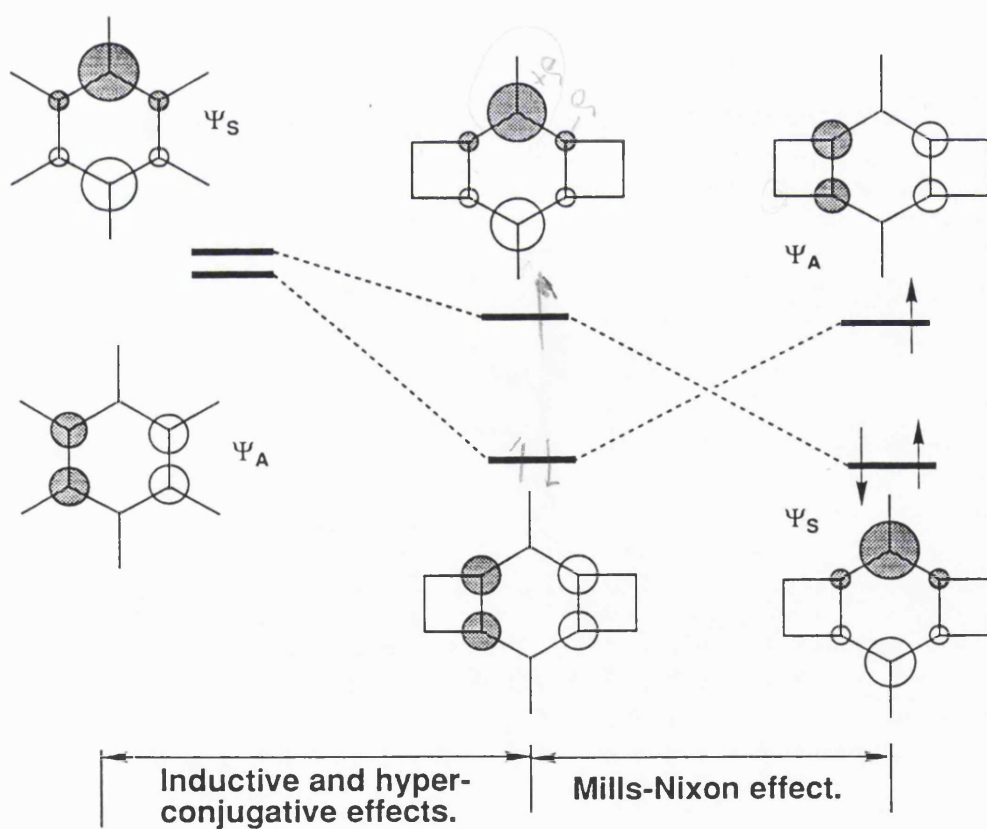


Figure 3.11. M.O. Energy levels of 3,6-dimethylbenzo[1,2:4,5]dicyclobutene.

3.3.2. Benzocyclopentenes:-

The e.s.r. spectra have indicated that the S.O.M.O. of the benzocyclopentene radical cations (3.4)⁺ and (3.5)⁺ and (3.4b)⁺, like that of the corresponding benzocyclobutene radical cations, is Ψ_A , but the vertical ionisation energies in the literature for (3.9) and (3.7),⁶ (3.15) and (3.6),⁷ and (3.16) and (3.18),⁷ (Figure 3.12), do not show clearly the relative electronic effects of the methyl and cyclo-(CH₂)₃ groups.

Again, therefore we have oxidised mixtures of hexamethylbenzene (3.9) and 3,6-dimethyl-benzo[1,2:4,5]dicyclopentene (3.4), and of (3.9) and 4,5,6,7-tetramethylbenzocyclopentene (3.5) under the conditions where each compound separately gives a strong persistent e.s.r. spectrum. This time, the e.s.r. spectra of both solutions showed the spectra consisting of about 90% (3.9)⁺ and 10% of the other component. These results are less clear cut than those obtained with the benzocyclobutenes, but they suggest that an *ortho* pair of methyl groups repels electrons more strongly than does a cyclo-(CH₂)₃ group, and the relative electron releasing ability is *ortho*-methyl > cyclo-(CH₂)₃ > cyclo-(CH₂)₂.

The ordering of the energy level thus appears again to be dominated by angle strain: recent *ab initio* M.O. calculation¹⁶ suggest that the Mills-Nixon effect associated with the cyclopentene moiety, is the same as illustrated for the cyclobutene analogue in Figure 3.10 and Figure 3.11.

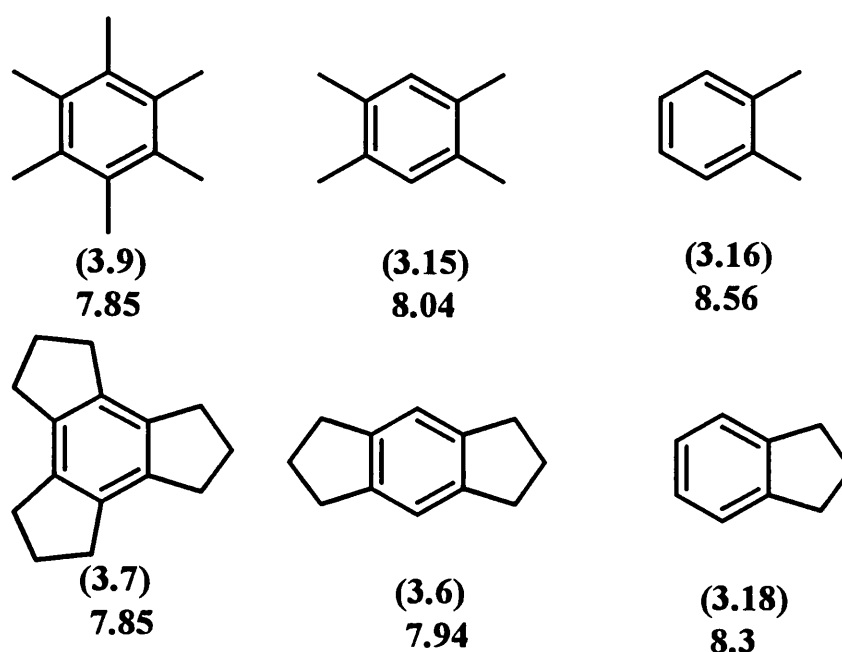


Figure 3.12 Vertical ionisation energies (eV)

3.3.3. Benzocyclohexenes:-

Angle strain within the fused cyclohexene rings should now be small, and the ordering of the energy levels would be expected to be due simply to the inductive and hyperconjugative effects of the β -protons in the methylene groups.

The e.s.r. spectra of the radical cations of the benzocyclohexenes (3.11)⁺ and (3.12)⁺ have been described in Avila's thesis¹⁷, and showed that the radical cations (3.11)⁺ and (3.12)⁺ have the unpaired electron situated principally in the Ψ_s M.O.. Vertical ionisation energies for (3.9) and (3.10), (3.15) and (3.13), and (3.16) and (3.19), in Figure (3.13) suggest that cyclo-(CH₂)₄ groups repels electrons *more* strongly than do an *ortho* pair of methyl groups, and if this sequence held in solution, the S.O.M.O. of the radical cation (3.11)⁺ and (3.12)⁺ would be expected to be Ψ_A M.O.. Unfortunately, we could not find any single set of conditions under which both methylated and the cyclo-(CH₂)₄-annelated compounds would give strong e.s.r. spectra, and we could not carry out meaningful competitive oxidation reactions.

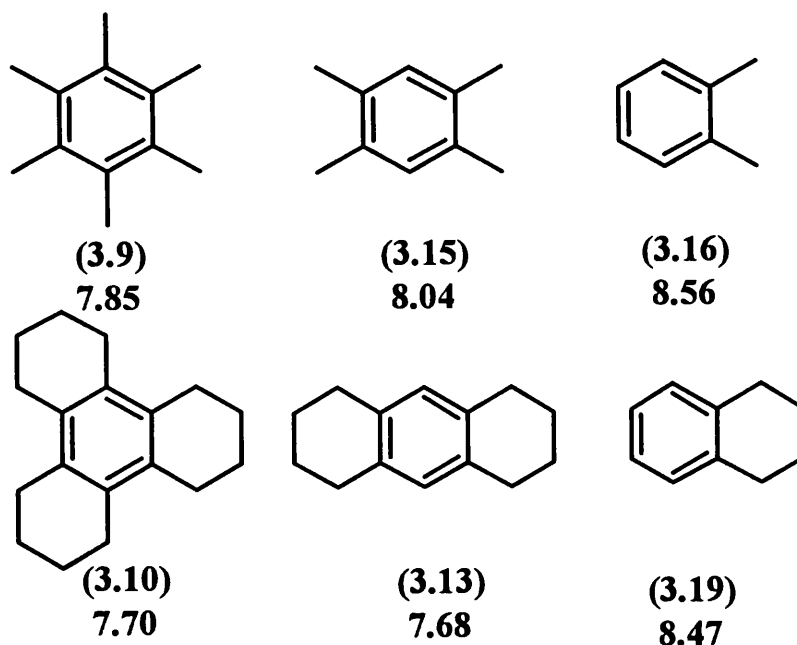


Figure 3.13. Vertical ionisation energies (eV).

Hexamethylbenzene (3.9) shows a strong e.s.r. spectrum of the radical cation on photolysis of solutions in $\text{Hg}(\text{TFA})_2/\text{TFAH}$, or $\text{Tl}(\text{TFA})_3/\text{TFAH}$, or H_2SO_4 , but dodecahydrobenzotricyclohexene (3.10) showed a spectrum only in dichloromethane containing AlCl_3 . When (3.9) and (3.10) were oxidised in mixture with $\text{Hg}(\text{TFA})_2/\text{TFAH}$, or $\text{Tl}(\text{TFA})_3/\text{TFAH}$ with photolysis, both components $(3.9)^+$ and $(3.10)^+$ were recorded. The former was rather stronger, but the spectrum of $(3.10)^+$ alone cannot be observed under these conditions. The experiment shows that the ionisation energies are rather similar under these conditions.

In addition, there is a further, and perhaps related, problem associated with these spectra of benzocyclohexene radical cations $(3.11)^+$ and $(3.12)^+$. The benzo[1,2:4,5]-dicyclohexene radical cation $(3.13)^+$ shows a total unpaired electron density ($\Sigma\rho$) 1.01, confirming the Q value for the cyclo- $(\text{CH}_2)_4$ groups in the cyclohexene ring, which was derived from benzotricyclohexene (3.10), but 3,4,5,6-tetramethylbenzocyclohexene (3.11) and 3,6-dimethylbenzo[1,2:4,5]dicyclohexene (3.12), show very low values of $\Sigma\rho_{\text{C}\alpha}$ of 0.65 and 0.71 respectively. We note that in both radical cations the S.O.M.O. is Ψ_s and that in both radical cations the electron deficiency occurs at all the arene ring atoms: in the Ψ_s M.O., the unpaired electron density should be $\frac{1}{3}$ on the C_2 axis, and $1/12$ at the other positions.

The cause of the discrepancy is not clear, but we note here briefly a number of factor which might be relevant.

(a). The spectra may have been wrongly analysed. This seems unlikely. The simulation of the spectrum of $(3.11)^+$ is very good.

(b). We have worked with Hückel unpaired electron densities rather than McLachlan spin densities. However, this treatment usually has the effect of making large coupling constants larger and small one smaller (perhaps changing the sign), but all the coupling constants in $(3.11)^+$ and $(3.12)^+$ are too small.

(c). We have ignored the excess charge effect. For α -protons, modification of the McConnell equation [eqn. (3.1)] to include this effect is shown in equation (3.4),^{18,19} where $Q = -26.6$ G and $K = -12$ G.

$$\underline{a}(\text{H}_\alpha) = Q_\alpha \rho_{\text{C}\alpha} + K \rho_{\text{C}\alpha}^2 \quad (3.4)$$

This is a small perturbation to the McConnell equation. If a similar equation applies to coupling of β -protons, where Q and K have the same sign, this would not be able to account for the low values of $\Sigma\rho_{C\alpha}$ in (3.11) and (3.12).

(d). The molecules may be distorted, and equations (3.1) and (3.3) assume sp^2 hybridisation in a planar arene. The methylene groups benzo[1,2:4,5]dicyclohexene (3.13) have been shown to be 3.8° out of the plane of the arene ring,^{20,21} but this compound shows $\Sigma\rho_{C\alpha} = 1.01$. A similar and perhaps larger distortion may occur in compounds (3.11) and (3.12) which are more sterically congested.

(e). Interaction between the methyl groups and the cyclohexene rings might affect the $\cos^2\theta$ term in equation (3.2). We have therefore prepared two compounds, 4,5-dimethyl-benzocyclohexene and 3,6-dimethylbenzocyclohexene, and attempted to examine the effect. Unfortunately, we could not obtain any useful spectra when the two compounds were treated with a variety of oxidizing agents [TFAH with or without $Hg(TFA)_2$, $Tl(TFA)_3$, or H_2SO_4 ; $AlCl_3/CH_2Cl_2$; DDQ/TFAH with or without $MeSO_3H$, or CF_3SO_3H ; all with or without photolysis].

References

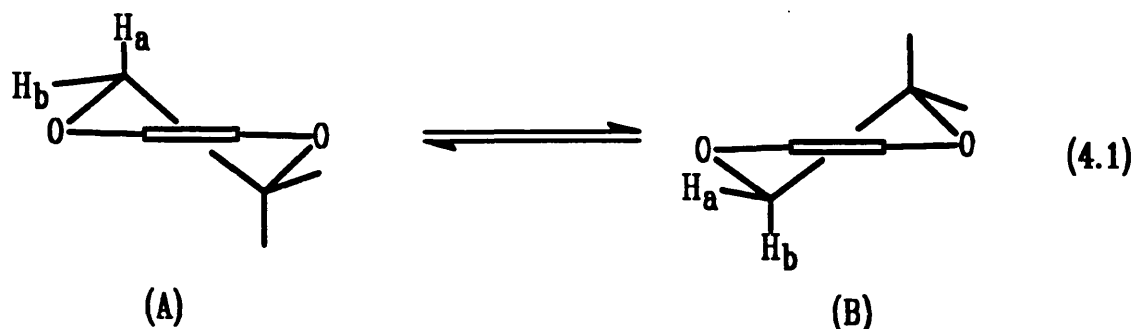
1. F. Gerson, *High Resolution E.S.R. Spectroscopy*, Wiley-Verlag Chemie, Berlin, 1976.
2. R.M. Dessau, S. Shih and E.I. Heiba, *J. Am. Chem. Soc.*, 1970, **92**, 412.
3. S.G. Lias, J.E. Bartmess, J.E. Liebman, J.L. Holmes, R.D. Levin and W.G. Mallard, *J. Phys. Chem., Ref. Data*, 1988, **17**, Suppl. 1.
4. A.D. McLachlan, *Mol. Phys.*, 1960, **3**, 233.
5. H. Bock, *Angew. Chem., Int. Engl.*, 1977, **16**, 613
6. F. Brogli, E. Giovannina, E. Heilbronner and R. Schurter, *Chem. Ber.*, 1973, **106**, 961.
7. C. Santiago, R.W. Gandour, K.N. Houk, W. Nutakul, W.E. Cravey and R.P. Thummel, *J. Am. Chem. Soc.*, 1978, **100**, 3730.
8. W.H. Mills and I.G. Nixon, *J. Chem. Soc.*, 1930, 2510.
9. M.J. Collins, J.E. Gready, S. Sternhell and C.W. Tansy, *Aust. J. Chem.*, 1990, **43**, 1547.
10. R. Boese and D. Blaser, *Angew. Chem., Int. Ed. Engl.*, 1988, **27**, 304
11. R. Boese and D. Blaser, in *Strain and its Implications in Organic Chemistry*, eds., A. de Maijere and S. Blechert, Kluwer Academic Publishers, Dordrecht, 1989.
12. R. Benassi, S. Ianelli, M. Nardelli and F. Taddei, *J. Chem. Soc., Perkin Trans. 2*, 1991, 1381.
13. M. Eckert-Maksic, A. Lesar and Z.B. Maksic, *J. Chem. Soc., Perkin Trans. 2*, 1992, 993.
14. R.A. Finnegan, *J. Org. Chem.*, 1965, **30**, 1333.
15. A. Streitwieser, G.R. Ziegler, P.C. Mowery, A. Lewis and R.G. Lawler, *J. Am. Chem. Soc.*, 1968, **90**, 1357.
16. J.E. Bloor, M. Eckert-Maksić, M. Hodošček, Z.B. Maksić and K. Pojanec, *New J. Chem.*, 1993, **17**, 157.
17. D.V. Avila, Ph.D., Thesis, University of London, 1990.

18. J.R. Bolton, in *Radical Ions*, ed. E.T. Kaiser and L. Kevan, Interscience, New York, 1968, Chap.1.
19. J.P. Colpa and J.R. Bolton, *Mol. Phys.*, 1963, **6**, 309.
20. M.A. Wilson, A.M. Vassallo, M.I. Burgaer, P.J. Collins, B.W. Skelton and A.H. White, *J.Phys.Chem.*, 1986, **90**, 3944.
21. H. Van Koningsveld and J.M.A. Baas, *Acta Crystallogr., Sect. C*, 1984, **40**, 311.
22. R.P. Thummel and W. Nutakul, *J. Org. Chem.*, 1978, **43**, 3170.

Chapter 4. Conformational Inversion of Derivatives of Benzo-1,4-dioxane Radical Cations

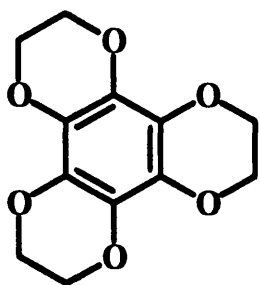
4.1. Background

The e.s.r. spectra of the radical cations of dioxene, 2,3-dimethyldioxene and benzo-1,4-dioxane in fluid solution have been observed in this research group by A.G. Davies and C.J. Shields.¹ The *pseudo*-axial and *pseudo*-equatorial protons (equation 4.1) of the methylene groups in the half-chair dioxene rings are distinguished by different hyperfine coupling constants, and simulation of the spectra over a range of temperatures has given the Arrhenius parameters for the ring inversion.

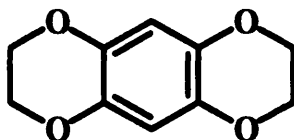


Later, D.V. Avila examined and characterised the tris(ethylenedioxy)benzene radical cation (4.0)⁺ by variable temperature e.s.r. spectroscopy.² He found a substantial ring inversion barrier (e.g. $E_a = 11.30 \text{ kcal mol}^{-1}$) in the dioxenes; in comparison, the activation energy for inversion of the cyclohexene ring in the dodecahydrotriphenylene radical cation (3.10)⁺ is $4.80 \text{ kcal mol}^{-1}$.

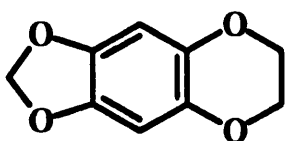
In this chapter, we extend this study to an investigation of the factors governing this high inversion barrier particularly in some less sterically hindered molecules such as benzo[1,2-b:4,5-b']bis-1,4-dioxane (4.1), (4.2), (4.3), (4.4) and (4.5).



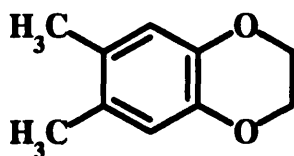
(4.0)



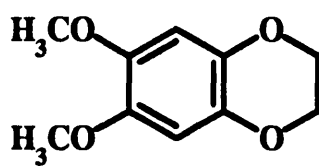
(4.1)



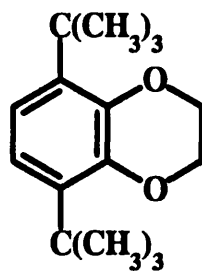
(4.2)



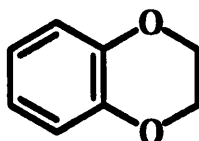
(4.3)



(4.4)



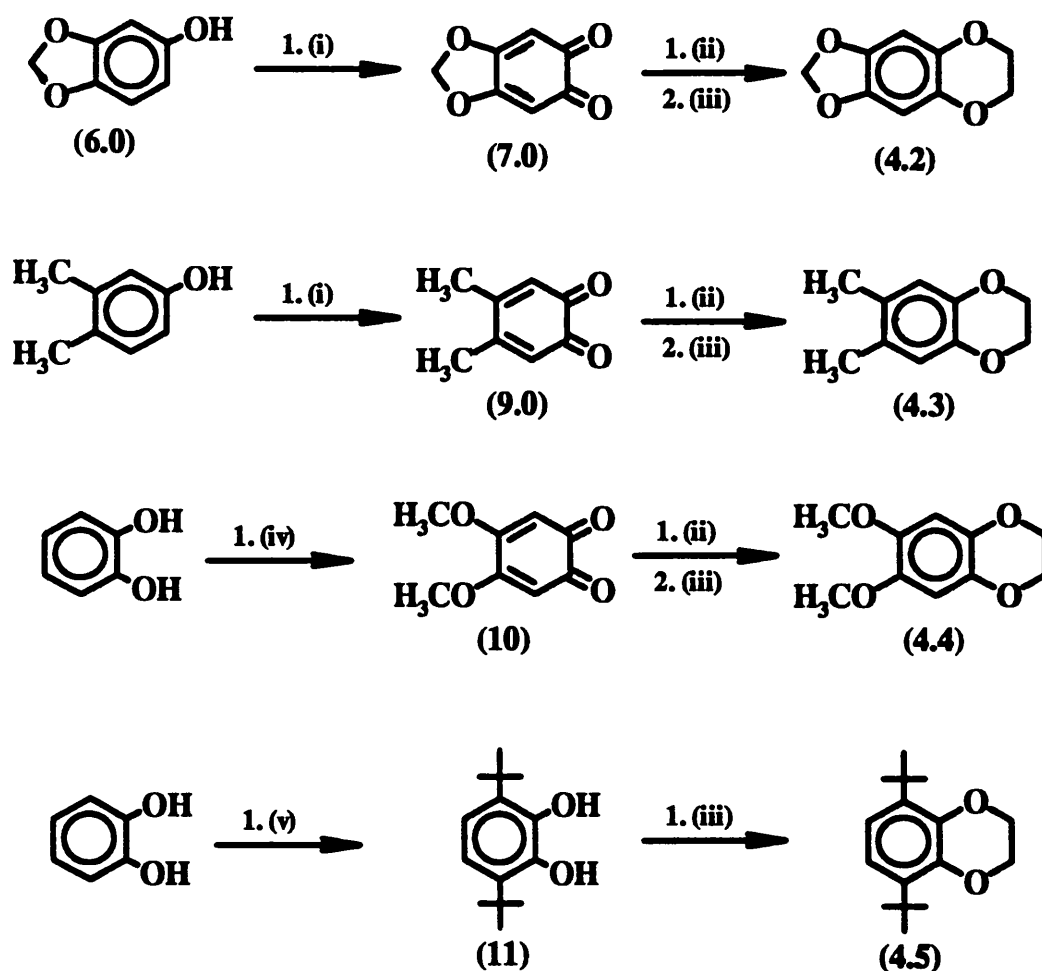
(4.5)



(4.6)

4.2. Results.

The compounds tris(ethylenedioxy)benzene (4.0) and benzo[1,2-d:4,5-d']bis-1,4-dioxane (4.1) were supplied by Dr. R. Lapouyade (University of Bordeaux 1). The benzo-1,4-dioxanes (4.2), (4.3), (4.4) and (4.5) were prepared by ethylenation of the appropriate catechol with 1,2-dibromoethane in acetone containing potassium carbonate (Scheme 4.1).

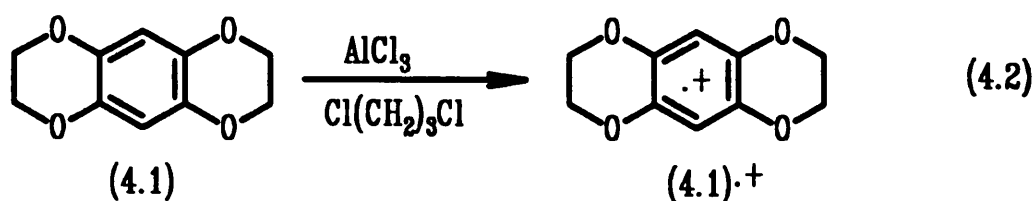


Conditions: (i) Fremy's salt; (ii) $\text{Na}_2\text{S}_2\text{O}_4(\text{aq})$; (iii) $\text{BrCH}_2\text{CH}_2\text{Br}$, K_2CO_3 , in acetone at 120°C ; (iv) $\text{NaIO}_3/\text{MeOH}$ and (v) titanium catecholate, *iso*-butylene in xylene at 110°C .

Scheme 4.1

4.2.1. Benzo[1,2-d:4,5-d']bis-1,4-dioxane (4.1)

The e.s.r. spectrum of (4.1)^{•+} was readily observable without photolysis when benzo[1,2-d:4,5-d']bis-1,4-dioxane (4.1) was dissolved in concentrated sulphuric acid, trifluoroacetic acid containing thallium(III) trifluoroacetate, liquid sulphur dioxide containing fluorosulphonic acid, or 1,3-dichloropropane containing aluminium chloride. At 321 K, the spectrum consisted of a pure nonet of triplets (Figure 4.0a).



In $\text{ClCH}_2\text{CH}_2\text{CH}_2\text{Cl}/\text{AlCl}_3$, (4.1)^{•+} could be studied between 174-321 K. At about 304 K, the intensity of the nonet decreased (Figure 4.0b), then at about 278 K, the nonet splitting was lost (Figure 4.0c), and near 223 K, the spectrum was unsymmetrical about the central line. We managed to obtain the following hyperfine coupling constants: $\underline{a}(2\text{H})$ 0.86 G, $\underline{a}(4\text{H}_{ax})$ 2.16 G and $\underline{a}(4\text{H}_{eq})$ 0.28 G at 223K. Computer simulation of these spectra over the temperature range 253-321 K gave the Arrhenius plot shown in Figure 4.1, with $\log_{10}A$ is 16.22, and the inversion barrier (E_a) 11.05 kcal mol⁻¹ for conformational equilibrium (equation 4.1).

The 400 MHz ¹H N.M.R. spectrum of (4.1) in CHF_2Cl containing 10% CD_2Cl_2 was recorded down to 130 K. The 1,2-dioxyethane group gave a signal at δ 4.22 at 293 K, and this showed no sign of broadening and separating into separate signals for axial and equatorial protons at the lowest temperature.

4.2.2. 1,3-Dioxolo[4,5-g]benzo-1,4-dioxane (4.2)

There appears to be no report in the literature of the study by variable temperature e.s.r. spectroscopy of the 1,3-dioxolo[4,5-g]benzo-1,4-dioxane radical cation (4.2)^{•+}.

The e.s.r. spectrum of (4.2)^{•+} is readily accessible by treatment of the compound (4.2) with $\text{Ti}^{3+}/\text{TFAH}$, $\text{FSO}_3\text{H}/\text{SO}_2$ or $\text{AlCl}_3/\text{CH}_2\text{Cl}_2$. The most appropriate conditions for generating this radical cation for variable temperature e.s.r. studies are in 1,3-dichloropropane containing AlCl_3 .

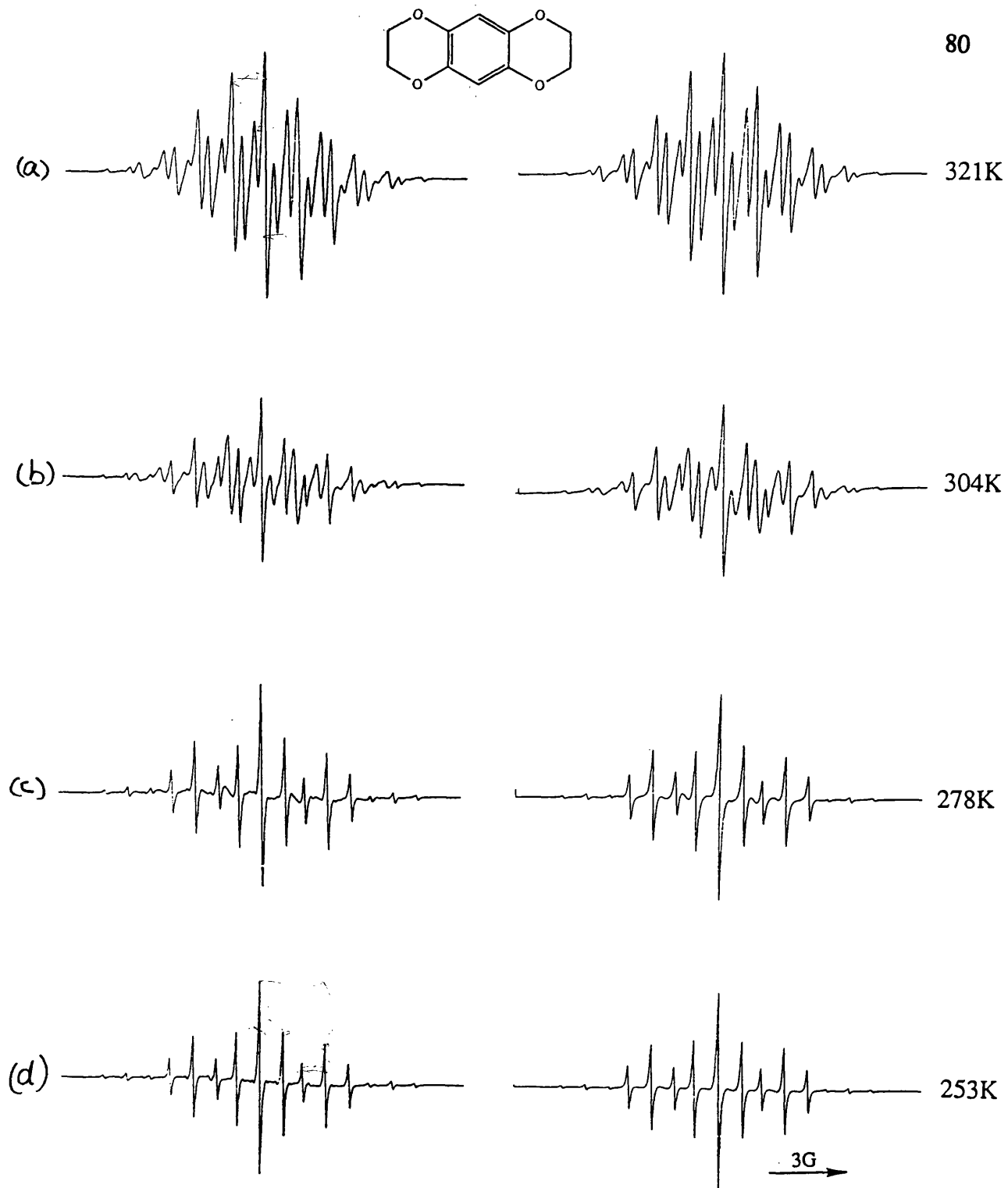


Figure 4.0. The e.s.r. spectra (left) and simulations (right) of the benzo[1,2-d:4,5-d']bis-1,4-dioxane radical cation (4.1)⁺ in ClCH₂CH₂CH₂Cl/AlCl₃.

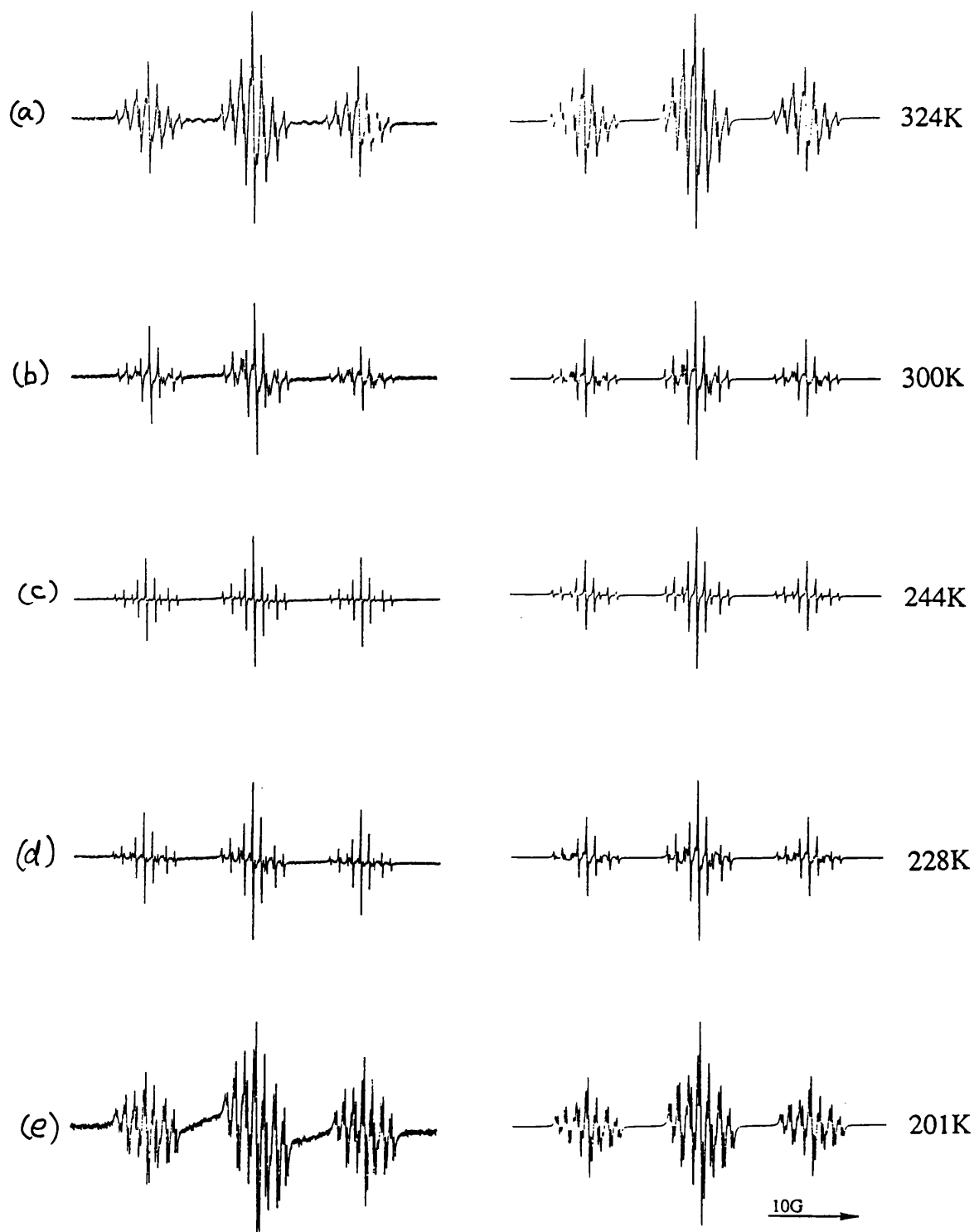
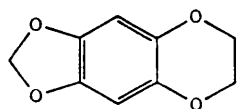


Figure 4.2. The e.s.r. spectra (left) and simulations (right) of the 1,3-dioxolo[4,5-g]benzo-1,4-dioxane radical cation (4.2)⁺ in ClCH₂CH₂CH₂Cl/AlCl₃.

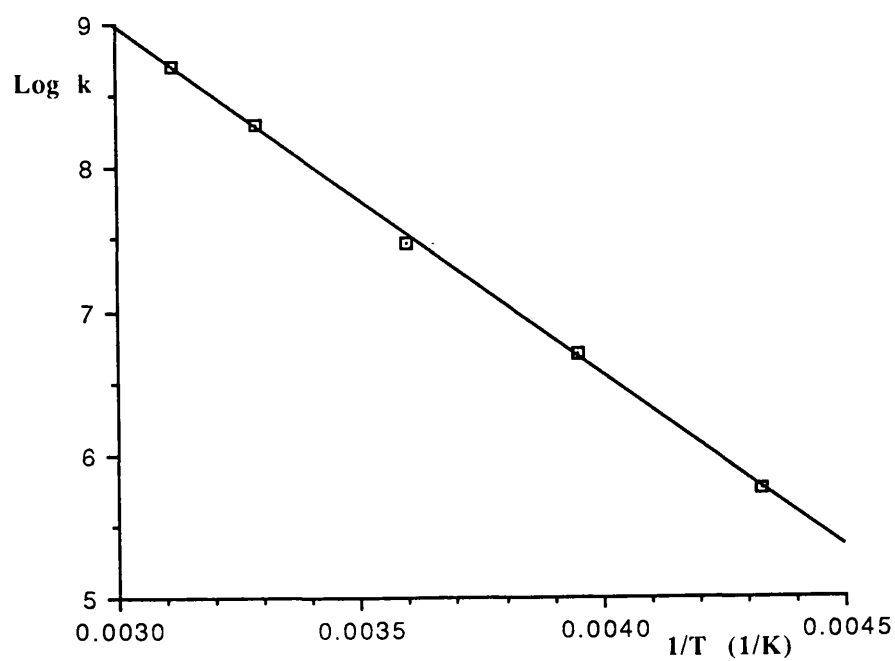


Figure 4.1. Arrhenius plot for the conformational inversion of (4.1)⁺.

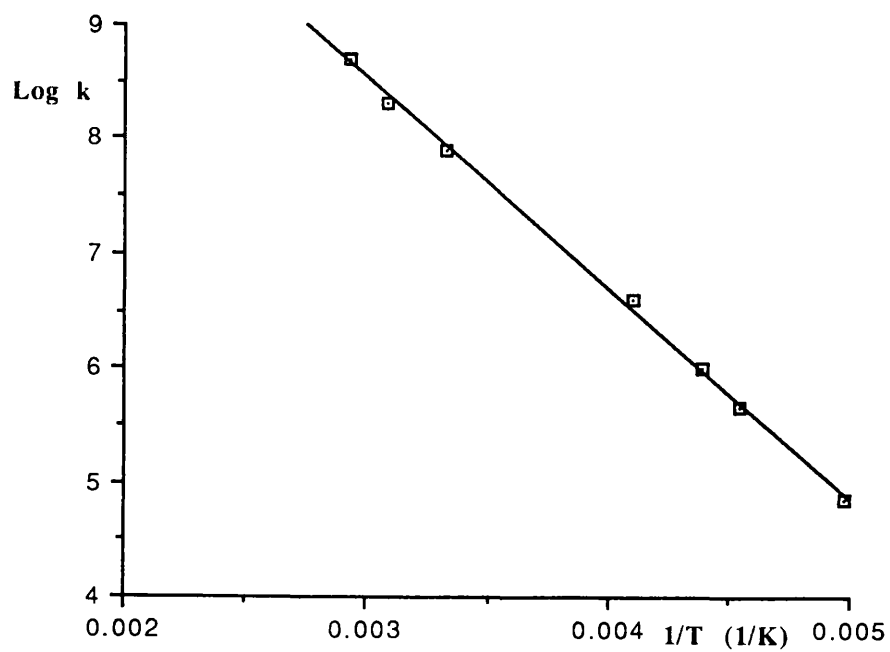
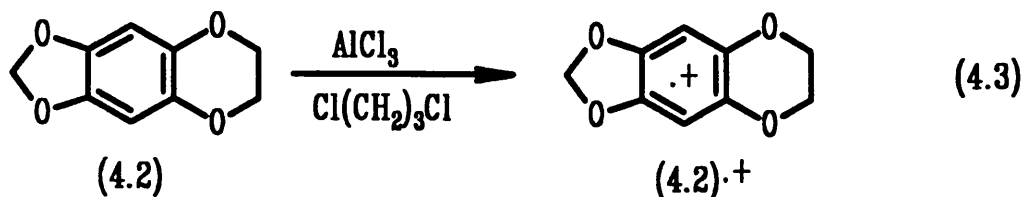
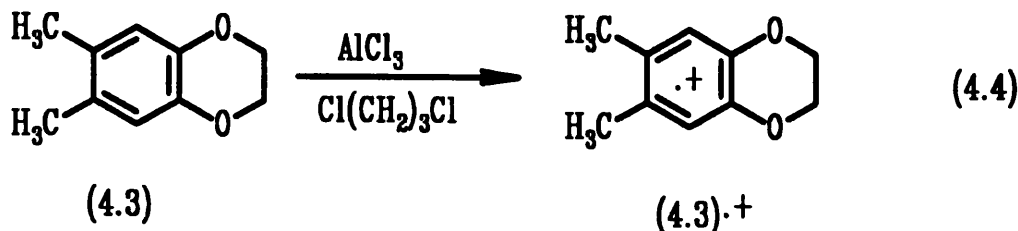


Figure 4.3. Arrhenius plot for the conformational inversion of (4.2)⁺.



At 321 K, the spectrum (Figure 4.2a) consisted of a triplet of quintets of triplets with $\underline{a}(2\text{H})$ 12.08 G, $\underline{a}(4\text{H})$ 1.24 G and $\underline{a}(2\text{H})$ 0.98 G. At around 244 K, the spectrum (Figure 4.2c) showed some alternating linewidth effect and the quintets were lost. Finally, at 201 K, the spectrum illustrated in Figure 4.2d was obtained, and showed the couplings to the methylene protons in the $-\text{OCH}_2\text{CH}_2\text{O}-$ resolved into a triplet of triplets, resulting from non-equivalent axial and equatorial methylene protons. The spectra were computer-simulated over the temperature range 201-324 K and gave the Arrhenius plot shown in Figure 4.3, and with $\log_{10}A = 14.07$ and $E_a = 8.45 \text{ kcal mol}^{-1}$.

4.2.3. 6,7-Dimethylbenzo-1,4-dioxane (4.3)

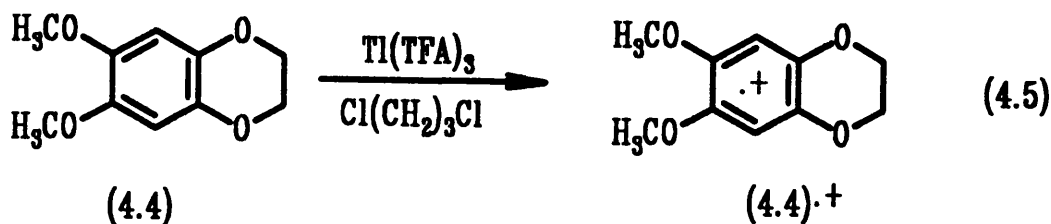


The spectrum of the radical cation of 6,7-dimethylbenzo-1,4-dioxane (4.3) has not been observed before. We found that the spectrum of $(4.3)^{\bullet+}$ could be recorded when (4.3) was dissolved in $\text{Ti}^{3+}/\text{TFAH}$ or $\text{FSO}_3\text{H}/\text{SO}_2$.

If the compound (4.3) was oxidised in 1,3-dichloropropane containing AlCl_3 , it gave the temperature-dependent e.s.r. spectra in Figure 4.4 which, at 189 K, consists of a septet of triplets of triplets of triplets with $\underline{a}(6\text{H})$ 7.00 G, $\underline{a}(2\text{H})$ 0.70 G, $\underline{a}(2\text{H}_{ax})$ 3.30 G and $\underline{a}(2\text{H}_{eq})$ 0.70 G.

At about 209 K, the spectrum of $(4.3)^{\bullet+}$ shows a strong alternating linewidth effect, then at near 345 K the coupling to the four methylene protons became a quintet. These spectra could be kinetic simulated for determining the kinetics of ring inversion process (Figure 4.5), giving $\log_{10}A = 13.64$ and $E_a = 7.43 \text{ kcal mol}^{-1}$.

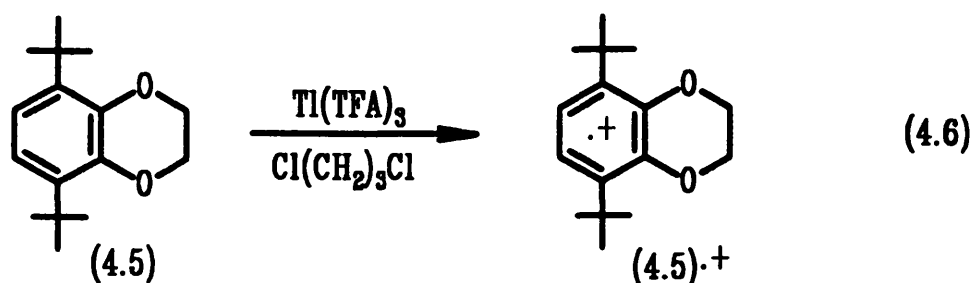
4.2.4. 6,7-Dimethoxybenzo-1,4-dioxane (4.4)



The e.s.r. spectrum of the 6,7-dimethoxybenzo-1,4-dioxane radical cation (4.4)^{•+} has not been reported previously.

A solution of 6,7-dimethoxybenzo-1,4-dioxane (4.4) in 1,3-dichloropropane containing thallium(III) trifluoroacetate at 313 K showed a spectrum of (4.4)^{•+} with $\underline{a}(6\text{H})$ 2.20 G, $\underline{a}(2\text{H})$ 0.82 G and $\underline{a}(4\text{H})$ 1.14 G (Figure 4.6). At 292 K, alternate lines became significantly broad, then at about 203 K the spectrum could be analysed in terms of $\underline{a}(6\text{H})$ 2.20 G, $\underline{a}(2\text{H})$ 0.82 G, $\underline{a}(2\text{H}_{\text{ax}})$ 2.08 G and $\underline{a}(2\text{H}_{\text{eq}})$ 0.20 G. Computer simulation of these spectra gave the rate constants for the ring inversion process which are shown in the Arrhenius plot in Figure 4.7, and gave $\log_{10}A = 14.45$ and $E_a = 8.85 \text{ kcal mol}^{-1}$. The spectra also indicate free rotation of the methoxy groups.

4.2.5. 5,8-Di-*tert*-butylbenzo-1,4-dioxane (4.5)



The e.s.r. spectrum of the radical cation of 5,8-di-*tert*-butylbenzo-1,4-dioxane (4.5) was observed by Bubnov *et al.* from a solution of compound (4.5) in dichloromethane containing thallium(III) trifluoroacetate with a small amount of TFAH. At high temperature, the spectrum showed $\underline{a}(2\text{H})$ 4.20 G and $\underline{a}(4\text{H})$ 2.65 G. Variable temperature e.s.r. spectroscopy was carried out between 153 and 353 K and provided, for the ring inversion barrier, $E_a = 5.00 \text{ kcal mol}^{-1}$ and $\log_{10}A = 11.96$.⁵

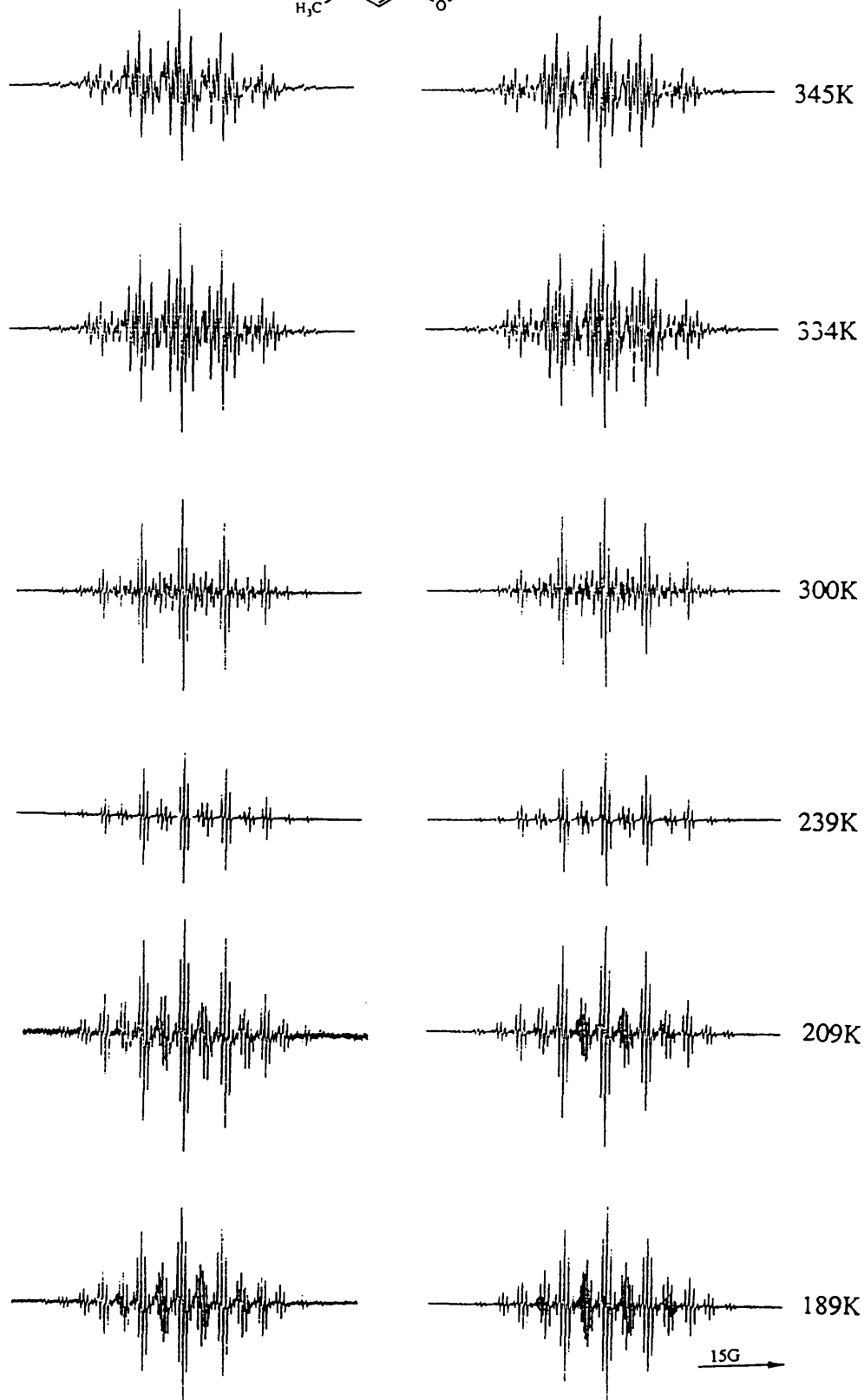
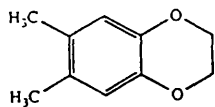


Figure 4.4. The e.s.r. spectra (left) and simulations (right) of the 6,7-dimethylbenzo-1,4-dioxane radical cation (4.3)⁺ in $\text{ClCH}_2\text{CH}_2\text{CH}_2\text{Cl}/\text{AlCl}_3$.

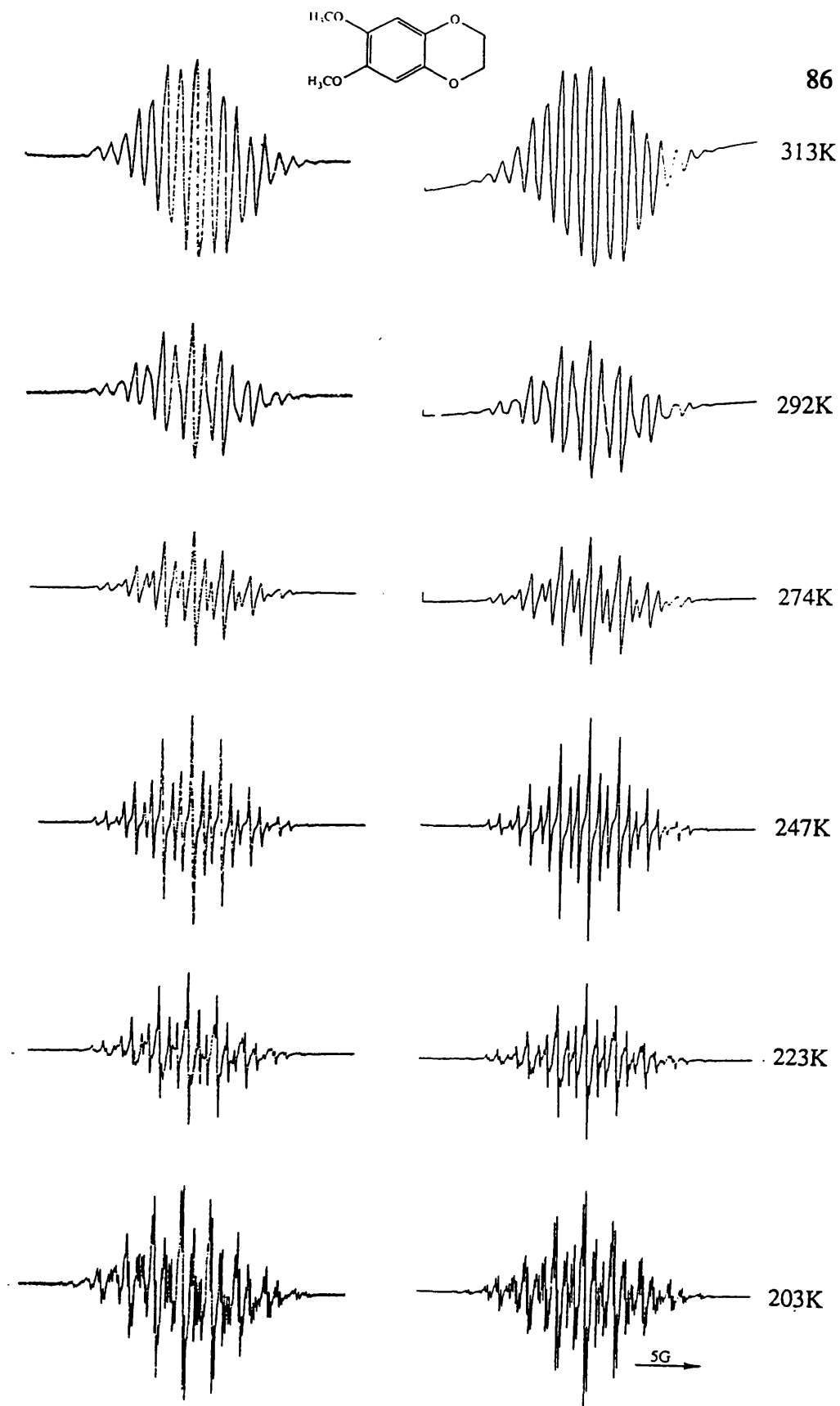


Figure 4.6. The e.s.r. spectra (left) and simulations (right) of the 6,7-dimethoxybenzo-1,4-dioxane radical cation (4.4)⁺ in ClCH₂CH₂CH₂Cl/AlCl₃.

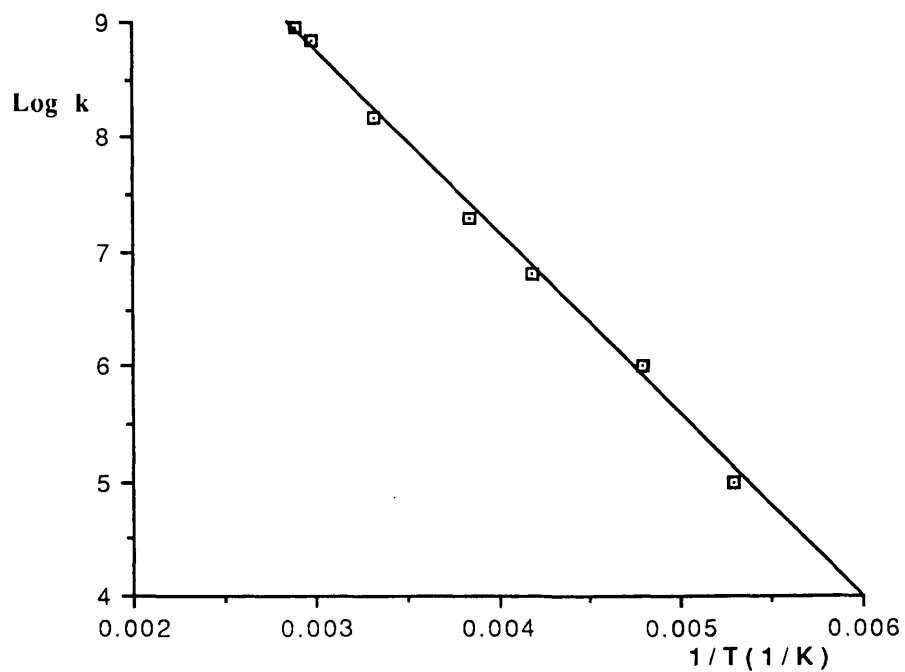


Figure 4.5. Arrhenius plot for the conformational inversion of (4.3)⁺.

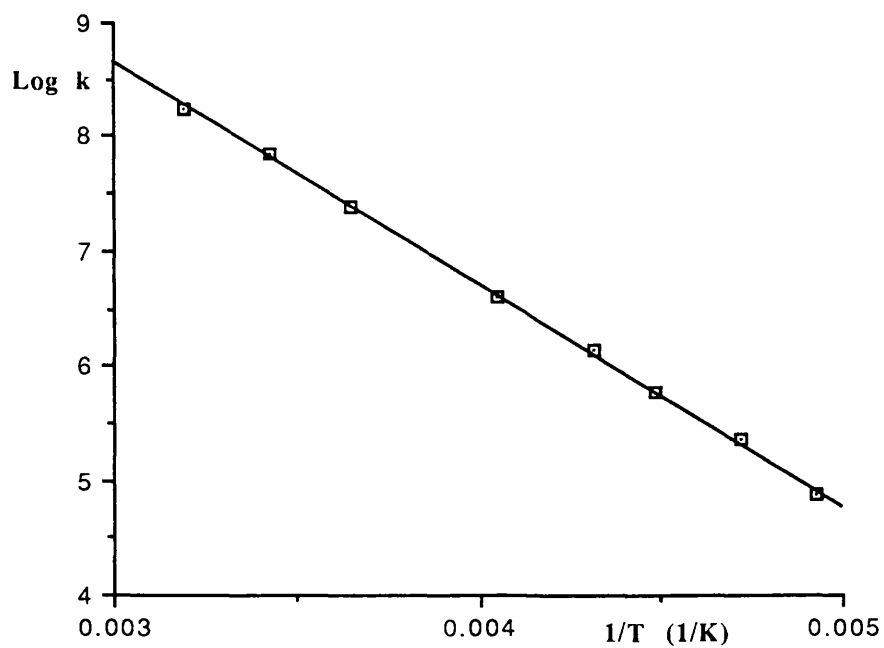
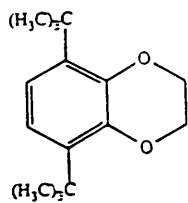


Figure 4.7. Arrhenius plot for the conformational inversion of (4.4)⁺.



88

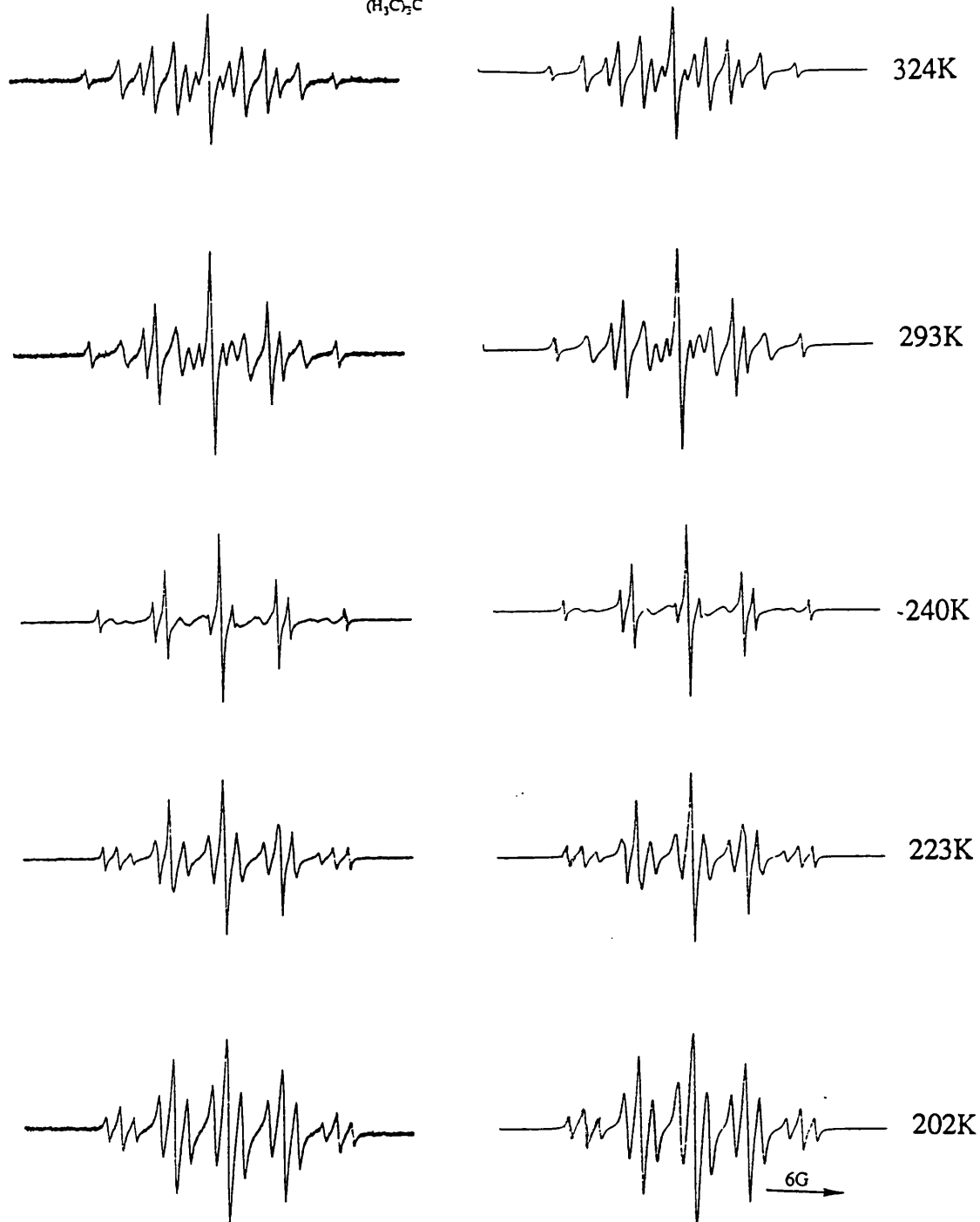


Figure 4.8. The e.s.r. spectra (left) and simulations (right) of the 5,8-di-*tert*-butylbenzo-1,4-dioxane radical cation (4.5)⁺ in $\text{ClCH}_2\text{CH}_2\text{CH}_2\text{Cl}/\text{Ti}(\text{TFA})_3$.

If we used 1,3-dichloropropane with one drop of TFAH instead of dichloromethane, the solution showed a strong spectrum of $(4.5)^+$ without photolysis. About 333 K the spectrum showed $\underline{a}(2H)$ 4.30 G and $\underline{a}(4H)$ 2.60 G. Between 324 and 202 K, alternate lines in the quintet broadened and resolved into two separate signals so that at low temperature the spectra could be analysed with $\underline{a}(2H)$ 4.30 G, $\underline{a}(2H_{ax})$ 4.10 G and $\underline{a}(2H_{eq})$ 1.10 G (Figure 4.8). Kinetic simulation of these spectra gave the Arrhenius plot in Figure 4.9, which gives $\log_{10}A = 13.71$ and $E_a = 7.63 \text{ kcal mol}^{-1}$ for the ring inversion process of $(4.5)^+$.

The inversion barrier measured by Bubnov is a lot smaller than the one we found, but our spectra are of much better quality than those reported previously. Also we have at least two further radical cations [e.g. $(4.3)^+$ and $(4.4)^+$] with similar high values. We note also that their $\log_{10}A$ value is smaller than ours.

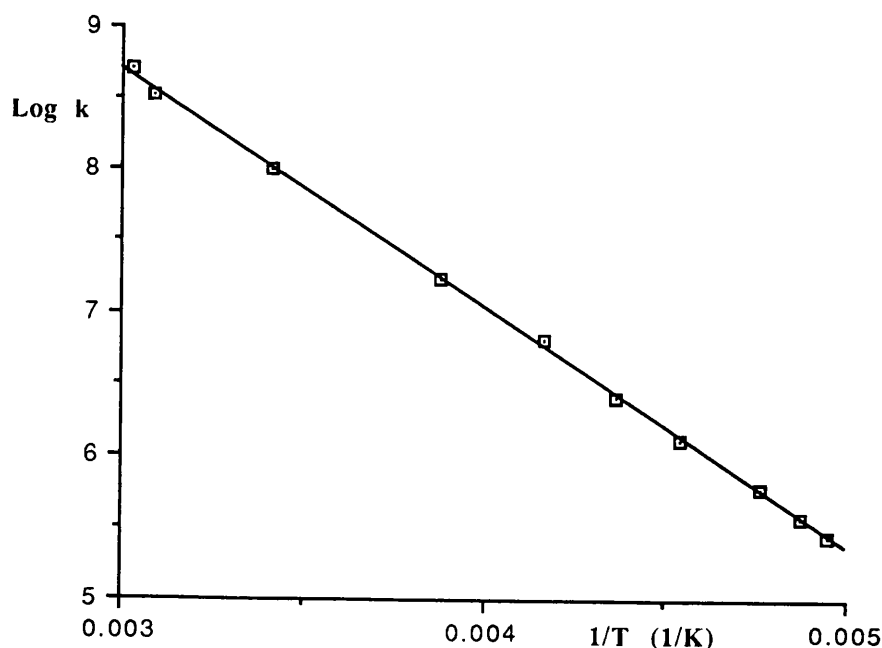


Figure 4.9. Arrhenius plot for the conformational inversion of $(4.5)^+$.

Table 4.0. The e.s.r. spectra of benzo-1,4-dioxanes and benzocyclohexenes radical cations, and Arrhenius parameters for equation (4.1).

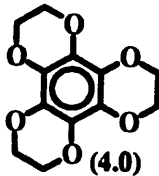
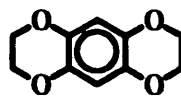
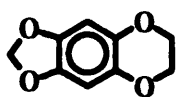
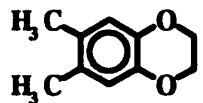
Radical Cations	$\underline{a}(H_{ax})/G$		$\underline{a}(H_{eq})/G$		$\underline{a}(H)/G$ Others		Ratio $\underline{a}(H_{ax})/\underline{a}(H_{eq})$	$E_a/$ kcal mol ⁻¹	log ₁₀ A	g-factor	Ref.
 (4.0)	6H	1.13	6H	0.17	-		6.6	11.30	16.00	2.0038	(b)
 (4.1)	4H	2.16	4H	0.28	2H	0.86	7.7	11.05	16.22	2.0042	(a)
 (4.2)	2H	2.20	2H	0.28	2H	0.94	7.8	8.45	14.07	2.0040	(a)
 (4.3)	2H	3.30	2H	0.70	2H	0.70	4.71	7.43	13.64	2.0039	(a)
					6H	7.00					

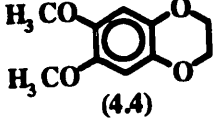
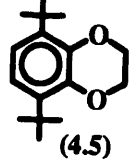
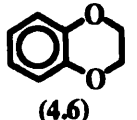

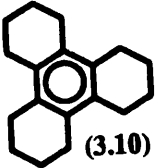
Table 4.0 (continued) Radical Cations	$\underline{a}(\text{H}_{\text{ax}})/\text{G}$	$\underline{a}(\text{H}_{\text{eq}})/\text{G}$	$\underline{a}(\text{H})/\text{G}$ Others	Ratio $\underline{a}(\text{H}_{\text{ax}})/\underline{a}(\text{H}_{\text{eq}})$	E_a kcal mol ⁻¹	log ₁₀ A	g-factor	Ref.
 (4.4)	2H 2.08	2H 0.20	2H 0.82 6H 2.20	10.5	8.85	14.45	2.0038	(a)
 (4.5)	2H 4.10	2H 1.10	2H 4.30	3.73	7.63 [5.00]	13.71 [11.96]	2.0037	(a) [(c)]
 (4.6)	2H 4.01	2H 0.95	2H 0.40 2H 4.57	4.22	8.29	15.1	2.0038	(e)

Table 4.0 (continued) Radical Cations	$\underline{a}(H_{ax})/G$	$\underline{a}(H_{eq})/G$	$\underline{a}(H)/G$ Others	Ratio $\underline{a}(H_{ax})/\underline{a}(H_{eq})$	E_a kcal mol ⁻¹	log ₁₀ A	g-factor	Ref.
 (3.13)	4H 20.15	4H 10.85	-	1.86	4.00	12.8	2.0029	(d)
 (3.10)	6H 13.31	6H 7.17	-	1.85	4.80	12.8	2.0028	(d)

(a) Present Work, (b) See Ref. 2, (c) See Ref. 5, (d) See Ref. 3 and (e) See Ref. 1.

4.3. Discussion

The e.s.r. spectra of the radical cations (4.0)⁺-(4.6)⁺ containing the -OCH₂CH₂O- group often show significant hyperfine interactions attributed these methylene protons. We believe the interaction is principally via hyperconjugative coupling between the C-H bond and the unpaired spin densities located on the oxygen atom.⁶

The Hückel model predicts that the H.O.M.O. of benzo-1,3-dioxole and of its radical cation should have a node between the terminal atoms of the O-C=C-O system as shown in Figure 4.10.⁷

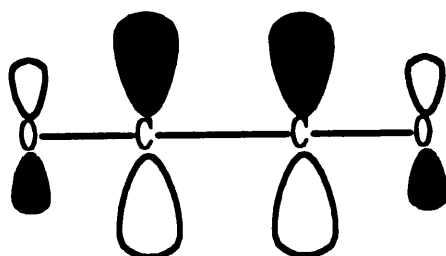


Figure 4.10.

The ratio of $\underline{a}(H_{ax})/\underline{a}(H_{eq})$ varies between 3.7 and 10.5 in our five benzo-1,4-dioxane radical cations and does not remain constant at 4.22 as found in ref. 1 for benzo-1,4-dioxane itself and some 1,4-dioxenes.¹

We have found that the barrier to inversion (equation 4.1) is particularly high for the benzo-1,4-dioxane radical cations (4.0)⁺-(4.6)⁺.

The cause of this high barrier has not been fully understood, but we note here a number of factors which might be relevant.

(a) Preliminary variable temperature n.m.r. spectroscopic studies have been made of tris(ethylenedioxy)benzene (4.0) and benzo[1,2-b:4,5-b']bis[1,4]dioxane (4.1). At room temperature, the ¹H n.m.r. spectra of (4.0) and (4.1) gave a singlet signal for the methylene groups, and these separated into separate signals for axial and equatorial protons at a similar temperature (130 K). From these preliminary results, we therefore suggest that the energy barrier in the neutral molecules should be similar. Our results in Table 4.0 show that the inversion barrier of the radical cations (4.0)⁺ and (4.1)⁺ are similar, but that of (4.0)⁺ appears to be slightly higher. This is probably due to intramolecular lone-pair/lone-pair repulsion in (4.0)⁺ which is illustrated in Figure 4.11.

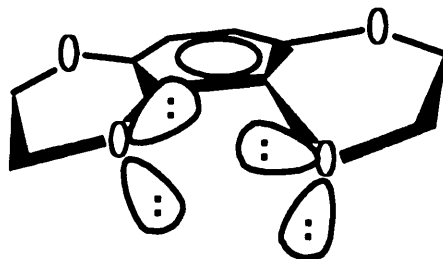


Figure 4.11. Intramolecular lone-pair/lone-pair repulsion.

(b) These molecules contained an extended conjugated system. If the transition state is planar, the inversion process involves twisting about the terminal O-C bonds where the wave function in Figure 4.10 is locally antibonding, and this would increase the activation energy for achieving the transition state.

(c) A C-O bond is normally accepted to be substantially shorter than the corresponding C-C bond. X-Ray diffraction studies of compounds (4.0) and (4.1) have not been reported. An alternative way to estimate the molecular structures is to use a molecular modelling program such as the Desktop Molecular Modeller (DTMM) ver. 2.0, which can carry out a molecular energy minimization. This suggested that the C-O bond in compound (4.0) is shorter than the C-C bond in compound (3.10) (Figure 4.12). In a flexible ring system, if the bonds become shorter it requires a higher activation energy to achieve the inversion process.

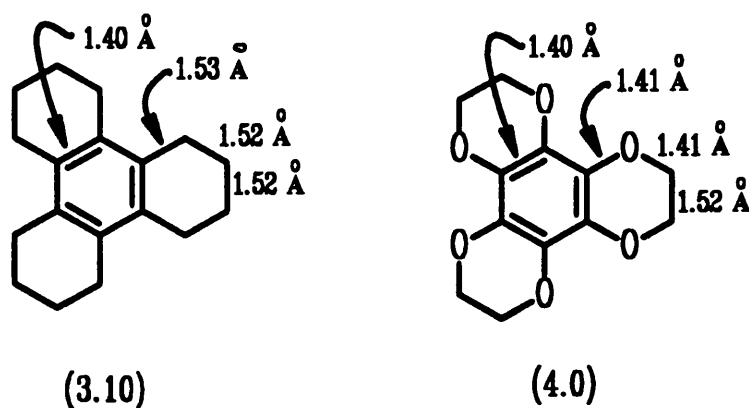


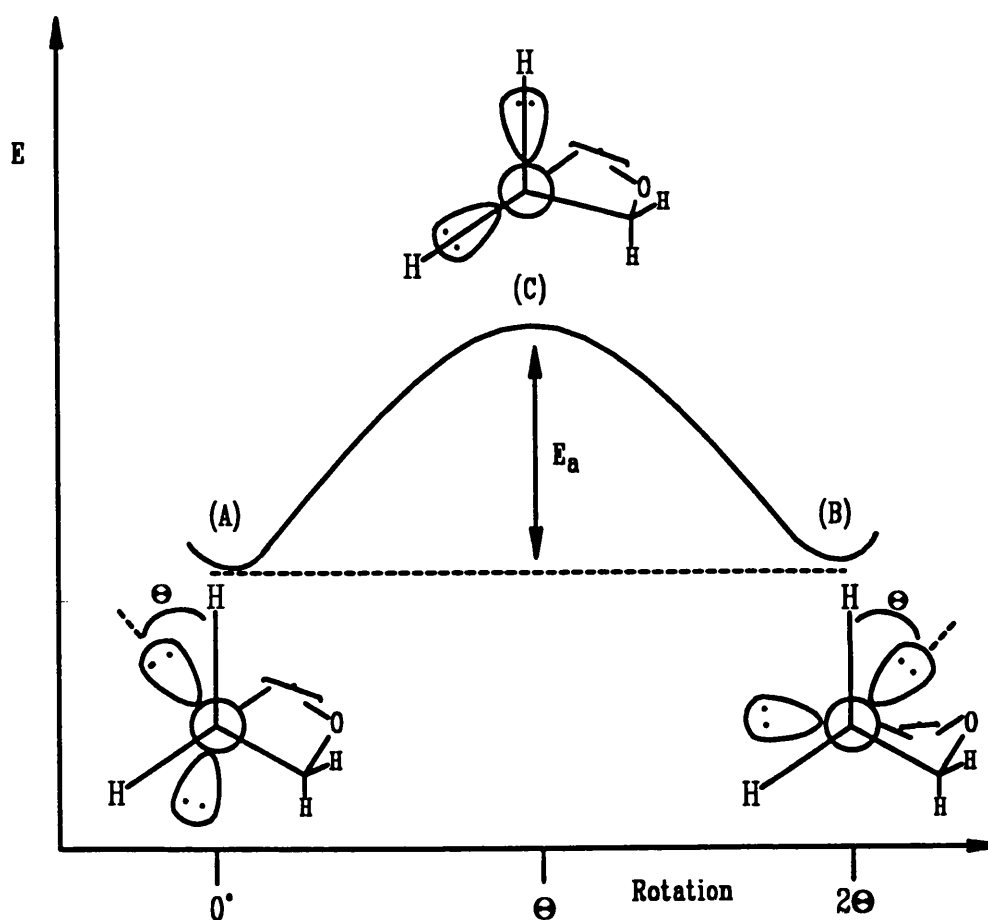
Figure 4.12. Energy minimization of molecules (4.0) and (3.10).

(d) In 1970, R.J. Gillespie described the Valency Shell Electron Pair Repulsion (VSEPR) theory that could predict the shape of molecules. The VSEPR theory states:^{8,9}

(i) A non-bonding or lone-pair is larger and occupies more space on the surface than a bonding pair.

(ii) The relative repelling ability is lone-pair/lone-pair > lone-pair/bonding pair > bonding pair/bonding pair.

According to Gillespie's arguments, the inversion process can be illustrated in Scheme 4.2 [(A) \rightleftharpoons (C) \rightleftharpoons (B)]. This suggests that the energies required to achieve the transition state (C) in the benzo-1,4-dioxane should be greater than in the benzocyclohexenes, because the lone-pair/bonding pair repel more strongly than the bonding-pair/bonding-pair.



Scheme 4.2. Gillespie's model of VSEPR

References

1. A.G. Davies, C.J. Shields, J.C. Evans and C.C. Rowlands, *Can. J. Chem.*, 1989, **67**, 1748.
2. D.V. Avila and A.G. Davies, Unpublish work.
3. D.V. Avila , A.G. Davies and M.L. Girbal, *Tetrahedron*, 1990, **46**, 1999.
4. W. Dixon and D. Murphy, *J. Chem. Soc., Perkin Trans. 2*, 1976, 1823.
5. N.A. Malysheva, A.I. Prokof'ev, N.N. Bubnov, S.P. Solodovinkov, T.I. Prokof'ev, V.B. Vol'eva, V.V. Ershov and M.I. Kabachnik, *Izv. Akad. Nauk SSSR. Ser. Khim.*, 1988, **5**, 1040.
6. P.D. Sullivan, *J. Phys. Chem.*, 1970, **74**, 2563.
7. J. Fleischhauer, S. Ma, W. Schleker, K. Gersonde, H. Twilfer and F. Dallacker, *Z. Naturforsch, A*, 1982, **37A**, 680.
8. R.J. Gillespie, *J. Chem. Edu.*, 1970, **47**, 18.
9. R.J. Gillespie, *Chem. Soc. Rev.*, 1992, **21**, 59.

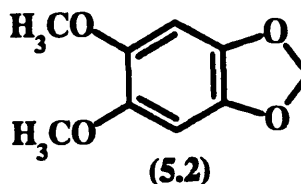
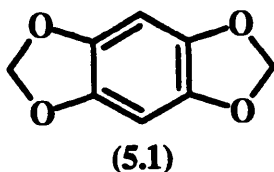
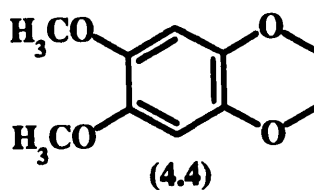
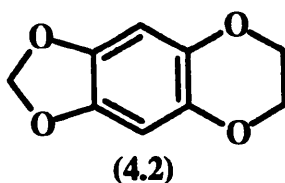
Chapter 5. Radical Cations of Alkoxybenzenes

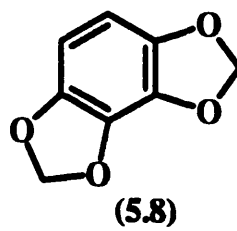
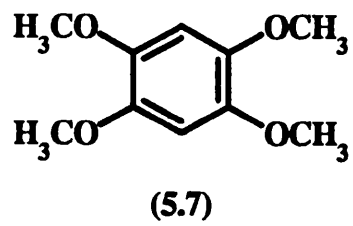
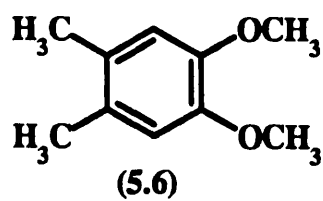
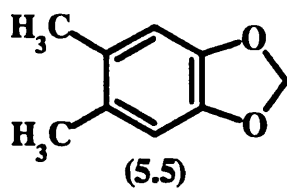
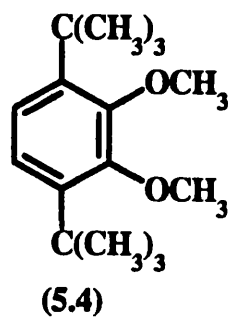
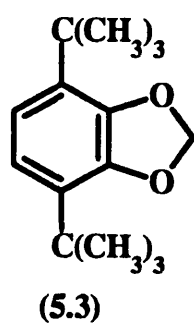
5.1. Background.

In 1966 and 1977, Sullivan and his co-workers reported the observation of *p*-dialkoxybenzene radical cations by variable temperature e.s.r. spectroscopy in liquid nitromethane with aluminium chloride.^{1,2}

Later, Dixon and Murphey oxidised a number of *o*-alkoxybenzenes using cerium(IV) in concentrated sulphuric acid in a flow system. They found that, the aliphatic proton hyperfine coupling in the 1,2-dimethoxybenzene radical cation (5.10)⁺ is substantially smaller than in the 1,3-benzodioxole radical cation (5.9)⁺, and this was explained in terms of the molecular orbital model of hyperconjugation.³

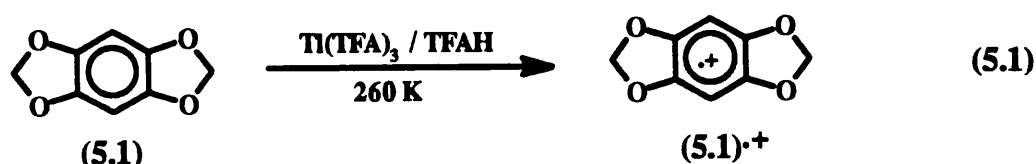
This chapter reports an e.s.r. investigation of further radical cations of *o*-alkoxybenzenes and their derivatives, and provides further examples that relate to the Dixon and Murphy interpretation.





5.2. Results

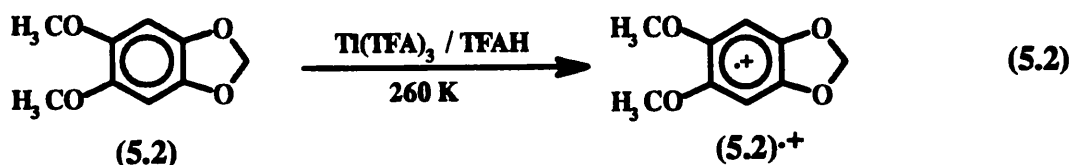
5.2.1. Benzo[1,2-d:4,5-d']bis-1,3-dioxole (5.1)



A good e.s.r. spectrum of the benzo[1,2-d:4,5-d']bis-1,3-dioxole radical cation (5.1)^{•+} was recorded by Fleischhaur *et al.* by oxidation of compound (5.1) using cerium(IV) and concentrated sulphuric acid in a flow system.^{4,5} The spectrum showed $\underline{a}(4\text{H})$ 11.67 G and $\underline{a}(2\text{H})$ 1.03 G, and the g-factor is 2.0042.

The radical cation (5.1)^{•+} seems to be very stable in our static system. When (5.1) was dissolved in trifluoroacetic acid containing thallium(III) trifluoroacetate at 260 K, it gave a yellowish solution which showed a strong and persistent spectrum of the radical cation (5.1)^{•+} (Figure 5.1 and Table 5.0).

5.2.2. 5,6-Dimethoxybenzo-1,3-dioxole (5.2)

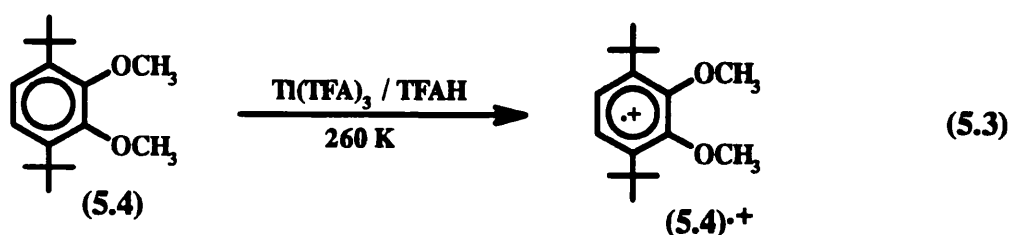


The e.s.r. spectrum of the radical cation of 5,6-dimethoxybenzo-1,3-dioxole (5.2) has not been reported previously. In the dark, a solution of compound (5.2) in trifluoroacetic acid containing thallium(III) trifluoroacetate at 260 K gave rise to a spectrum which we ascribed to (5.2)^{•+} (Figure 5.2). This was analysed and confirmed by computer simulation: $\underline{a}(2\text{H})$ 11.41 G, $\underline{a}(6\text{H})$ 2.22 G, $\underline{a}(2\text{H})$ 0.96 G and g 2.0041.

The same spectrum of (5.2)^{•+} could be generated by other static techniques (e.g. $\text{AlCl}_3/\text{CH}_2\text{Cl}_2$ or $\text{FSO}_3\text{H}/\text{SO}_2$) and it seems to be very stable under these conditions. The

proton hyperfine coupling constants correlate well with the values in the benzo[1,2-d:4,5-d']bis-1,3-dioxole radical cation (5.1)⁺ and 1,2,4,5-tetramethoxybenzene radical cation (5.7)⁺ (see Table 5.0).

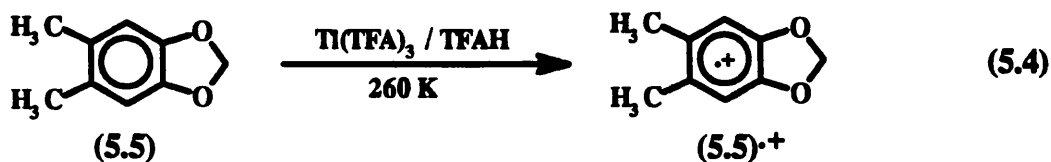
5.2.3. 3,6-Di-*tert*-butyl-1,2-dimethoxybenzene (5.4)



The e.s.r. spectrum of 3,6-di-*tert*-butyl-1,2-dimethoxybenzene radical cation (5.4)⁺ has been observed by Bubnov *et al.* from a solution of 3,6-di-*tert*-butyl-1,2-dimethoxybenzene (5.4) containing $\text{Ti(TFA)}_3/\text{TFAH}$ at 260 K, and gave $a(6\text{H})$ 2.08 G and $a(2\text{H})$ 4.20 G.⁶

We obtained the spectrum of (5.4)⁺ from (5.4) in $\text{Ti(TFA)}_3/\text{TFAH}$, and also by photolysis of a solution of (5.4) in trifluoroacetic acid in the presence of mercury(II) trifluoroacetate at 260 K with U.V. light which was attenuated to 10% of its intensity by a neutral filter, and passed through Pyrex glass (Figure 5.3). The coupling constants are close to the values in the literature (see Table 5.0).

5.2.4. 5,6-Dimethylbenzo-1,3-dioxole (5.5)



When 5,6-dimethylbenzo-1,3-dioxole (5.5) was added to a solution of trifluoroacetic acid containing thallium(III) trifluoroacetate at 260 K, it gave a yellowish solution. Without photolysis, this solution showed a strong, well resolved, persistent e.s.r. spectrum of the 5,6-dimethylbenzo-1,3-dioxole radical cation (5.5)⁺, which could be simulated with

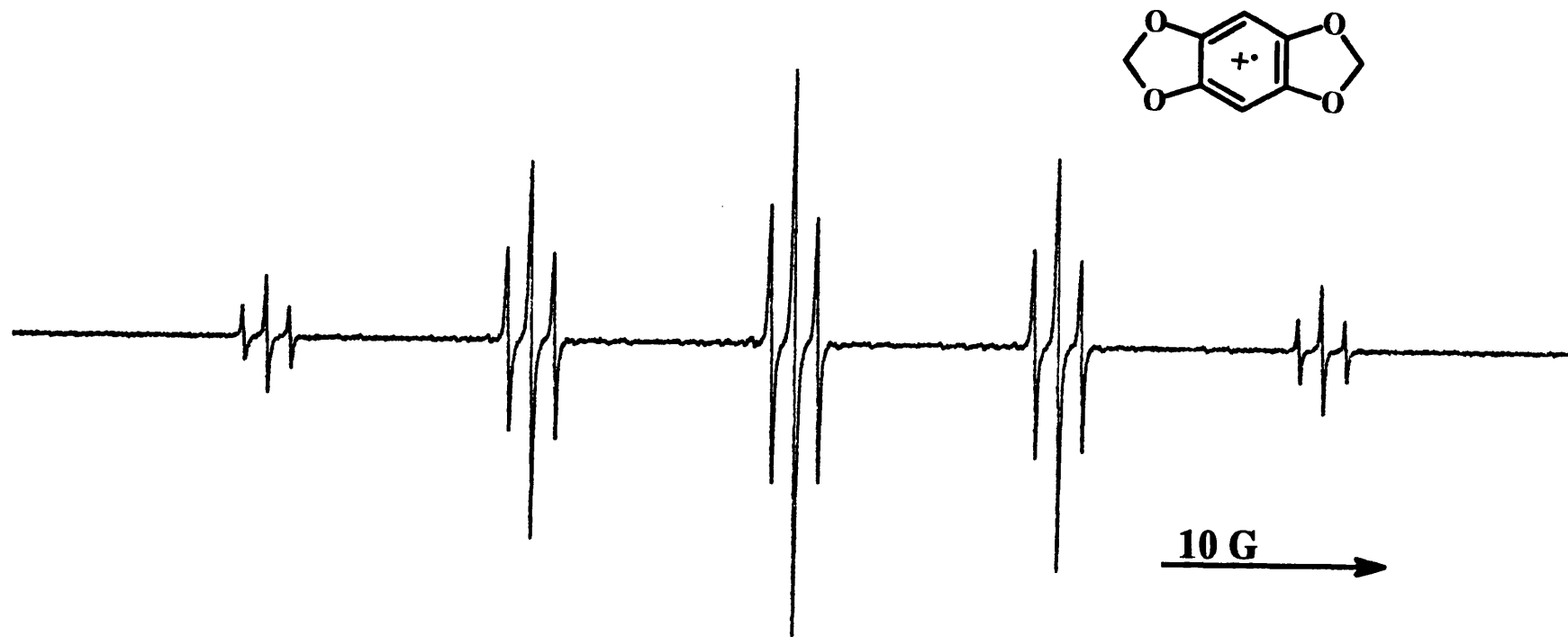


Figure 5.1. E.s.r. spectrum of the benzo[1,2-d:4,5-d']bis-1,3-dioxole radical cation (5.1)⁺ in TFAH/Tl(TFA)₃ at 260 K.

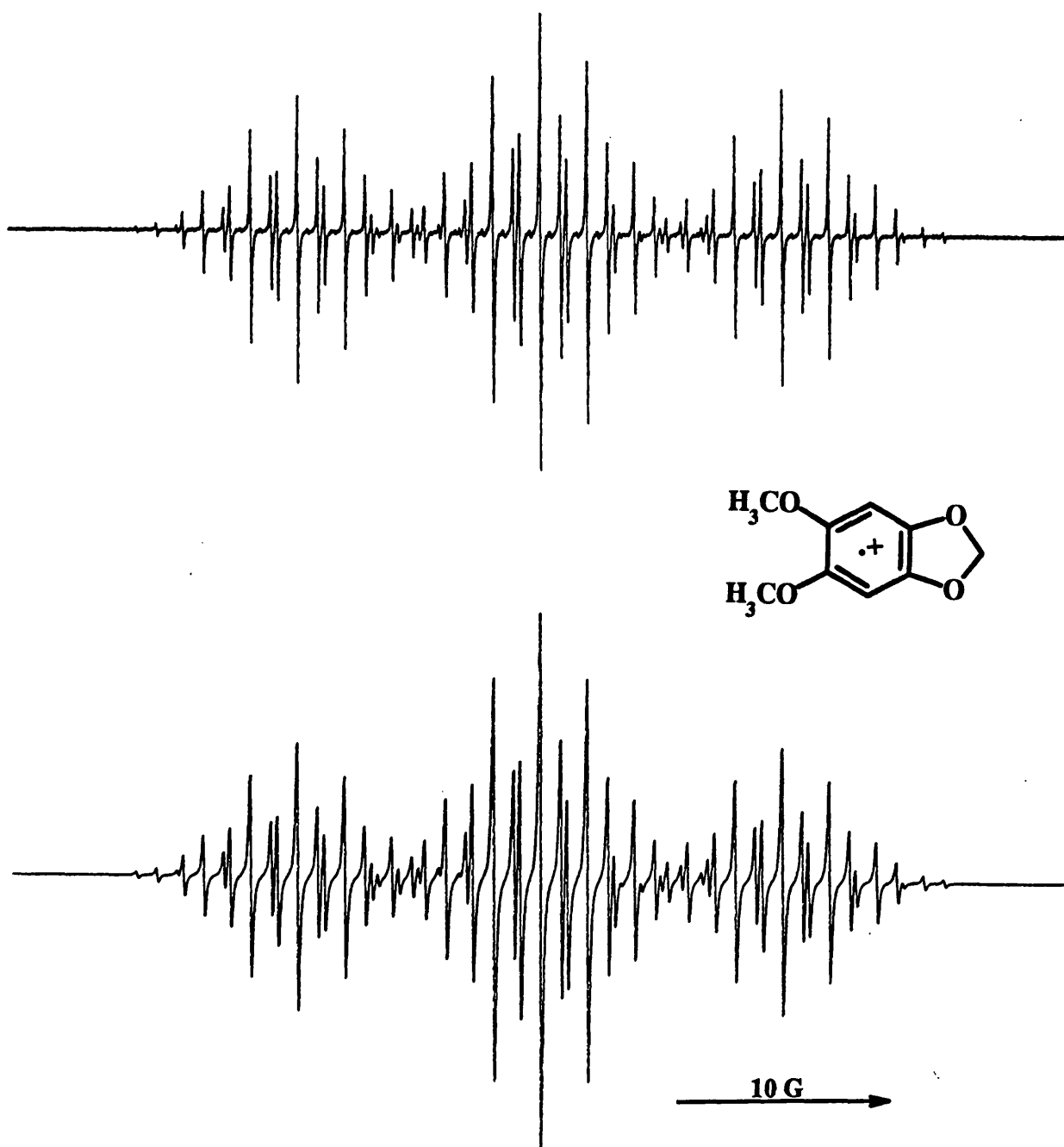


Figure 5.2. E.s.r. spectrum (top) and simulation (bottom) of the 5,6-dimethoxybenzo-1,3-dioxole radical cation (5.2)^{·+} in TFAH/Tl(TFA)₃ at 260 K.

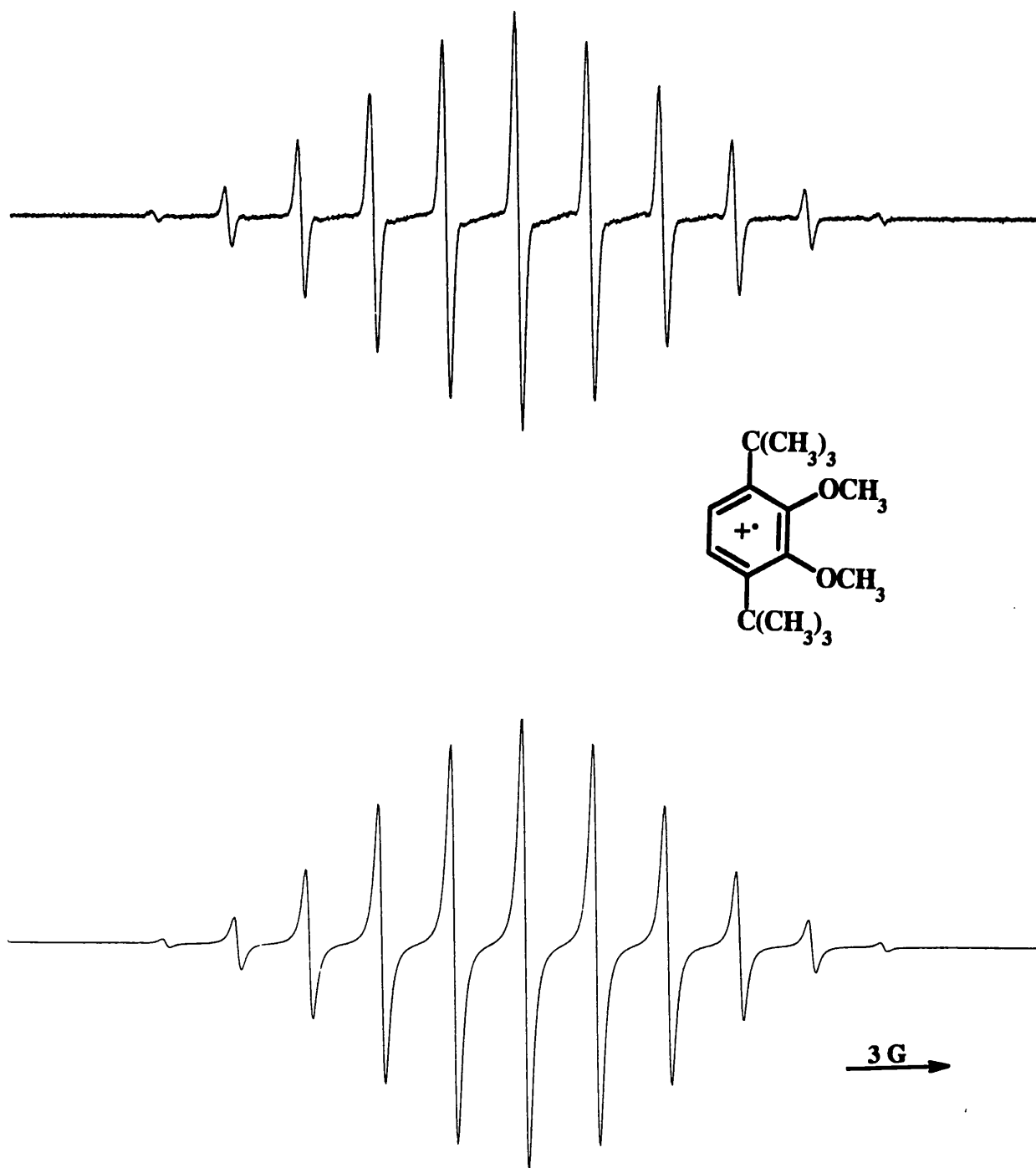


Figure 5.3. E.s.r. spectrum (top) and simulation (bottom) of the 3,6-di-*tert*-butyl-1,2-dimethoxybenzene radical cation (5.4)⁺ in TFAH/Hg(TFA)₂ at 260 K.

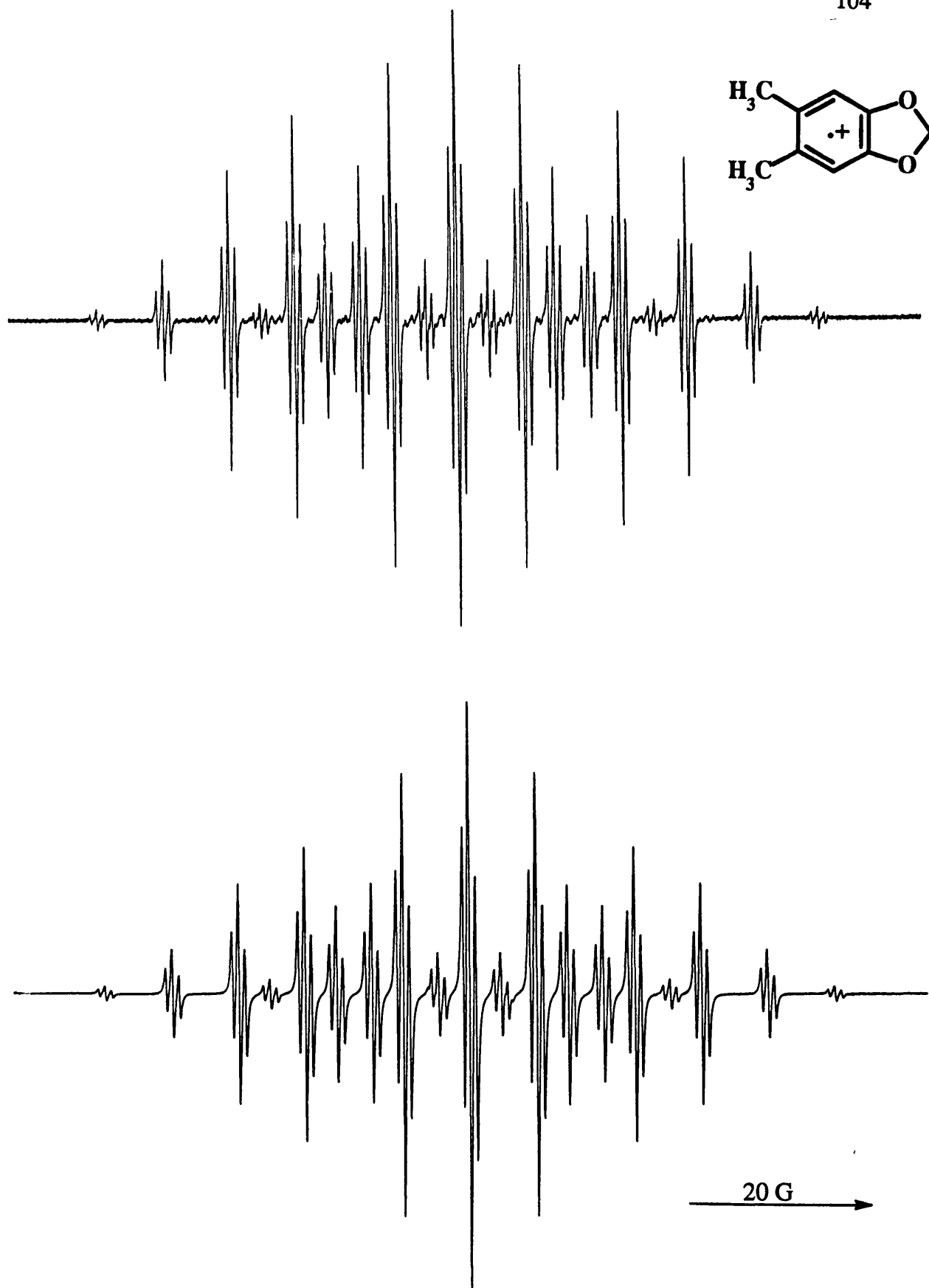
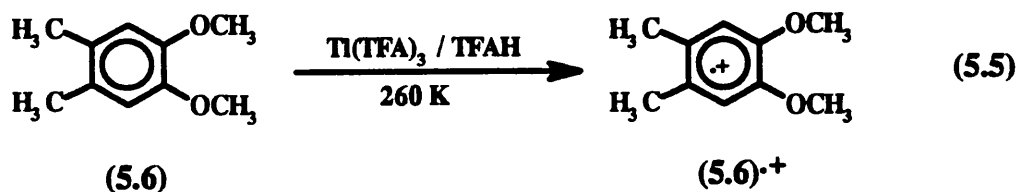


Figure 5.4. E.s.r. spectrum (top) and simulation (bottom) of the 5,6-dimethylbenzo-1,3-dioxole radical cation (5.5)⁺ in TFAH/Tl(TFA)₃ at 260 K.

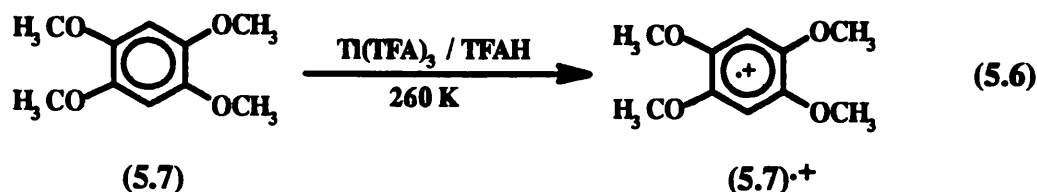
the following hyperfine coupling constants: $a(2H)$ 18.04 G, $a(6H)$ 7.30 G, $a(2H)$ 0.71 G and g 2.0038 (Figure 5.4).

5.2.5. 1,2-Dimethoxy-4,5-dimethylbenzene (5.6)



When 1,2-dimethoxy-4,5-dimethylbenzene (5.6) was dissolved in trifluoroacetic acid containing thallium(III) trifluoroacetate at 260 K, it gave a yellowish solution, which in the dark, gave a strong and persistent e.s.r. spectrum of the 1,2-dimethoxy-4,5-dimethylbenzene radical cation (5.6)^{·+}, which is shown in Figure 5.5, with the hyperfine coupling constants: $a(6H)$ 3.01 G, $a(2H)$ 0.58 G, $a(6H)$ 7.22 G and g 2.0034.

5.2.6. 1,2,4,5-Tetramethoxybenzene (5.7)

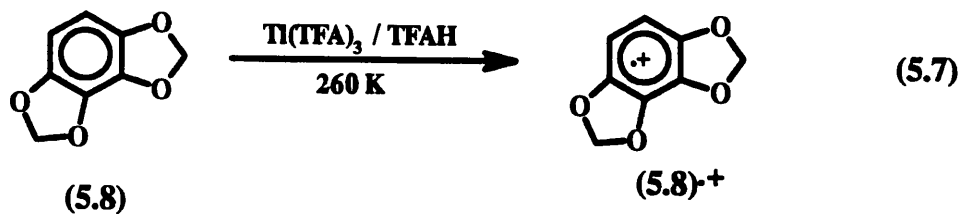


There have been several publications on the 1,2,4,5-tetramethoxybenzene radical cation (5.7)^{·+} that involved e.s.r. spectroscopy⁷ and TRIPLE resonance.⁸

Sullivan and Brette report the e.s.r. spectrum of (5.7)^{·+} in $\text{AlCl}_3/\text{MeNO}_2$, with $a(2H)$ 2.26 G, $a(2H)$ 0.89 G and g 2.0039, and the TRIPLE resonance study suggests that both the proton hyperfine coupling constants have the same positive sign.

We obtained the same spectrum of (5.7)^{·+} from (5.7) in trifluoroacetic acid containing thallium(III) trifluoroacetate at 260 K (Figure 5.6). The hyperfine coupling constants are similar to the values reported previously (see Table 5.0).

5.2.7. Benzo[1,2-d:3,4-d']bis-1,3-dioxole (5.8)



The e.s.r. spectrum of the benzo[1,2-d:3,4-d']bis-1,3-dioxole radical cation (5.8)⁺ was observed by Fleischhauer *et al.* in a flow system,^{4,5} with the coupling constant: $\underline{a}(4\text{H})$ 8.91 G and $\underline{a}(2\text{H})$ 2.98 G.

If compound (5.8) was dissolved in a solution of trifluoroacetic acid containing thallium(III) trifluoroacetate at 260 K, it gave a yellowish solution, which showed the spectrum of (5.8)⁺, and with following coupling constants: $\underline{a}(4\text{H})$ 9.02 G, $\underline{a}(2\text{H})$ 3.05 G, and g 2.0037 (Figure 5.7).

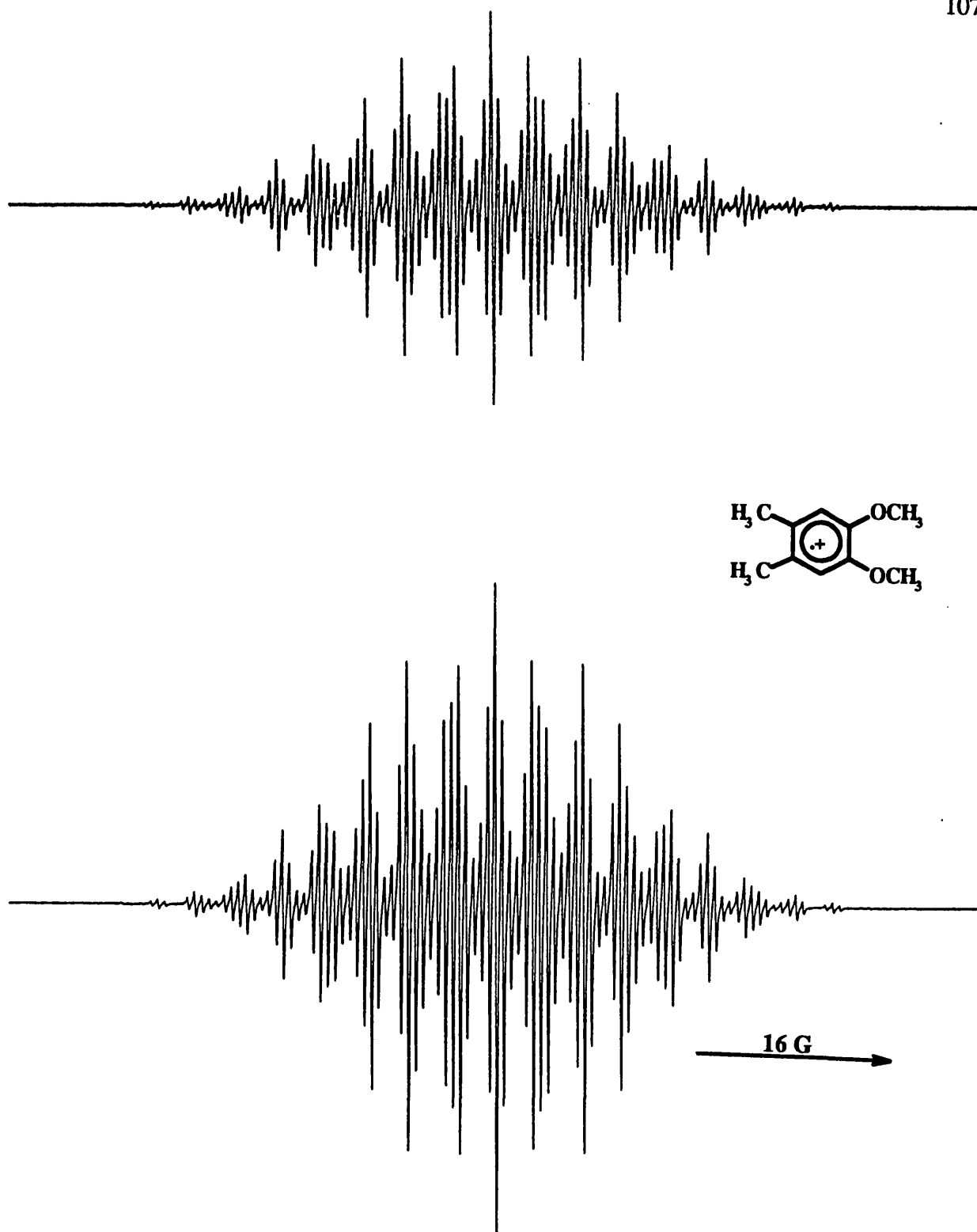


Figure 5.5. E.s.r. spectrum (top) and simulation (bottom) of the 1,2-dimethoxy-4,5-dimethylbenzene radical cation (5.6)⁺ in TFAH/Tl(TFA)₃ at 260 K.

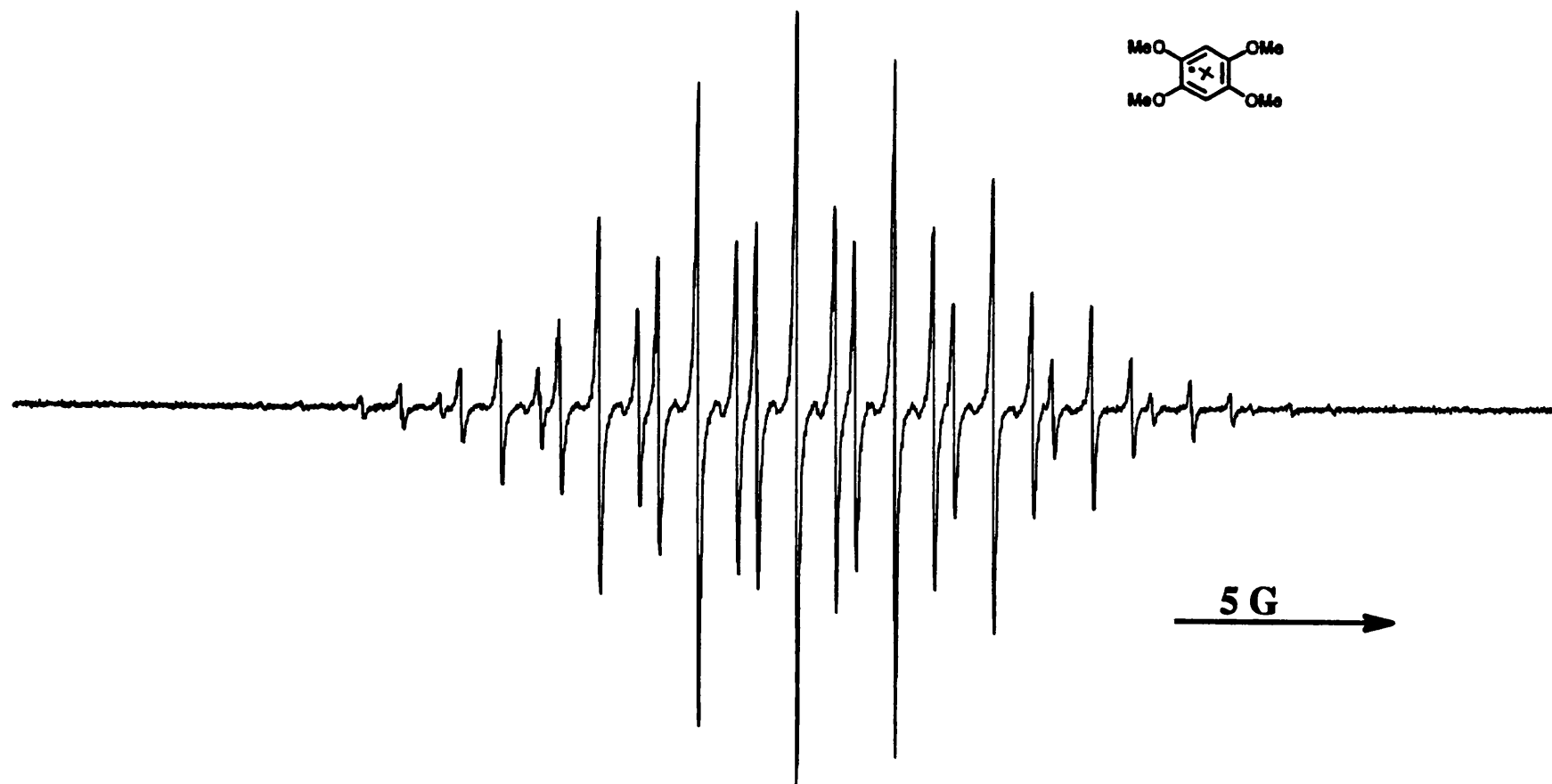


Figure 5.6. E.s.r. spectrum of the 1,2,4,5-tetramethoxybenzene radical cation (5.7)⁺ in TFAH/Tl(TFA)₃ at 260 K.



Figure 5.7. E.s.r. spectrum of the benzo[1,2-d:3,4-d']bis-1,3-dioxole radical cation (5.8)⁺ in TFAH/Tl(TFA)₃ at 260 K.

Table 5.0.

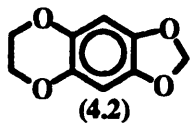
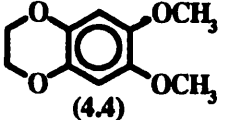
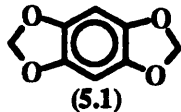
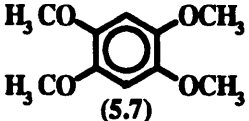
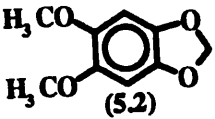
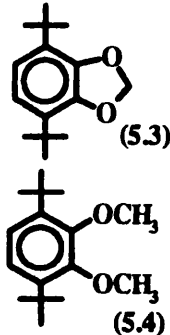
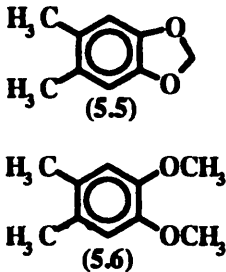
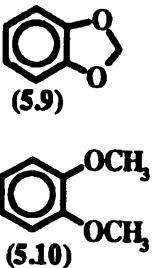
Radical cations	$\underline{a}(\text{H})/\text{G}$ in CH_3 or OCH_2O	$\underline{a}(\text{H})/\text{G}$ Others	Ratio $\underline{a}(\text{H}_{\text{OCH}_2\text{O}})/\underline{a}(\text{H}_{\text{OCH}_3})$	g-factor
 (4.2)	2H (OCH_2O) 12.08	4H ($\text{OCH}_2\text{CH}_2\text{O}$) 1.24 2H (Ar) 0.94	5.49	2.0040
 (4.4)	6H (OCH_3) 2.20	4H ($\text{OCH}_2\text{CH}_2\text{O}$) 1.14 2H (Ar) 0.94		2.0038
 (5.1)	4H (OCH_2O) 11.79	2H (Ar) 1.03	5.21	2.0042
 (5.7)	12 (OCH_3) 2.20	2H (Ar) 0.86		2.0040
 (5.2)	2H (OCH_2O) 11.41 6H (OCH_3) 2.22	2H (Ar) 0.96	5.14	2.0041

Table 5.0 (continued) Radical cations	$\underline{a}(\text{H})/G$ in CH_3 or OCH_2O	$\underline{a}(\text{H})/G$ Others	Ratio $\underline{a}(\text{H}_{\text{OCH}_2\text{O}})/\underline{a}(\text{H}_{\text{OCH}_3})$	g-factor
 <p>(5.3)</p> <p>(5.4)</p>	<p>2H (OCH_2O) 21.41</p> <p>6H (OCH_3) 2.09</p>	<p>2H (Ar) 4.55</p> <p>2H (Ar) 4.17</p>	<p>10.24</p>	<p>2.0041</p> <p>2.0034</p>
 <p>(5.5)</p> <p>(5.6)</p>	<p>2H (OCH_2O) 18.04</p> <p>6H (OCH_3) 3.01</p>	<p>2H (Ar) 0.71</p> <p>6H (CH_3) 7.30</p> <p>2H (Ar) 0.58</p> <p>6H (CH_3) 7.22</p>	<p>6.00</p>	<p>2.0038</p> <p>2.0034</p>
 <p>(5.9)</p> <p>(5.10)</p>	<p>2H (OCH_2O) 21.90</p> <p>6H (OCH_3) 3.25</p>	<p>2H (Ar) 0.40</p> <p>2H (Ar) 4.90</p> <p>2H (Ar) 0.16</p> <p>2H (Ar) 4.90</p>	<p>6.74</p>	<p>2.0039</p> <p>2.0034</p>

5.3. Discussion

5.3.1. Hyperfine coupling to the protons in OCH₃ and OCH₂O groups.

The e.s.r. spectra of the alkoxybenzene radical cations are listed in Table 5.0. These radical cations containing the -OCH₃ and -OCH₂O- groups show hyperfine coupling to the protons of these two groups.

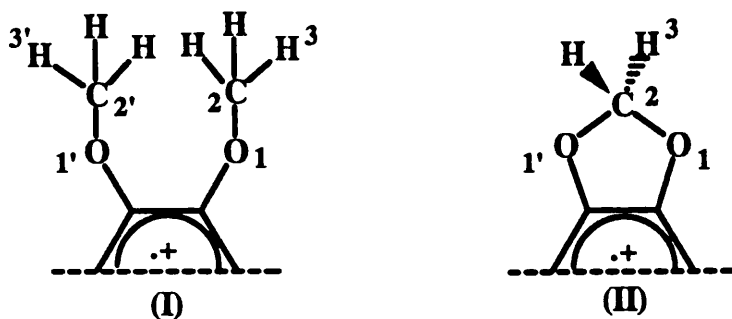
P.D. Sullivan ascribed the hyperfine coupling to hyperconjugation between the protons and the unpaired spin located on the oxygen atom, and this is expected to have a positive sign.² The coupling constant could be simply described by equation 5.8.

$$\underline{a}(\text{H}_x) = Q_x \rho_o \quad (5.8)$$

Q_x should be positive and represents the hyperconjugative interaction ($X = -\text{OCH}_3$ or $-\text{OCH}_2\text{O}-$), and ρ_o is the spin densities in the p_x orbital of the oxygen atom.

5.3.1a. M.O. hyperconjugation model.

Since the aliphatic proton coupling in radical cation (I) and (II) both arise from hyperconjugation^{2,3} (Scheme 5.1), they should be proportional to the spin densities on the adjacent oxygen atom (equation 5.8).



Scheme 5.1.

We can consider the alkoxy fragment [(I) and (II)] in more detail in order to understand where the coupling constants in these two hydrogen groups are so different. The secular equations for calculating spin delocalisation due to hyperconjugation mechanism are, for (I), as follows:³

$$(\alpha_C - E_O)(C_2 - C_{2'}) + B_{12}C_1 + B_{1'2'}C_{1'} + B_{23}C_3 + B_{2'3'}C_{3'} = 0 \quad (5.9)$$

$$B_{23}C_2 + B_{2'3'}C_{2'} + (\alpha_X - E_O)(C_3 + C_{3'}) = 0 \quad (5.10)$$

and for (II)

$$(\alpha_C - E_O')C_2 + B_{12}C_1 + B_{1'2'}C_{1'} + B_{23}C_3 + B_{2'3'}C_{3'} = 0 \quad (5.11)$$

$$B_{23}C_2 + B_{2'3'}C_{2'} + (\alpha_X - E_O')C_3 = 0 \quad (5.12)$$

where α_C and α_X are the Coulomb integrals of the carbon π -orbital and the hydrogen group orbital of π -symmetry, respectively; B_{12} , $B_{1'2'}$, B_{23} , and $B_{2'3'}$ are resonance integrals, and C the coefficients of the atomic orbitals. E_O and E_O' are the energies of the odd electron orbital in the two cases and it would be expected that $(E_O - E_O')$ is small. The spin density ρ_X in the hydrogen group orbital "X" can then be calculated:

for (I) when $X = \text{OCH}_3$

$$\rho_{\text{OCH}_3} = C_3 C_{3'} \approx \rho_O (B_{12} B_{1'2'}) / (B_{23} B_{2'3'}) \quad (5.13)$$

and for (II) when $X = \text{OCH}_2\text{O}$

$$\rho_{\text{OCH}_2\text{O}} = C_3^2 \approx 4\rho_O (B_{12} B_{1'2'}) / (B_{23} B_{2'3'}) \quad (5.14)$$

The coupling constants of the aliphatic protons will depend on the dihedral angle, θ , which determines the nature of the hydrogen group orbitals.

For (I)

$$\underline{a}(\text{H}_{\text{OCH}_3}) = \rho_{\text{OCH}_3} Q \langle \cos^2 45^\circ \rangle = \frac{1}{3} \rho_{\text{OCH}_3} Q \quad (5.15)$$

and for (II)

$$\underline{a}(\text{H}_{\text{OCH}_2\text{O}}) = \rho_{\text{OCH}_2\text{O}} Q \langle \cos^2 30^\circ \rangle = \frac{1}{2} \rho_{\text{OCH}_2\text{O}} Q \quad (5.16)$$

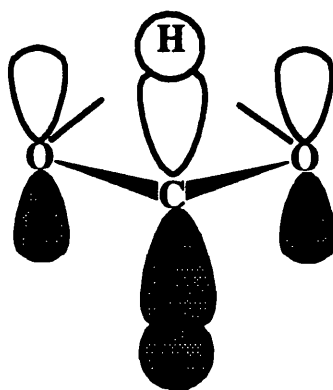
The predicted ratio of the aliphatic coupling constants becomes:

$$\underline{a}(\text{H}_{\text{OCH}_2\text{O}}) / \underline{a}(\text{H}_{\text{OCH}_3}) = (\frac{1}{2} \times 4) / (\frac{1}{3}) = 6$$

The ratio agrees reasonably well with a number of our experimental measurements which are illustrated in Table 5.0. There is disagreement between the compounds (5.3) and (5.4) and we have noted that the aliphatic proton coupling constant of (5.4)⁺ is slightly smaller than the others. The reason for this disagreement is not clear but it might be caused by the steric effects between the *tert*-butyl group and alkoxy moieties.

5.3.1b. Whiffen's Model

In Table 5.0, all the spectra show a large proton hyperfine coupling to the methylene protons in the -OCH₂O- group. This can be interpreted in terms of the model of the π - σ - π delocalised S.O.M.O. (Scheme 5.2) which was proposed by D.H. Whiffen in his original work on the interpretation of the e.s.r. spectrum for cyclohexadienyl radicals.⁹ The extent of the delocalisation is due to the coefficients on the oxygen atoms having the same sign in the half filled orbital of benzo-1,3-dioxoles.



Scheme 5.2. Whiffen's model.

References

1. W.F. Forbes, P.D. Sullivan and H.M. Wang, *Canad. J. Chem.*, 1966, **44**, 1501.
2. P.D. Sullivan, *J. Phys. Chem.*, 1970, **74**, 2563.
3. W.T. Dixon and D. Murphy, *J. Chem. Soc., Perkin Trans. 2*, 1976, 1823.
4. J. Fleischhauer, S. Ma, W. Schleker, K. Gersonde, H. Twilfer and F. Dallacker, *Z. Naturforsch.*, 1982, **37A**, 680.
5. J. Fleischhauer and S. Ma, *Ch'eng-kung Ta Hsueh Pao, K'O Chi, I Hsuech Pien*, 1986, **21**, 51.
6. N.A. Malysheva, A.I. Prokof'ev, N.N. Bubnov, S.P. Solodovnikov, T.I. Prokof'eva, V.B. Vol'eva, V.V. Ershov and M.I. Kabachnik, *Izv. Akad. Nauk SSSR, Ser. Khim.*, 1988, 1040.
7. P.D. Sullivan and N.A. Brette, *J. Phys. Chem.*, 1975, **79**, 474.
8. S.A. Fairhursh, I.M. Smith, L.H. Sutcliffe and S.M. Taylor, *Org. Magn. Reson.*, 1982, **18**, 231.
9. D.H. Whiffen, *Mol. Phys.*, 1963, **6**, 233.

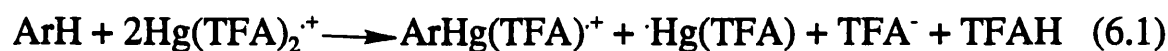
Chapter 6. Mercuration of Aromatic Radical Cations

6.1. Background

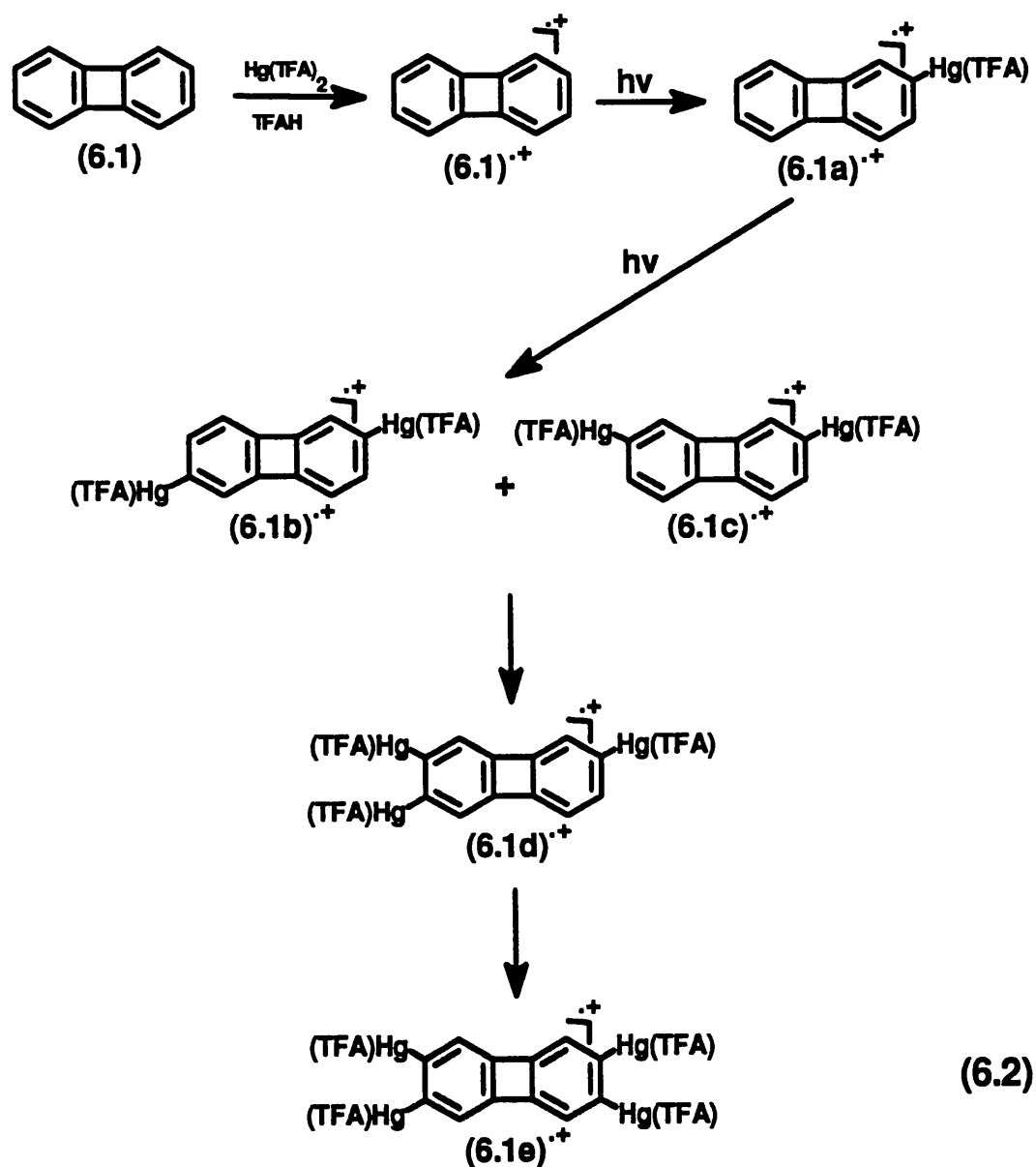
One of the most convenient techniques for the one electron oxidation of π -conjugated aromatic compounds to the corresponding radical cations was developed by Kochi and his co-workers. It involves photolysis of a solution of the arenes in trifluoroacetic acid containing mercury(II) trifluoroacetate.¹⁻³

From a study of the oxidation of various methylbenzenes, Kochi and his co-workers concluded that the reaction mechanism involved the initial formation of a charge-transfer complex between the arene and the mercury(II) trifluoroacetate and this was confirmed by single crystal X-ray diffraction studies of the hexamethylbenzene complex. Irradiation into the charge-transfer band then induced electron-transfer, and back electron-transfer was minimised by rapid dissociation of the counterion $\text{Hg}(\text{TFA})_2^-$ (see equation 1.5 in Chapter 1.).

We have using this technique for preparing radical cations of aromatic compounds for e.s.r. spectroscopy study, and we found that sometimes the aromatic ring was undergoing mercurideprotonation (equation 6.1).



In particular, biphenylene (6.1) was shown to undergo progressive mercuration in the β -positions.⁴ During a period of about 3 hr, the e.s.r. spectra of the zero-, mono-, di-, tri-, and tetra- β -mercurated biphenylene radical cations ($6.1^+ \text{--} 6.1e^+$) were identified (equation 6.2). Each mercuration step brought about a reduction in the g-factor of the radical cation.



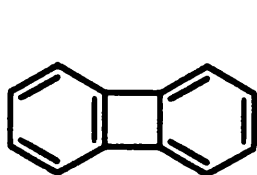
All the compounds reported previously show similar behaviour:

- (a) The aromatic protons with the largest hyperfine coupling constants are replaced by mercury.
- (b) Mercuration reduces the g -factor of the radical cations.
- (c) For the nuclei involved in the mercurideprotonation process, $\underline{a}(^{199}\text{Hg})/\underline{a}(^1\text{H}) \approx 20.6$.

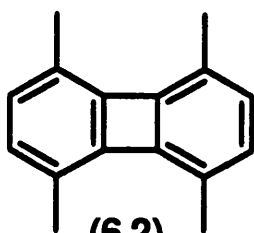
We have been interested in the way the nature of the anionic ligand, X in ArHgX , influences the magnitude of the mercury-199 hyperfine coupling, $\underline{a}(^{199}\text{Hg})$.

Initially, was done by generating the mercurated radical cations with *in situ*

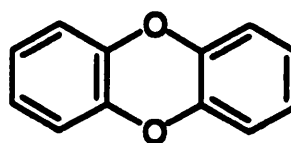
This provided a potential route for the formation of new radical cations of mercurated arenes under acid conditions. We now report some results on the effect of the nature of the anionic ligand X on the magnitude of $a(^{199}\text{Hg})$ in mercury-containing organic radical cations ArHgX^+ .



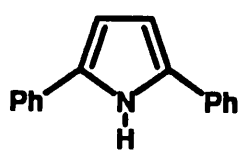
(6.1)



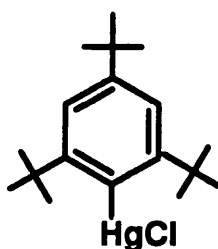
(6.2)



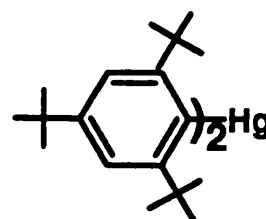
(6.3)



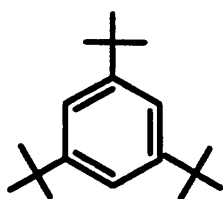
(6.4)



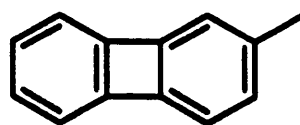
(6.5)



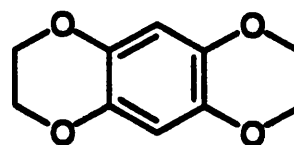
(6.6)



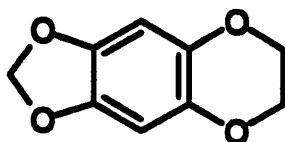
(6.7)



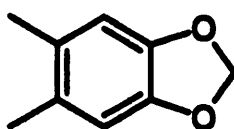
(6.8)



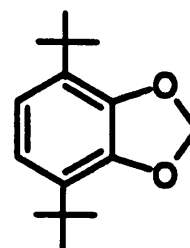
(4.1)



(4.2)



(5.5)



(5.3)

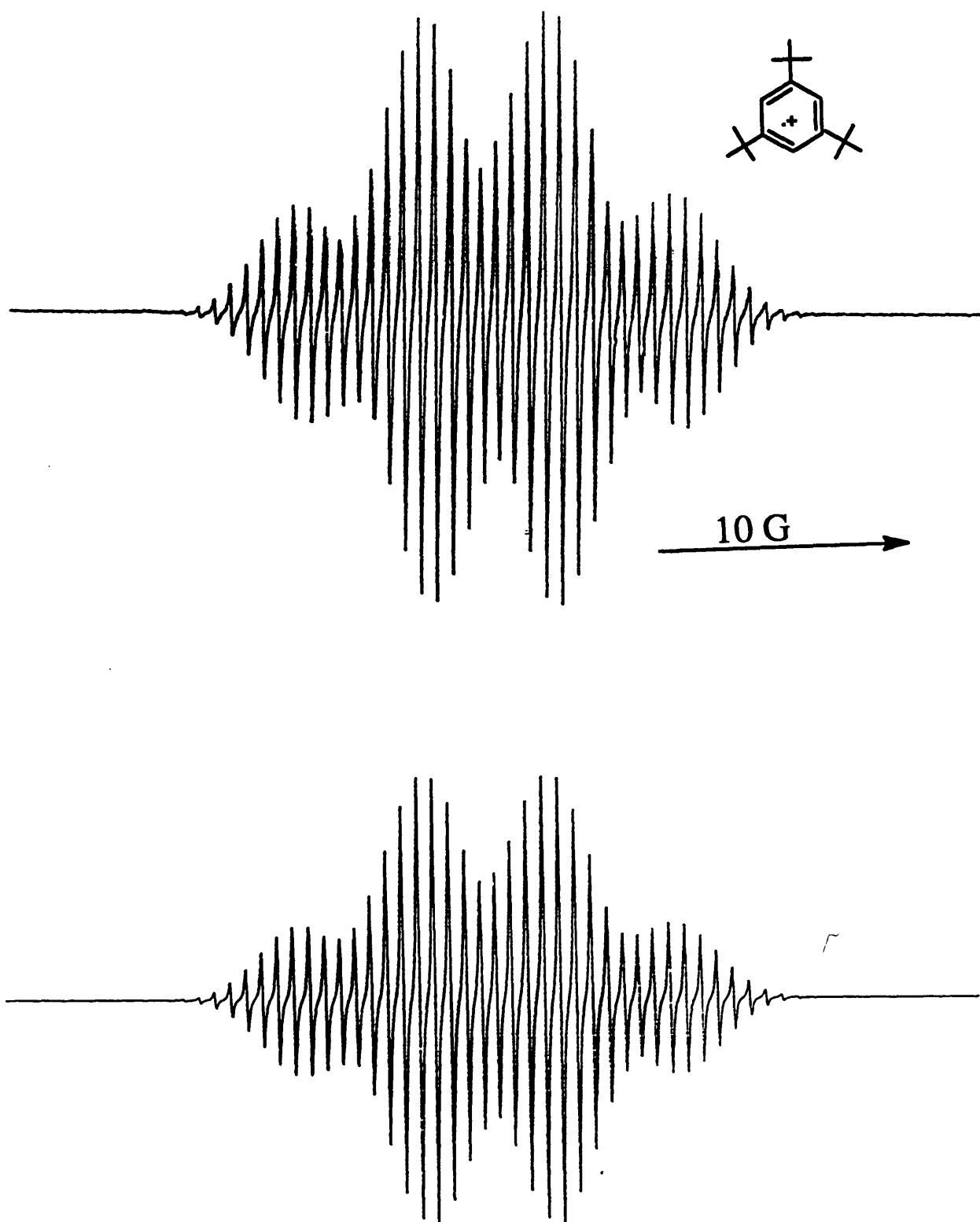


Figure 6.1. E.s.r. spectrum (top) and simulation (bottom) of the 1,3,5-tri-*tert*-butylbenzene radical cation (6.7)⁺ in TFAH/Hg(TFA)₂ at 260 K.

6.2. Results

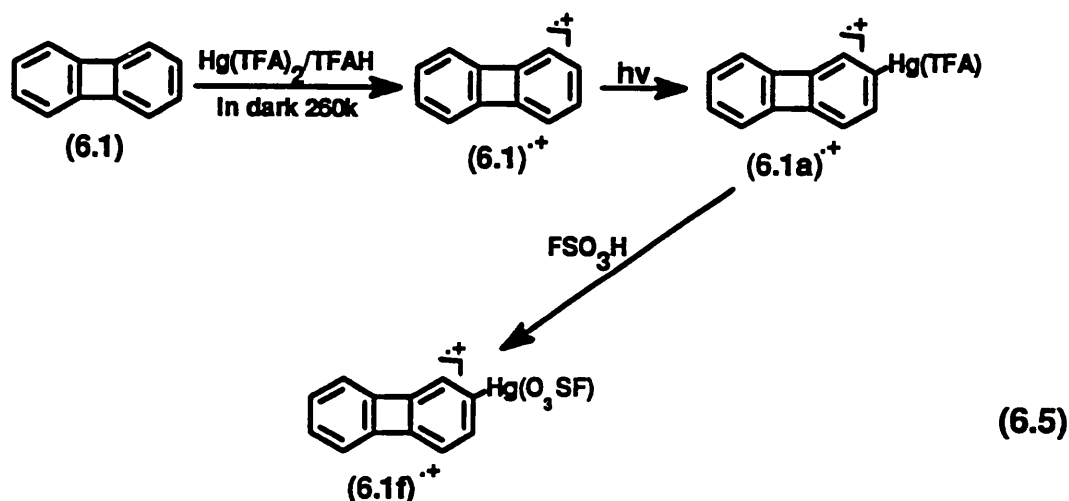
6.2.1. Biphenylene (6.1)

When biphenylene (6.1) was dissolved in trifluoroacetic acid, a good e.s.r. spectrum of the biphenylene radical cation $(6.1)^{\cdot+}$, consisting of a quintet of quintets, was observed, with the hyperfine coupling constants: $a(4H_a)$ 0.20 G and $a(4H_b)$ 3.60 G.

A solution of biphenylene (6.1) in trifluoroacetic acid containing mercury(II) trifluoroacetate at 260 K gave a light orange solution, and without photolysis this solution showed the same quintet of quintets spectrum of $(6.1)^{\cdot+}$. Photolysis of the same solution with 10% Pyrex-filtered U.V. light then gave the spectrum of the mono-mercurated radical cation $(6.1a)^{\cdot+}$ with $a(4H_a)$ 0.20 G, $a(3H_b)$ 3.60 G and $a(^{199}\text{Hg})$ 76.71 G. After the mono-mercuration was complete, the e.s.r. tube was removed from the spectrometer cavity. The sample was kept at 260 K and flushed with nitrogen gas and then a few drops of fluorosulphonic acid (FSO_3H) was added into the solution, giving a white precipitate. This precipitate indicated that $\text{Hg}(\text{O}_3\text{SF})_2$ was formed.

The sample was replaced in the e.s.r. spectrometer cavity. Without photolysis, this sample showed the spectrum of the radical cation, $(6.1)^{\cdot+}$. If the sample was irradiated with 10% Pyrex-filtered U.V. light, the spectrum showed a good quartet splitting in its ^{199}Hg satellites due to the mono-mercurated biphenylene radical cation with $a(^{199}\text{Hg})$ 88.15 G, $a(3H_b)$ 3.60 G and $a(4H_a)$ 0.20 G, and g-factor 2.0014 (Figure 6.2).

We conclude therefore that the trifluoroacetate anion in the $(6.1a)^{\cdot+}$ has been replaced by a fluorosulphonate anion to give $(6.1f)^{\cdot+}$ (equation 6.5).



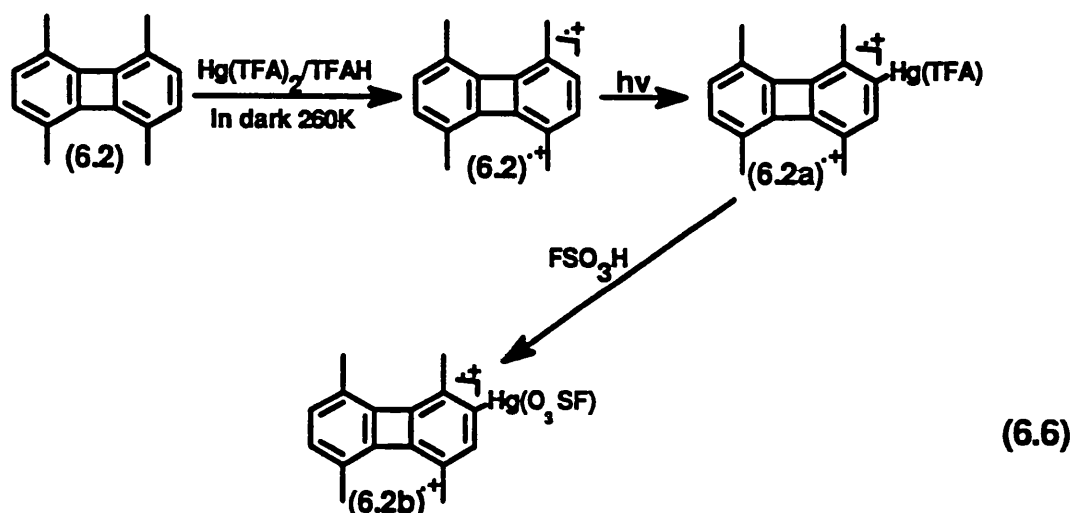
With prolonged photolysis of the solution of (6.1f)⁺ the spectrum changed back to the original biphenylene radical cation (6.1)⁺. This is probably due the fact that protodemercuration had occurred.

We made many attempts to exchange the trifluoroacetate group of the mono-mercurated biphenylene radical cation (6.1a)⁺ with other acids: methanesulphonic acid and trifluoromethanesulphonic acid, both gave a similar $a(^{199}\text{Hg})$ 76.7 G, and hydrogen chloride, chlorosulphonic acid and sulphuric acid gave only the biphenylene radical cation (6.1)⁺.

6.2.2. 1,4,5,8-Tetramethylbiphenylene (6.2)

A spectrum of the 1,4,5,8-tetramethylbiphenylene radical cation (6.2)⁺ was observed by Davies and his co-workers, from a solution of 1,4,5,8-tetramethylbiphenylene (6.2) in trifluoroacetic acid containing thallium(III) trifluoroacetate at 260 K.⁷ The spectrum appears as a 1:4:6:4:1 quintet due to coupling to the 4 β -protons, with $a(4\text{H}_\beta)$ 3.25 G, and any coupling to the 12 protons of the 4 α -methyl groups was lost in the linewidth.

When compound (6.2) was treated with mercury(II) trifluoroacetate in trifluoroacetic acid, it showed the same quintet spectrum of (6.2)⁺. When this sample was irradiated with 10% U.V. light passed through Pyrex glass, mercurideprotonation occurred, and the initial quintet was largely transformed into a quartet. We assign the quartet central spectrum and quartet satellites to the mono-mercurated species (6.2a)⁺. The hyperfine coupling by ^{199}Hg is 69.86 G and the g-factor is reduced from 2.0025 as it is in (6.2)⁺ to 2.0014 (6.2a)⁺.

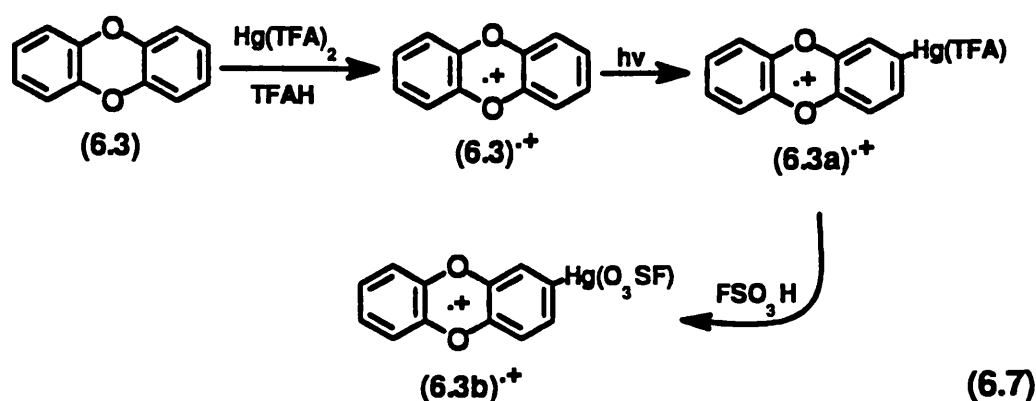


Photolysis was stopped when the mono-mercuration was completed. A few drops of FSO_3H were quickly added to the sample and the solution was degassed. Then the sample was returned to the e.s.r. spectrometer cavity. When this solution was irradiated with Pyrex-filtered 10% U.V. light, it gave a spectrum showing an overlapping quintet and quartet as the central spectrum, and quartet satellites (Figure 6.3), and the hyperfine coupling by ^{199}Hg was now 80.28 G. Again, we assign the central quartet spectrum and the quartet satellite to the mono-mercurated species $(6.2b)^+$ (equation 6.6). The quartet spectrum satellites were lost if the photolysis of the sample was prolonged, presumably because of protiodemercuration.

6.2.3. Dibenzodioxin (6.3)

Dibenzodioxin (6.3) in trifluoroacetic acid containing thallium(III) trifluoroacetate at 260 K gave a blue solution that showed a good e.s.r. spectrum of the dibenzodioxin radical cation $(6.3)^+$ consisting of a quintet with $\underline{a}(4\text{H}_\delta)$ 2.20 G.

When dibenzodioxin (6.3) was dissolved in TFAH containing $\text{Hg}(\text{TFA})_2$ at 260 K it gave a yellowish solution. Without photolysis, this solution showed the same quintet e.s.r. spectrum of $(6.3)^+$. Photolysis of the solution with 10% Pyrex-filtered U.V. light, caused mercurideprotonation and gave the spectrum of the monomercurated radical cation $(6.3a)^+$ with $\underline{a}(3\text{H}_\delta)$ 2.20 G and $\underline{a}(^{199}\text{Hg})$ 43.20 G.⁸ After 15 min, the spectrum indicated that the sample contained only the monomercurated species $(6.3a)^+$.



This sample was then removed from the e.s.r. spectrometer cavity, a few drops of FSO_3H were quickly added and the solution was degassed with nitrogen, and the sample

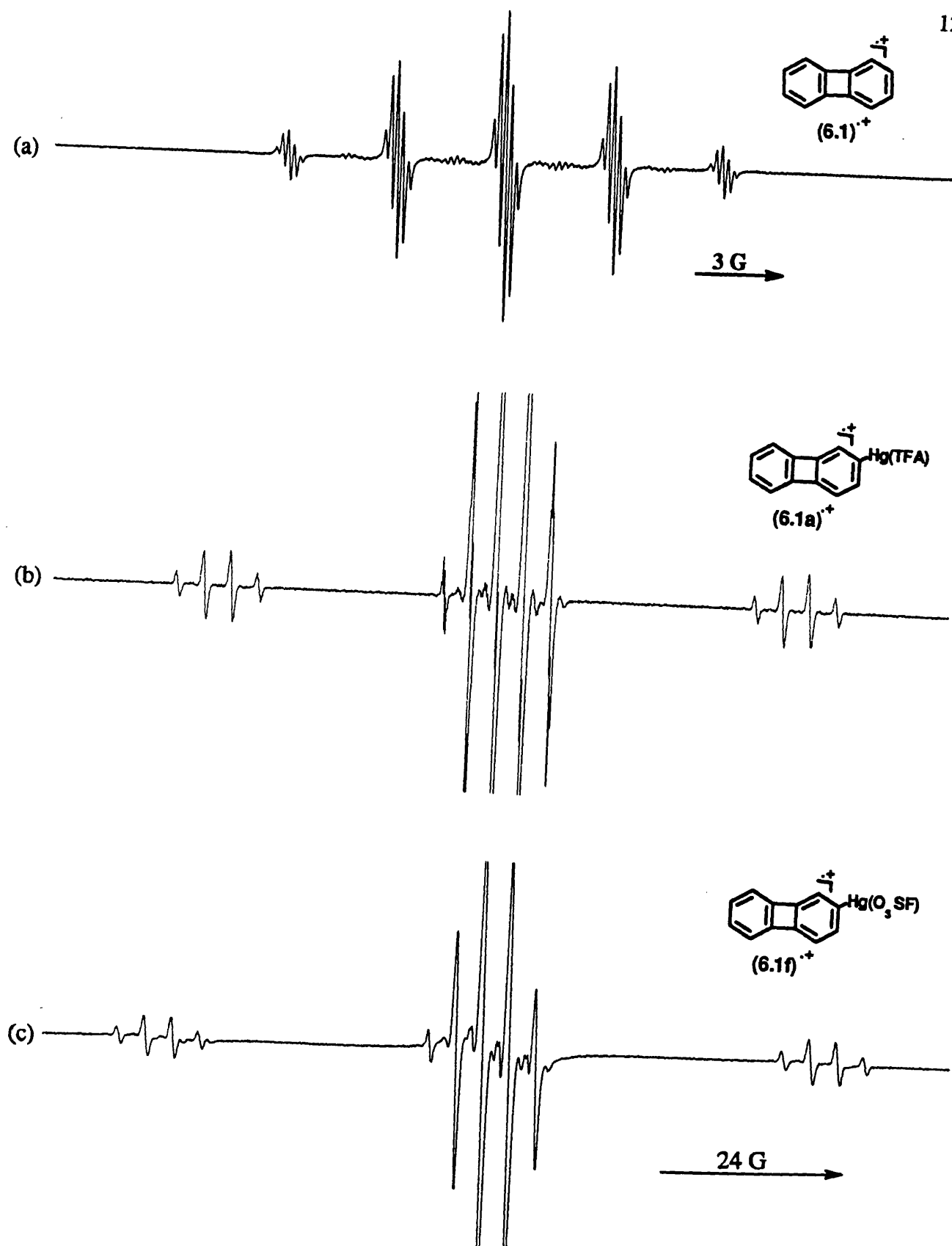


Figure 6.2. E.s.r. spectra of radical cations in TFAH at 260 K. (a) Biphenylene $(6.1)^{\bullet+}$. (b) Monomercurated biphenylene $(6.1a)^{\bullet+}$. (c) Monomercurated biphenylene $(6.1f)^{\bullet+}$.

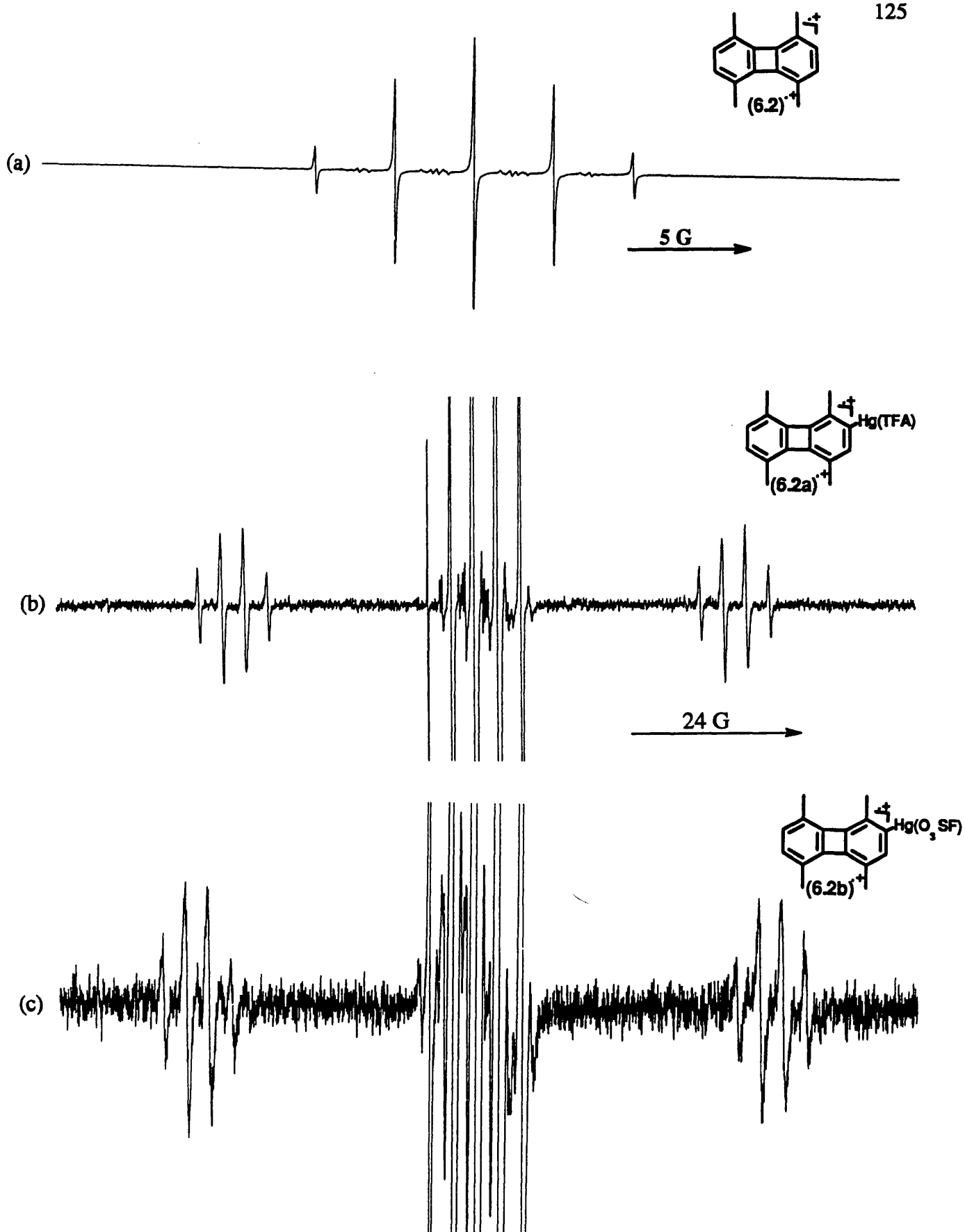


Figure 6.3. E.s.r. spectra of radical cations in TFAH at 260 K. (a) 1,4,5,8-tetramethylbiphenylene $(6.2)^{\cdot+}$. (b) Monomercurated 1,4,5,8-tetramethylbiphenylene $(6.2a)^{\cdot+}$. (c) Monomercurated 1,4,5,8-tetramethylbiphenylene $(6.2b)^{\cdot+}$.

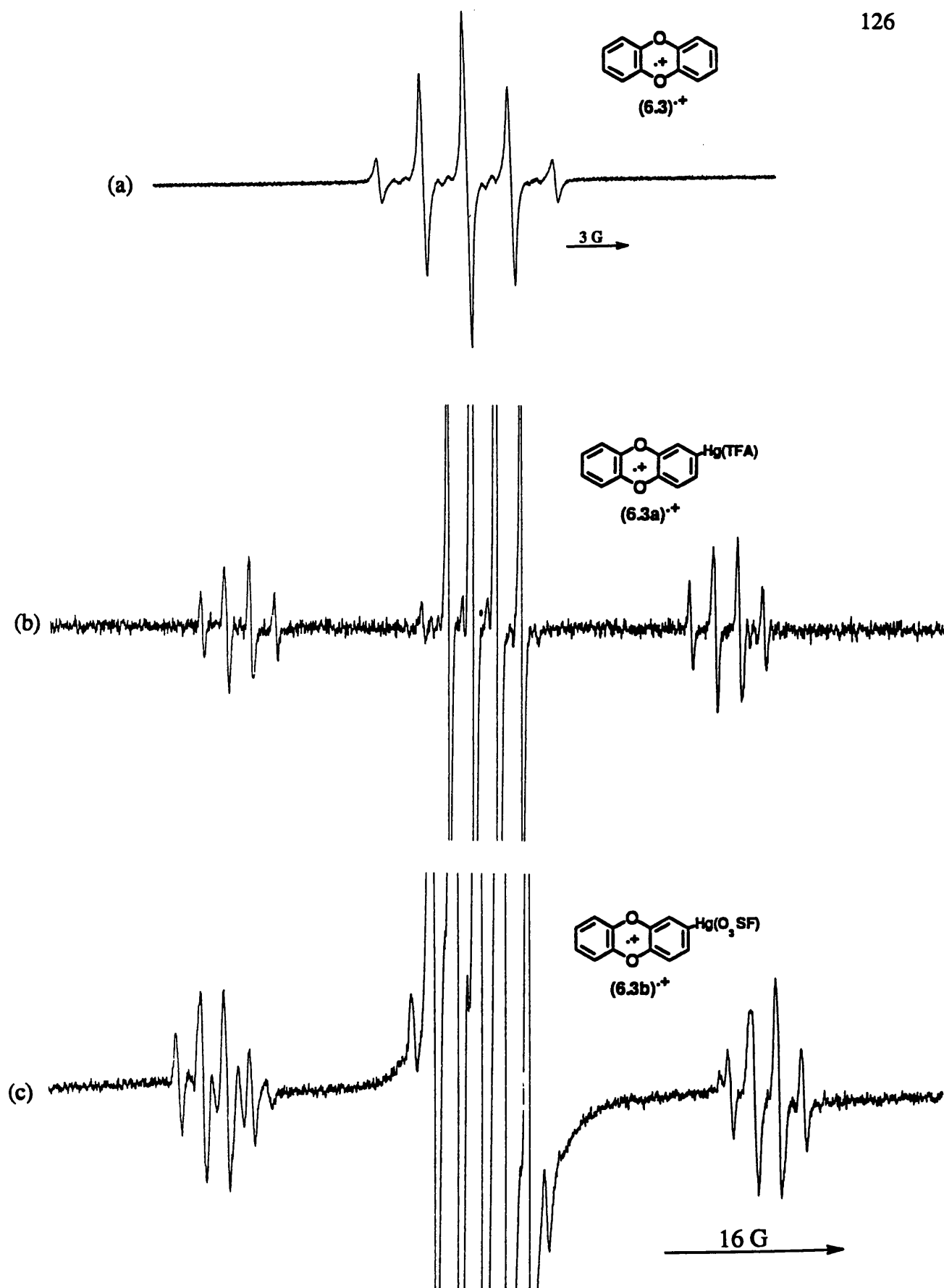
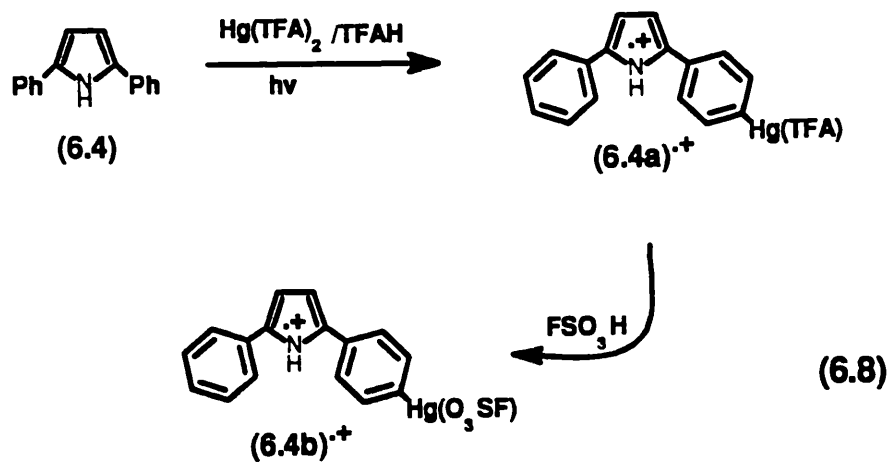


Figure 6.4. E.s.r. spectra of radical cations in TFAH at 260 K. (a) Dibenzodioxin $(6.3)^{\bullet+}$. (b) Monomercurated dibenzodioxin $(6.3a)^{\bullet+}$. (c) Monomercurated dibenzodioxin $(6.3b)^{\bullet+}$.

was returned into the cavity. Photolysis with 10% Pyrex-filtered U.V. light then showed the spectrum of the monomercurated radical cation $(6.3b)^+$ with $a(3H_\beta)$ 2.20 G and $a(^{199}\text{Hg})$ 49.30 G (see equation 6.7 and Figure 6.4).

6.2.4. 2,5-Diphenylpyrrole (6.4)

A very weak e.s.r. spectrum of the 2,5-diphenylpyrrole radical cation $(6.4)^+$ had been reported, when the compound (6.4) was dissolved in trifluoroacetic acid containing thallium(III) trifluoroacetate at 260 K. This spectrum could not be analysed, but photolysis of a solution in TFAH containing $\text{Hg}(\text{TFA})_2$ gave a spectrum which suggested that mercurideprotonation had occurred,⁹ and showed satellites due to mercury-199 hyperfine coupling, $a(^{199}\text{Hg})$ 64.30 G. It appears that only mono-mercuration had taken place, because no satellites which should be observable if two ^{199}Hg atoms entered into coupling, could be detected at higher gain. Later, the site of mercuration was assigned to the *para*-(4'-)-position of the phenyl groups which show $a(\text{H})$ *ca.* 3.31 G (6.4) (Figure 6.5).



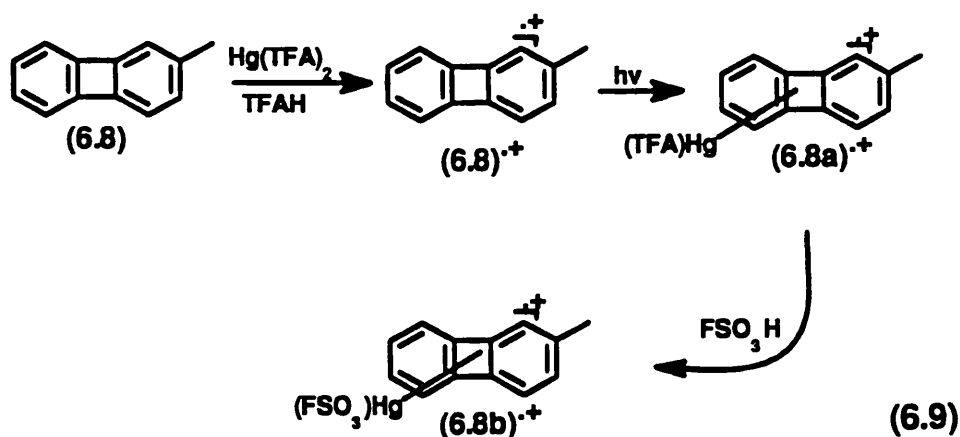
We carried out the same experiment but with the addition of a few drops of fluorosulphonic acid. Upon photolysis, this sample gave a spectrum that showed mercury satellites with $a(^{199}\text{Hg})$ 74.67 G rather than $a(^{199}\text{Hg})$ 64.30 G. We assign this to the radical cation, $(6.4b)^+$, where the mercury atom is associated with the fluorosulphonate anion (equation 6.8). Both monomercurated radical cations shown the same g-factor of 2.0020.

6.2.5. 2-Methylbiphenylene (6.8)

Photolysis of a solution of 2-methylbiphenylene (6.8) in dichloromethane containing AlCl_3 at 243 K gave a strong e.s.r. spectrum of the 2-methylbiphenylene radical cation $(6.8)^{\cdot+}$, which can be analyzed in terms of the following hyperfine coupling constants: $\underline{a}(1\text{H})$ 0.18 G, $\underline{a}(1\text{H})$ 0.55 G, $\underline{a}(1\text{H})$ 2.97 G, $\underline{a}(1\text{H})$ 3.56 G, $\underline{a}(1\text{H})$ 4.20 and $\underline{a}(3\text{H})$ 5.50 G.

2-Methylbiphenylene (6.8) in trifluoroacetic acid containing mercury(II) trifluoroacetate at 260 K gave a light orange solution. This solution showed the same e.s.r. spectrum of $(6.8)^{\cdot+}$ without photolysis. If the sample was irradiated with 10% Pyrex-filtered light, it showed a spectrum with mercury satellites with $\underline{a}(^{199}\text{Hg})$ 91.85 G. After about 10 min, the spectrum showed purely the monomercurated species $(6.8a)^{\cdot+}$. This spectrum progressively changed when irradiation was continued, but unfortunately the spectrum was not strong enough for the mercury satellites due to dimercuration to be identified.

We assign the position of mono-mercuration to that where the proton shows $\underline{a}(1\text{H})$ 4.20 G, so that the ratio between the incoming mercury [$\underline{a}(^{199}\text{Hg})$ 91.85 G, $(6.8a)^{\cdot+}$], and the outgoing proton [$\underline{a}(1\text{H})$ 4.20 G $(6.8)^{\cdot+}$] is 21.8. The g-factor was reduced from 2.0026 $(6.8)^{\cdot+}$ to 2.0018 $(6.8a)^{\cdot+}$. We could not assign the position where the mercuration occurred, but we believe it might be one of the three (3,6,7)- β -positions in the compound (6.8).



If a few drops of fluorosulphonic acid were added to the monomercurated species $(6.8a)^{\cdot+}$, it gave a white precipitate in a yellowish solution. When this solution was

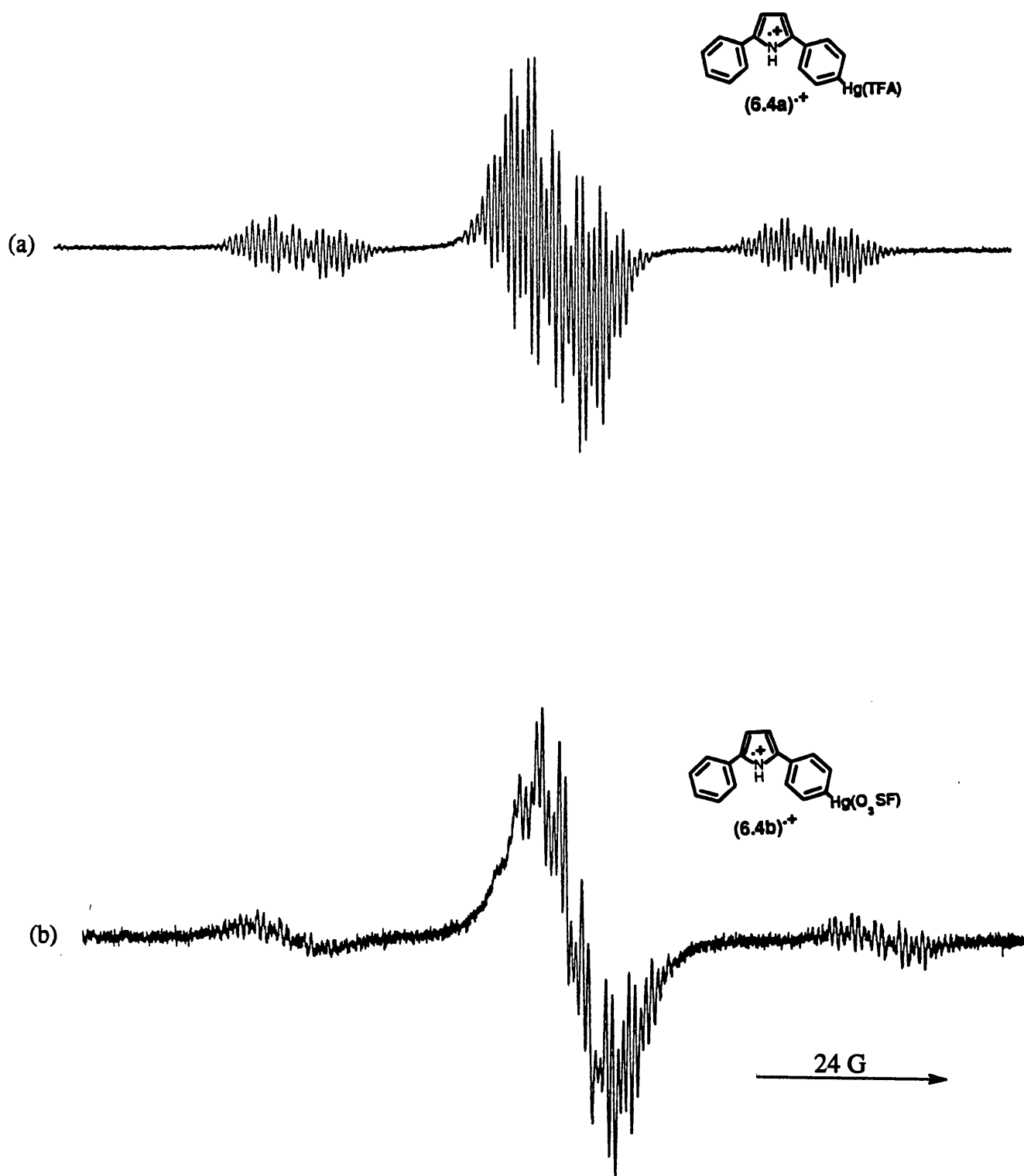


Figure 6.5. E.s.r. spectra of radical cations in TFAH at 260 K. (a) Monomeric 2,5-diphenylpyrrole (6.4a)⁺. (b) Monomeric 2,5-diphenylpyrrole (6.4b)⁺.

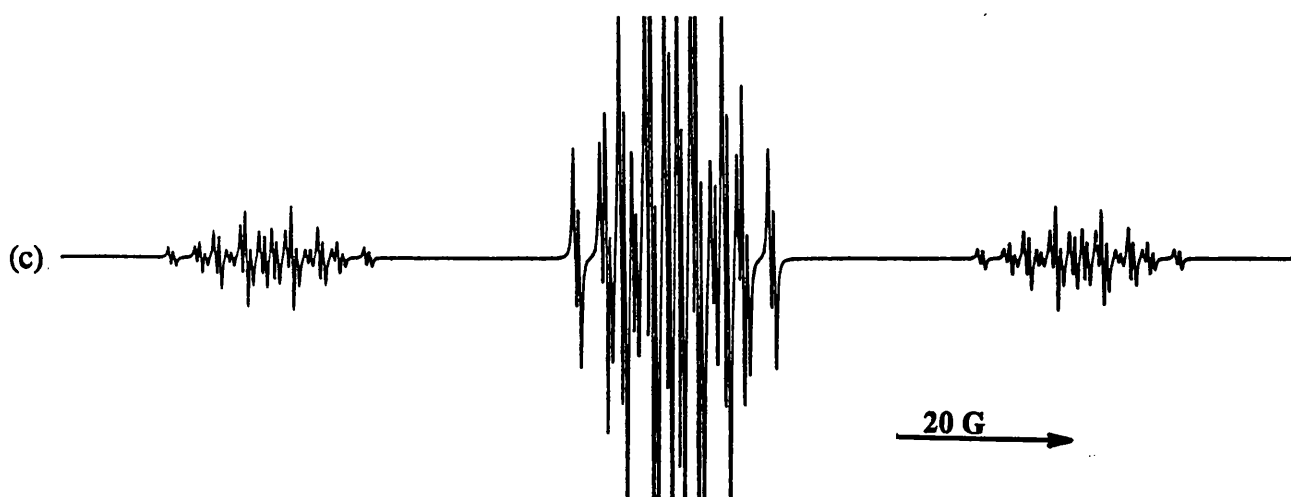
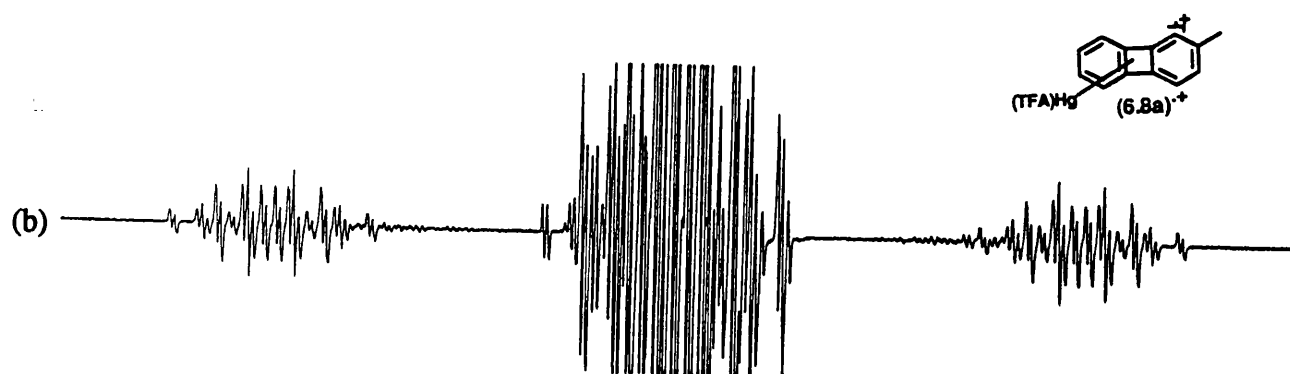
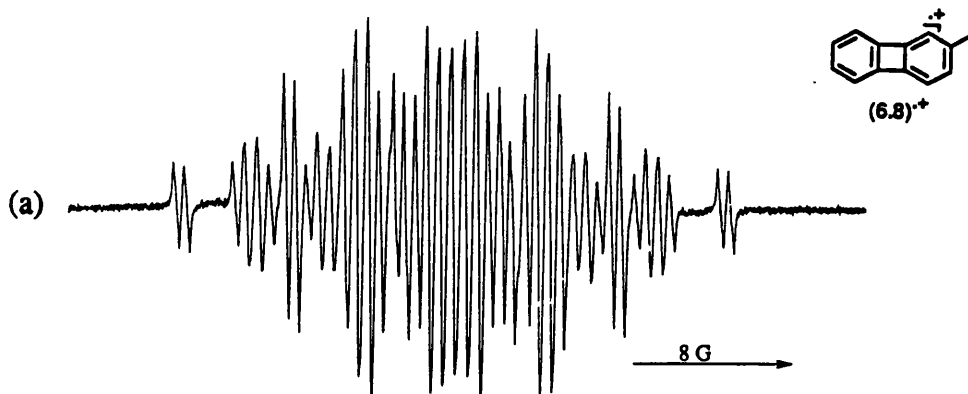


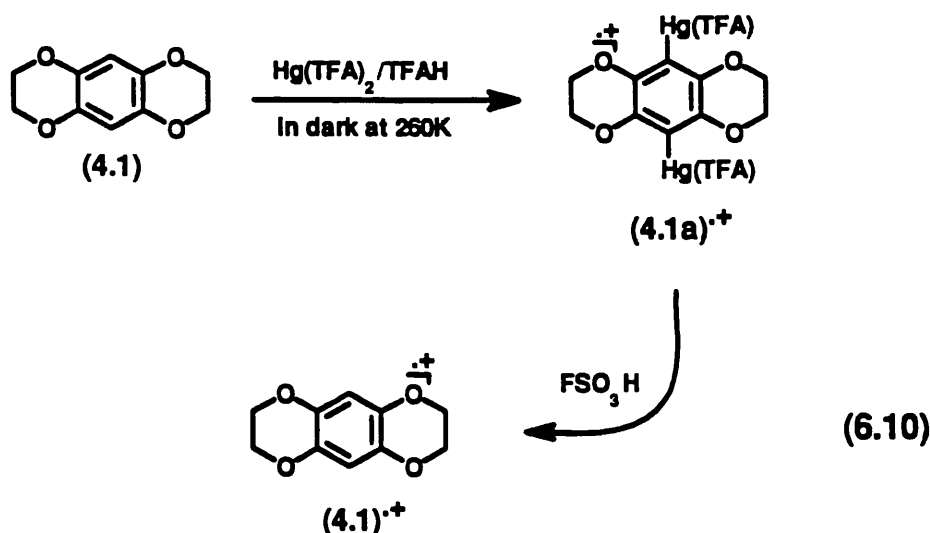
Figure 6.6. E.s.r. spectra of radical cations in TFAH at 260 K. (a) 2-Methylbiphenylene (6.8)⁺. (b) Monomercurated 2-methylbiphenylene (6.8a)⁺. (c) Computer simulation of the spectrum 6.6b.

photolysed with 10% Pyrex-filtered U.V. light, it gave a weak e.s.r. spectrum containing mercury satellites with $\underline{a}(^{199}\text{Hg})$ 104.83 G, which can be ascribed to the monomercurated species $(6.8b)^+$ (Figure 6.6 and equation 6.9). After 2 min, the parent hydrocarbon radical cation $(6.8)^+$ was observed.

6.2.6. Benzo[1,2-b:4,5-b']bis-1,4-dioxane (4.1)

Benzo[1,2-b:4,5-b']bis-1,4-dioxane (4.1) in 1,3-dichloropropane containing AlCl_3 gave a yellowish solution and a series of temperature dependent e.s.r. spectra were observed, which result from conformational inversion of the dioxene ring in $(4.1)^+$ which has already illustrated in Chapter 4.

If the compound (4.1) was dissolved in trifluoroacetic acid containing mercury(II) trifluoroacetate at 260 K it gave a yellowish solution. In the dark, this solution gave a weak e.s.r. spectrum which is different from the spectrum of (4.1) in $\text{AlCl}_3/\text{ClCH}_2\text{CH}_2\text{CH}_2\text{Cl}$ at 260 K. The intensity of the spectrum increased when the sample was irradiated with 30% Pyrex-filtered U.V. light (Figure 6.8b).



We assign the spectrum in Figure 6.8b to the dimercurated radical cation $(4.1a)^{\bullet+}$. The two aromatic ring protons with $\underline{a}(2\text{H})$ 0.90 G appear to have been replaced by two mercury atoms, with $\underline{a}(^{199}\text{Hg})$ 12.72 G at 260 K. If the sample temperature was now raised to 330 K, it showed a strong spectrum (Figure 6.8c) of the dimercurated radical cation $(4.1a)^{\bullet+}$, consisting of a nonet with mercury satellites, and this spectrum can be simulated reasonably well as illustrated in Figure 6.8d. The g-factor increased from 2.0044 $(4.1)^{\bullet+}$ to 2.0049 $(4.1a)^{\bullet+}$.

If the dimercurated species (4.1a)⁺ was quenched with a few drops of fluorosulphonic acid at 260 K, it gave a white precipitate in a yellowish solution. It showed the e.s.r. spectrum of (4.1)⁺, even when the sample was irradiated with U.V. light (equation 6.10).

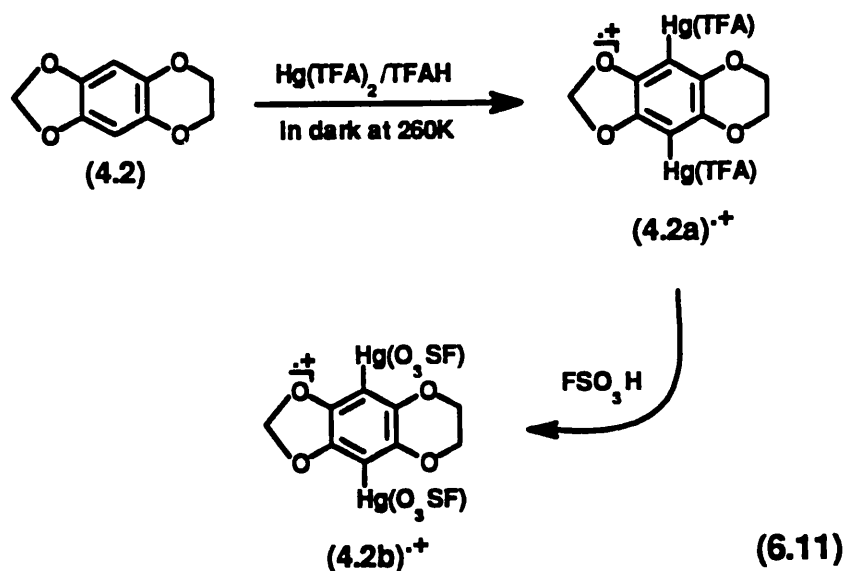
6.2.7. 1,3-Dioxolo[4,5-g]benzo-1,4-dioxane (4.2)

The radical cation, (4.2)⁺, was observed from a solution of compound (4.2) in 1,3-dichloropropane containing AlCl₃. At 260 K the spectrum showed a substantial alternating linewidth effect due conformational exchange of the axial and equatorial protons of the methylene groups of the dioxene ring, which has already discussed in Chapter 4.

If the compound (4.2) was dissolved in trifluoroacetic acid containing mercury(II) trifluoroacetate at 260 K, it gave rise to a good e.s.r. spectrum without photolysis, but the spectrum did not appear to be associated with the radical cation (4.2)⁺.

The spectrum showed that the two aromatic ring protons with $\underline{a}(2H)$ 0.94 G at the *para*-positions were missing and signals developed in the gaps within the triplet which was due to the two methylene protons. The signals appears to be mercury satellites due to the dimercurated species (4.2a)⁺ with $\underline{a}(^{199}\text{Hg})$ 13.72 G (Figure 6.9b). We were unable to record the spectrum of any monomercurated species. When the spectrum was recorded at 333 K, all four methylene protons in the dioxene ring became equivalent (Figure 6.9c) and this spectrum can be simulated as shown in Figure 6.9d.

For the first time, we are able to generate a mercurated radical cation directly from the neutral mercurated compound. We have successfully prepared the dimercurated compound (4.2a) by treating the compound (4.2) in a solution of TFAH containing Hg(TFA)₂.



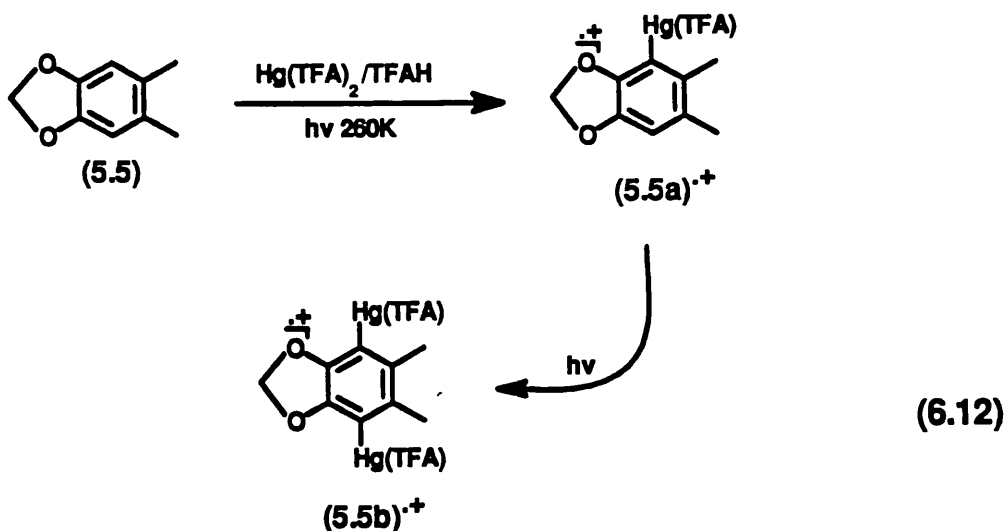
When compound (4.2a) was dissolved in trifluoroacetic acid containing thallium(III) trifluoroacetate at 260 K, it gave the same spectrum of (4.2a)⁺.

A few drops of fluorosulphonic acid were added to the solution containing the dimercurated species (4.2a)⁺, then the sample was photolysed with U.V. light at 10% intensity and filtered through Pyrex glass, and gave a spectrum containing ¹⁹⁹Hg satellites with $\underline{a}(^{199}\text{Hg})$ 15.85 G, as shown in Figure 6.9e (equation 6.11).

We assign the spectrum in Figure 6.9e to the dimercurated radical cation (4.2b)⁺, contaminated with un-mercurated and monomercurated species. After about 30 min, only the spectrum of (4.2)⁺ was recorded.

6.2.8. 5,6-Dimethylbenzo-1,3-dioxole (5.5)

An excellent e.s.r. spectrum of the 5,6-dimethylbenzo-1,3-dioxole radical cation (5.5)⁺ was observed as reported in Chapter 5 from a solution of compound (5.5) in trifluoroacetic acid containing thallium(III) trifluoroacetate at 260 K. The radical cation (5.5)⁺ shows the following hyperfine coupling constants: $\underline{a}(2\text{H})$ 18.04 G, $\underline{a}(6\text{H})$ 7.30 G and $\underline{a}(2\text{H})$ 0.71 G, and g-factor 2.0044.



When compound (5.5) was added to a solution of trifluoroacetic acid containing mercury(II) trifluoroacetate at 260 K it gave a yellowish solution. This solution showed no e.s.r. spectrum without photolysis. If this solution was irradiated with 30% Pyrex-

filtered U.V. light it showed a spectrum of the monomercurated radical cation (5.5a)⁺ which is illustrated in Figure 6.10b. We could not locate the hyperfine coupling to ¹⁹⁹Hg in spectrum 6.10b. With prolonged photolysis, a spectrum was obtained which appeared to be that of the dimercurated radical cation (5.5b)⁺, which is illustrated in Figure 6.10c. The principal ¹⁹⁹Hg satellites lie within the main body of the spectrum and contribute to the complication. The spectrum 6.10c can be simulated reasonably well in terms of 100% of dimercurated species (5.5b)⁺, with satellites due to ¹⁹⁹Hg hyperfine coupling, $a(^{199}\text{Hg})$ 9.18 G (equation 6.12).

When the dimercurated species (5.5b)⁺ was quenched by fluorosulphonic acid at 260 K, it gave a yellowish solution containing a white precipitate; this sample showed the spectrum of the radical cation (5.5)⁺.

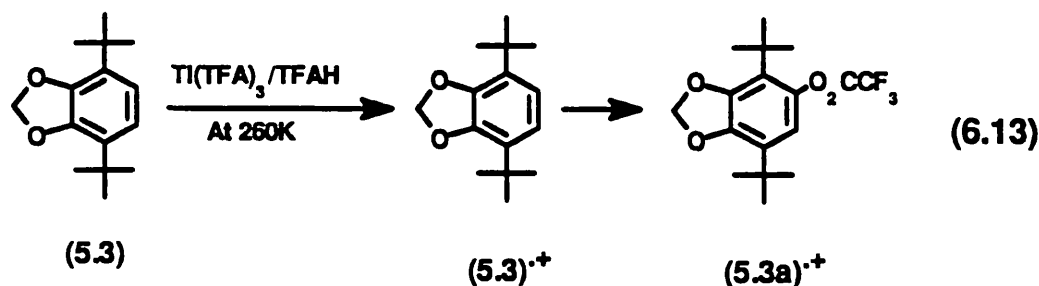
6.2.9. 4,7-Di-*tert*-butylbenzo-1,3-dioxole (5.3)

In the dark, 4,7-di-*tert*-benzo-1,3-dioxole (5.3) in dichloromethane containing AlCl₃ gave rise to a strong spectrum of the radical cation (5.3)⁺, with the hyperfine coupling constants: $a(2\text{H})$ 4.55 G and $a(2\text{H})$ 21.41 G.

Oxidation of the compound (5.3) with thallium(III) trifluoroacetate in trifluoroacetic acid at 260 K gave a yellowish solution, which without photolysis led to the appearance of several different e.s.r. spectra over a period of time. The initial spectrum is the familiar (5.3)⁺ which is illustrated in Figure 6.11a. After about 5 min, this was replaced by the spectrum in Figure 6.11b, which appeared to consist of the spectrum with $a(2\text{H})$ 4.55 G and $a(2\text{H})$ 21.41 G in (5.3)⁺, and further signals were developed in the gaps of the small triplets. After, 30 min at 260 K, it gave the spectrum shown in Figure 6.11c, with $a(1\text{H})$ 4.00 G and $a(2\text{H})$ 21.71 G. After about 1 hr a weaker spectrum 6.11c was recorded, and after a total of 1½ hr, no spectrum of any radical cation could be detected.

It seems unlikely that these changes could be due to thallation of the aromatic rings as ²⁰³Tl (29.52% abundance) and ²⁰⁵Tl (70.48% abundance) each have a nuclear spin of ½ and no hyperfine coupling by these isotopes could be observed. Sullivan has reported,¹¹ and we have confirmed, that thallium(III) trifluoroacetate brings about trifluoroacetoxylation of anthracene in the 9,10-positions where the proton hyperfine coupling constant is the largest, and it seems probable that we are observing trifluoroacetoxylation of compound (5.3) in the benzene ring where $a(2\text{H})$ is 4.55 G.

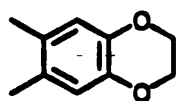
We assign the spectrum in Figure 6.11c to the 4,7-di-*tert*-butyl-5-(trifluoroacetoxy)benzo-1,3-dioxole radical cation (5.3a)^{•+} (equation 6.13). The *g*-factor increases from 2.00466 as it is in (5.3)^{•+} to 2.00481 in (5.3a)^{•+}.



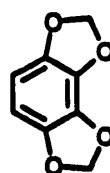
To investigate the effect of the conditions on the trifluoroacetylation, a few drops of trifluoroacetic anhydride were added to a solution of the compound (5.3) in TFAH containing $\text{Ti}(\text{TFA})_3$ at 260 K. The spectrum showed a marked increase in the rate of trifluoroacetylation (total 30 min). Photolysis weakened the spectrum.

It is interesting that, when $\text{Ti}(\text{TFA})_3$ was replaced by $\text{Hg}(\text{TFA})_2$ in a solution of TFAH containing compound (5.3) at 260 K it gave a yellowish solution. Without photolysis, this solution showed a strong e.s.r. spectrum of (5.3)^{•+}. If this solution was irradiated with Pyrex-filtered U.V. light that gave a relatively weak spectrum of (5.3)^{•+}, under no conditions of temperature or photolysis could we observe distortion of the spectrum or the appearance of satellites, which would indicated the occurrence of mercuration or trifluoroacetylation.

6.2.10. 6,7-Dimethylbenzo-1,4-dioxane (4.3) and benzo[1,2-d:3,4-d']bis-1,3-dioxole (5.8)



(4.3)



(5.8)

Compounds (4.3) and (5.8) in trifluoroacetic acid were treated with thallium(III) trifluoroacetate, which readily oxidised both to the corresponding familiar radical cations (4.3)⁺ (in Chapter 4) and (5.8)⁺ (in Chapter 5).

If compounds (4.3) and (5.8) were dissolved in TFAH containing Hg(TFA)₂ at 260 K, no e.s.r. spectra could be observed. If these solutions were photolysed with 100% Pyrex-filtered U.V. light, both showed a weak and complicated spectrum, which could not to be analyzed. This might be related to some kind of ring opening or mercuration.

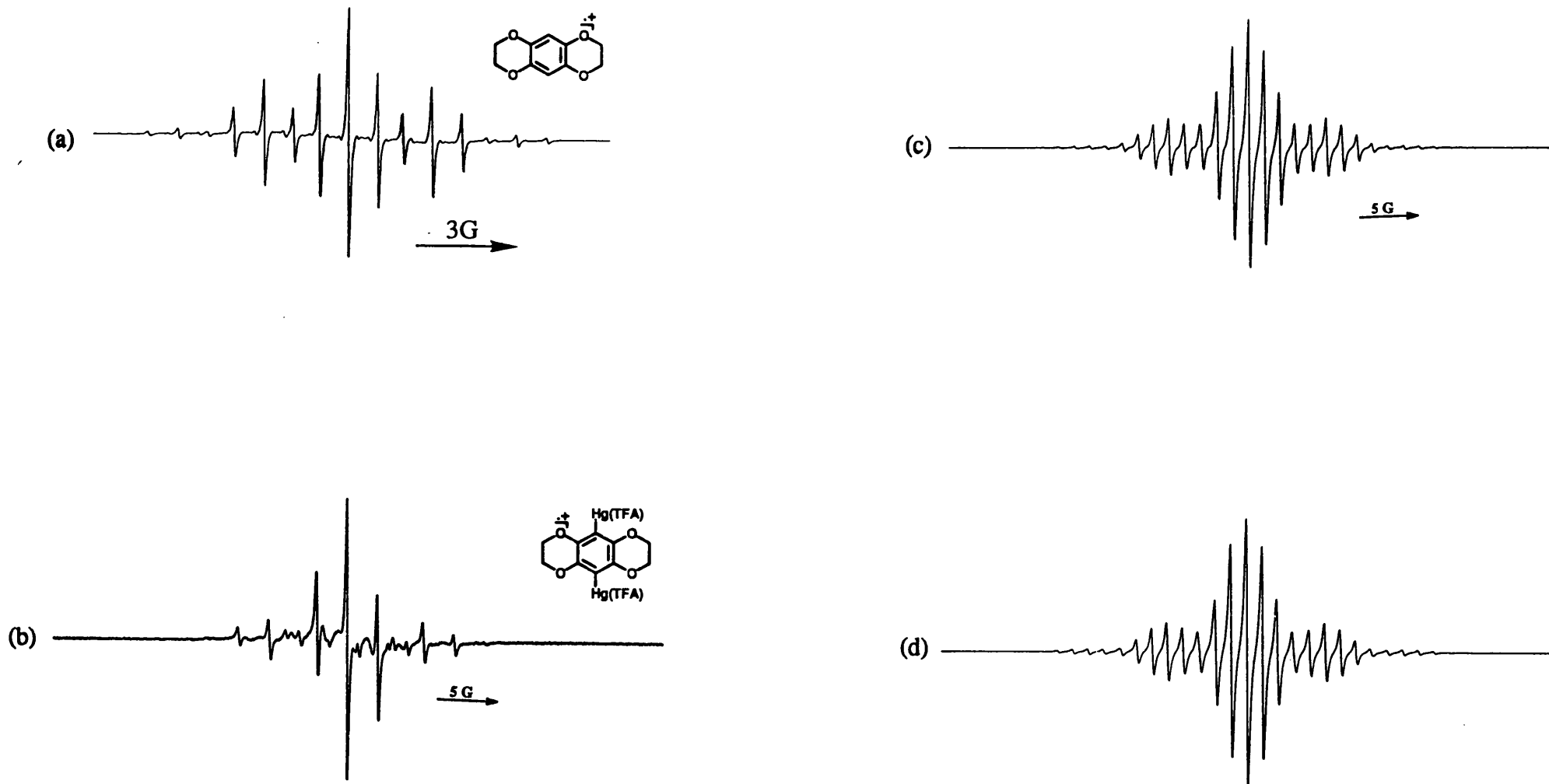


Figure 6.8. E.s.r. spectra of radical cations in TFAH. (a) $(4.1)^{\bullet+}$ at 260 K. (b) $(4.1a)^{\bullet+}$ at 260 K. (c) $(4.1a)^{\bullet+}$ at 330 K (d) Computer simulation of the spectrum 6.8c.

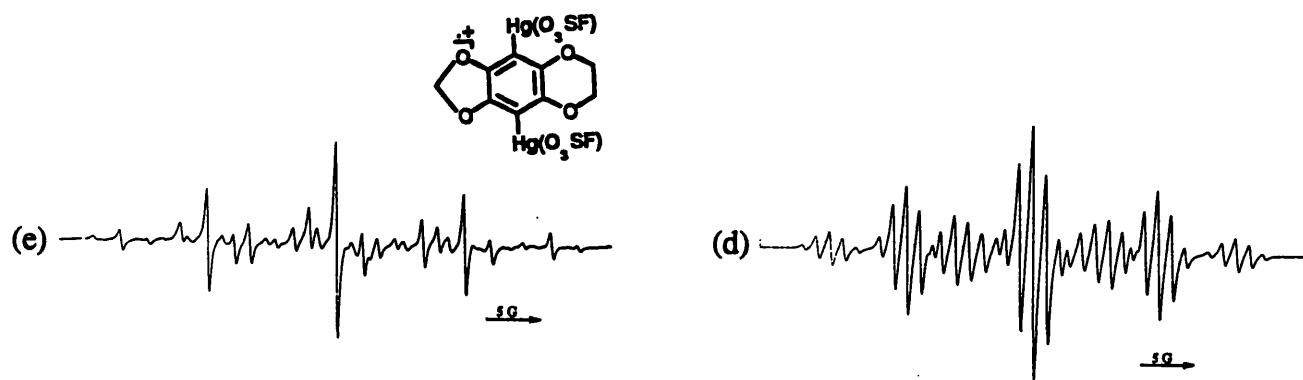
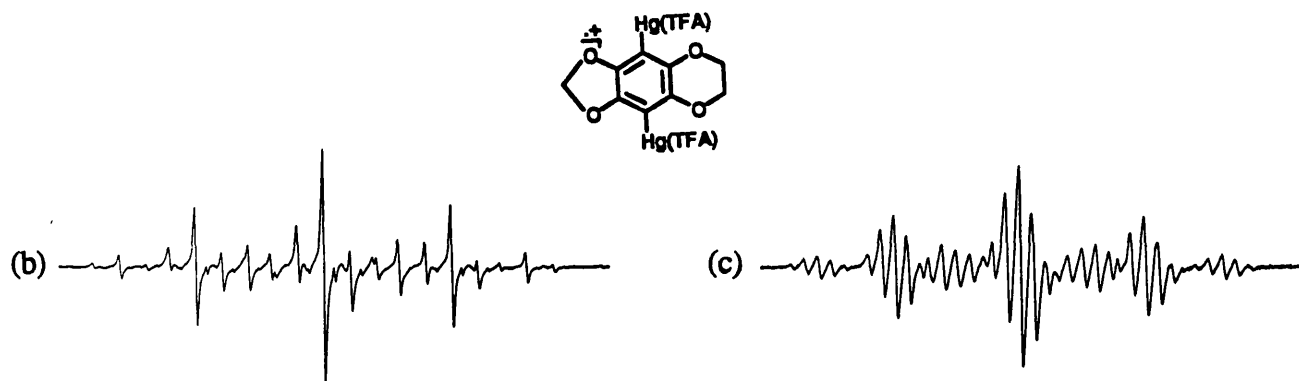
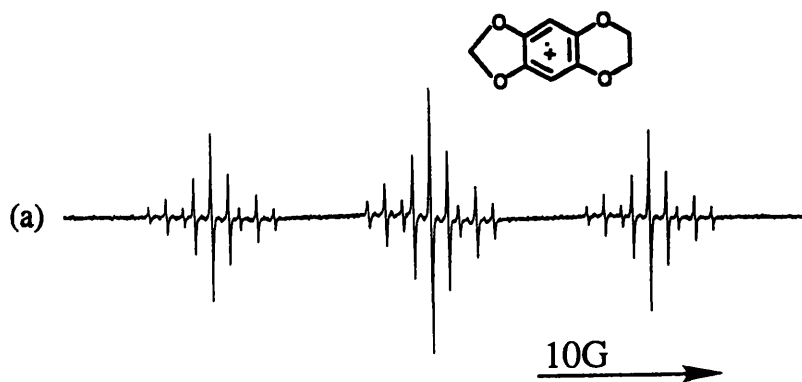


Figure 6.9. E.s.r. spectra of radical cations in TFAH. (a) $(4.2)^+$ at 260 K. (b) $(4.2a)^+$ at 260 K. (c) $(4.2a)^+$ at 333 K. (d) Computer simulation of the spectrum 6.8c. (e) $(4.2b)^+$ at 260 K.

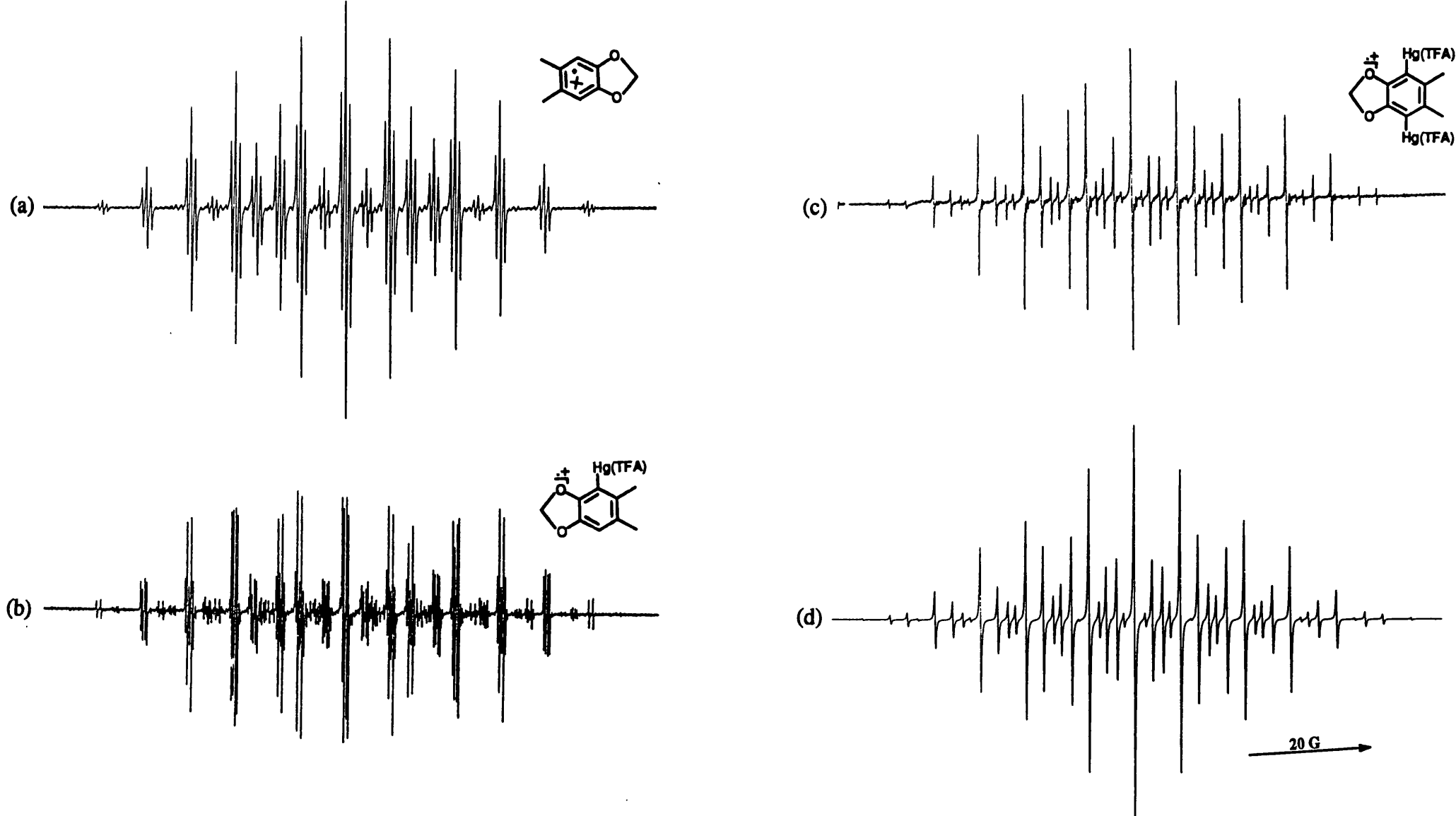


Figure 6.10. E.s.r. spectra of radical cations in TFAH at 260 K. (a) 5,6-Dimethylbenzo-1,3-dioxole (5.5)⁺. (b) Monomercurated 5,6-dimethylbenzo-1,3-dioxole (5.5a)⁺. (c) Dimercurated 5,6-dimethylbenzo-1,3-dioxole (5.5b)⁺. (d) Computer simulation of the spectrum 6.10c.

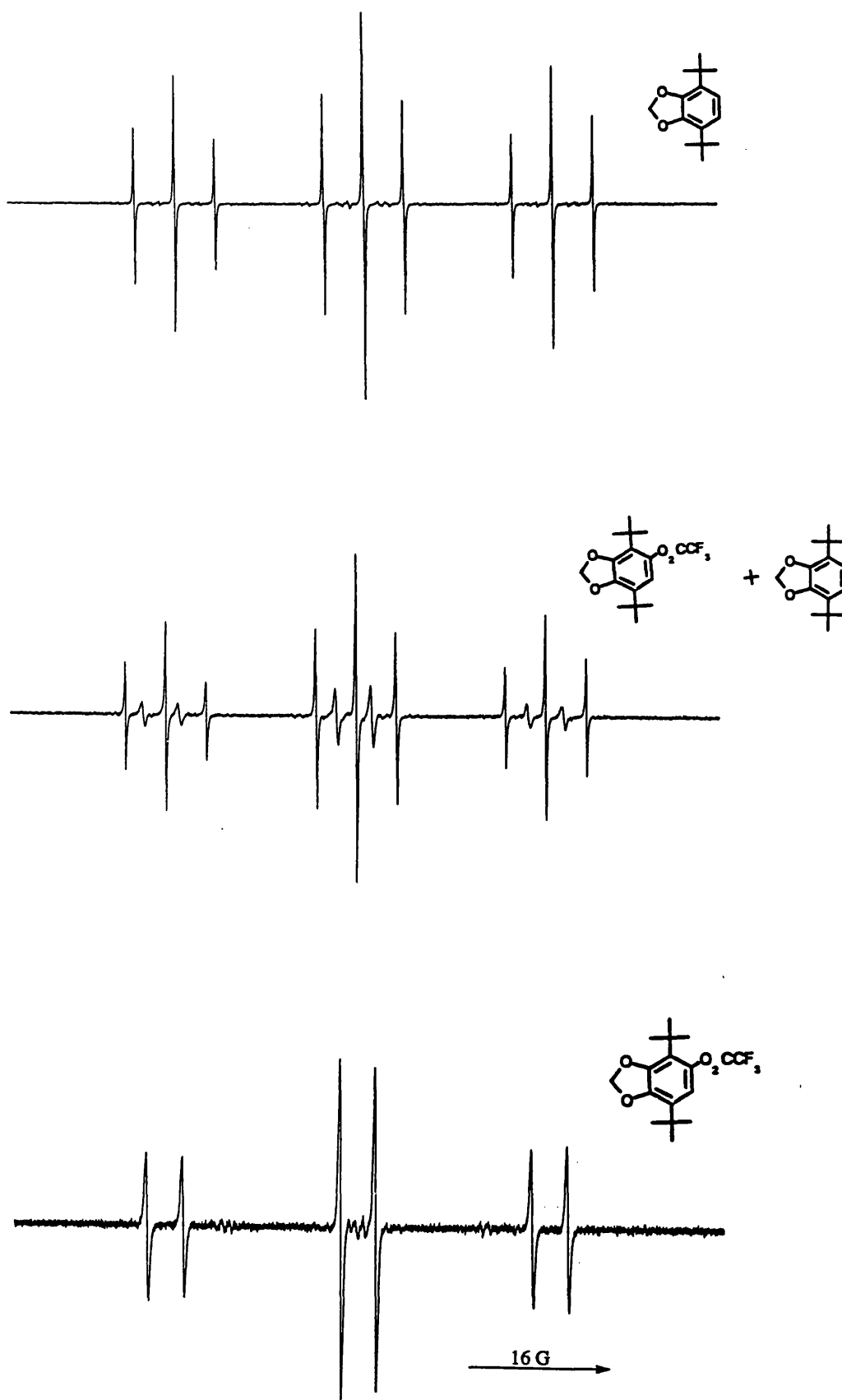
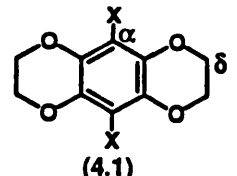
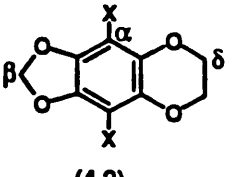
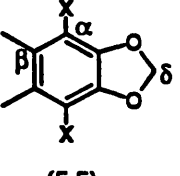


Figure 6.11. E.s.r. spectra of radical cations in TFAH at 260 K. (a) 4,7-Di-*tert*-butylbenzo-1,3-dioxole (5.3)⁺. (b) Non- and monotrifluoroacetylated 4,7-di-*tert*-butylbenzo-1,3-dioxole (5.3)⁺ and (5.3a)⁺. (c) Monotrifluoroacetylated 4,7-di-*tert*-butylbenzo-1,3-dioxole (5.3a)⁺.

Table 6.1. E.s.r. spectra of mercurated arene radical cations at 260 K.

Radical cations	ArH ⁺	$\underline{a}(\text{H})/G$	$\underline{a}(\text{X})/G$ (X= ¹ H, ¹⁹⁹ Hg-TFA ^b or ¹⁹⁹ Hg-FSO ^c)		g-factors	$\underline{a}(\text{Hg})/\underline{a}(\text{H})$	$\underline{a}(\text{Hg-FSO})/\underline{a}(\text{Hg-TFA})$
 (4.1)	(4.1) ⁺	4H _{ax} +4H _{eq} (δ) 2.45	2H(α)	0.90	2.0044	-	-
	(4.1a) ⁺	4H _{ax} +4H _{eq} (δ) 2.45	2Hg-TFA(α)	12.45	2.0048	13.81	-
 (4.2)	(4.2) ⁺	2H _{ax} +2H _{eq} (δ) 2.48 2H(β) 11.60	2H(α)	0.94	2.0046	-	-
	(4.2a) ⁺	2H _{ax} +2H _{eq} (δ) 2.48 2H(β) 11.70	2Hg-TFA(α)	13.72	2.0052	14.6	-
	(4.2b) ⁺	2H _{ax} +2H _{eq} (δ) 2.48 2H(β) 11.70	2Hg-FSO(α)	15.85	2.0054	16.9	1.157
 (5.5)	(5.5) ⁺	6H(β) 7.30 2H(δ) 18.04	2H(α)	0.71	2.0044	-	-
	(5.5a) ⁺	3H(β) 7.18 3H(β) 7.53 2H(δ) 18.00	1H(α) 0.71 1Hg-TFA(α) <i>a</i>	-	-	-	-
(5.5b) ⁺	6H(β) 7.50 2H(δ) 17.90	2Hg-TFA(α)	9.18	2.0047	12.91	-	

^a $\underline{a}(\text{¹⁹⁹Hg})$ cannot be resolve. ^b ¹⁹⁹Hg-TFA = a trifluoroacetate anion attached to the mercury atom. ^c ¹⁹⁹Hg-FSO = a fluorosulphonate anion attached to a mercury atom.

Table 6.2. E.s.r. spectra of mercurated arene radical cations at 260 K.

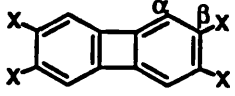
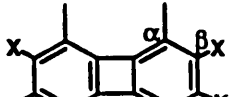
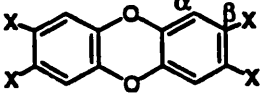
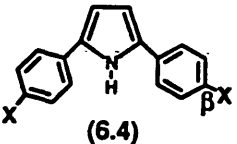
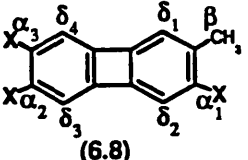
Radical ions	ArH ⁺	$\underline{a}(\text{H})/\text{G}$	$\underline{a}(\text{X})/\text{G}$ (X=H, ¹⁹⁹ Hg-TFA or ¹⁹⁹ Hg-FSO)	g-factors	$\underline{a}(\text{Hg})/\underline{a}(\text{H})$	$\underline{a}(\text{Hg-FSO})/\underline{a}(\text{Hg-TFA})$		
 (6.1)	(6.1) ⁺	4H(α)	0.20	4H(β)	3.60	2.0025	-	-
	(6.1a) ⁺	4H(α)	0.20	3H(β) 1Hg-TFA(β)	3.60 76.71	2.0014	21.3	-
	(6.1f) ⁺	4H(α)	0.20	3H(β) 1Hg-FSO(β)	3.60 88.15	2.0014	24.5	1.150
 (6.2)	(6.2) ⁺	12H(α)	<0.15	4H(β)	3.25	2.0025	-	-
	(6.2a) ⁺			3H(β) 1Hg-TFA(β)	3.25 69.86	2.0014	21.5	-
	(6.2b) ⁺			3H(β) 1Hg-FSO(β)	3.25 80.28	2.0014	24.7	1.149
 (6.3)	(6.3) ⁺	4H(α)	<0.005	4H(β)	2.20	2.0039	-	-
	(6.3a) ⁺			3H(β) 1Hg-TFA(β)	2.20 43.20	2.0031	19.6	-
	(6.3b) ⁺			3H(β) 1Hg-FSO(β)	2.20 49.30	2.0031	22.4	1.143

Table 6.2. (continued) Radical cations	ArH ⁺	<u>a</u> (H)/G		<u>a</u> (X)/G		g-factors	<u>a</u> (Hg)/ <u>a</u> (H)	<u>a</u> (Hg-FSO)/ <u>a</u> (Hg-TFA)
 (6.4)	(6.4) ⁺	<i>i</i>		H(B)	<i>i</i>	<i>ii</i>	-	-
	(6.4a) ⁺	<i>i</i>		1Hg-TFA(B)	64.30	<i>ii</i>	-	-
	(6.4b) ⁺	<i>i</i>		1Hg-FSO(B)	74.67	<i>ii</i>	-	1.161
 (6.8)	(6.8) ⁺	3H(B)	5.50	1H(α_y)	2.97 ^b	2.0026	-	-
		1H(δ_z)	0.18 ^a	1H(α_y)	3.56 ^b			
		1H(δ_z)	0.55 ^a	1H(α_y)	4.20 ^b			
		2H(δ_z)	<0.05 ^a					
	(6.8a) ⁺	3H(B)	5.20	1H(α_y)	3.00 ^b	2.0018	21.8	-
		1H(δ_z)	0.18 ^a	1H(α_y)	3.60 ^b			
	1H(δ_z)	0.55 ^a	1Hg-TFA(α_y)	91.85 ^b				
(6.8b) ⁺	3H(B)	5.20	1H(α_y)	3.00 ^b	2.0018	24.9	1.142	
	1H(δ_z)	0.18 ^a	1H(α_y)	3.60 ^b				
	1H(δ_z)	0.55 ^a	1Hg-FSO(α_y)	104.83 ^b				

ⁱ a(H) could not be resolve. [#] g-Factors could not be resolve. ^a $\delta_z = \delta_1$, or δ_2 , or δ_3 . ^b $\alpha_y = \alpha_1$, or α_2 , or α_3 .

6.3. Discussion

6.3.1. ^{199}Hg Satellites

The isotopic nuclear spins and natural abundance of various isotopes of mercury are illustrated in Table 6.3.

Table 6.3. The isotopic composition and the spin in naturally occurring mercury.

Isotopes	Spin	Natural Abundances/%
^{196}Hg	0	0.146
^{198}Hg	0	10.02
^{199}Hg	1/2	16.84
^{200}Hg	0	23.13
^{201}Hg	3/2	13.22
^{202}Hg	0	29.80
^{203}Hg	0	6.85

The e.s.r. spectra of mercury-containing organic compounds in solution that have been reported apart from our own work, relate to complexes of some nitroxyl¹² and semiquinones^{13,14} radicals, and these record only ^{199}Hg but not ^{201}Hg hyperfine coupling. Similarly, ^{199}Hg - ^1H coupling is well documented in N.M.R. spectroscopy, but ^{201}Hg - ^1H coupling has not been observed. Fullam and Symons, however, have detected both ^{199}Hg and ^{201}Hg hyperfine coupling in the radicals $\text{CH}_3\text{HgCH}_2\cdot$ and $\text{BrHgCH}_2\cdot$ in the solid state.¹⁵

In our e.s.r. spectra we observed ^{199}Hg but not ^{201}Hg hyperfine coupling. This is probably due to rapid relaxation induced by the nuclear quadrupole moment, which broadens the signals of the e.s.r. spectra of the radicals containing this isotope (^{201}Hg) beyond detectability.

The relative intensity of the combined pair of ^{199}Hg satellites to that of the central spectrum which is due to the spin-free isotopomers in a monomercurated radical should be 16.84:69.94 (or 1:4.15), and this is approximately what we observe. Similarly, the intensities of the secondary, and tertiary, ^{199}Hg satellites arising from the radical cations

containing two or three ^{199}Hg atoms, respectively, agree approximately with predictions.

Wan found mercuration reduced the g-factor of the radical, and rationalised the low g-factors in terms of the spin-orbital coupling which results from p_{π} - d_{π} overlap.¹²⁻¹⁴

6.3.2. Site of Mercuration.

When the parent hydrocarbon contains nonequivalent aromatic protons, mercurideprotonation occurs at the position where the proton hyperfine coupling is greatest (usually $a(\text{H}) > 2.0$ G), which is where the S.O.M.O. of the hydrocarbon radical cation and the local coefficient of the M.O. of the H.O.M.O. of the hydrocarbon is greatest. Photolysis with U.V. light filtered through Pyrex glass is often necessary for mercuration to be observed, but the use of unfiltered U.V. light always led to a rapid decay of the spectrum.

When mercuration occurs, the hyperfine coupling of the remaining protons and the ^{13}C hyperfine coupling (if it can be detected) is not changed. This implies that the mercury substituent has essentially no effect on the electron distribution and that the coefficients of the S.O.M.O. are unchanged by the mercuration.

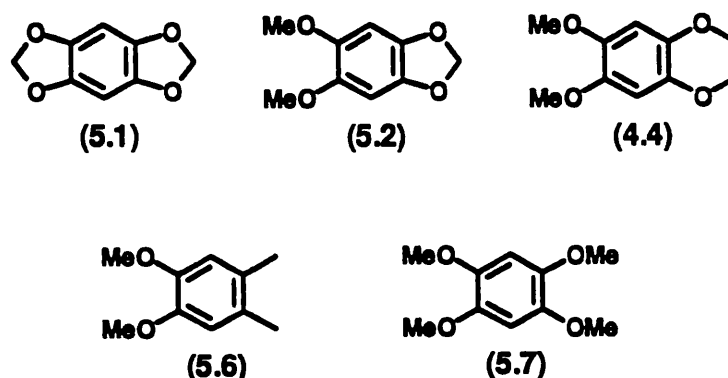
6.3.3. Mercuration of Compounds (4.1), (4.2) and (5.5).

Recently, we have observed that mercurideprotonation occurs at the position where the proton hyperfine coupling constant is small ($a(\text{H}) < 1.0$ G) in compounds (4.1), (4.2) and (5.5).

These compounds (4.1), (4.2) and (5.5) are derivatives of benzene where the 1,2- and 4,5-positions are occupied by $-\text{OCH}_2\text{O}-$, or $-\text{OCH}_2\text{CH}_2\text{O}-$ or methyl groups, but the *para* (or 3,6)-positions remain unoccupied. The e.s.r. spectra indicated that the S.O.M.O. of the radical cations (4.1)⁺, (4.2)⁺ and (5.5)⁺ has the Ψ_A M.O. configuration and the hyperfine coupling at the *para*-position in (4.1)⁺ is 0.90 G, in (4.2)⁺ is 0.94 G and in (5.5)⁺ is 0.71 G, and at the other four positions is relatively high (see Table 6.1).

When compounds (4.1), (4.2) and (5.5) in TFAH were treated with $\text{Hg}(\text{TFA})_2$, the spectra indicated that mercuration occurred at the *para*-position where the proton hyperfine coupling constant is small. This is the first set of the examples where mercurideprotonation occurs at positions with low spin density. Only in the case of compound (5.5) was photolysis essential for mercuration.

To investigate further examples of similar systems, 6,7-dimethoxy-1,4-benzodioxane (4.4), benzo[1,2-d:4,5-d']bis-1,3-dioxole (5.1), 5,6-dimethoxybenzo-1,3-dioxole (5.2), 4,5-dimethyl-1,2-dimethoxybenzene (5.6) and 1,2,4,5-tetramethoxybenzene (5.7) in trifluoroacetic acid were treated with mercury(II) trifluoroacetate. All the five compounds were readily oxidized to the corresponding familiar radical cations. Under no conditions of temperature or photolysis could we observe distortion of the spectra or the appearance of Hg satellites, which would indicate the occurrence of mercuration.



6.3.4. The Ratio $\underline{a}(^{199}\text{Hg})/\underline{a}(^1\text{H})$

Davies and McGuchan reported that the ratio of the hyperfine coupling by mercury-199 which is introduced to that by the proton which is displaced is approximately constant, with $\underline{a}(^{199}\text{Hg})/\underline{a}(^1\text{H})$ *ca.* 20.6,⁸ making it possible to predict the value of $\underline{a}(^{199}\text{Hg})$ in new species and to locate the ^{199}Hg satellites more readily.

This implies a proportionality between the spin density on the ring α -carbon and on the attached mercury atom according to a McConnell-like equation 6.14:¹⁶

$$\underline{a}(^{199}\text{Hg}) = Q_{\text{C-Hg}}\rho_{\text{C}\alpha} \quad (6.14)$$

where the constant $|Q_{\text{C-Hg}}| = 20.6Q_{\text{C-H}}$. Gerson has recommended values of $Q_{\text{C-H}}$ for radical cations of -35.1 G based on H.M.O. electron densities c^2 , and -25.4 G based on the more accurate McLachlan spin densities, which leads to the corresponding values for $Q_{\text{C-Hg}}$ of -723 and -523 G, respectively.¹⁷

As replacement of hydrogen by mercury almost does not perturb the S.O.M.O. of

the radical cation, so the spin polarisation of the C-H and C-Hg σ -bonding electron pair should be similar, placing similar spin densities on the hydrogen and mercury. In that case, if bonding by hydrogen utilized the 1s-orbital and that by mercury utilizes a pure 6sp-hybrid, with 50% s-character (and no p_π - p_π or p_π - d_π involvement), the ratio $\underline{a}(^{199}\text{Hg})/\underline{a}(^1\text{H})$ should be approximately equal to $A_o(^{199}\text{Hg})/2A_o(^1\text{H})$, where $A_o(^{199}\text{Hg})$ is the isotropic coupling to mercury (41880 MHz)¹⁸ and $A_o(^1\text{H})$ is the isotropic coupling to hydrogen (1422 MHz).

This predicts a value of $\underline{a}(^{199}\text{Hg})/\underline{a}(^1\text{H})$ of *ca.* 15, as compared with that of 20.6 which was observed previously.⁸ The discrepancy between these two values has been rationalised on the model proposed by Fullam and Symons,¹⁵ who generated radicals $\cdot\text{CH}_2\text{HgX}$ and $\text{Me}\dot{\text{C}}\text{HHgX}$ (X= Me, I, Br, or Cl) by γ -radiolysis of the solid matrixes at 77 K and found that $\underline{a}(^{199}\text{Hg})$ increased from 220 G to 450 G as the electronegativity of X increased in above sequence. They suggested that when X was more electronegative than the organic ligand, the Hg-X bond involved largely the mercury 6p_z-orbital, so the C-Hg bond involved mainly the 6s-orbital and the spin polarisation of the C-Hg σ -bond was more effective. In our system, the ligand X in ArHgX^+ is presumably the electronegative trifluoroacetate group, therefore, the Hg-TFA bond has a p-contribution greater than 50% and Ar-Hg bond has a s-contribution greater than 50%.

6.3.4a. A New Ratio $\underline{a}(^{199}\text{Hg})/\underline{a}(^1\text{H})$ when the ligand X is Fluorosulphonate (FSO)

As shown in Table 6.2 and Figure 6.12, the replacement of the trifluoroacetate (TFA) anion by a fluorosulphonate (FSO) anion, gave an increase of $\underline{a}(^{199}\text{Hg})$ as the electronegativity of the anion increased, and the constant $Q_{\text{C-Hg}}$ increased by *ca.* 14% to a new value of ratio of $\underline{a}(^{199}\text{Hg-FSO})/\underline{a}(^1\text{H})$ *ca.* 23.5. Our experimental results are accommodated well by this electronegativity argument.

As far as this project is concerned, we could not extend examinations to other ligands (eg. Cl, Br, or ClSO_3) in our strong acid conditions. This is probably caused by rapid protodemercuration when the mercury atom is associated with a highly electronegative ligand. Even the e.s.r. spectra of our mercurated radical cation containing fluorosulphonate group did not live very long.

6.3.4b. Unusual Low Ratio $\underline{a}(^{199}\text{Hg})/\underline{a}(^1\text{H})$

Table 6.1 and Figure 6.13 illustrate ratios of $\underline{a}(^{199}\text{Hg})/\underline{a}(^1\text{H})$ *ca.* 13.8 which is significantly lower than the earlier estimate of *ca.* 20.6 for the HgTFA group.

There is a further, and maybe related problem associated with the spectra of (4.1a)⁺, (4.2a)⁺ and (5.5b)⁺: these show a slight increase in the g-factor on mercuration, rather than the decrease which is previously observed.

The cause of these two discrepancies is not clear, but we suggest a number of factors which may be relevant.

(a) We note that all three compounds (4.1), (4.2) and (5.5) are derivatives of the degenerate (Ψ_A and Ψ_S M.O.) benzene ring. The earlier studies involved only non-degenerate molecules (eg. biphenylene or dibenzodioxin). The S.O.M.O. of the radical cations and the mercurated radical cations [(4.1a)⁺, (4.2a)⁺ and (5.5b)⁺] is Ψ_A . If the energy gap between Ψ_A and Ψ_S levels becomes larger when two mercury atoms are introduced to the benzene ring at the *para*-positions, this might explain the low value of $\underline{a}(^{199}\text{Hg})$. This seems unlikely, as the spectra showed that the other hyperfine coupling constants are essentially unaffected by mercuration.

(b) The mercurated molecules might be co-ordinated with other ligands which have electron releasing ability. We suggest that the lone pair electrons on the oxygen atom in these molecules may form intramolecular dative covalent bonds to the nearest mercury atoms (Figure 6.14). This could reduce the s-character contribution in the Ar-Hg bond and make the hyperfine coupling by spin polarisation of the C-Hg σ -bond less effective. However, stereochemically, this intramolecular bond seems rather unlikely.

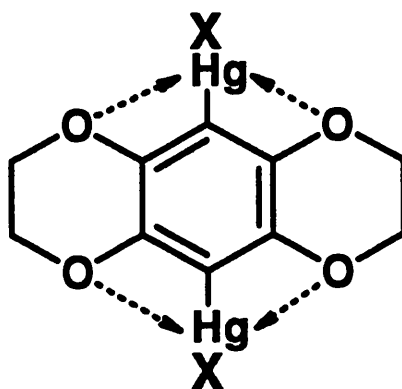


Figure 6.14. Intramolecular dative covalent bond to the mercury atoms.

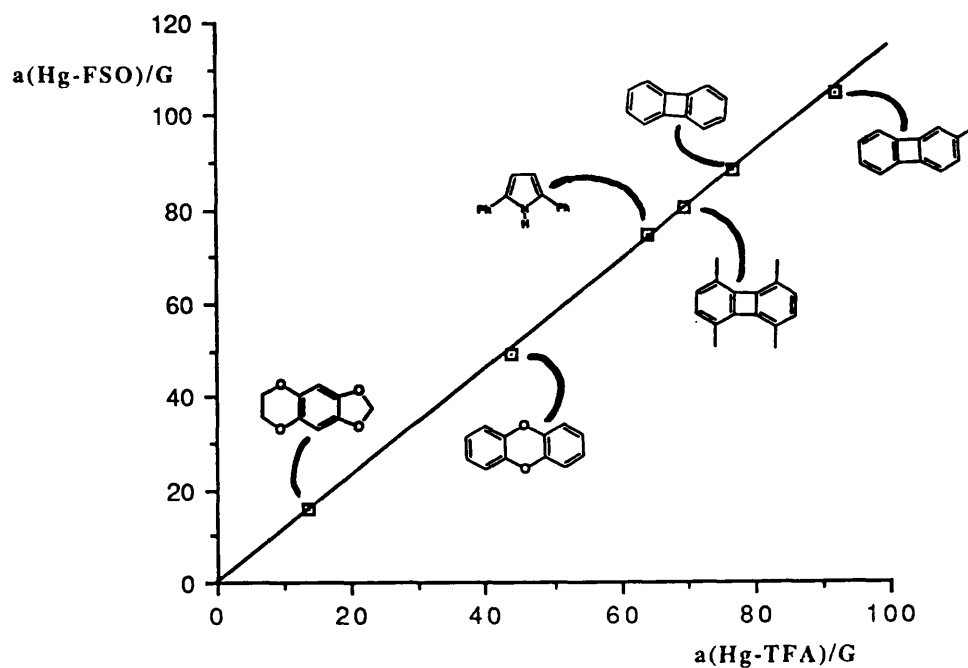


Figure 6.12. Plot of $\underline{a}(^{199}\text{Hg-FSO})$ against $\underline{a}(^{199}\text{Hg-TFA})$.

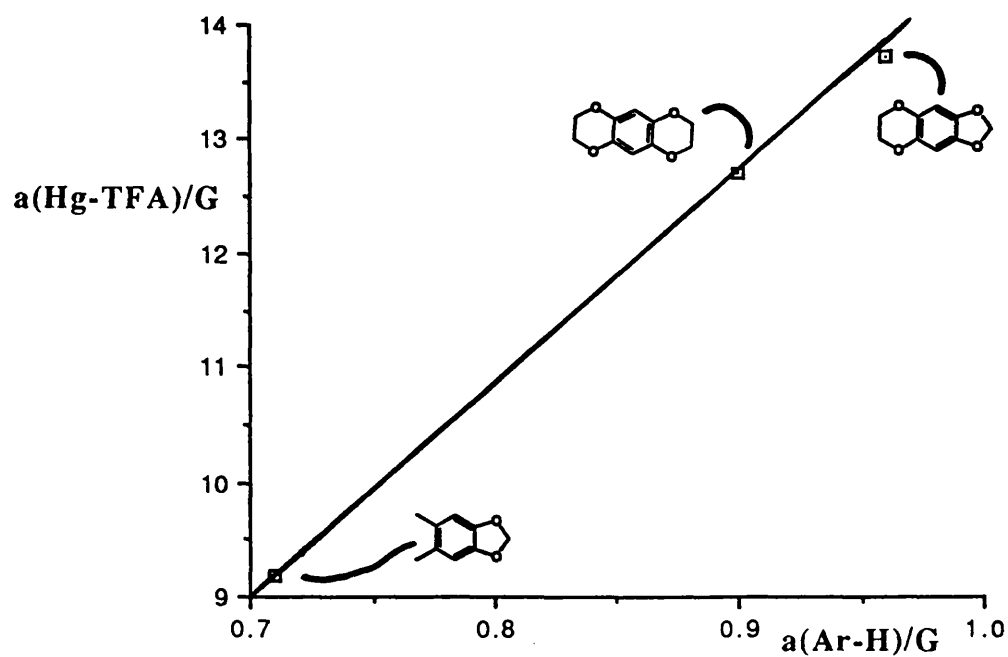


Figure 6.13. Plot of $\underline{a}(^{199}\text{Hg-TFA})$ against $\underline{a}(^1\text{H})$ for the process of mercurideprotonation.

(c) Since these radical cations were generated in trifluoroacetic acid solution. The molecules might form a complex with the -OH group in TFAH as illustrated in Figure 6.15. Again, if the lone pair electrons on the -OH group complexed to the mercury atom, the hybridisation of the C-Hg bond would be more sp^3 than sp and the lower s -character could give a lower coupling.

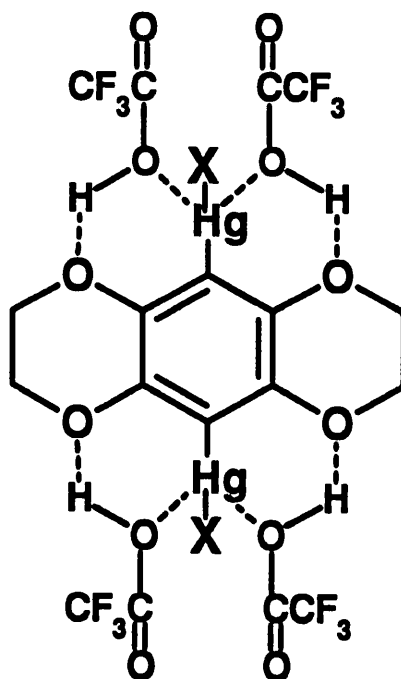
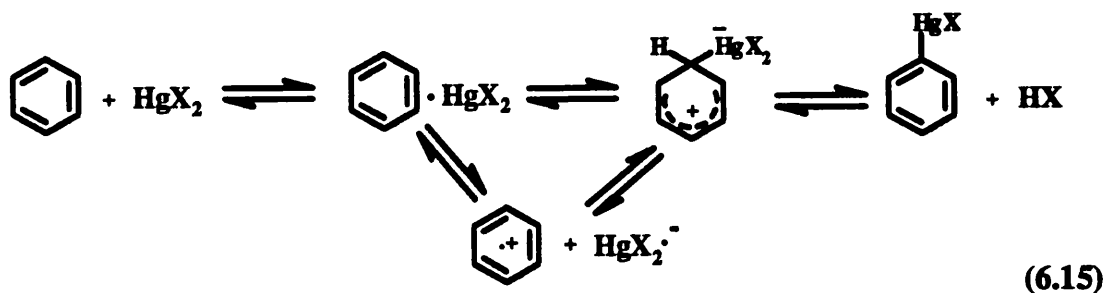


Figure 6.15. Intermolecular Complex.

6.3.5. Mechanism of Mercuration

Aromatic mercuration is usually accepted to involve attack of the electrophile $Hg(TFA)_2$ to first form a charge-transfer complex, then a Wheland intermediate, followed by elimination of TFAH (equation 6.15).



In the compounds we have studied (e.g. (4.1), (4.2) and (5.5)), the mercuration occurs before the sample is irradiated with U.V. light and could be accommodated by this mechanism.

With other compounds, however (e.g. biphenylene), the mercuration is slow in the dark, but relatively fast when the sample is photolysed. The e.s.r. spectra show that this photolysis enhances electron transfer in the charge-transfer complex to produce a radical ion pair; collapse of the radical ion pair then leads to mercuration (equation 6.15).

Aromatic mercuration and thallation by mercury(II) trifluoroacetate or thallium(III) trifluoroacetate occur equally readily, and it is interesting that we observe the e.s.r. spectra of mercurated species so frequently, but we have not yet observed the spectra of the thallated species. Two factors probably account for this. First, thalliodeprotonation is reversible, and under our condition, the parent hydrocarbon ArH will be present together with the thallated compound, $\text{ArTl}(\text{TFA})_2$. Second, thallation appears to attract electrons from the ring and thereby increases the ionisation potential of the thallated compound.

6.3.6. Trifluoroacetoxylation

It is interesting that we do not observe trifluoroacetoxylation more frequently, because this should reduce the ionisation potential of the arene. Sullivan has shown that anthracene undergo trifluoroacetoxylation with $\text{Tl}(\text{TFA})_3$ at the 9- and 10-positions.¹¹ Photolysis of arenethallium bis(trifluoroacetates) has been shown to lead to the formation of some aryl trifluoroacetates.^{19,20,21} Generation of the spectrum of the 9,10-bis-(trifluoroacetoxy)anthracene, which we observe from anthracene in TFAH in presence of $\text{Tl}(\text{TFA})_3$, may indicate that, at least in this system, trifluoroacetoxylation proceeds through thallation.

Our recent example of trifluoroacetoxylation of 4,7-di-*tert*-butylbenzo-1,3-dioxole (5.3) in TFAH/ $\text{Tl}(\text{TFA})_3$, leads to the formation of the mono-(trifluoroacetoxy)-4,7-di-*tert*-butylbenzo-1,3-dioxole spectrum only, and not the di-trifluoroacetoxy species. This might be due to protonation of the oxygen which increases the ionisation potential of the π -system.

References

1. W. Lau, J.C. Huffman and J.K. Kochi, *J. Am. Chem. Soc.*, 1982, **104**, 5515
2. W. Lau and J.K. Kochi, *J. Org. Chem.*, 1986, **51**, 1801.
3. W. Lau and J.K. Kochi, *J. Am. Chem. Soc.*, 1986, **108**, 6720.
4. J.L. Courtneidge, A.G. Davies, D.C. McGuchan and S.N. Yazdi, *J. Organomet. Chem.*, 1988, **341**, 63.
5. J.K. Kochi, *Inorg. Chem.*, 1980, **19**, 2749.
6. G.B. Deacon and D. Tunaley, *J. Organomet. Chem.*, 1978, **156**, 403.
7. D.V. Avila, A.G. Davies, M.L. Girbal and K.M. Ng, *J. Chem. Soc., Perkin Trans. 2*, 1990, 1693.
8. A.G. Davies and D.C. McGuchan, *Organometallic*, 1991, **10**, 329.
9. D.V. Avila and A.G. Davies, *J. Chem. Soc., Perkin Trans. 2*, 1991, 1111.
10. N.A. Malysheva, A.I. Prokof'ev, N.N. Bubnov, S.P. Solodovnikov, T.I. Prokof'eva, V.B. Vol'eva, V.V. Ershov and M.I. Kabachnik, *Izv. Akad. Nauk SSSR, Ser. Khim.*, 1988, **5**, 1040.
11. P.D. Sullivan, E.M. Menger, A.H. Reddoch and D.H. Paskovich, *J. Phys. Chem.*, 1978, **82**, 1158.
12. J.N. Helbert, P.W. Kopf and E.H. Poindexter, *J. Chem. Soc., Dalton Trans.*, 1975, 998.
13. K.S. Chen, R.T. Smith and J.K.S. Wan, *Can. J. Chem.*, 1978, **56**, 2503.
14. D. Weir, D.A. Hutchinson, J. Russell and J.K.S. Wan, *Can. J. Chem.*, 1982, **60**, 703.
15. B.W. Fullam and M.C.R. Symons, *J. Chem. Soc., Dalton Trans.*, 1974, 1086.
16. H.M. McConnell, *J. Chem. Phys.*, 1956, **24**, 764.
17. F. Gerson, *High Resolution E.S.R. Spectroscopy*, Wiley, New York, 1976.
18. J.R. Morton and K. Preston, *J. Magn. Reson.*, 1978, **30**, 577.
19. A. McKillop and E.C. Taylor, *Comprehensive Organometallic Chemistry*, G.

Wilkinson, F.G. Stone and E.W. Abel, Eds., Pergamon Press, Oxford, 1982, Vol. 7, 499.

20. A. McKillop, J.D. Hunt, J.S. Fowler, E.C. Taylor, G. McGillivray and F. Kienzle, *J. Am. Chem. Soc.*, 1971, 93, 4841.
21. A. McKillop and E.C. Taylor, *Acc. Chem. Res.*, 1970, 3, 338.

Chapter 7. Radical Ions of Benzenoid Systems

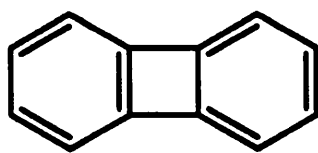
7.1. Background.

As already described in Chapter 1, Hückel molecular orbital calculations can predict the molecular structure of many alternant π -systems. The e.s.r. spectra of the radical ions can also be calculated with this simple theory, but the results are rather poor. More advanced treatments such as the McLachlan method have improved the prediction.¹

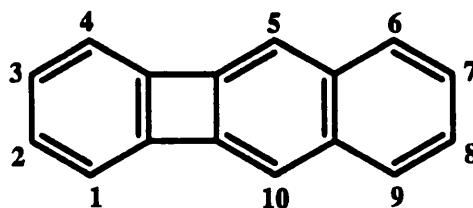
Biphenylene is an interesting molecule because it contains a central four-membered ring. The e.s.r. spectra of the biphenylene radical ions showed that all the hyperfine coupling constants in the biphenylene radical cation are larger than in its radical anion, and this could be interpreted in terms of the pairing principal.² The pairing theorem states that in alternant hydrocarbon radical anions and cations, the spin densities at corresponding positions should be the same. This implies the variation in the proton hyperfine coupling constants between corresponding radical anions and cations is due to change in the constant, Q_{CH} , and not to a redistribution of the spin densities.³

In this Chapter, attention is focused on the proton hyperfine coupling constants of the corresponding radical anions and the radical cations, of molecules such as benzo[b]biphenylene (7.1), binaphthylene (7.2) and tribenzo[12]annulene (7.3).

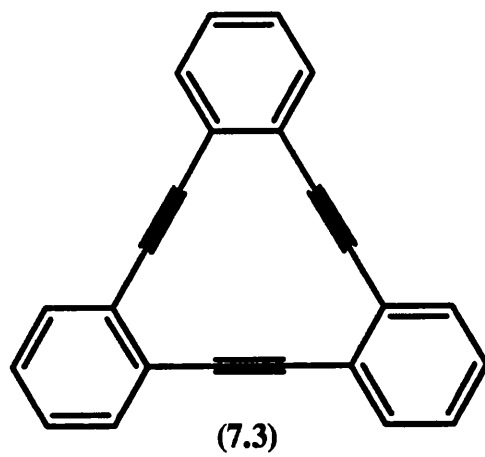
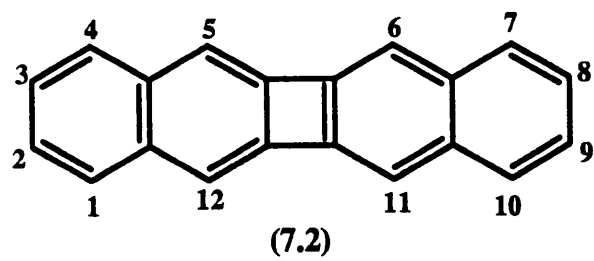
Many of the e.s.r. spectra of the benzo-derivatives radical anions are well known, but the spectra of the corresponding radical cations are absent from the literature. In recent years a number of new methods have been developed for the generation of the radical cations for study by e.s.r. spectroscopy, and we have applied these new techniques to the generation of the radical cations of benzo-derivatives.



(6.1)



(7.1)



7.2. Results.

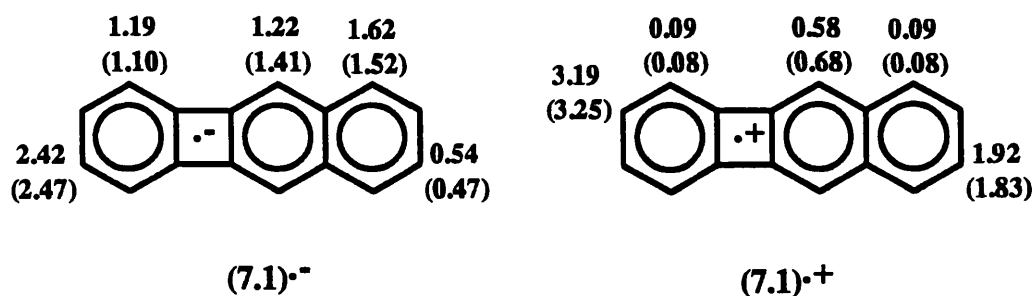
The compounds benzo[b]biphenylene (7.1), binaphthylene (7.2) and tribenzo[12]annulene (7.3) were supplied by Dr. M.K. Shepherd (University of North London).

7.2.1. Benzo[b]biphenylene (7.1)

The e.s.r. spectra of the benzo[b]biphenylene radical anion (7.1)⁻ and radical cation (7.1)⁺ have been reported previously, by F. Gerson.⁴ The radical anion (7.1)⁻ was formed by reduction of parent (7.1) with potassium metal in 1,2-dimethoxyethane (DME), and the radical cation (7.1)⁺ was prepared by oxidation of (7.1) either with concentrated sulphuric acid or AlCl₃/CH₃NO₂.

We observed a similar spectrum of the radical anion (7.1)⁻ when compound (7.1) was treated with potassium metal in THF containing a small amount of benzo-18-crown-6 ether. This solution was light blue and gave the spectrum of the radical anion (7.1)⁻ which is illustrated in Figure 7.1.

Again, the same spectrum of the benzo[b]biphenylene radical cation (7.1)⁺ was recorded if compound (7.1) was dissolved in a solution of Tl(TFA)₃/TFAH at 273 K (Figure 7.2). The hyperfine coupling constants are given in Scheme 7.0, and the results agree well with the literature.⁴



Scheme 7.0. $a(^1\text{H})$ in Gauss of (7.1)^{•-} and (7.1)^{•+}; data from the literature are given in brackets.

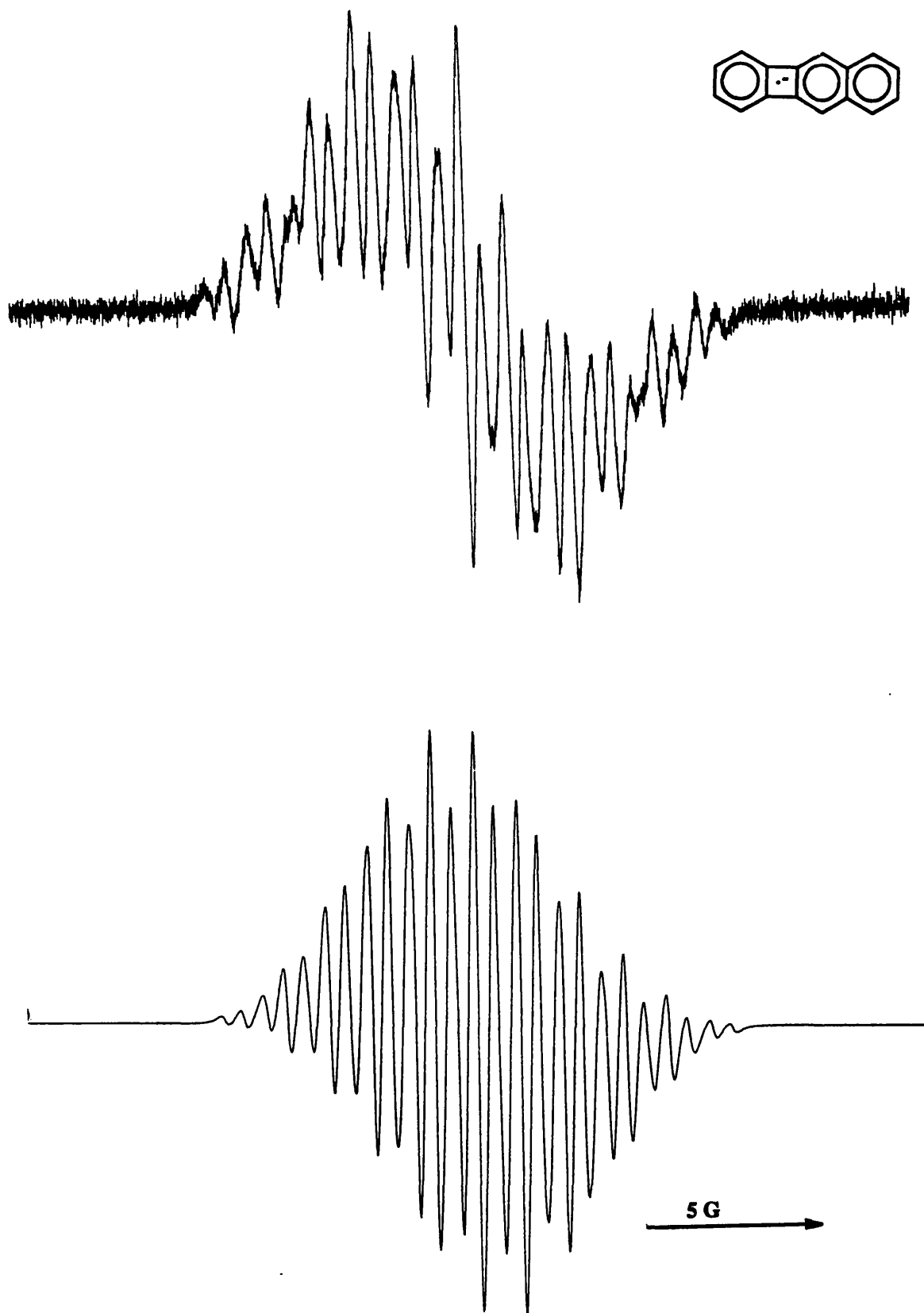


Figure 7.1. (top) E.s.r. spectrum and (bottom) simulation of (7.1) \cdot K⁺ in THF at 243 K.

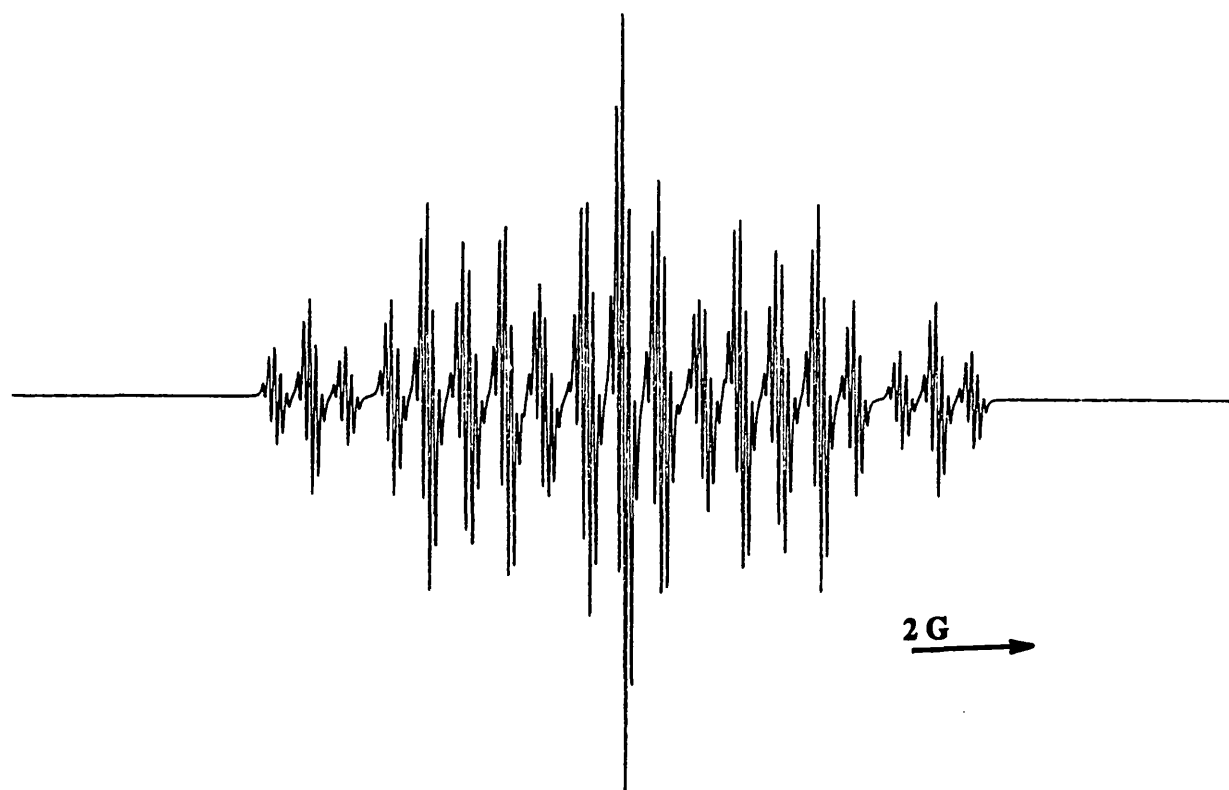
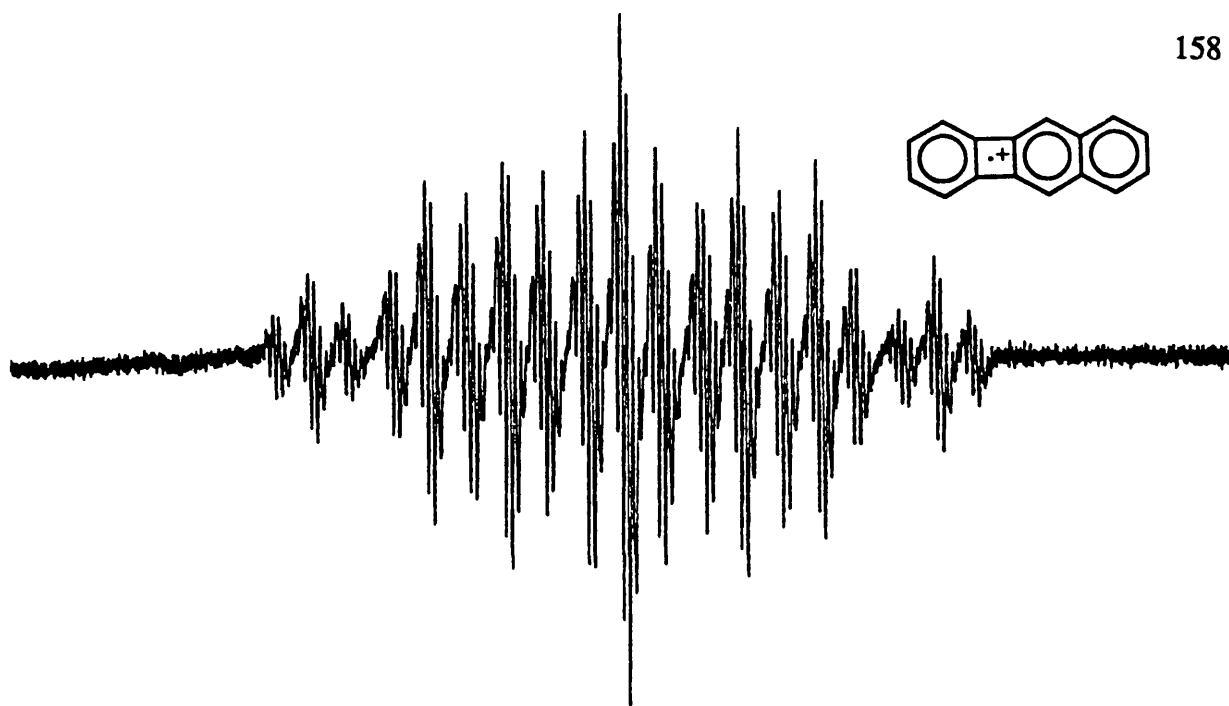
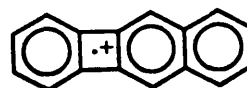


Figure 7.2. (top) E.s.r. spectrum and (bottom) simulation of (7.1)⁺ in TFAH/Tl(TFA)₃ at 273 K.

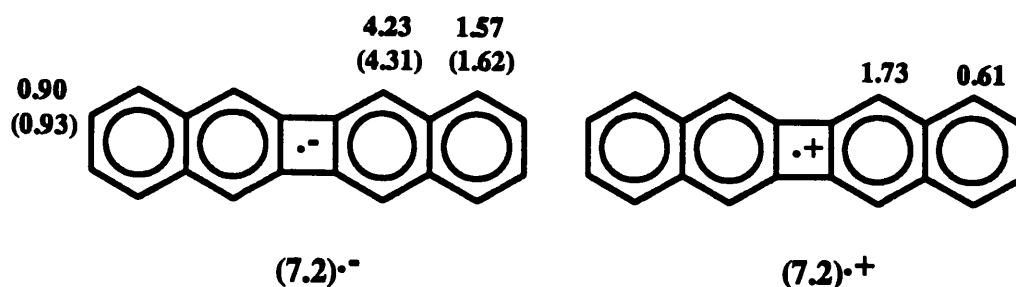
7.2.2. Binaphthylene (7.2)

An excellent spectrum of the binaphthylene radical anion $(7.2)^{\cdot-}$ was observed by Carrington and Dos Santos-Veiga from a solution of binaphthylene (7.2) in 1,2-dimethoxyethane containing potassium metal.⁵

When THF was used instead of DME, we observed the same spectrum of $(7.2)^{\cdot-}$ which is illustrated in Figure 7.3. The hyperfine coupling constants are showed in Scheme 7.1.

The spectrum of the binaphthylene radical cation $(7.2)^{\cdot+}$ is absent from the literature, and Carrington and Dos Santos-Veiga failed to observe it with a solution of (7.2) in concentrated sulphuric acid.⁵

The spectrum which we assign to the binaphthylene radical cation $(7.2)^{\cdot+}$ is shown in Figure 7.4. It was observed when (7.2) was dissolved in trifluoroacetic acid containing thallium(III) trifluoroacetate at 260 K, and we have subsequently obtained the same spectrum also by using DDQ or mercury(II) trifluoroacetate in trifluoroacetic acid. The measured hyperfine coupling constants are showed in Scheme 7.1.



Scheme 7.1. $a(^1\text{H})$ in Gauss of $(7.2)^{\cdot-}$ and $(7.2)^{\cdot+}$; data from the literature are given in brackets.

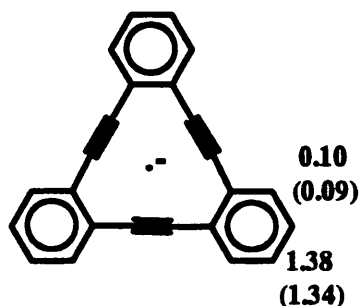
7.2.3. Tribenzo[12]annulene (7.3)

The e.s.r. spectrum of tribenzo[12]annulene radical anion $(7.3)^{\cdot-}$ was observed from a solution tribenzo[12]annulene (7.3) in DME with potassium metal at 298 K.⁶

When tribenzo[12]annulene (7.3) was dissolved in THF containing potassium metal and a small amount of benzo-18-crown-6 ether at 243 K, it gave a light blue solution

which this solution gave a spectrum consisting of a septet of septets [$\underline{a}(6\text{H})$ 1.38 G and $\underline{a}(6\text{H})$ 0.10 G, g 2.0026] (Figure 7.5).

The e.s.r. spectrum of the radical cation of tribenzo[12]annulene (7.3) has not been reported previously. In trifluoroacetic acid containing thallium(III) trifluoroacetate at 260 K, it gave the spectrum shown in Figure 7.6, with $\underline{a}(6\text{H})$ 1.29 G, and g 2.0025 (see Scheme 7.2).



Scheme 7.2. $\underline{a}(^1\text{H})$ in Gauss of (7.3) $^{\cdot+}$; data from the literature are given in brackets.

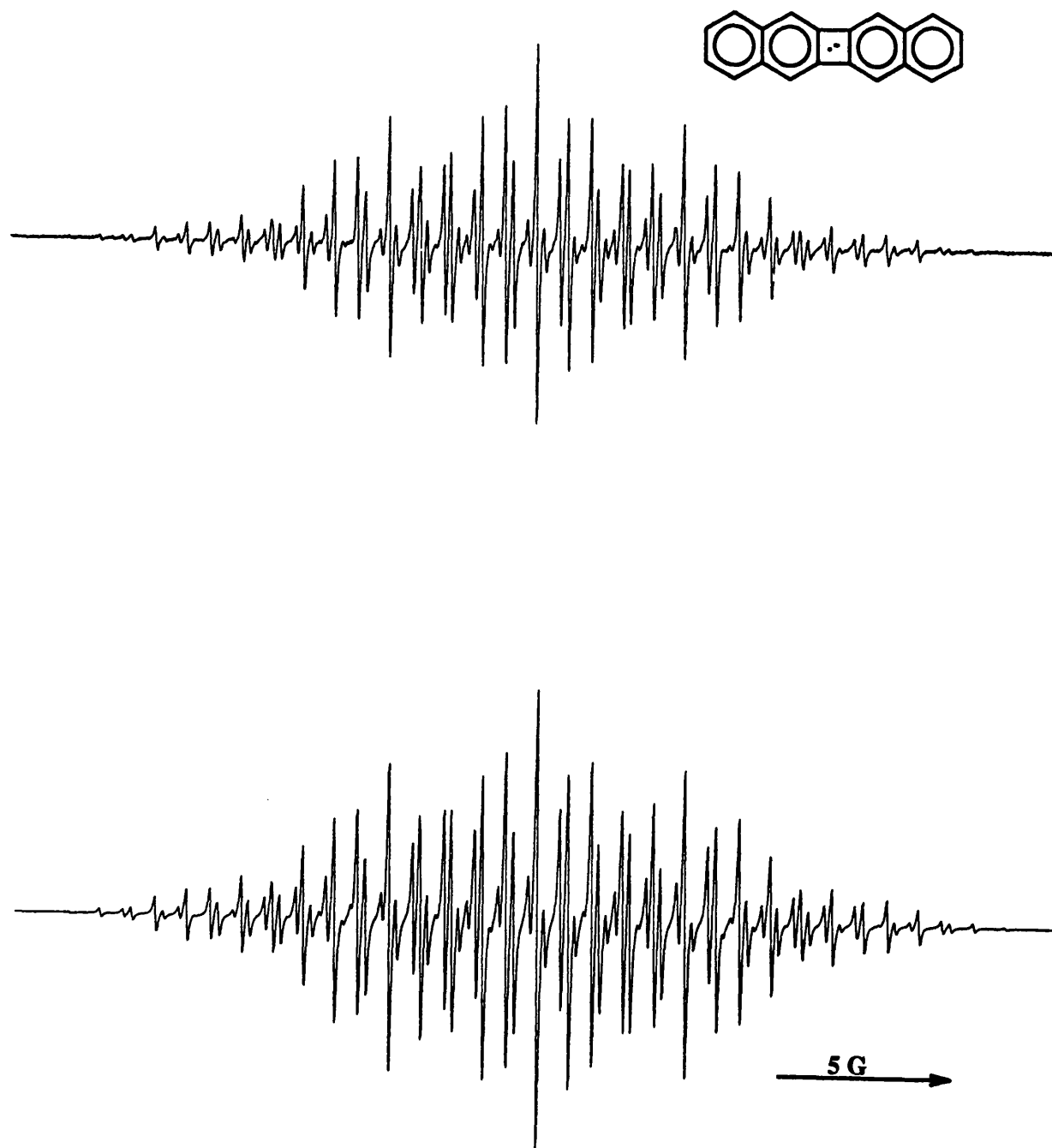


Figure 7.3. (top) E.s.r. spectrum and (bottom) simulation of $(7.2)^{\cdot+}K^+$ in THF at 243 K.

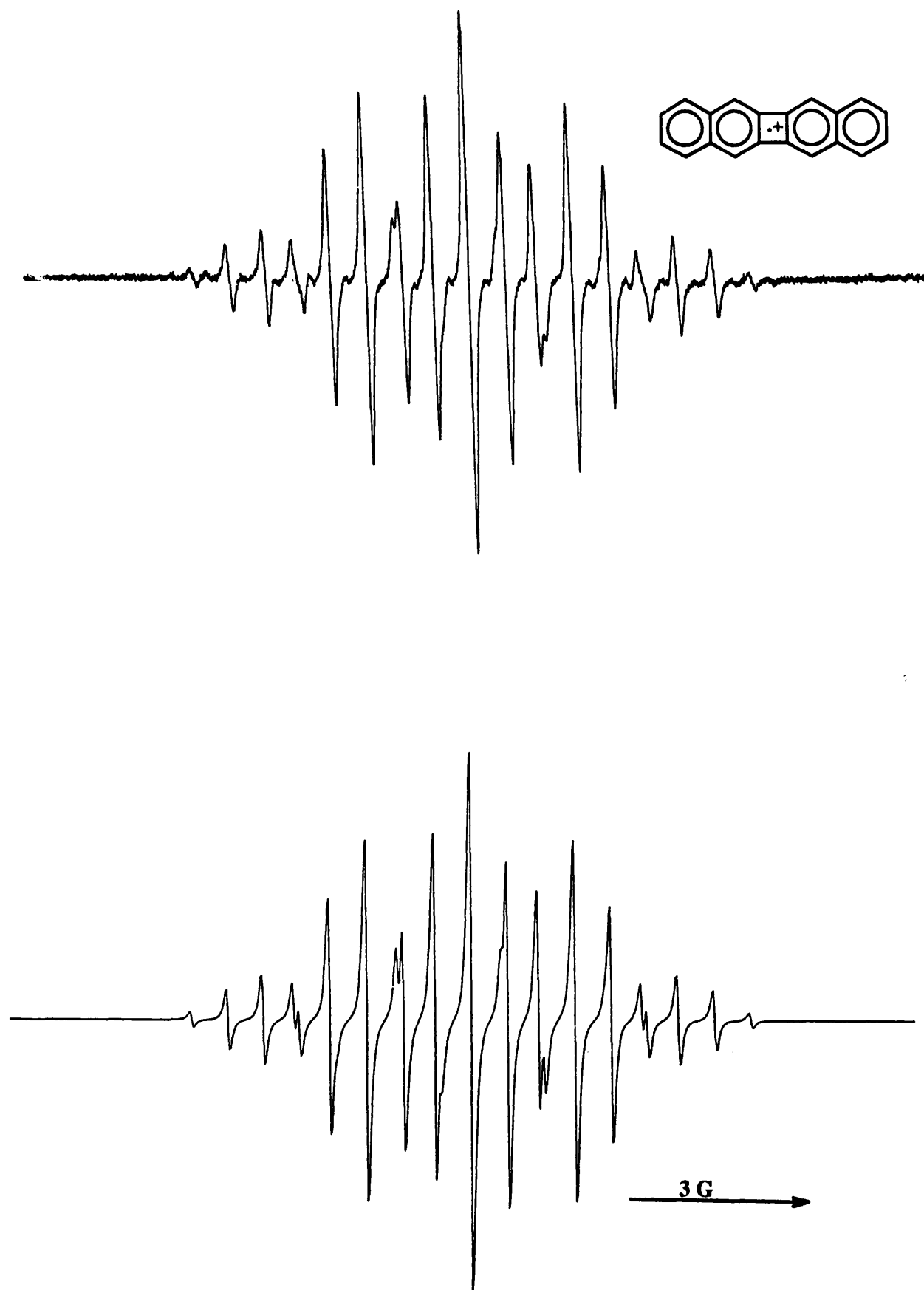


Figure 7.4. (top) E.s.r. spectrum and (bottom) simulation of (7.2)⁺ in TFAH/Tl(TFA)₃ at 260 K.

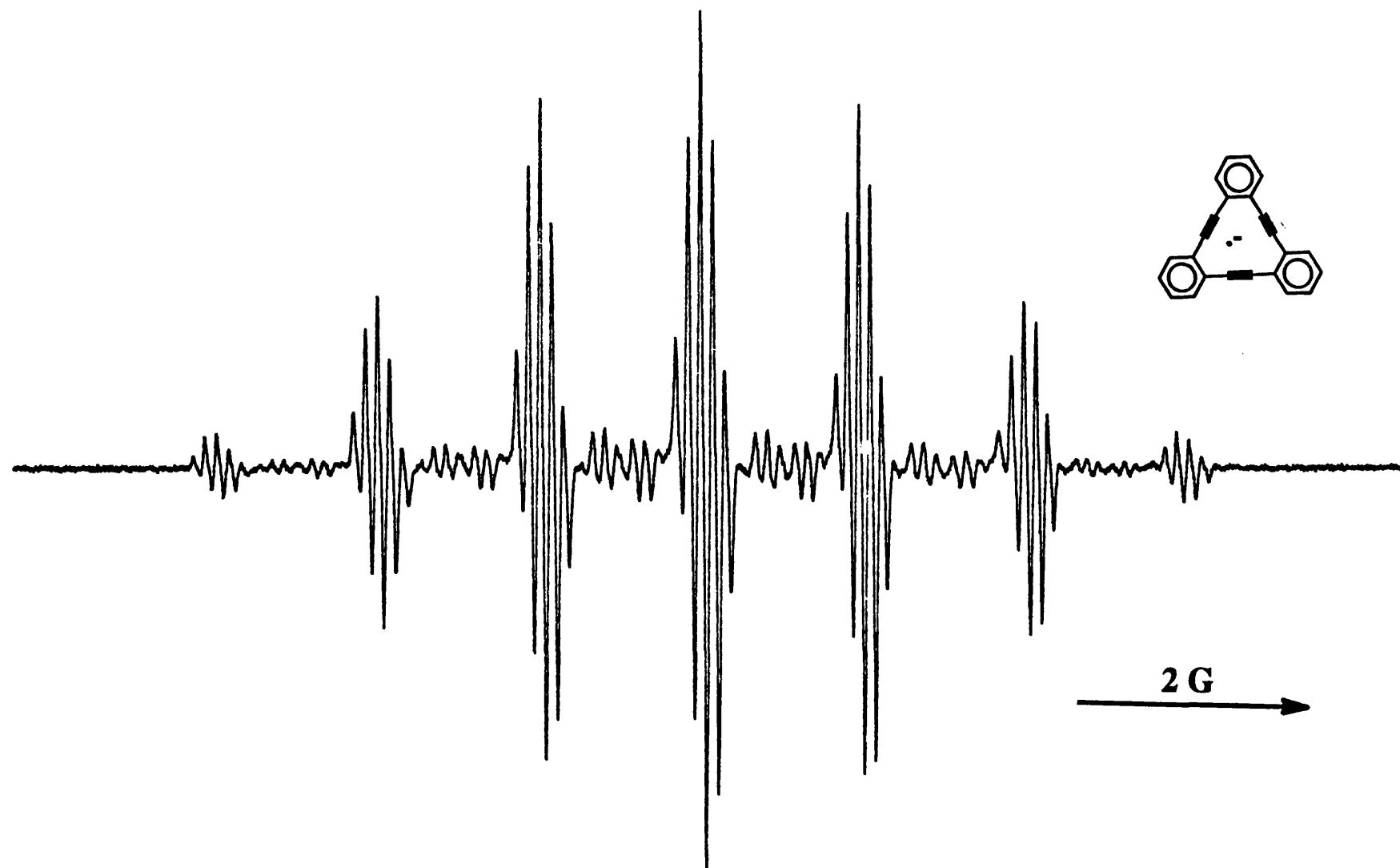


Figure 7.5. E.s.r. spectrum of (7.3)[•]K⁺ in THF at 243 K.

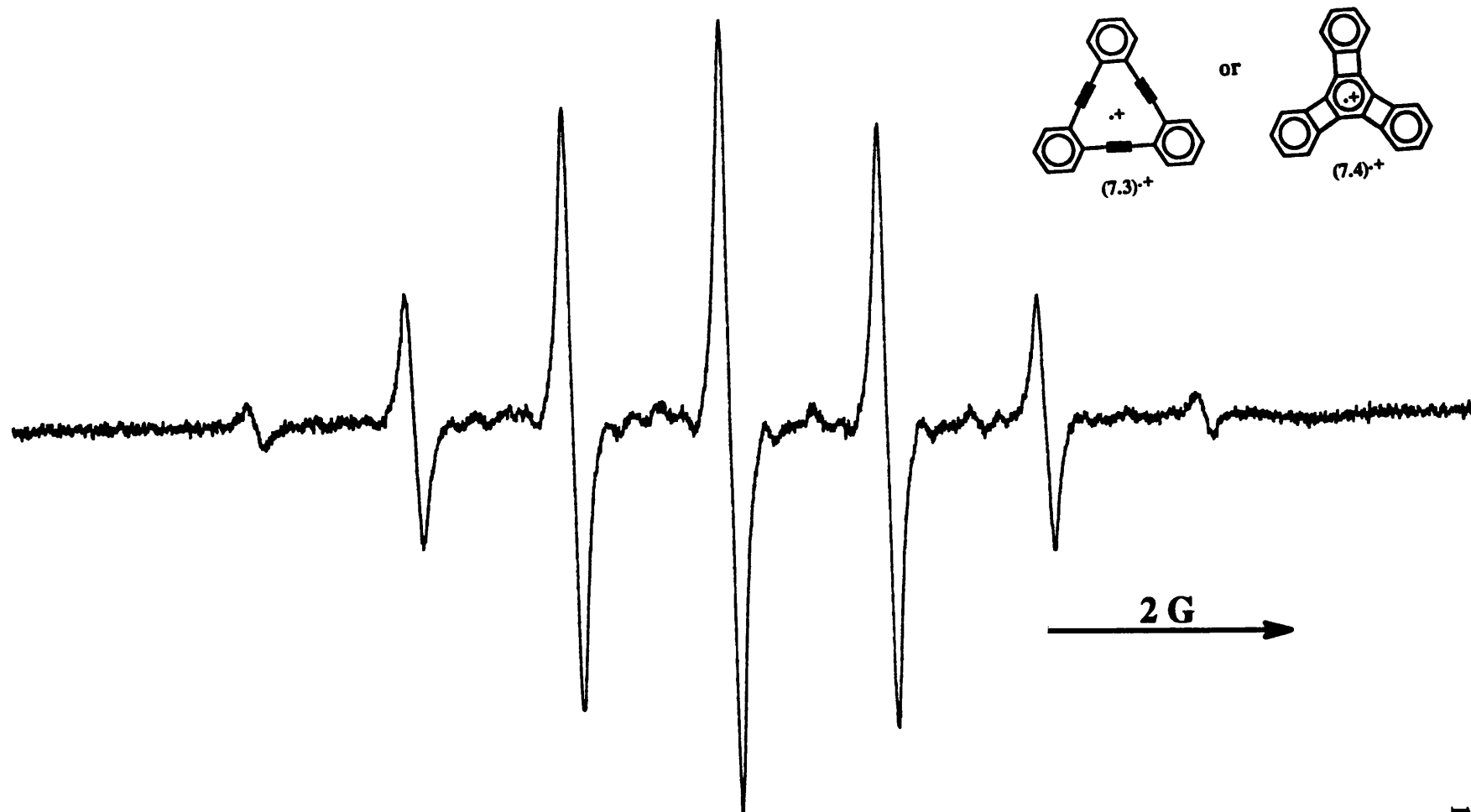


Figure 7.6. E.s.r. spectrum obtained from (7.3) in TFAH/Tl(TFA)₃ at 260 K.

7.3. Discussion.

7.3.1. Benzo[b]biphenylene (7.1) and binaphthylene (7.2)

As both benzo[b]biphenylene (7.1) and binaphthylene (7.2) are alternant hydrocarbons, the absolute values of the Hückel coefficients at corresponding positions in the H.O.M.O. and in the L.U.M.O. are the same if the molecule is accepted to be planar. If the spin densities ρ are taken to be equal to c^2 (c is a Hückel coefficient), the hyperfine coupling constants at corresponding positions in the radical cation and anion are given by the McConnell equation 7.1, and should therefore differ only insofar as the constant Q differs in the two species.

$$\underline{a}(\text{H}) = Q\rho \quad (7.1)$$

We found that the proton hyperfine coupling constants of the radical cations (7.1)⁺ and (7.2)⁺ are less than those of the corresponding radical anions.

This is opposite to the order which is usually observed, where the coupling constants for the radical cation are greater than those for the corresponding radical anion. This has been ascribed to the effect of the positive charge which concentrates the spin density in the singly occupied p-orbital.⁷

In our case therefore, either the pairing theorem or the charge effect theorem is breaking down. The only previous example of this of which we are aware is Gerson's study of benzo[b]biphenylene radical anion and radical cation. They suggested that in this structure the pairing theorem was breaking down.⁴

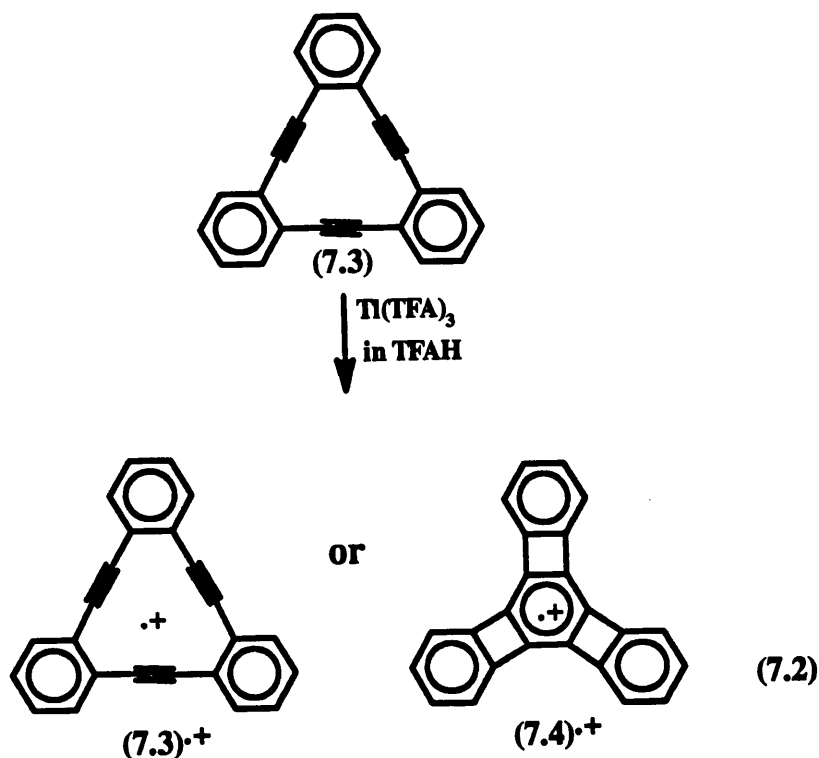
It is not clear to us what special factors cause these few molecules to give these anomalous results.

If we compare the hyperfine coupling constants of binaphthylene radical ions, the ratios of $\underline{a}_1(4\text{H})$ 0.61 G and $\underline{a}_5(4\text{H})$ 1.73 G in (7.2)⁺ [1 : 2.83], and $\underline{a}_1(4\text{H})$ 1.57 G and $\underline{a}_5(4\text{H})$ 4.23 G in (7.2)⁻ [1 : 2.70] are indeed the same. This suggests that the spin densities at the corresponding position in (7.2)⁻ and (7.2)⁺ are identical. Unfortunately, we were unable to measure any $\underline{a}(^{13}\text{C})$ values from carbon-13 satellites of these spectra.

7.3.2. Tribenzo[12]annulene (7.3).

It would be very interesting to study the species generated by oxidation of the tribenzo[12]annulene (7.3).

In our previously experience, if a mixture of a dialkylacetylene and AlCl_3 in dichloromethane is photolysed in an e.s.r. cavity, a strong spectrum of the tetra-alkyl cyclobutadiene radical cation is observed. On the other hand, under the same conditions, diphenylacetylene shows the radical cation of triphenylazulene (see Chapter 1). We expected that compound (7.3) might show the spectrum of the radical cation, $(7.4)^{\cdot+}$, when (7.3) was oxidised in fluid solution (equation 7.2). The simplicity of the spectrum which we observed (Figure 7.6) would be compatible with either $(7.3)^{\cdot+}$ or $(7.4)^{\cdot+}$, but not with an azulene-type product. It could be difficult to distinguish the species $(7.4)^{\cdot+}$ from $(7.3)^{\cdot+}$, since they both carried the same number of the protons. The best way to prove the formation of $(7.4)^{\cdot+}$ from the oxidation of (7.3), would be to oxidise tris-(benzocyclobutadiene)benzene (7.4) to the corresponding radical cation $(7.4)^{\cdot+}$, but the time available did not allow us to undertake this difficult preparation.



References

1. A.D. McLachlan, *Mol. Phys.*, 1960, **3**, 233.
2. J.R. Bolton and G.K. Fraenkel, *J. Chem. Phys.*, 1964, **40**, 3307.
3. J.R. Bolton, P.R. Hindle and J. Dos Santos-Veiga, *J. Chem. Phys.*, 1968, **48**, 4703.
4. F. Gerson, W.B. Martin Jr., F. Sondheimer and H.N.C. Wong, *Helv. Chim. Acta*, 1975, **58**, 2431.
5. A. Carrington and J. Dos Santos-Veiga, *Mol. Phys.*, 1962, **5**, 285.
6. H. Brunner, K.H. Hausser, M. Rawitscher and H.A. Staab, *Tetrahedron Lett.*, 1966, 2775.
7. J.P. Colpa and J.R. Bolton, *Mol. Phys.*, 1963, **6**, 309.

Chapter 8.

Experimental

8.1. SYNTHESIS.

8.1.1 1,4-Di-(chloromethyl)2,3,5,6-tetramethylbenzene (3.1a)^{3,4}

Durene (25 g, 185 mmol) was dissolved in petroleum (60 cm³) and mixed with 40% formaldehyde (60 cm³, 750 mmol), zinc chloride (8 g) and conc. hydrochloric acid (60 cm³). The mixture was heated with stirring on an oil bath at 90° C while conc. hydrochloric acid was added dropwise into the mixture to hold the hydrochloric acid level constant. After three hours, the oil layer was separated while hot and set aside to cool. The organic layer was treated with a fresh formaldehyde-conc. HCl mixture as described above, and an additional amount of crude product was obtained. A total of four such treatments of the original durene solution gave a white crude product. This was washed with bicarbonate solution and distilled water, then dissolved in dichloromethane and dried with calcium chloride. The solvent was removed. The crude product was washed with warmed pentane (150 cm³). The yield of undissolved white solid was 11g (26%), m.p. 192-194 ° C (Lit.³ m.p. 193-194 ° C).

¹H N.M.R. 400 MHz (CDCl₃) δ: 4.7 (4H, s, 2CH₂) and 2.36 (12H, s, 4CH₃).

8.1.2. 3,6-Dimethylbenzo[1,2:4,5]dicyclobutene (3.1)

1,4-Di-(chloromethyl)2,3,5,6-tetramethylbenzene (3.1a) (3.0 g, 0.013 mmol) was sublimed into a hot zone (700 ° C) quartz tube at 0.05 mmHg pressure (see Figure 8.1). The brown pyrolysate was condensed immediately at the exit of the pyrolysis tube onto a cold finger (liq. N₂) and the product was dissolved in pentane (50 cm³), washed with saturated bicarbonate solution, and dried with sodium sulphate. The product was purified by chromatography on silica gel (100% pentane). 3,6-Dimethylbenzo[1,2:4,5]dicyclo-

butene (2) was obtained as white crystals (0.4 g, 19%), and m.p. 118-119 °C (Lit.⁶ m.p. 119-120 °C).

¹H N.M.R. 200 MHz (CDCl₃) δ_H: 2.01 (6H, s, 2CH₃) and 2.99 (8H, s, 4CH₂).

Lit.⁶ (CDCl₃) δ_H: 2.04 (6H, s, 2CH₃) and 3.00 (8H, s, 4CH₂).

8.1.3. Pentamethylbenzylchloride (3.2a)³

A mixture of pentamethylbenzene (25 g, 169 mmol), 40% formaldehyde (60 cm³, 750 mmol), zinc chloride (10.0 g) as a catalyst and conc. hydrochloric acid (60 cm³) was heated with stirring on an oil bath, while conc. hydrochloric acid was added dropwise to maintain the HCl level. After 3 h, the oil layer was set aside to cool. This was treated with a fresh formaldehyde-conc. hydrochloric acid mixture as described above and an additional amount of crude product was obtained. The crude product was washed with bicarbonate solution, dissolved in dichloromethane and dried over sodium sulphate, to yield white crystals (pentane; 28.6 g). M.p. 81-82 °C. (Lit.³ 82-84 °C)

¹H N.M.R. (CDCl₃) δ_H: 4.73 (2H, s, CH₂), 2.22 (6H, s, CH₃), 2.23 (3H, s, CH₃) and 2.35 (6H, s, CH₃).

8.1.4. 3,4,5,6-Tetramethylbenzocyclobutene (3.2)

Pentamethylbenzylchloride (3.2a) (13.6 g, 69 mmol) was sublimed into the hot zone (700 °C) a quartz tube at 0.1 mmHg pressure (see Figure 8.1). The pyrolysate was condensed immediately at exit of the pyrolysis tube on a cold finger (lqd. N₂). The brown mixture was dissolved in pentane (100 cm³), washed with carbonate solution and dried with sodium sulphate. The product was first purified by chromatography on silica gel (100% pentane). At this stage, the product was contained a small amount of hexamethylbenzene (1%) by ¹H N.M.R.. A further purification, again by chromatography on silica gel (100% pentane), gave white crystals, (from methanol; 0.9 g, 8%) m.p. 144 °C. (Found: C, 89.90; H, 10.18. C₁₂H₁₆ requires C, 89.94; H, 10.06%).

m/z(70eV): 160(100%, M⁺), 159(21.2%), 147(30.7%), 146(18.4%), 145(95.5%), 130(48%) and 117(23.6%); Acc. Mass (C₁₂H₁₆) found: 160.1234, Calc. 160.1251.

^1H N.M.R. (CDCl_3) δ_{H} : 3.01 (4H, s, sCH_2), 2.16 (6H, s, 2CH_3) and 2.09 (6H, s, 2CH_3).
 ^{13}C N.M.R. (CDCl_3) δ_{C} : 14.53 (Me), 15.87 (Me), 26.93 (Methylene), 128.30 (Ar) 133.51 (Ar) and 141.12 (Ar).

8.1.5. Benzo[1,2:4,5]dicyclobutene (3.3)

4,6-Di-(chloromethyl)-m-xylene (1.70 g, 8.37 mmole) was distilled into the hot zone (750 °C) of a quartz tube at about 0.1 mmHg pressure. The brown mixture was condensed immediately at the end of the pyrolysis tube onto a cold finger (liq N_2)². The condensate was dissolved in pentane (50 cm^3), washed with bicarbonate solution and dried with sodium sulphate. The separation was carried out by column chromatography with 100% pentane. The first fraction was collected and recrystallised from 100% methanol, giving white crystals (yield 0.10 g, 10%), m.p. 101-102 °C (Lit.⁶ 100-101 °C).
 ^1H N.M.R. 200 MHz (CDCl_3) δ_{H} : 6.76 (2H, s, Ar) and 3.09 (8H, s, 4CH_2).
 Lit.⁶ (CDCl_3) δ_{H} : 6.80 (2H, s, Ar) and (8H, s, 4CH_2)

8.1.6. 4,7-Dimethyl-indan-1-one (3.4a)³

A mixture of β -chloropropionyl chloride (35 g, 220 mmol) and p-xylene (22 g, 210 mmole) in carbon disulphide (35 cm^3) was added dropwise to a fine powder of aluminium chloride (40 g, 300 mmole) covered with carbon disulphide (170 cm^3). The mixture was stirred at room temperature for 3 h. then the carbon disulphide was removed. A brown oily complex was obtained, conc. sulphuric acid (300 cm^3) was added and the mixture was heated at 90 °C for 45 min with stirring. After cooling, ice (500 g) was added followed by ether-benzene. The organic layer was washed with water and carbonate solution and dried over sodium sulphate. The solvent was removed to give a white solid, which was recrystallised from methanol as white crystals, 20.46 g (60%); m.p. 75-76 °C (Lit.³ 76-77 °C).
 ^1H N.M.R. (CDCl_3) δ_{H} : 7.23 (1H, d, Ar); 7.00 (1H, d, Ar); 2.94 (2H, m, CH_2); 2.64 (2H, m, CH_2); 2.58 (3H, s, CH_3) and 2.88 (3H, s, CH_3).

8.1.7. 3,6-Dimethylbenzocyclopentene (3.4b)⁵

Zinc powder (120 g) was amalgamated by stirring a mixture with mercuric chloride (12 g), conc. hydrochloric acid (60 cm³) and water (150 cm³) for a few minutes and decanting the aqueous solution. The ketone (3.4a) (35.5 g, 220 mmol) was dissolved in toluene (50 cm³), then the amalgamated zinc was mixed with water (50 cm³), conc. hydrochloric acid (200 cm³) and the ketone solution in a 3-necked flask. The mixture was refluxed for 22 h, with addition of conc. hydrochloric acid (70 cm³) every 6 h. After cooling, the aqueous layer was extracted with ether (2 x 50 cm³). The organic layer was washed with bicarbonate solution, and with water and dried over sodium sulphate. The product was separated by reduced pressure distillation to give 23 g (71%) b.p. 77-78 °C at 4 mmHg. (Lit.⁵ b.p. 94-97 °C at 10mmHg).

¹H N.M.R. (CDCl₃) δ_H: 6.91 (2H, s, Ar); 2.87 (4H, t, CH₂); 2.25 (6H, s, CH₃) and 2.09 (2H, q, CH₂).

8.1.8. 4,8-Dimethyl-S-hydroindan-1-one (3.4c)

A solution of β-chloropropionyl chloride (18.3 g, 144 mmol) and 4,7-dimethylindane (3.4b) (21 g, 144 mmol) in carbon disulphide (20 cm³) was added, dropwise over 45 minutes to a fine powder of aluminium chloride (23 g, 170 mmol) covered with carbon disulphide (100 cm³). The mixture was stirred for 3 h and stood overnight at room temperature. After removal of the carbon disulphide, a dark brown residue was formed; conc. sulphuric acid (250 cm³) was added and refluxed for 1.5 h. After cooling, the mixture was hydrolysed with ice, then, ether was added. The aqueous layer was extracted with more ether and the ether was dried over sodium sulphate, to give a brown solid. The product was purified by chromatography on silica gel, eluting with dichloromethane, and was obtained as white crystals (from methanol, 6 g; 20%); m.p. 128-130 °C. Found: C, 84.26; H, 8.32; C₁₄H₁₆O requires C, 83.96; H, 8.05%.

¹H N.M.R. (CDCl₃) δ_H: 2.12 (2H, q, CH₂); 2.20 (3H, s, CH₃); 2.54 (3H, s, CH₃); 2.70 (2H, m, CH₂); 2.80-2.90 (6H, m, CH₂).

¹³C N.M.R. (CDCl₃) δ_C: 14.36 (Me); 14.39 (Me); 23.74; 24.62; 30.75; 32.01;

37.44; 127.87 (Ar); 131.07 (Ar); 132.89 (Ar); 143.05 (Ar); 149.97 (Ar); 153.96 (Ar) and 208.26 (>C=O).

Mass Spectrum: C₁₄H₁₆O: Acc. Mass. Calc. 200.1201; found: 200.1199; m/z (70eV): 200 (100%, M⁺); 185 (11.32%); 172 (29.44%); 158 (28.57%); 157 (51.58%) and 143 (30%).

8.1.9. 3,6-Dimethylbenzo[1,2:4,5]dicyclopentene (3.4)

Zinc powder (100 g) was amalgamated by stirring a mixture with mercuric chloride (10 g), conc. hydrochloric acid (6 cm³) and water (150 cm³) for 5 minutes and decanting the aqueous solution. The ketone (3.4c) (6 g, 30 mmol) was dissolved in toluene (50 cm³), then the amalgamated zinc was mixed with water (50 cm³), and conc. hydrochloric acid (200 cm³) and the ketone (3.4c) solution in a 3-necked flask. The mixture was refluxed for 20 h. After cooling, the aqueous layer was extracted with ether (2 x 50 cm³). The organic layer was washed with water and dried over sodium sulphate. The solvent was removed to give a white solid, which was recrystallised from methanol:hexane (10:1) as white crystals 2.75 g (41%); m.p. 108-109 °C. Found: C, 90.16; H, 9.89; C₁₄H₁₈ requires C, 90.26; H, 9.74%.

¹H N.M.R. (CDCl₃) δ_H: 2.85 (8H, t, CH₂); 2.10 (4H, q, CH₂) and 2.17 (6H, s, CH₃).

¹³C N.M.R. (CDCl₃) δ_C: 15.97 (Me); 24.99; 31.47; 126.57 (Ar); 140.90 (Ar).

Mass Spectra: C₁₄H₁₈ Acc. Mass: Calc. 186.1408; found: 186.1420.

m/z (70eV): 186 (53.4%); 185 (17%); 172 (17.3%) and 171 (100%).

8.1.10. 4,5,6,7-Tetramethyl-indan-1-one (3.5a)¹

Durene (49 g, 366 mmol) and ethyl 3-chloropropionate (50 g, 366 mmol) was mixed in a 3-necked flask, and then fine aluminium chloride (240 g) was added slowly with stirring. The mixture was stirred and heated at 145 °C for 1.5 h. The crude product was poured over ice and extracted with ether. The dark green organic layer was washed with water and dried over magnesium sulphate. The solvent was removed, leaving a dark green mobile oil. Distillation under reduced pressure gave a yellowish liquid which solidified to yellow crystals; m.p. 136 °C (Lit.¹ 150 °C), yield 8.5 g; b.p. 120 °C (0.05

mmHg), [Lit.¹ b.p. 132 °C (0.01 mmHg)].

¹H N.M.R. (CDCl₃) δ_H: 2.22 (3H, s, CH₃), 2.23 (3H, s, CH₃), 2.25 (2H, m, CH₂), 2.27 (3H, s, CH₃), 2.32 (2H, m, CH₂) and 2.61 (3H, s, CH₃).

8.1.11. 3,4,5,6-Tetramethylbenzocyclopentene (3.5)^{1,5}

Zinc powder (120 g) was amalgamated by stirring a mixture with mercuric chloride (12 g), conc. hydrochloric acid (6 cm³) and water (150 cm³) and decanting the aqueous solution. The ketone (3.5a) (8.3 g, 44 mmol) was dissolved in toluene (50 cm³), then, the amalgamated zinc was mixed with water (100 cm³), conc. hydrochloric acid (350 cm³) and the ketone (3.5a) in a 3-necked flask. The mixture was refluxed for 20 h, with addition of conc. hydrochloric acid (70 cm³) every 6 h. After cooling, the aqueous solution was extracted with ether (50 cm³). The ether-toluene mixture was washed with water, and with sodium bicarbonate solution and dried over sodium sulphate. The product was purified by chromatography on silica gel, eluting with pentane. The product was obtained as white crystals (from methanol, 2.37 g, 31%) and m.p. 96-97 °C (Lit.¹ m.p. 99-100 °C). Found: C, 89.85; H, 10.37 C₁₃H₁₈ requires C, 89.56; H, 10.41%.

¹H N.M.R. (CDCl₃) δ_H: 2.89 (4H, t, CH₂), 2.20 (12H, s, CH₃) and 2.04 (2H, q, CH₂).

¹³C N.M.R. (CDCl₃) δ_C: 15.96 (Me), 16.73 (Me), 24.21 (Methylene), 32.52 (Methylene), 129.34 (Ar), 132.71 (Ar) and 139.88 (Ar).

8.1.12. Sesamol (3,4-methylenedioxyphenol) (6.0)

Under ice cooling, hydrogen peroxide (30%, 50 cm³) was added to formic acid (85%, 167 cm³). The solution was left to stand at room temperature for 1 h, then this solution was added to a cooled solution (-5 °C) of piperonal (50.0 g 333 mmol) in formic acid (85%, 500 cm³). The mixture was allowed to stand for 22 hours at -15 °C, then it was hydrolysed with 3 l of ice-water at -10 °C for 30 min, which gave a green precipitate. The solid was collected by filtration under suction. The solid was dissolved in warm NaOH (2M), cooled and acidified with diluted HCl. The mixture was extracted with ether. The ether layer was neutralised with water and dried with Na₂SO₄. The

product was purified by distillation b.p. 64 °C at 0.08 mmHg(Lit.⁷ b.p. 110-112 °C at 4 mmHg). Yield 13.65 g (30%).

¹H N.M.R. 200 MHz (CDCl₃) δ: 6.63 (1H, d, ArH), 6.41 (1H, d, ArH), 6.20 (1H, d,d, ArH), 5.90 (2H, s, -O-CH₂-O-) and 4.80 (1H, s, Ar-OH).

8.1.13. 5,6-Dioxobenzo-1,3-dioxole (7.0)⁷

A solution of KH₂PO₄ (2 g) in water (30 cm³) was added to sesamol (6.0) (13.65 g, 96 mmol) in acetone (30cm³). This mixture was added to a solution of Fremy's salt²⁰ (70.0 g) in water (300 cm³), and the mixture was shaken until a yellow solution resulted. This was extracted with chloroform (1500 cm³). The organic layer was dried over MgSO₄ and the solvent was removed, yielding a yellow-orange solid, 12.3 g (78%), m.p. 201 °C. This product was used directly for the next step without further purification.

¹H N.M.R. 200 MHz (CDCl₃) δ_H: 6.09 (2H, s, -O-CH₂-O-) and 6.03 (2H, s, ArH).

8.1.14. 5,6-Dihydroxybenzo-1,3-dioxole (8.0)⁷

An excess of a saturated aqueous solution of sodium dithionite was added to a suspension of o-benzoquinone (7.0) (12.0 g, 77 mmol) , ether (150 cm³) and water (500 cm³) in a separating funnel, until the mixture was colourless. The aqueous solution was extracted with ether (50 cm³). The ether layer was dried over MgSO₄, and the solvent was removed to give a colourless crystals, 9.1 g (75%), m.p. 159 °C (Lit⁷. m.p. 159 °C).

8.1.15. Benzo[1,2-d:4,5-d']bis-1,3-dioxole (5.1)⁷

5,6-Dihydroxybenzo-1,3-dioxole (8.0) (8.0 g, 51 mmole) was dissolved in dried DMF (30 cm³), then dried bromochloromethane (7.8 g, 60 mmole) and K₂CO₃ (8.1 g, 58 mmole) were added to the solution. The mixture was heated for 30 h at 100°C (bath temp.) under N₂. The solid was filtered off and then washed the with DMF (5 cm³),and dissolved in ether (500 cm³). The ether layer was washed with water, NaOH solution (0.5 M) and then with water. The organic layer was dried with MgSO₄. The solvent was

removed and the product was recrystallisation from cyclohexane giving colourless needles (0.79 g, 9%), m.p. 142-144 °C (Lit.⁷ m.p. 141 °C).

¹H N.M.R. (CDCl₃) 200 MHz δ_{H} : 5.86 (4H, s, -OCH₂O-) and 6.48 (2H, s, ArH).

8.1.16. 5,6-Dimethoxybenzo-1,3-dioxole (5.2)⁷

5,6-Dihydroxy-1,2-dioxole (8.0) (2.0 g, 13 mmole) was dissolved in dried acetone (30 cm³), then K₂CO₃ (2.0 g, 14.5 mmole), and dimethyl sulphate (6.0 g, 47.6 mmole) were added. The mixture was heated at 100 °C (bath temp.) for 12 h under N₂. After cooling, the solvent was removed under reduced pressure, and water (100 cm³) was added. The aqueous solution was extracted with ether (2 × 30 cm³). The organic layer was washed with more water and dried over MgSO₄. The solvent was evaporated and the product was purified by two recrystallisations from cyclohexane; yield 0.5 g (21%), m.p. 110-111 °C (lit.⁷ m.p. 111 °C).

¹H N.M.R. 200 MHz (CDCl₃) δ_{H} : 3.80 (6H, s, OMe), 5.87 (2H, s, -OCH₂O-) and 6.57 (2H, s, ArH).

8.1.17. 1,3-Dioxolo[4,5-g]benzo-1,4-dioxane (4.2)⁷

A mixture of 5,6-dihydroxybenzo-1,3-dioxole (8.0) (8.0 g, 51 mmole), 1,2-dibromoethane (19.0 g, 100 mmole), dried K₂CO₃ (20.0 g, 144 mmole) and dry acetone (170 cm³) was heated at 120 °C (bath temp.) for 20 hours under N₂. After cooling, the solvent was removed and ether (100 cm³) was added. The ether layer was washed with water, aqueous NaOH (0.5 M) and water, then dried over MgSO₄. The solvent was removed under reduced pressure and the product was recrystallised from cyclohexane. Yield 2.96 g (32%), m.p. 88-89 °C (Lit.⁷ m.p. 89 °C).

¹H N.M.R. 200 MHz (CDCl₃) δ_{H} : 4.17 (4H, s, -OCH₂CH₂O-), 5.83 (2H, s, -OCH₂O-) and 6.41 (2H, s, ArH).

8.1.18. 1,2-Dimethyl-1,2-benzoquinone (9.0)⁸

A solution of KH_2PO_4 (17.0 g, 125 mmole) in water (100 cm^3), and of Fremy's salt²⁰ (90.0 g, 335 mmole) in water (3 l) were added to 3,4-dimethylphenol (16.0 g, 131 mmole) in acetone (50 cm^3) in one portion. The mixture was shaken until a red solution was formed, then the aqueous layer was extracted with chloroform. The organic layer was dried over Na_2SO_4 and the solvent was removed on a rotatory evaporator at room temperature giving red crystals 11.0 g (62%), m.p. 104-106 °C (Lit.⁸ m.p. 105-107 °C). ^1H N.M.R. 200 MHz (CDCl_3) δ_{H} : 2.13 (6H, d, CH_3) and 6.22 (2H, q, ArH).

8.1.19. 6,7-Dimethylbenzo-1,4-dioxane (4.3)⁹

4,5-Dimethyl-1,2-benzoquinone (9.0) (2.0 g, 14.7 mmole) was reduced to the corresponding catechol in chloroform solution with aqueous sodium dithionite. The crude catechol was dissolved in dry acetone (40 cm^3) under N_2 , followed by 1,2-dibromoethane (4.0 g, 21 mmole) and K_2CO_3 (4.0 g, 29 mmole). The mixture was stirred and heated at 120 °C (bath temp.) for 20 h. After cooling, the solvent was removed, and water was added. The aqueous layer was extracted with ether (3 \times 25 cm^3), and the ether layer was washed with dilute KOH solution and water, then dried over MgSO_4 . The solvent was removed and the product was purified by column chromatography (eluant, petroleum spirit:ether 5:1); yield 0.7 g (33%), m.p. 71-74 °C (Lit.⁹ 72-74 °C).

^1H N.M.R. 200 MHz (CDCl_3) δ_{H} : 2.14 (6H, s, CH_3), 4.21 (4H, s, $-\text{OCH}_2\text{CH}_2\text{O}-$) and 6.64 (2H, s, ArH).

8.1.20. 5,6-Dimethylbenzo-1,3-dioxole (5.5)¹⁰

4,5-Dimethyl-1,2-benzoquinone (9.0) (4.5 g, 33 mmole) was reduced to the corresponding catechol in chloroform solution with aqueous sodium dithionite. The dried crude catechol was dissolved in dried DMF (40 cm^3) under N_2 , and bromochloromethane (9.4 g, 72 mmole) and K_2CO_3 (19.0 g) were added. The mixture was heated under N_2 at 120°C (bath temp.) for 16 h. After cooling, the solid was filtered off and washed with

ether ($2 \times 20 \text{ cm}^3$). The organic layer was washed with water, aqueous KOH and water, then dried over MgSO_4 . The solvent was evaporated under reduced pressure and column chromatography of the crude product (eluant, petroleum spirit:ethyl acetate 5:1) afforded (5.5) (0.4 g, 8%) as colourless crystals, m.p. 43-45 °C (Lit.¹⁰ 43-47 °C).

^1H N.M.R. 200 MHz (CDCl_3) δ_{H} : 2.16 (6H, s, CH_3), 5.86 (2H, s, $-\text{OCH}_2\text{O}-$) and 6.63 (2H, s, ArH).

8.1.21. 4,5-Dimethyl-1,2-dimethoxybenzene (5.6)¹⁰

4,5-Dimethyl-1,2-benzoquinone (9.0) (2.0 g, 14.7 mmole) was reduced in chloroform solution with aqueous sodium dithionite to the corresponding catechol. The dried catechol was dissolved in aqueous KOH (10.0 g in 21 cm^3 water). The mixture was cooled in an ice bath and dimethyl sulphate (10 cm^3) was added dropwise over 10 min. The mixture was stirred at rm. temp. for 3 h. The aqueous layer was extracted with ether ($2 \times 25 \text{ cm}^3$). The ether was washed with water and brine, and dried over MgSO_4 . The solvent was removed under reduced pressure and column chromatography (eluant, petroleum spirit:ethyl acetate 5:1) yielded (5.6) 0.5 g (20%), m.p. 41-43 °C (Lit.¹⁰ 43-44 °C).

^1H N.M.R. 200 MHz (CDCl_3) δ_{H} : 2.14 (6H, s, CH_3), 3.78 (6H, s, OCH_3) and 6.50 (2H, s, ArH).

8.1.22. 4,5-Dimethoxy-1,2-benzoquinone (10)¹¹

Sodium iodate (40.0 g, 200 mmole) was added to a solution of catechol (11.0 g, 100 mmole) in dry methanol (800 cm^3) at room temperature with stirring, then the mixture was stirred for 20 hours at 60 °C. After filtration, the filtrate was concentrated to about 200 cm^3 under reduced pressure and then cooled to -15 °C to give a deep orange precipitate, which was filtered off. Recrystallisation of the solid from methanol afforded the product (10.0) as deep orange needle crystals (5.6 g, 33%), m.p. 230-232 °C (Lit.¹² 225-227 °C).

^1H N.M.R. 200 MHz (CDCl_3) δ_{H} : 3.88 (6H, s, OCH_3) and 5.75 (2H, s, ArH).

8.1.23. 6,7-Dimethoxy-1,4-benzodioxane (4.4)¹³

4,5-Dimethoxy-1,2-benzoquinone (10.0) (2.0 g, 11.9 mmole) was reduced to the corresponding catechol with a saturated solution of sodium dithionite. A mixture of 1,2-dibromoethane (4.5 g, 23.8 mmole), K₂CO₃ (5.0 g) and the catechol in dried acetone were heated under reflux at 130 °C (bath temp.) and with stirring for 6 h. After cooling, the solvent was removed under reduced pressure, and water was added. The aqueous solution was extracted with ether (2 × 50 cm³). The ether layer was washed with dilute NaOH, water and brine, and dried over MgSO₄. The solvent was removed by evaporation. Sublimation of the crude solid [0.1 mmHg at 80-90 °C (bath temp.)] afforded compound (4.4) (0.38 g, 16%) as colourless crystal, m.p. 91-92 °C (Lit.¹³ 90-90.5 °C) (Found: C, 61.10; H, 6.35, C₁₀H₁₂O₄ requires C, 61.22; H, 6.16%).

¹H N.M.R. 200 MHz (CDCl₃) δ_H: 3.79 (6H, s, OCH₃), 4.20 (4H, s, -OCH₂CH₂O-) and 6.45 (2H, s, ArH).

8.1.24. 3,6-Di-*tert*-butylcatechol (11)¹⁴

A mixture of catechol (27.0 g, 245 mmole), dry xylene (30 cm³), titanium catecholate¹⁴(1.0 g) and *iso*-butylene (60 cm³) were heated in an autoclave at 110°C (about 15 atm. pressure) for 3 h. After removal of the excess solvent, the mixture was distilled and the fraction (11) (b.p. 100 °C at 0.3 mmHg) [Lit.¹⁴ 141-145 °C at 5 mmHg] was collected. The product was further purified by recrystallisation from hexane; yield 9.0 g (16%), m.p. 94-96 °C (Lit.⁴ 96-96.5 °C).

¹H N.M.R. 200 MHz (CDCl₃) δ_H: 1.39 (18H, s, *t*-butyl), 5.35 (2H, s, OH) and 6.76 (2H, s, ArH).

8.1.25. 5,8-Di-*tert*-butylbenzo-1,4-dioxane (4.5)¹⁵

3,6-Di-*tert*-butylcatechol (11) (2.0 g, 9 mmole), 1,2-dibromoethane (4.0 g, 18 mmole), potassium carbonate (4.5 g) and dry acetone (40 cm³) were heated under reflux at 120°C (bath temp.) for 24 h. After cooling, the solvent was removed and water was

added. The aqueous solution was extracted with ether (2 x 50 cm³) and the ether layer was washed with dilute NaOH, water, and brine and dried over MgSO₄. The solvent was removed under reduced pressure and the product was chromatographed with petroleum spirit. The first fraction afforded compound (4.5) as a white solid (1.1 g, 49%); m.p. 44-45 °C (Lit.¹⁵ 48-49 °C). Found: C, 77.24; H, 9.84 C₁₆H₂₄O₂ requires C, 77.38; 9.74%. ¹H N.M.R. 200 MHz (CDCl₃) δ_H: 1.34 (18H, s, *t*-butyl), 4.25 (4H, s, -OCH₂CH₂O-) and 6.75 (2H, s, ArH).

8.1.26. 4,7-Di-*tert*-butylbenzo-1,3-dioxole (5.3)¹⁵

A mixture of 3,6-di-*tert*-butylcatechol (11) (4.0 g, 18 mmole), bromochloromethane (4.65 g, 36 mmole) and potassium carbonate (11.0 g) in dry DMF (40 cm³) was heated for 20 h at 120 °C (bath temp.). After cooling, the solid was filtered off and washed with ether. Water (70 cm³) was added to the filtrate and the aqueous solution was extracted with ether (2 x 80 cm³). The ether layer was washed with dilute NaOH, water and brine, and then dried over MgSO₄. After removal of the solvent, the product was purified by column chromatography (eluant, petroleum spirit) and yield 1.5 g (36%), m.p. 39-40 °C (Lit.¹⁵ 41-42 °C). Found: C, 76.24; H, 9.60 C₁₅H₂₂O₂ requires C, 76.88; H, 9.46%. ¹H N.M.R. 200 MHz (CDCl₃) δ_H: 1.33 (18H, s, *t*-butyl), 5.90 (2H, s, -OCH₂O-) and 6.71 (2H, s, ArH).

8.1.27. 3,6-Di-*tert*-butyl-1,2-dimethoxybenzene (5.4)¹⁵

3,6-Di-*tert*-butylcatechol(11) (2.0 g, 9 mmole) was dissolved in aqueous potassium hydroxide (6.4 g in 16 cm³ of water) at room temperature, then dimethyl sulphate (16 cm³) was added dropwise. The mixture was stirred and heated at 70-80 °C (bath temp.) for 2 h. After cooling, the aqueous layer was extracted with ether (2 x 30 cm³). The ether layer was washed with water and brine, and dried over MgSO₄. The solvent was removed under reduced pressure and then column chromatography of the crude solid (eluant, petroleum spirit) afforded (5.4) (0.6 g, 27%), m.p. 74.5-75 °C. Found: C, 76.54; H, 10.70 C₁₆H₂₆O₂ requires C, 76.74; H, 10.47%.

^1H N.M.R. 200 MHz (CDCl_3) δ_{H} : 1.35 (18H, s, *t*-butyl), 3.82 (6H, s, OMe) and 6.91 (2H, s, ArH).

8.1.28. 2,5-Dimethoxy-1,4-benzoquinone (12)¹⁶

Freshly prepared *p*-benzoquinone (44.0 g, 400 mmole) was added to a solution of fresh fused zinc chloride (48.0 g, 350 mmole) in methanol (250 cm³). The mixture was heated under reflux on a water bath; after 15 min. a red-brown solid separated. The mixture was refluxed for a total of 30 min. and then cooled in a ice-bath overnight. The brown solid was separated by filtration under suction. The solid was washed with cooled methanol and dried in air; yield 36.0 g (53%); m.p. 255-260 °C.

^1H N.M.R. 200 MHz (CDCl_3) δ_{H} : 3.84 (6H, s, OMe) and 6.72 (2H, s, ArH).

8.1.29. 2,5-Dimethoxy-hydroquinone (13)¹⁶

Boiling water (150 cm³) was added into a mixture of 2,5-dimethoxy-1,4-benzoquinone (12) (7.0 g, 41.6 mmole) and sodium dithionite (15.0 g). The mixture was shaken for about 2 min. and then cooled in an ice-bath. The solid was collected by filtration under suction and washed with water. The crude solid (13) was dried under vacuum, yield 5.1 g, 72%, m.p. 166-169°C. The crude product was used directly for the next step.

^1H N.M.R. 200 MHz (CDCl_3) δ_{H} : 3.81 (6H, s, OMe), 5.20 (2H, s, OH) and 6.57 (2H, s, ArH).

8.1.30. 1,2,4,5-Tertamethoxybenzene (5.7)¹⁶

A solution of the crude 2,5-dimethoxyhydroquinone (13) (5.0 g, 29 mmole), sodium dithionite (1.0 g) and dimethyl sulphate (20 cm³) in methanol (20cm³) was stirred in an ice bath and aqueous sodium hydroxide (10.0 g in 20 cm³ of water) was added over 1½ h. The mixture was heated to 70-80 °C for 20 min. and then diluted with water (50 cm³), and cooled to 5 °C. The product (5.7) was obtained as nearly colourless needles m.p. 101-102 °C (Lit.¹⁶ 102-103 °C); yield 2.5 g (41%).

¹H N.M.R. 200 MHz (CDCl₃) δ_H: 3.84 (12H, s, Me) and 6.60 (2H, s, ArH).

8.1.31. Dibenzo-*p*-dioxin (6.3)¹⁷

o-Chlorophenol (20.5 g, 108 mmole), potassium carbonate (11.0 g) and copper powder (1.2 g) were heated at 170-180 °C (bath temp.) for 3 h with mechanical stirring. After cooling, aqueous potassium hydroxide (20.0 g in 500 cm³ of water) was added. The mixture was refluxed for another 30 min.. The mixture was cooled and extracted with ether (2 x 50 cm³). The ether layer was washed with aqueous KOH, and with water and dried over Na₂SO₄. After removal of the solvent, a yellowish solid was obtained. The product (6.3) was purified by sublimation at 80 °C (0.05 mmHg), yield 0.72 g (3%); m.p. 119-120 °C (Lit.¹⁷ 119 °C).

¹H N.M.R. 200 MHz (CDCl₃) δ_H: 6.80-6.91(8H, m, ArH).

8.1.32. 1,4-Diphenyl-1,4-butanedione (14)¹⁸

Succinyl chloride (32.0 g, 206 mmole) was added to a mixture of finely powdered aluminium chloride (70.0 g, 543 mmole) in benzene (500 cm³) at 60 °C over 15 min. The mixture was refluxed for 20 min. in a water bath then poured into crush ice (1 kg). Boiling water (500 cm³) was added into the ice mixture to form two layers. The top organic layer was repeatedly washed with hot water (5 x 500 cm³), then dried over MgSO₄. The solvent was removed and the solid was recrystallised from ethanol as white crystals yielding (14) 15.0 g (30%); m.p. 144-145 °C (Lit.¹⁸ 145 °C)

¹H N.M.R. 200 MHz (CDCl₃) δ_H: 3.46 (4H, s, -CH₂-) and 7.40-8.01 (10H, m, ArH).

8.1.33. 2,5-Diphenylpyrrole (6.4)¹⁹

A mixture of 1,4-diphenyl-1,4-butanedione (14) (10.0 g, 42 mmole) and ammonium acetate (20.0 g) in acetic acid (100 cm³) was refluxed for 20 h. After cooling, this solution was poured into cold water (200 cm³) to causes precipitation. The crude solid was collected by filtration under suction, and then dried in air. Recrystallisation from

ethanol afforded (6.4) 6.0 g (65%); m.p. 140-142 °C (Lit.¹⁹ 142-143 °C).

¹H N.M.R. 200 MHz (CDCl₃) δ_H: 6.58 (2H, s, -CH=), 7.20-7.50 (10H, m, ArH) and 8.60 (1H, s, NH).

8.1.34. Bis(trifluoroacetato-*p*-)(1,3-dioxolo[4,5-*g*]benzo-1,4-dioxane)-dimercury (4.2a)

A solution of 1,3-dioxolo[4,5-*g*]benzo-1,4-dioxane (4.2) (0.4 g, 2.22 mmole) in dichloromethane (5 cm³) was added to a mixture of trifluoroacetic acid and mercuric trifluoroacetate (3.5 g, 8.22 mmole). A white precipitate was formed. The mixture was stirred at 60°C for 15 min and then poured into water (50 cm³). The resulting precipitate was separated by filtration under suction and washed thoroughly with water, and dried in vacuum, yielding the crude bis(trifluoroacetate) (4.2a), 1.5 g (85%).

¹H N.M.R. 400 MHz (DMSO-*d*₆) δ_H: 4.14 (4H, s, -OCH₂CH₂O-) and 5.84 (4H, s, -OCH₂O-).

8.1.35. Other compounds

4,5-Dimethoxybenzo-15-crown-5 (2.7) was supplied by Prof. M. L. Truter. Benzo[*b*]biphenylene (7.1), binaphthylene (7.2) and tribenzo[12]annulene (7.3) were supplied by M. K. Shepherd. Benzo[1,2-*d*:4,5-*d'*]bis[1,4]dioxane (4.1) and benzo[1,2-*d*:3,4-*d'*]bis[1,3]dioxole (5.8) were supplied by Dr. R. Lapouyade.

Most other compounds and reagents were supplied by the Aldrich Chemical Company.

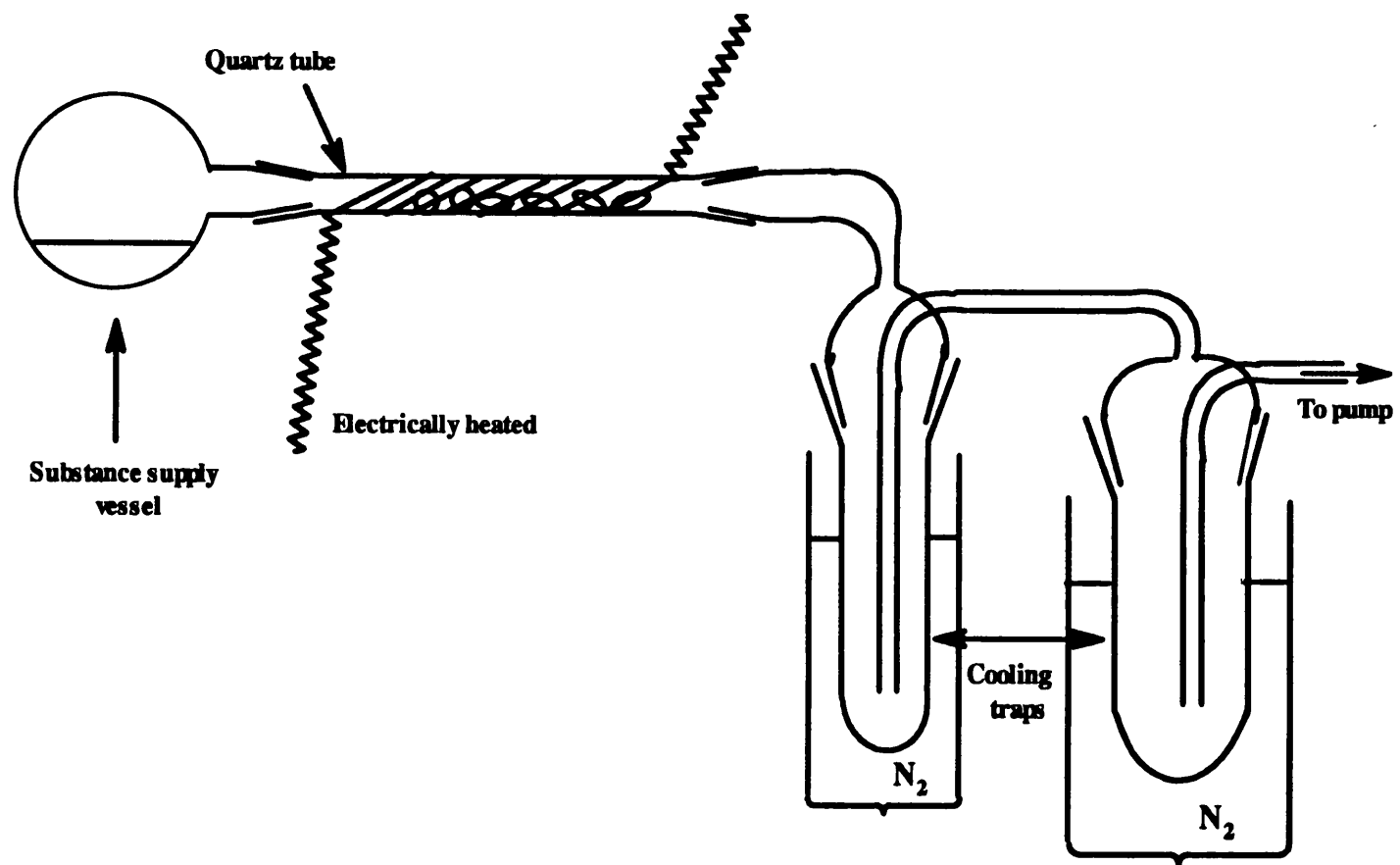


Figure 8.1. Flash vacuum pyrolysis apparatus with external heating.

8.2. E.S.R. Spectroscopy

E.S.R. Spectra were recorded on a Bruker ESP300 or occasionally a Varian E109 spectrometer operating in the microwave region in *ca.* 9.2 GHz. Both spectrometers were fitted with a 500W high pressure mercury arc, provided with neutral (metal gauze 3, 10 and 30% transmittance) and glass filters (soda and Pyrex glass), focused on the cavity.

The infra-red radiation could cause a rise in the sample temperature, and was removed by passing the light beam through an aqueous solution containing $\text{CoSO}_4 \cdot 7\text{H}_2\text{O}$ (0.07M), $\text{NiSO}_4 \cdot 7\text{H}_2\text{O}$ (0.38M) and H_2SO_4 (0.04M). This solution was kept in a quartz cell filled with a water cooled condenser.

The g-factors were determined with a Gaussmeter and the microwave frequency counter was calibrated with the pyrene radical anion (2.002710).²¹

The unknown g-factor could then be calculated from the resonance condition,

$$h\nu_0 = g\beta B_0$$

h is Planck's constant, ν_0 is the microwave frequency, β is the Bohr magneton and B_0 is the field at the centre of resonance.

Computer simulations of experimental spectra were carried out with the Bruker EPR-Simulation program version 1.0 or the ESRXN program for kinetic spectra.

8.3. Preparation of samples for e.s.r. spectroscopy.

8.3.1. Oxidants

All samples were prepared in the e.s.r. tube as illustrated in Figure 8.2.

8.3.1a. DDQ in TFAH containing a few drops of stronger acid.

A solution of DDQ (*ca.* 2 mg) in TFAH (1 cm³) was degassed with nitrogen at 260 K for *ca.* 3 min. The substrate (0.05 mg) was added into the solution mixture, and few drops of a stronger acid (e.g. MeSO_3H or $\text{CF}_3\text{SO}_3\text{H}$) was added. The solution was further degassed.

8.3.1b. $\text{Hg}(\text{TFA})_2$ or $\text{Tl}(\text{TFA})_3$ in TFAH.

A mixture of either $\text{Hg}(\text{TFA})_2$ or $\text{Tl}(\text{TFA})_3$ (5 mg) in TFAH (1 cm³) at 260 K was degassed with a stream of nitrogen. The substrate (0.05 mg) was added into the mixture

and the solution was degassed for *ca.* 2 min.

8.3.1c. Aluminium chloride in dichloromethane.

A solution of the substrate (0.05 mg) and of AlCl_3 (*ca.* 10 mg), was dissolved in dichloromethane (1 cm^3) at 240 K. The solution was degassed with a stream of nitrogen for *ca.* 5 min.

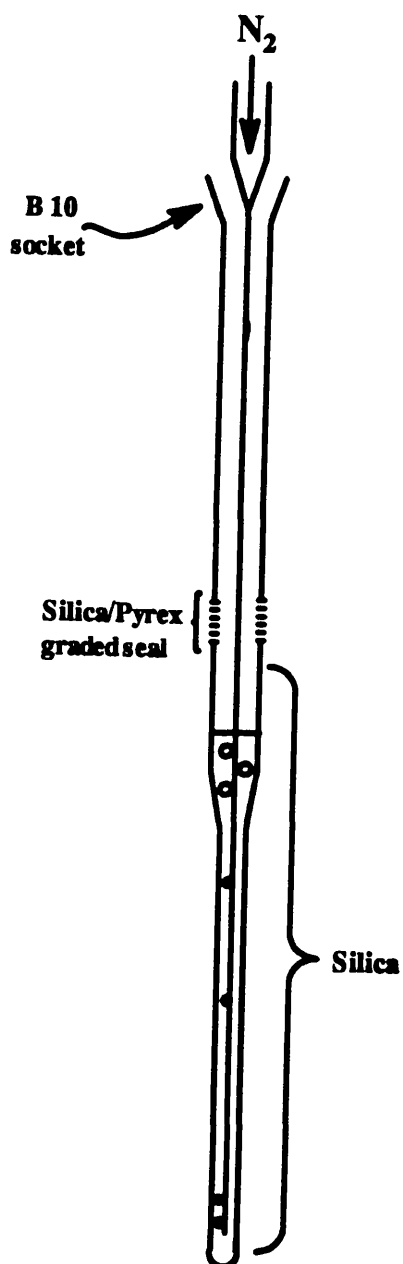


Figure 8.2. Apparatus for radical cation preparation.

8.3.2. Reductants

Radical anions were prepared by contacting a solution of substrate (0.03 mg) in solvent (THF or DME) (1 cm³) with potassium or sodium mirror in a sealed silica tube. The electron-transfer process could be activated by sonication.

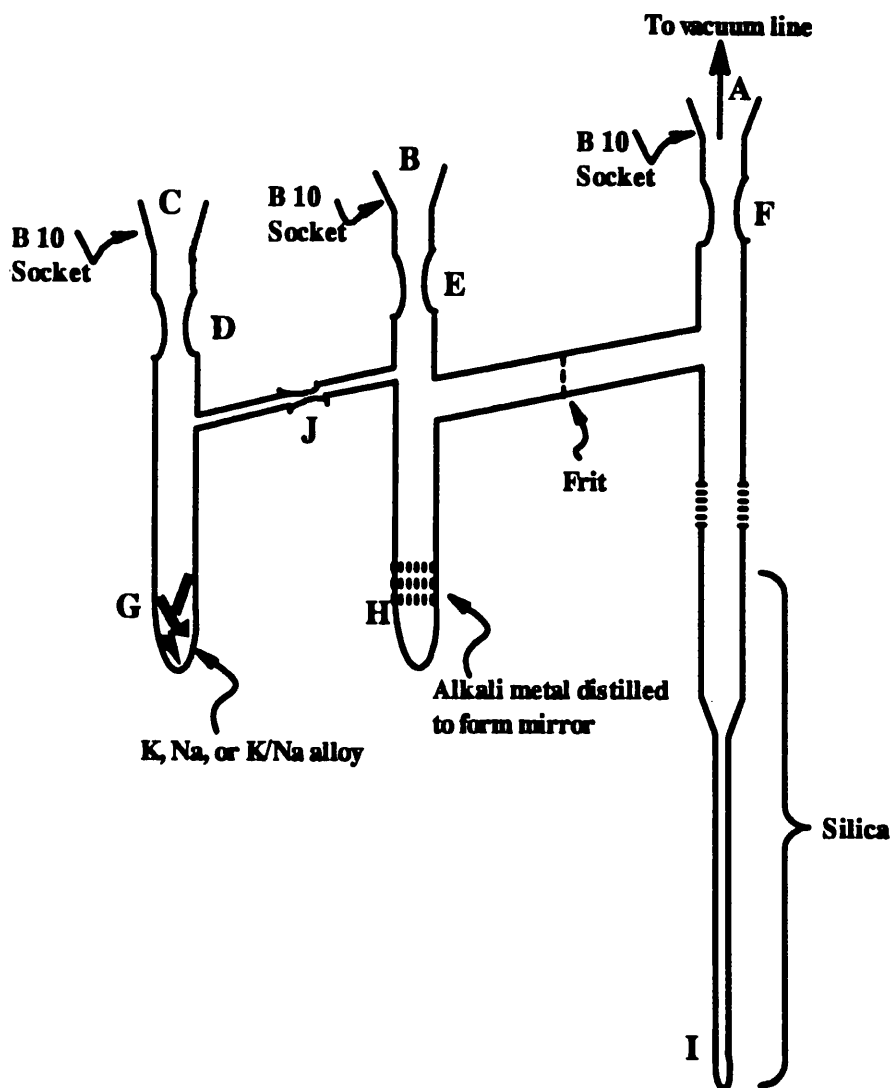


Figure 8.3. Apparatus for preparation of radical anions.

Preparation of the radical anions using potassium, or sodium was carried out in the apparatus illustrated in Figure 8.3 and by the following method:

- (1) The apparatus was predried in an oven (*ca.* 100 °C, 12 h) and then cooled in an

inert gas (Ar or N₂). All further operations were conducted under an inert atmosphere.

- (2) A weighed amount of substrate (0.03 mg) was placed in tube I through A.
- (3) Freshly cut alkali metal (K, or Na) (*ca.* 0.3 g) was washed with dry ether and placed in tube G through C, and then B and C were stoppered.
- (4) The apparatus was connected through A to a vacuum line (0.01 mmHg).
- (5) Points D and E were sealed and cut, and then a portion of the alkali metal was carefully distilled over to tube H. After that, point J was sealed and cut.
- (6) Predried solvent (THF or DME) (*ca.* 1 cm³) was condensed into the tube via A.
- (7) The solution was degassed by 3-4 freeze-pump-thaw cycles.
- (8) Point F was sealed and cut.
- (9) The solution of the substrate was brought into contact with the alkali metal mirror.

8.4. N.M.R. Spectroscopy.

N.M.R. Spectra were recorded on either a Varian VXR 400, a Varian XL 200 or a Jeol PMX 60 spectrometer.

References

1. R. Criegee, F. Förg, H-A. Brune and D. Schönleber, *Chem. Ber.*, 1964, **86**, 52.
2. GüGther Seybold, *Angew. Chem. Int. Ed. Engl.*, 1977, **16**, 365.
3. M.J. Rhoud and P.J. Flory, *J. Am. Chem. Soc.*, 1950, **72**, 2217.
4. H.E. Cier and H.L. Wilder, U.S.P. 3,755,473.
5. L. Fieser and M. Fieser, *Reagent for Organic Synthesis*, Wiley-Int., Vol. 1, 1287.
6. R. Gray, L.G. Harruff, J. Krymowski, J. Peterson and V. Vockelheide, *J. Am. Chem. Soc.*, 1978, **100**, 2892.
7. F. Dallacker, W. Edelmann and A. Weiner, *Liebigs. Ann. Chem.*, 1968, **719**, 112-118.
8. H.J. Teuber, *Org. Synth.*, 1972, **52**, 88.
9. F. Dallacker, G. Reichrath and G. Schnakers, *Z. Naturforsch.*, 1979, **34b**, 624.
10. C.D. Snyder and H. Rapoport, *J. Am. Chem. Soc.*, 1972, **94**, 227.
11. T. Morimoto, Y. Itoh, T. Kakuta and M. Hirano, *Bull. Chem. Soc. of Japan*, 1979, **52**, 2169.
12. H-W. Wanzlick and U. Jahnke, *Chem. Ber.*, 1968, **101**, 3744.
13. A.V. El'tsov, *Zhurnal Obshchei Khimii.*, 1963, **33(6)**, 2006.
14. I.S. Belostotskaya, N.L. Komissarova, E.V. Dzhuaryan and V.V. Ershov, *Izv. Akad. Nauk. SSSR, Ser. Khim.*, 1972, **7**, 1594.
15. V.V. Ershov, *Izv. Akad. Nauk. SSSR, Ser. Khim.*, 1980, **10**, 2414.
16. F. Benington, R.D. Morin and L.C. Clark, *J. Org. Chem.*, 1955, **20**, 102.
17. H. Gilman and J.J. Dietrich, *J. Am. Chem. Soc.*, 1957, **79**, 1939.
18. R.E. Lutz, *Org. Synth.*, 1940, **20**, 29.
19. P.A. Kalter and A. Kreutzberger, *J. Org. Chem.*, 1960, **25**, 554.

20. S.W. Horgan, D.C. Lankin and H. Zimmer, *Chem. Rev.*, 1971, **71**, 229.
21. B. Segal, M. Kaplan and G.K. Fraenkel, *J. Chem. Phys.*, 1965, **43**, 4191.